

ERRATA

p II line 29: “lipid-water interfaces provided” for “lipid-water interfaces, provided”

p 31 line 23: “does not, however, appear” for “does not however appear”

p 113 line 31: “the low amounts of α -helix and β -sheet structures” for “the low amount of the α -helix and the β -sheet”

ADDENDUM

p IV table column 3 row 4: delete “Submitted” and read “In press”

p IV table column 3 row 5: delete “Submitted” and read “Published”

p XIV line 11: delete “Submitted to *Langmuir*, August 2011” and read “*Langmuir*, in press”

p XIV line 13: delete “Submitted to *Langmuir*, August 2011” and read “*Langmuir* **2011**, 27, 14757-14766”

p XIV line 16: delete “, in press” and read “**2012**, 27, 91-101”

p 6 line 4: delete “strength” and read “range”

p 54 legend Figure 3A: the unmatched β -Lg stabilized emulsion should be the blue line; the baseline corrected β -Lg stabilized emulsion should be the red line.

p 88 line 12: delete “the surface charge...electrostatic screening” and read “the Debye screening length and hence the measurable effective charge, i.e. the ζ -potential measured at the finite distance from the droplet surfaces”

p 90 line 17: after “were retained.” add “ However, comparison between the two surfaces should be considered carefully because at low pH, α -La can exist as a molten globule state,^{43,44,46} which may have less stable tertiary structure than the native protein, resulting in the variability of the dimension of the adsorbed protein as seen in Figure 1B”

p 119 line 10: delete “the surface charge...electrostatic screening” and read “the Debye screening length and hence the measurable effective charge, i.e. the ζ -potential measured at the finite distance from the droplet surfaces”

p 122 line 1: delete “SRCD results were also obtained (Appendix 5.1 Figure 6A) that” and read “Another SRCD study has also measured β -casein structure at emulsion interfaces by following the methods developed in this study and the results”

p 122 line 16: delete “SRCD,” and read “SRCD,¹⁷⁻²⁵”

p 122 line 17: delete “proposed...Figure 5.5” and read “shown in Figure 5.5 for comparison to the adsorbed β -Lg layer at the oil-water interface proposed in Chapter 3”

p 170 add at the end of para 2: “However, one should be aware of the contribution of the non-adsorbed β -casein to the SRCD spectra. It is not possible to use centrifugation techniques to determine how much free β -casein was not adsorbed at the interface because the complex internal structure of liquid crystalline nanoparticles cannot be separated into serum and lipid phase. Future studies could investigate a range of β -casein concentrations without Pluronic F127 and identify the ‘threshold’ β -casein concentration to stabilize the nanoparticles, which in turn can provide information on the amount of β -casein adsorption to lipid nanoparticles.”

p 192 line 7: delete “; and 4)...conformational changes of β -casein.”

P 193 line 27: delete “, either retained...interface or”

p 195 add at the end of para 3: “As discussed in Chapter 6, there is no experimental evidence showing how much β -casein was adsorbed. In this regard, further studies using a range of β -casein concentrations to stabilize the lipid nanoparticles are needed to provide a deeper understanding of the effect of the relative amount of protein adsorption on nanoparticle stability.”

Comment on data reproducibility:

To obtain reliable DPI sensorgrams, SRCD spectra, FFTF spectra, SAXS spectra, each condition was measured at least twice on two different samples, the difference between sensorgrams/spectra was less than 0.5%. To obtain representative confocal images of emulsions and TEM of liquid crystalline nanoparticles, each condition was measured on two different samples with at least 10 images taken for each sample.

Comment on DPI study:

The comparison between the adsorbed protein layers on the hydrophobic C18 surface and the hydrophilic silicon oxynitride surface should be interpreted carefully in Chapters 3-5. One could argue that the comparison is not possible because different pHs of the buffer were used in the DPI system and also different concentrations of protein solution were used for injection onto the chip surface. In regard to different concentrations, as can be seen in Chap 3 Fig 1, Chap 4 Fig 1 and Chap 5 Fig 5.1, the adsorbed protein layer had similar deposited mass between the two surfaces for each protein, regardless of the fact that different protein concentrations were used in the initial solution. This indicates that a similar amount of protein was adsorbed on the two surfaces, making the comparison possible and justified. In regard to different pHs, it has been shown by previous studies that the secondary and tertiary structure of β -Lg in solution remains stable even at pH 2¹. In the case of α -La, it is known that a molten globule state of α -La exists under low pH and thereby interpretation of the DPI results should be more careful. More discussion is added as shown in the addendum. Despite the results on the silicon oxynitride surface at pH 3, results from protein adsorption to the C18 surface at pH 7 clearly show that hydrophobic interaction can induce significant protein structural changes. Future investigations could involve a study of the adsorbed protein layer on the hydrophobic C18 layer under pH 3 conditions for comparison.

Reference for addendum:

- (1) El-Zahar, K.; Sitohy, M.; Dalgalarondo, M.; Choiset, Y.; Metro, F.; Haertle, T.; Chobert, J.-M. *Purification and physicochemical characterization of ovine β -lactoglobulin and α -lactalbumin*. *Nahrung - Food* **2004**, *48*, 177-183.

Notice 1

Under the Copyright Act 1968, this thesis must be used only under the normal conditions of scholarly fair dealing. In particular no results or conclusions should be extracted from it, nor should it be copied or closely paraphrased in whole or in part without the written consent of the author. Proper written acknowledgment should be made for any assistance obtained from this thesis.

Notice 2

I certify that I have made all reasonable efforts to secure copyright permissions for third-party content included in this thesis and have not knowingly added copyright content to my work without the owner's permission.

Protein Adsorption at Oil-Water Interfaces
Interfacial Structure and Function of Proteins
in Emulsions

Jiali Zhai

Bsc. (Hons), Bsc. (Biotechnology)

A Thesis for the Degree of Doctor of Philosophy

Department of Biochemistry and Molecular Biology
Monash University

August 2011

Table of Contents

Abstract.....	I
Declaration for thesis	III
Declaration for chapters.....	V
Acknowledgements	XIII
List of publications.....	XIV
List of abbreviations.....	XV
Chapter 1	
Introduction.....	1
1.1 General considerations.....	2
1.2 Oil-in-water emulsions.....	3
1.2.1 Composition and formation	3
1.2.2 Colloidal interactions	4
1.2.2.1 <i>van der Waals interactions</i>	5
1.2.2.2 <i>Hydrophobic interactions</i>	6
1.2.2.3 <i>Electrostatic interactions</i>	6
1.2.2.4 <i>Steric interactions</i>	8
1.2.3 Physical stability	9
1.2.3.1 <i>Creaming/Sedimentation</i>	9
1.2.3.2 <i>Flocculation</i>	10
1.2.3.3 <i>Coalescence</i>	11
1.3 Protein adsorption at oil-water interfaces of emulsions.....	12
1.3.1 Molecular forces and structures of proteins in solution	13
1.3.2 Interfacial properties of proteins.....	15
1.3.3 Characterization of protein interfacial structure	16
1.3.3.1 <i>X-Ray/Neutron reflectometry</i>	16
1.3.3.2 <i>Dual polarization interferometry</i>	17
1.3.3.3 <i>Fourier transform infrared spectroscopy</i>	18
1.3.3.4 <i>Tryptophan emission fluorescence spectroscopy</i>	19
1.3.3.5 <i>Circular dichroism spectroscopy</i>	20
1.4 Interfacial structure and function of milk proteins in emulsions.....	22
1.4.1 β -Lactoglobulin.....	23
1.4.2 α -Lactalbumin	26
1.4.3 β -Casein	27

1.5 Lipid liquid crystalline nanostructured particles.....	29
1.6 Project aims and thesis outline	32
References	34
Chapter 2	
Changes in β-lactoglobulin conformation at the oil-water interface of emulsions studied by synchrotron radiation circular dichroism spectroscopy	50
References	56
<i>Appendix 2.1: Supporting Information.....</i>	<i>58</i>
Chapter 3	
Structural rearrangement of β-lactoglobulin at different oil-water interfaces and its effect on emulsion stability	62
References	71
<i>Appendix 3.1: Supporting Information.....</i>	<i>73</i>
Chapter 4	
Conformational changes of α-lactalbumin adsorbed at oil-water interfaces: Interplay between protein structure and emulsion stability	76
References	96
<i>Appendix 4.1: Supporting Information.....</i>	<i>109</i>
Chapter 5	
Interfacial structure and stabilizing function of β-casein at oil-water interfaces of emulsions	112
References	124
<i>Appendix 5.1: Conformational changes to deamidated wheat gliadins and β-casein upon adsorption to oil-water emulsion interfaces.....</i>	<i>127</i>
Chapter 6	
Revisiting β-casein as a stabilizer for lipid liquid crystalline nanostructured particles.....	159
References	175
<i>Appendix 6.1: Supporting Information.....</i>	<i>186</i>
Chapter 7	
Discussion and conclusion	188
References	198

Abstract

Protein adsorption at oil-water interfaces of emulsions is an important process in the manufacture of many emulsion-based products in food and pharmaceutical industries. It is widely known that for protein-stabilized oil-in-water emulsions, the interfacial structure of proteins adsorbed at oil-water interfaces plays an active role in controlling the physical stability of the emulsions. However, the colloidal properties of emulsions such as the strong scattering and high absorbance of light have severely limited the ability of spectroscopic techniques to measure the interfacial structure of proteins. The lack of studies that systematically investigate the interfacial structure of proteins adsorbed at oil-water interfaces has limited our understanding of how the adsorption process mediates protein structural change and in turn the physical stability of the protein-stabilized emulsions. To address this issue, there is therefore great need to employ novel biophysical techniques that provide molecular level understanding of the interfacial structure of proteins adsorbed at oil-water interfaces.

This thesis explores three biophysical techniques, i.e. synchrotron radiation circular dichroism (SRCD) spectroscopy, front-face tryptophan fluorescence (FFTF) spectroscopy and dual polarization interferometry (DPI), to study the interfacial structure of proteins adsorbed at oil-water interfaces of emulsions. The strong light from the synchrotron radiation source significantly enhanced the sensitivity of SRCD spectroscopy in measuring optically turbid emulsions. SRCD spectroscopy proved to be a powerful technique providing information on both the secondary and tertiary structure of proteins adsorbed at oil-water interfaces. Studies using FFTF spectroscopy in this thesis provided specific information on changes in the tertiary folding of globular proteins adsorbed at oil-water interfaces. DPI was employed in this thesis as a sensing technique to measure the geometric dimensions of proteins (thickness and density) adsorbed at planar hydrophobic interfaces mimicking oil-water interfaces of emulsions. Using the techniques of SRCD, FFTF and DPI, the interfacial structures of three proteins, i.e. β -lactoglobulin (β -Lg), α -lactalbumin (α -La) and β -casein, adsorbed at oil-water interfaces were therefore characterized at a molecular level. These milk proteins are common components of emulsifiers used in many food emulsions and have been frequently used as model proteins in studies of protein adsorption.

Studies on the interfacial structure of β -Lg adsorbed at oil-water interfaces of two model emulsions (hexadecane-in-water and tricaprilyn-in-water emulsions) showed that upon adsorption to oil-water interfaces, β -Lg changed from its native globular structure (3.6 nm in diameter) rich in β -sheet into an open flat structure with a non-native secondary structure with heat-resistant, α -helical-rich characteristics. The β -Lg layer adsorbed at planar hydrophobic surfaces mimicking oil-water interfaces of emulsions was shown to be thin (~ 1 nm) and dense (~ 1 g/cm³). The droplet

surfaces surrounded by the β -Lg interfacial layers were negatively charged (approximately -60 mV of ζ -potential), providing electrostatic repulsion between the emulsion droplets. Parallel studies on the physical stability of β -Lg-stabilized emulsions showed that these emulsions were resistant to droplet flocculation under the condition of heating up to 90 °C. However, increasing the ionic strength by adding 120 mM NaCl reduced the strength of the electrostatic interactions and thus caused β -Lg-stabilized emulsions to undergo heat-induced droplet flocculation.

Studies on the interfacial structure of α -La adsorbed at oil-water interfaces showed that α -La also underwent a significant structural change. Adsorption caused a loss of the well-defined globular structure of α -La ($2.5 \times 3.2 \times 3.7$ nm in crystal structure dimension) accompanied by the formation of a non-native, heat-resistant, α -helical-rich secondary structure. This structural change resulted in a thin (~ 1 nm) and dense (~ 1 g/cm³) layer of α -La, which was negatively charged (approximately -49 mV of ζ -potential). The main stabilization mechanism of α -La-stabilized emulsions was therefore also electrostatic repulsion. Like β -Lg-stabilized emulsions, α -La-stabilized emulsions were resistant to droplet flocculation under the condition of heating up to 90 °C. Interestingly, α -La-stabilized emulsions displayed better stability than β -Lg-stabilized emulsions under the condition of heating in the presence of 120 mM NaCl, mainly due to the lack of inter-droplet disulfide bonding reactions between the interfacial α -La layers.

Studies on β -casein, a flexible protein with a large amount of unordered secondary structure, showed that adsorption to oil-water interfaces induced the formation of the non-native α -helical structure in β -casein. The β -casein layer adsorbed at the planar hydrophobic surface was thicker (~ 5 nm) and more diffuse (0.4 g/cm³) than the β -Lg and α -La layers. The droplet surfaces surrounded by the β -casein layers were also negatively charged (-40 mV of ζ -potential). This interfacial structure of β -casein provided both electrostatic and steric repulsion between the droplets of β -casein-stabilized emulsions, which showed excellent resistance to droplet flocculation under conditions of heating up to 90 °C and 120 mM NaCl addition. This interfacial structure and function of β -casein in oil-in-water emulsions led to a study exploring the ability of β -casein as a stabilizer in another colloidal system, i.e. lipid liquid crystalline nanostructured particles, which are important systems in drug delivery applications. Results obtained from this study revealed that β -casein adsorbed to lipid-water interfaces, provided steric stabilization and favoured the formation of the hexagonal liquid crystalline phase in these lipid nanostructured particles.

Overall, studies in this thesis have advanced our understanding of how adsorption to oil-water or lipid-water interfaces leads to changes in the structure of proteins and in turn how it impacts on their function as stabilizers for colloids containing oil or lipid particles, which have implications in areas such as improvement of food emulsion stability and development of new drug delivery systems.

Declaration for Thesis

In accordance with Monash University Doctorate Regulation 17/Doctor of Philosophy and Master of Philosophy (MPhil) regulations the following declarations are made:

I hereby declare that this thesis contains no material which has been accepted for the award of any other degree or diploma at any university or equivalent institution and that, to the best of my knowledge and belief, this thesis contains no material previously published or written by another person, except where due reference is made in the text of the thesis.

This thesis includes two original papers published in peer reviewed journals and two manuscripts submitted to peer reviewed journals. The core theme of the thesis is to develop biophysical approaches for direct measurement of the interfacial structure of proteins adsorbed at oil-water or lipid-water interfaces and to use these new methods to understand the interfacial structure-function relationship of proteins in colloids containing oil or lipid particles. The ideas, development and writing up of all the papers in the thesis were the principal responsibility of myself, the candidate, working within the Department of Biochemistry and Molecular Biology under the supervision of Professor Marie-Isabel Aguilar. The inclusion of co-authors reflects the fact that the work came from active collaboration between researchers and acknowledges input into team-based research.

In the case of Chapters 2, 3, 4, and 6, my contribution to the work involved the following:

Thesis chapter	Publication title	Publication status	Nature and extent of candidate's contribution
2	Changes in β -lactoglobulin conformation at the oil/water interface of emulsions studied by synchrotron radiation circular dichroism spectroscopy	Published	Manuscript preparation; carried out experimental procedures and data analysis; participated in project co-ordination between co-authors; 70%
3	Structural rearrangement of β -lactoglobulin at different oil-water interfaces and its effect on emulsion stability	Published	Manuscript preparation; carried out experimental procedures and data analysis; participated in project co-ordination between co-authors; 75%
4	Conformational changes of α -lactalbumin adsorbed at oil-water interfaces: Interplay between protein structure and emulsion stability	Submitted	Manuscript preparation; carried out experimental procedures and data analysis; participated in project co-ordination between co-authors; 75%
6	Revisiting β -casein as a stabilizer for lipid liquid crystalline nanostructured particles	Submitted	Manuscript preparation; carried out experimental procedures and data analysis; participated in project co-ordination between co-authors; 70%

Candidate's signature:

.....

Date:

.....

Declaration for Chapter 2

In the case of Chapter 2, the nature and extent of my contribution to the work was the following:

Nature of contribution	Extent of contribution (%)
Manuscript preparation; carried out experimental procedures and data analysis; participated in project co-ordination between co-authors	70

The following co-authors contributed to the work:

Name	Nature of contribution
Andrew J. Miles	Intellectual input on SRCD operation and analysis
Leonard Keith Pattenden	Intellectual input; refinements to the manuscript
Tzong-Hsien Lee	Intellectual input; refinements to the manuscript
Mary Ann Augustin	Intellectual input; refinements to the manuscript
B.A. Wallace	Intellectual input; refinements to the manuscript
Marie-Isabel Aguilar	Supervision; intellectual input; refinements to the manuscript
Tim J. Wooster	Supervision; intellectual input; refinements to the manuscript

Candidate's signature:

Date:

.....

.....

Declaration by co-authors

The undersigned hereby certify that:

- (1) the above declaration correctly reflects the nature and extent of the candidate's contribution to this work, and the nature of the contribution of each of the co-authors.
- (2) they meet the criteria for authorship in that they have participated in the conception, execution, or interpretation, of at least that part of the publication in their field of expertise;
- (3) they take public responsibility for their part of the publication, except for the responsible author who accepts overall responsibility for the publication;
- (4) there are no other authors of the publication according to these criteria;
- (5) potential conflicts of interest have been disclosed to (a) granting bodies, (b) the editor or publisher of journals or other publications, and (c) the head of the responsible academic unit; and
- (6) the original data are stored at the following location(s) and will be held for at least five years from the date indicated below:

Location(s)

Department of Biochemistry and Molecular Biology, Monash University, Clayton, Vic 3800, Australia
--

Co-authors' signature for Chapter 2:

Date:

Andrew J. Miles

27/7/2011

Leonard Keith Pattenden

27/7/2011

Tzong-Hsien Lee

27/7/2011

Mary Ann Augustin

08/08/2011

B.A. Wallace

28/7/2011

Marie-Isabel Aguilar

27/7/2011

Tim J. Wooster

16/8/2011

Declaration for Chapter 3

In the case of Chapter 3, the nature and extent of my contribution to the work was the following:

Nature of contribution	Extent of contribution (%)
Manuscript preparation; carried out experimental procedures and data analysis; participated in project co-ordination between co-authors	75

The following co-authors contributed to the work:

Name	Nature of contribution
Tim J. Wooster	Supervision; intellectual input; refinements to the manuscript
Søren V. Hoffmann	Intellectual input on SRCD operation and analysis
Tzong-Hsien Lee	Intellectual input on DPI operation and analysis
Mary Ann Augustin	Intellectual input; refinements to the manuscript
Marie-Isabel Aguilar	Supervision; intellectual input; refinements to the manuscript

Candidate's signature:

Date:

Declaration by co-authors

The undersigned hereby certify that:

- (1) the above declaration correctly reflects the nature and extent of the candidate's contribution to this work, and the nature of the contribution of each of the co-authors.
- (2) they meet the criteria for authorship in that they have participated in the conception, execution, or interpretation, of at least that part of the publication in their field of expertise;
- (3) they take public responsibility for their part of the publication, except for the responsible author who accepts overall responsibility for the publication;
- (4) there are no other authors of the publication according to these criteria;
- (5) potential conflicts of interest have been disclosed to (a) granting bodies, (b) the editor or publisher of journals or other publications, and (c) the head of the responsible academic unit; and
- (6) the original data are stored at the following location(s) and will be held for at least five years from the date indicated below:

Location(s)

Department of Biochemistry and Molecular Biology, Monash University, Clayton, Vic 3800, Australia
--

Co-authors' signature for Chapter 3:

Date:

Tim J. Wooster

16/8/2011

Søren V. Hoffmann

27/2-2011

Tzong-Hsien Lee

27/7/2011

Mary Ann Augustin

08/08/2011

Marie-Isabel Aguilar

27/7/2011

Declaration for Chapter 4

In the case of Chapter 4, the nature and extent of my contribution to the work was the following:

Nature of contribution	Extent of contribution (%)
Manuscript preparation; carried out experimental procedures and data analysis; participated in project co-ordination between co-authors	75

The following co-authors contributed to the work:

Name	Nature of contribution
Søren V. Hoffmann	Intellectual input on SRCD operation and analysis
Li Day	Intellectual input; refinements to the manuscript
Tzong-Hsien Lee	Intellectual input on DPI operation and analysis
Mary Ann Augustin	Intellectual input; refinements to the manuscript
Marie-Isabel Aguilar	Supervision; intellectual input; refinements to the manuscript
Tim J. Wooster	Supervision; intellectual input; refinements to the manuscript

Candidate's signature:

Date:

Declaration by co-authors

The undersigned hereby certify that:

- (1) the above declaration correctly reflects the nature and extent of the candidate's contribution to this work, and the nature of the contribution of each of the co-authors.
- (2) they meet the criteria for authorship in that they have participated in the conception, execution, or interpretation, of at least that part of the publication in their field of expertise;
- (3) they take public responsibility for their part of the publication, except for the responsible author who accepts overall responsibility for the publication;
- (4) there are no other authors of the publication according to these criteria;
- (5) potential conflicts of interest have been disclosed to (a) granting bodies, (b) the editor or publisher of journals or other publications, and (c) the head of the responsible academic unit; and
- (6) the original data are stored at the following location(s) and will be held for at least five years from the date indicated below:

Location(s)

Department of Biochemistry and Molecular Biology,
Monash University, Clayton, Vic 3800, Australia

Co-authors' signature for Chapter 4:

Date:

Søren V. Hoffmann

27/7-2011
.....

Li Day

08/08/2011
.....

Tzong-Hsien Lee

27/07/2011
.....

Mary Ann Augustin

08/08/2011
.....

Marie-Isabel Aguilar

27/7/2011
.....

Tim J. Wooster

16/8/2011.
.....

Declaration for Chapter 6

In the case of Chapter 6, the nature and extent of my contribution to the work was the following:

Nature of contribution	Extent of contribution (%)
Manuscript preparation; carried out experimental procedures and data analysis; participated in project co-ordination between co-authors	70

The following co-authors contributed to the work:

Name	Nature of contribution
Lynne Waddington	Intellectual input on cryo-TEM operation and analysis
Tim J. Wooster	Intellectual input; refinements to the manuscript
Marie-Isabel Aguilar	Supervision; intellectual input; refinements to the manuscript
Ben J. Boyd	Supervision; intellectual input; refinements to the manuscript

Candidate's signature:

Date:

.....

.....

Declaration by co-authors

The undersigned hereby certify that:

- (1) the above declaration correctly reflects the nature and extent of the candidate's contribution to this work, and the nature of the contribution of each of the co-authors.
- (2) they meet the criteria for authorship in that they have participated in the conception, execution, or interpretation, of at least that part of the publication in their field of expertise;
- (3) they take public responsibility for their part of the publication, except for the responsible author who accepts overall responsibility for the publication;
- (4) there are no other authors of the publication according to these criteria;
- (5) potential conflicts of interest have been disclosed to (a) granting bodies, (b) the editor or publisher of journals or other publications, and (c) the head of the responsible academic unit; and
- (6) the original data are stored at the following location(s) and will be held for at least five years from the date indicated below:

Location(s)

Department of Biochemistry and Molecular Biology, Monash University, Clayton, Vic 3800, Australia
--

Co-authors' signature for Chapter 6:

Date:

Lynne Waddington

..... 8/8/2011

Tim J. Wooster

..... 16/8/2011

Marie-Isabel Aguilar

..... 27/7/2011

Ben J. Boyd

..... 01/08/2011

Acknowledgements

First and foremost, I would like to sincerely thank my primary supervisors Prof. Mibel Aguilar at Monash and Dr. Tim Wooster at CSIRO, who have been inspiring mentors during the last three and half years and have given me endless support, advice and encouragement. You have guided me into becoming an independent scientist.

To my co-supervisors Dr. Tzong-Hsien (John) Lee at Monash and Dr. Mary Ann Augustin at CSIRO, I am always amazed at your extensive scientific knowledge and grateful for your numerous ideas and discussion to help the project development. I am also grateful to Dr. Li Day at CSIRO for all her support and advice, especially for her company during the after hour work at the synchrotron as well as at CSIRO.

I would also like to thank all the excellent scientists who trained and supported me in the SRCD work – Dr. Søren Hoffmann and Dr. Nykola Jones at ISA-ASTRID in Denmark, Dr. Andy Miles and Prof. Bonnie Wallace at Birkbeck College in UK as well as Dr. Len Pattenden.

The lipid nanoparticle work in this project would never have been possible without the support from Assoc. Prof. Ben Boyd at Monash Institute of Pharmaceutical Sciences. I would like to thank him for his insightful discussion and technical advice. Many thanks go to Lynne Waddington at CSIRO for her help on the cryo-TEM work.

I would also like to thank the Aguilar lab and the colleagues at CSIRO who have provided a welcome research environment for me to work. From the Aguilar lab, special thanks go to Ann Du, Sharon Unabia and Romila Gopalan for their friendship, laughs and company. From CSIRO, I would particularly like to thank Mi Xu, Dr. Benjamin Wong and Agustina Goh for their friendship and company, Dr. Roderick Williams, Dr. Lijiang Cheng and Phil Muller for their technical support.

This work was part of an ARC linkage project involving collaboration between Monash, ANU and Dairy Innovation Australia Limited (DIAL). I would like to thank all the collaborators – Dr. Martin Palmer and Dr. Sandra Ainsworth at DIAL and Prof. John White at ANU for their scientific discussion during the meetings. Special thanks go to June Tan at DIAL for her help on the protein purification work. I am thankful to all the financial bodies for providing the scholarship, the travel grant and the project funding – Monash, CSIRO, ARC, DIAL, ISA-ASTRID, Australian Synchrotron and AMRFP.

Last but not least, I would like to thank my family and friends, most importantly my parents Dongsheng Zhai and Yanhua Liu and my partner Bo Liu, for all their love, encouragement and understanding.

List of publications

1. Zhai, J., Miles, A.J., Pattenden, L.K., Lee, T.-H., Augustin, M.A., Wallace, B.A., Aguilar, M.-I., Wooster, T.J. *Changes in β -lactoglobulin conformation at the oil/water interface of emulsions studied by synchrotron radiation circular dichroism spectroscopy. *Biomacromolecules* **2010**, *11*, 2136-2142.*
2. Zhai, J., Wooster, T.J., Hoffmann, S.V., Lee, T.-H., Augustin, M.A., Aguilar, M.-I. *Structural rearrangement of β -lactoglobulin at different oil-water interfaces and its effect on emulsion stability. *Langmuir* **2011**, *27*, 9227-9236.*
3. Zhai, J., Hoffmann, S.V., Lee, T.-H., Augustin, M.A., Aguilar, M.-I., Wooster, T.J., *Conformational changes of α -lactalbumin adsorbed at oil-water interfaces: Interplay between protein structure and emulsion stability.* Submitted to *Langmuir*, August 2011.
4. Zhai, J., Waddington, L., Wooster, T.J., Aguilar, M.-I., Boyd, B.J. *Revisiting β -casein as a stabilizer for lipid liquid crystalline nanostructured particles.* Submitted to *Langmuir*, August 2011.
5. Wong, B.T., Zhai, J., Hoffmann, S.V., Aguilar, M.-I., Augustin, M.A., Wooster, T.J., Day, L. *Conformational changes to deamidated wheat gliadins and β -casein upon adsorption to oil-water emulsion interfaces. *Food Hydrocolloids*, in press.*

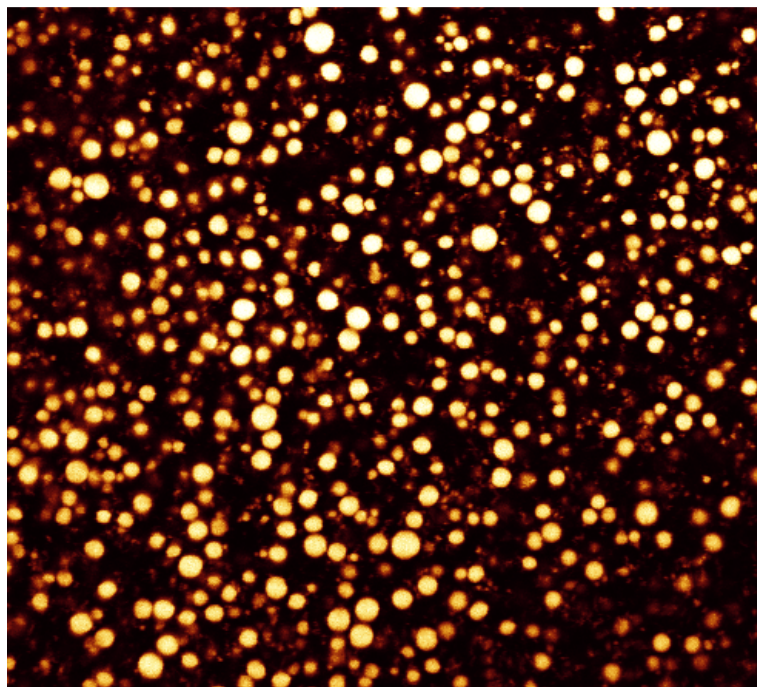
List of abbreviations

3D	Three-dimensional
DPI	Dual polarization interferometry
TM	Transverse magnetic
TE	Transverse electric
FTIR	Fourier transform infrared spectroscopy
CD	Circular dichroism spectroscopy
SRCD	Synchrotron radiation circular dichroism spectroscopy
β-Lg	β -Lactoglobulin
α-La	α -Lactalbumin
β-CN	β -Casein
BSA	Bovine serum albumin
DMPC	Dimyristoylphosphatidylcholine
DMPG	Dimyristoylphosphatidylglycerol
GMO	Glyceryl monooleate
PHYT	Phytantriol (3,7,11,15-tetramethyl-1,2,3-hexadecanetriol)
V₂	Inverse bicontinuous cubic phase
H₂	Inverse hexagonal phase
L₂	Inverse micellar phase
F127	Pluronic F127
IPMS	Infinite periodic minimal surfaces
SAXS	Small angle X-ray scattering
PPO	Polypropylene oxide
PEO	Polyethylene oxide
TEM	Transmission electron microscopy
O/W	Oil/water
RIME	Refractive index matched emulsions
RI	Refractive index
HPLC-MS	High performance liquid chromatography-mass spectrometry
Tris	Tris(hydroxymethyl)aminomethane

NaCl	Sodium chloride
SDS	Sodium dodecyl sulphate
D_{3,2}	Surface area moment mean diameter
D_{4,3}	Volume-weighted average mean diameter
MRE [θ]	Mean residue ellipticity
NRMSD	Normalized root-mean-square deviation
HT	High tension voltage
Γ	Surface coverage
Trycaprylin	Glyceryl trioctanoate
DLS	Dynamic light scattering
λ_{max}	Wavelength of maximum tryptophan emission
FFTF	Front-face tryptophan fluorescence
FESEM	Field emission scanning electron microscopy
Pdi	Polydispersity index
PDB	Protein data bank

Chapter 1

Introduction



A confocal image of a protein-stabilized oil-in-water emulsion

1.1 General considerations

Protein adsorption at interfaces is a common phenomenon in many biological and industrial processes. Interfaces can be divided into three major categories: liquid-liquid interfaces such as lipid bilayers and oil-water interfaces of emulsions; solid-liquid interfaces such as biosensor chips; and gas-liquid interfaces such as the air-water interface of foams. Protein adsorption at these interfaces mediates membrane protein interactions with lipid bilayers,¹⁻⁵ protein interactions with solid-supported surfaces in biosensors⁶⁻¹⁰ and protein interactions with oil-water or air-water interfaces for emulsification and stabilization.¹¹⁻¹⁵

This thesis mainly focuses on the adsorption process of milk proteins at oil-water interfaces of oil-in-water emulsions: how it affects milk protein structural properties and in turn the emulsion stability. There are many different types of emulsions such as macroemulsions, microemulsions and nanoemulsions depending on their particle sizes. The term ‘emulsion’ in this thesis refers to the oil-in-water macroemulsion (average particle size $>0.5 \mu\text{m}$) stabilized by milk proteins. The oil-water interface of emulsions thus corresponds to the surface of the oil droplets in emulsions. Emulsions are frequently used formulations in food and pharmaceutical industries.¹⁶⁻²⁰ The amphiphilic nature of proteins makes them good candidates as emulsifiers and stabilizers in emulsions. In particular, milk proteins such as sodium caseinate and whey protein isolate have been widely used in food emulsions.²¹⁻²⁵ Studies over the past decades have shown that the interfacial properties of milk proteins adsorbed at oil-water interfaces play a key role in determining the physicochemical properties of the emulsion, including texture, taste, average particle size and stability.²⁶⁻³⁰ It is not surprising, therefore, that characterization of milk protein interfacial properties and emulsion properties has received widespread interest in the field of food colloid and interface science.

This thesis also presents a study on the adsorption of milk proteins at lipid-water interfaces of lipid liquid crystalline nanostructured particles, which is a colloidal system of lipid liquid crystalline phases dispersed in an aqueous medium. In the last couple of decades, there has been considerable research into the formation and phase behaviour of lipid liquid crystalline nanostructured particles due to their great potential in areas such as controlled release of drugs and nutrients.³¹⁻⁴⁷ Lipid liquid crystalline nanostructured particles are usually stabilized by synthetic polymers. However, the development of a biocompatible stabilizer is important. Although there is little information on milk proteins as stabilizers for lipid liquid crystalline nanostructured particles to date, milk proteins are a logical choice as biocompatible stabilizers since they have shown excellent stabilizing function in oil-in-water emulsions.

This chapter provides an overview of the field of milk protein adsorption at oil-water interfaces of emulsions. First, a background introduction is given on oil-in-water emulsions, the

colloidal interactions and the physical stability (Section 1.2). Second, the current understanding of the molecular forces and properties of proteins in the native state in solution and adsorbed at oil-water interfaces is reviewed, with a focus on protein interfacial structure and its characterization by a range of biophysical techniques (Section 1.3). Third, a review of the interfacial structural properties of three individual milk proteins at oil-water interfaces and the relationship to emulsion stability is presented (Section 1.4). Fourth, a section on lipid liquid crystalline nanostructured particles is provided to introduce their phase behaviour, the stabilization by polymers and the potential of use of milk proteins as alternative stabilizers (Section 1.5). Last, the general aims of this project are outlined (Section 1.6).

1.2 Oil-in-water emulsions

Oil-in-water emulsions are familiar to everyone through daily usage and consumption. Examples of food oil-in-water emulsions are milk, mayonnaise, cream liqueurs, etc. Food manufacturers seek to produce emulsion-based products of desirable organoleptic properties and long shelf life for transport and storage, which relies on the scientific understanding of the emulsion properties. The purpose of this section is to give an overview of the composition and formation, the colloidal interactions and the physical stability of emulsions.

1.2.1 Composition and formation

An oil-in-water emulsion is a system of oil droplets dispersed in an aqueous phase. An emulsion is both compositionally and structurally complex. Nevertheless, it can be generally divided into three distinct regions: the oil phase; the interfacial layer; and the aqueous phase (Figure 1.1). Molecules in an emulsion partition themselves between the three regions depending on their polarity and surface activity. The dispersed oil phase may contain a variety of lipid-soluble components, such as triacylglycerols, fatty acids, sterols and vitamins. The interfacial layer is the narrow region surrounding the oil droplet and may contain a mixture of emulsifiers, such as small-molecule surfactants and large surface-active proteins and polysaccharides. The continuous aqueous phase may contain a mixture of water-soluble ingredients, such as salts, phospholipids, proteins and polysaccharides.

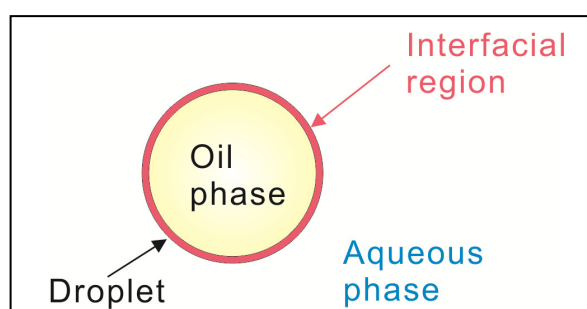


Figure 1.1: An oil-in-water emulsion can be divided into three regions: the oil phase which is the interior of the droplet, the narrow interfacial region surrounding the droplet, and the aqueous phase. Adapted from¹⁹

Emulsion formation can be achieved by emulsification, a process of converting the separate oil and aqueous phases into an emulsion by high energy input. The creation of an emulsion is thermodynamically unfavourable due to the large increase in the overall free energy, which can be represented by the following expression:

$$\Delta G_{\text{formation}} = \gamma \Delta A \quad (1.1)$$

where the free energy of formation ($\Delta G_{\text{formation}}$) is equal to the increase in the surface area between oil and water (ΔA) multiplied by the interfacial tension (γ). Oil-in-water macroemulsions are not thermodynamically stable because of the increase in the surface area between oil and water upon emulsification. The oil and aqueous phases rapidly separate into two distinct layers to achieve the global minimum state. However, it is possible to create a kinetically stable emulsion when emulsifiers are present in the system. Emulsifiers adsorb to oil-water interfaces during emulsification, reduce the interfacial tension (γ) and create an activation energy barrier (ΔG^*) against the transformation of the emulsion from the high to the low energy state (Figure 1.2). Hence, an emulsion can remain kinetically stable for a long period of time despite existing in a non-thermodynamically equilibrium state.

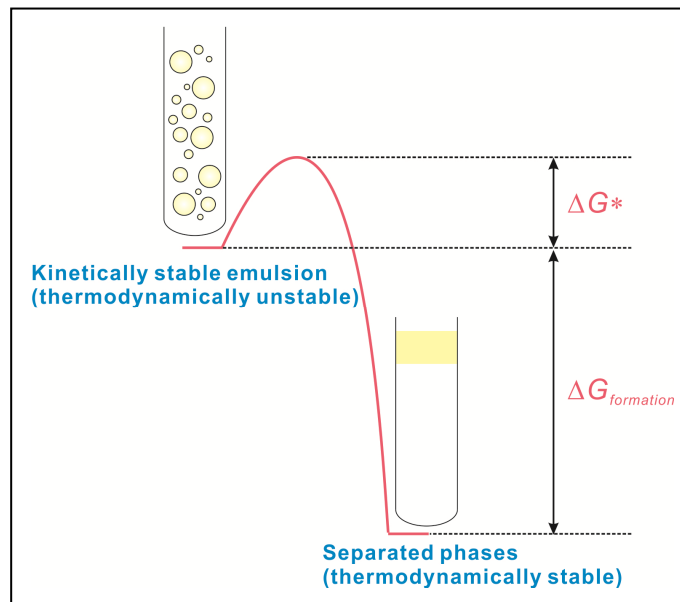


Figure 1.2: An emulsion system is thermodynamically unstable, but can be kinetically stable with a ΔG^* to overcome from the high to the low energy state. Adapted from¹⁹

1.2.2 Colloidal interactions

Colloidal interactions govern the kinetic stability of emulsions. In real food emulsions, colloidal interactions are very complex, arising from emulsion droplets, other colloidal particles and the ions and molecules in the aqueous phase.^{16, 19} Nevertheless, colloidal interactions between emulsion droplets can be understood in simple model emulsions. The overall interaction between a

pair of emulsion droplets can be described by the inter-droplet pair potential, which is the sum of all attractive and repulsive forces.¹⁹ The inter-droplet pair potential governs whether the two droplets remain as individual entities or aggregate. When the overall repulsive force dominates, the dispersion is stable. When the overall attractive force takes over, the emulsion droplets are likely to flocculate and/or to coalesce. There are various types of interactions that can occur between emulsion droplets, such as van der Waals interactions, hydrophobic interactions, electrostatic interactions, steric interactions, hydration interactions, depletion interactions, etc. This section focuses on four major types of colloidal interactions in protein-stabilized model emulsions.

1.2.2.1 van der Waals interactions

van der Waals interactions between emulsion droplets arise from the interactions between the molecules in the dispersed oil droplets, at the droplet interfacial layers and in the continuous aqueous phase.^{19, 48-50} Ultimately, van der Waals interactions arise from the fluctuating polarization of molecules and there are three types of forces: London dispersion forces (the interaction between two instantaneously induced dipoles), Debye/induction forces (permanent dipole-induced dipole interactions) and orientation forces (permanent dipole-permanent dipole interactions). The sum of all these inter-molecular interactions results in the van der Waals interactions that are attractive, strong and long range between emulsion droplets. These properties of the colloidal van der Waals interactions suggest that emulsion droplets always tend to flocculate (Section 1.2.3.2) and/or coalesce (Section 1.2.3.3) in the absence of any repulsive interactions.

According to various mathematical models for van der Waals interactions,^{19, 48-50} major factors controlling the van der Waals interactions between emulsion droplets are dependent on the properties of each phase as described by the Hamaker function, the droplet size, the droplet separation distance and the composition and thickness of the interfacial layer. General features of the van der Waals interactions between emulsion droplets are:

- 1) The inter-droplet van der Waals interactions are always attractive. The strength is described by the Hamaker function and depends on the physicochemical properties of the oil phase and the continuous aqueous phase, such as the dielectric constant, the refractive index and the electronic absorption frequency. In an oil-in-water emulsion, the oil phase and the continuous aqueous phase usually have different dielectric constants and refractive indices. A larger difference of these properties between the oil and the aqueous phase results in stronger van der Waals interactions between emulsion droplets.
- 2) The inter-droplet van der Waals interactions become stronger as the droplet size increases; the interactions become weaker when the droplet separation distance increases.

- 3) The orientation and induction contributions involving permanent dipoles influence the van der Waals interactions between emulsion droplets by the presence of electrolytes in the aqueous phase. Increasing the electrolyte concentration (higher ionic strength) can decrease the strength of the van der Waals interactions due to the accumulation of the counter-ions around the droplets, i.e. the electrostatic screening effect (Section 1.2.2.3).

1.2.2.2 Hydrophobic interactions

Hydrophobic interactions between emulsion droplets originate from inter-molecular hydrophobic interactions between molecules at the surfaces of emulsion droplets.¹⁹ Hydrophobic interactions refer to the self-association of the non-polar regions of molecules in an aqueous environment to minimize the thermodynamically unfavourable contact with water, which manifest itself as a strong attractive force.⁵⁰⁻⁵² Unlike van der Waals interactions which always exist between emulsion droplets, hydrophobic interactions only occur when the surfaces of the droplets contain some non-polar characters. This situation can arise either because there are insufficient emulsifiers to cover oil-water interfaces, leading to the exposure of non-polar oil molecules,^{53, 54} or because the emulsifiers themselves contain exposed non-polar regions.^{29, 30, 55} Therefore, factors influencing the inter-droplet hydrophobic interactions include: the droplet surface hydrophobicity, the extent of the emulsifier coverage of the emulsion droplet and the type of emulsifier adsorbed at the oil-water interface. The strength of the hydrophobic interactions increases as the surface hydrophobicity of the droplets increases. As emulsifiers, globular proteins can play an active role in determining the hydrophobic interactions between emulsion droplets as they can increase the surface hydrophobicity once adsorbed at the droplet surfaces, particularly upon heating.^{29, 30, 55}

1.2.2.3 Electrostatic interactions

Electrostatic interactions between emulsion droplets arise from the electrical charge carried on droplet surfaces.¹⁹ In the case of emulsions stabilized by the same type of emulsifier, the electrical charge on the droplet surfaces are the same, meaning the electrostatic interactions are repulsive. An isolated charged droplet surface contains an electrical double layer, i.e. one layer of ions directly adsorbed at the surface and one layer of counter-ions free in the bulk liquid, electrically neutralizes the first layer (Figure 1.3). When two droplets come together, the double layers of these two similarly charged droplets overlap and confine the counter-ions between the droplets to occupy a smaller volume, i.e. a decrease in entropy giving rise to a strong repulsive force.^{19, 56} The thickness of the double layer is related to the Debye screening length (κ^{-1});

$$\kappa^{-1} = \sqrt{\frac{\epsilon_0 \epsilon_R k T}{e^2 \sum n_i z_i^2}} \quad (1.2)$$

where ϵ_0 is the dielectric constant of a vacuum, ϵ_R is the relative dielectric constant of the solution, e is the elementary charge, n_{0i} is the concentration of ionic species of type i in the bulk electrolyte solution (in molecules per cubic meter) and z_i is their valency.

The strength of the electrostatic interactions between emulsion droplets depend on two electrical characteristics: the surface charge density and the electric surface potential.¹⁹ The surface charge density is the total amount of charge in a unit surface area, whereas the electrical surface potential is the free energy required to increase the surface charge density from zero to a certain value. The strength of the electrostatic interactions increases as the surface charge density and the surface potential increase. These two characteristics depend on many factors, such as the concentration and the type of emulsifiers adsorbed at the droplet surface as well as the environmental condition (pH, temperature and ionic strength).

Electrostatic repulsion is the major stabilizing mechanism in globular protein-stabilized emulsions, which are very sensitive to pH and ionic strength.^{29, 30, 55, 57-60} A pH close to the pI of the emulsifier can reduce the electrostatic interactions by reducing the number of ionized groups and hence reducing the surface charge density. Increasing the ionic strength by increasing the concentration and valency of ions (n_{0i} and z_i in Equation 1.2) reduces the Debye screening length, hence reducing the strength of electrostatic repulsion between emulsion droplets through the electrostatic screening effect (Figure 1.3). The electrostatic screening effect is the accumulation of counter-ions around the surface. The decreased thickness of the double layer results in weaker electrostatic repulsion and there is more potential for the droplets to flocculate.

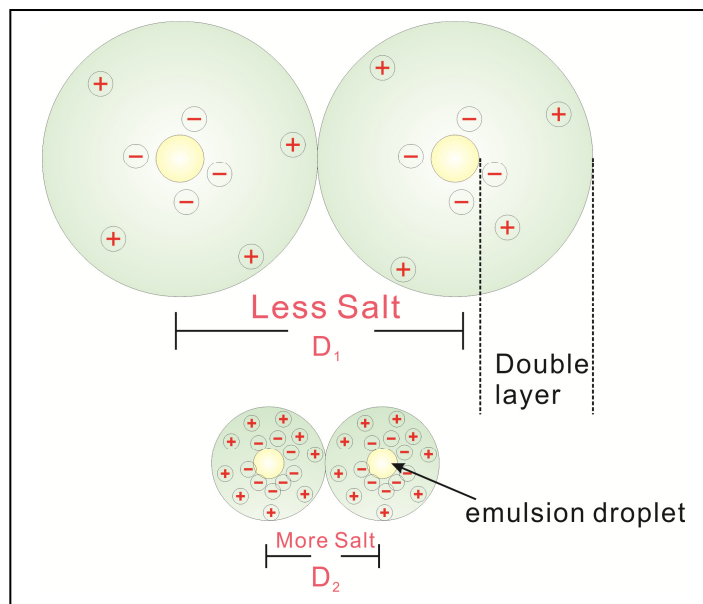


Figure 1.3: The electrostatic screening effect of salt addition on the double layers of charged emulsion droplets. The separation distance between two emulsion droplets can be significantly reduced by salt addition ($D_2 < D_1$) due to the decrease in the double layers, leading to weaker electrostatic interactions. Adapted from⁶¹

1.2.2.4 Steric interactions

Steric interactions between emulsion droplets are strong repulsive forces arising from overlap and compression of the interfacial layers when two droplets approach each other closely (Figure 1.4).¹⁹ When two emulsion droplets surrounded by steric interfacial layers approach each other, the overlap of the protruding segments of the interfacial layers causes a significant reduction in the conformational entropy of these segments, leading to strong repulsion between the two droplets (Figure 1.4). The overlap of the polymeric segments as two emulsion droplets approach each other induces an osmotic pressure gradient, which arises because of a local increase in the concentration of the polymeric segments in the narrow gap between the two droplets. This osmotic gradient pressure draws water from the bulk phase into the gap, thus preventing further approach of the droplets (Figure 1.4).

The strength of the steric interactions between emulsion droplets depends on increase in the thickness and density of the steric interfacial layers, which are determined by the emulsifier type and concentration.¹⁹ An emulsifier adsorbs at the droplet surface in a certain conformation in order to provide sufficient steric stabilization. It must have some segments that can strongly anchor the emulsifier at the droplet surface and other segments that protrude significantly into the aqueous phase (Figure 1.4). Flexible polymer emulsifiers often adopt this conformation and form thick interfacial layers at the droplet surfaces, providing effective steric stabilization (Section 1.3.2).¹³ In contrast, compact globular proteins lack the polymeric segments that can protrude into the aqueous phase and thus generally form relatively thin layers (Section 1.3.2).¹³

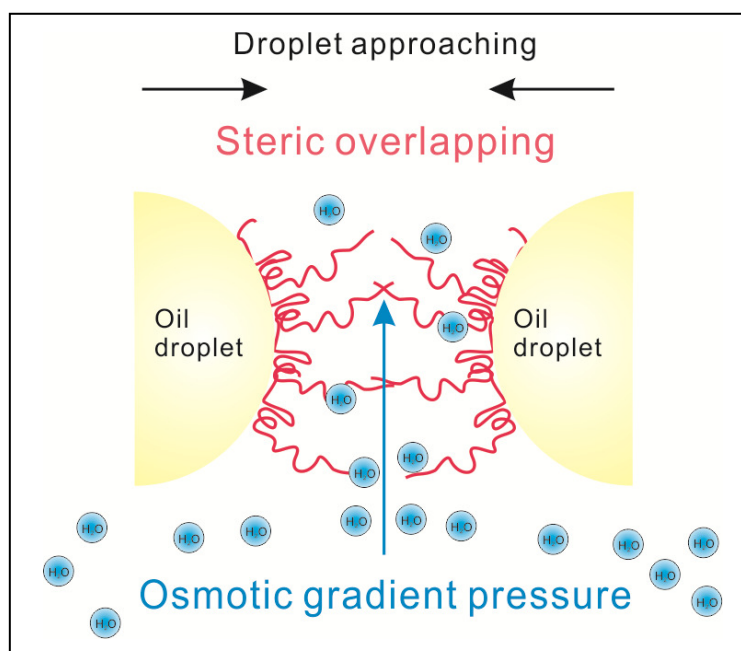


Figure 1.4: Steric interactions and the osmotic gradient pressure between the steric interfacial layers at the droplet surfaces. Adapted from¹²

Steric interactions and electrostatic interactions are the most common stabilizing mechanisms in food emulsions.^{12, 19} Steric interactions have one principal advantage over electrostatic interactions in that they are less sensitive to pH and ionic strength.^{57, 59, 60, 62} Electrostatic interactions can be reduced or screened by altering pH and increasing ionic strength (Section 1.2.2.3). In comparison, steric interactions are fairly insensitive to pH and ionic strength, unless the thickness of the steric layer is affected by pH and ionic strength.^{57, 62-65}

1.2.3 Physical stability

An oil-in-water macroemulsion is not thermodynamically stable but can be kinetically stable for a long period of time (Section 1.2.1). However, the kinetic stability of an emulsion can change with time due to a number of physical mechanisms. Understanding these mechanisms and the factors controlling them are important for identifying effective strategies to improve emulsion stability. Physical instability of emulsions involves changes in the spatial distribution of the emulsion droplets and the most common mechanisms are creaming/sedimentation, flocculation and coalescence (Figure 1.5). Two or more of these mechanisms may occur in an emulsion at the same time. The type of mechanisms that occur depends on the properties of the emulsion droplets, as well as environmental conditions, such as temperature, pH and ionic strength. This section summarizes the physical mechanisms of creaming/sedimentation, flocculation and coalescence.

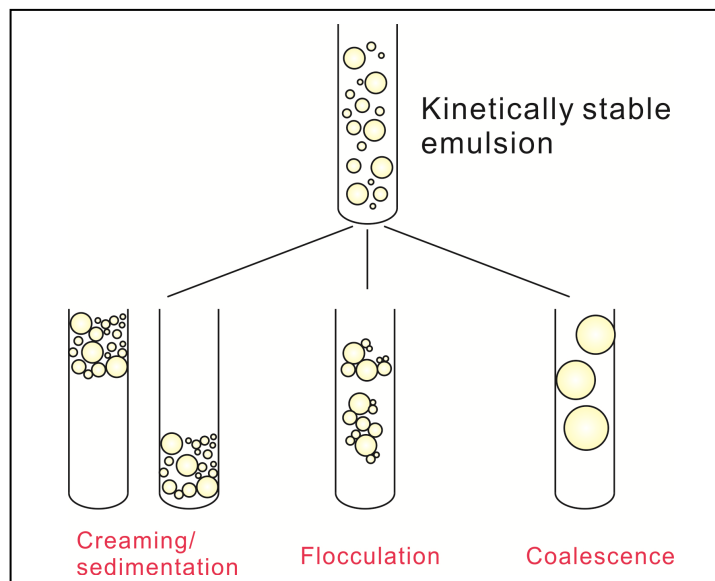


Figure 1.5: Schematic processes of physical instability of emulsions. Emulsion droplets may undergo creaming/sedimentation, flocculation and/or coalescence.

1.2.3.1 Creaming/Sedimentation

Creaming and sedimentation are gravitational separations due to the fact that oil droplets in an emulsion have a different density to that of the liquid surrounding them. Creaming refers to the upward movement of the oil droplets against gravity due to the fact that their density is lower than

the surrounding aqueous phase (Figure 1.5). Conversely, if the droplets have a higher density than the aqueous phase, sedimentation occurs as they move downward (Figure 1.5). The model emulsions used in the studies in this thesis contain oil droplets that have a lower density than the aqueous phase and hence only the creaming instability is introduced here. An emulsion that undergoes creaming results in a cream layer rich in oil droplets on top of a droplet-depleted bottom layer. The cream layer is more optically opaque and more viscous than the bottom layer (serum). Creaming is generally a reversible process and the droplets in the cream layer can be re-dispersed into the continuous phase by gentle shaking. However, the droplet-rich cream layer promotes flocculation (Section 1.2.3.2) and coalescence (Section 1.2.3.3) of droplets in close contact, which can be irreversible.

The physical basis of creaming is explained by Stokes law;

$$v = \frac{2gr^2\Delta\rho}{9\eta_0} \quad (1.3)$$

where v is the creaming velocity, g is acceleration due to gravity, r is the radius of the droplet, $\Delta\rho$ is the density difference between the oil phase and the aqueous phase and η_0 is the viscosity of the aqueous phase. According to Stokes law, the rate of creaming is controlled by three factors: the density difference between the oil phase and the continuous aqueous phase, the droplet size and the viscosity of the aqueous phase. Reducing the density difference decreases the rate of creaming. Increasing the viscosity of the aqueous phase is the most common method of controlling creaming in the food industry and it can be achieved by adding thickening agents such as hydrocolloids and polysaccharides.⁶⁶⁻⁷⁰ Decreasing the size of the droplets also reduces the rate of creaming. The size of the oil droplets in an emulsion is controlled by the emulsification condition and more importantly the ability of the emulsifier to lower the interfacial tension.

Stokes law can only be strictly applied to an isolated rigid spherical particle suspended in an ideal liquid and to dilute emulsions.¹⁹ In practice, droplet creaming may be controlled by other factors. The droplet concentration of an emulsion is another factor affecting the creaming velocity. An emulsion with a high droplet concentration has a lower creaming velocity (v) compared to an emulsion with a low droplet concentration due to the close packing of the droplets, which increases the viscosity (η_0) of the continuous phase. The final thickness of the cream layer also depends on the initial droplet concentration and the effectiveness of the droplet packing.^{12, 19}

1.2.3.2 Flocculation

Flocculation refers to the process whereby two or more droplets approach together and become associated with each other without losing their individual structural integrity (Figure 1.5). The process of droplet flocculation in emulsions originates from two factors: the collision

frequency and the collision efficiency. The dominant mechanisms contributing to the collision frequency in droplet flocculation include Brownian motion, gravitational separation and applied mechanical forces.¹⁹ When there is no external mechanical force, the collision frequency decreases as the viscosity of the continuous phase increases and also as the velocity of the droplets due to gravity decreases, both of which retard droplet flocculation.

The major interactions contributing to the collision efficiency in droplet flocculation include van der Waals forces (which are attractive), electrostatic and steric interactions (which are repulsive) between emulsion droplets (Section 1.2.2). Depending on the type of emulsifier adsorbed at the droplet surfaces, other interactions, such as hydrophobic interactions when globular proteins are employed as the emulsifier, may also become important in influencing the rate of flocculation. A net attractive force accelerates the rate of flocculation whereas a net repulsive force retards the flocculation process. Therefore, an effective method to control droplet flocculation in emulsions is to increase the repulsive interactions between the droplets.

Two other types of flocculation can exist in emulsions and they are bridging and depletion flocculation. Bridging flocculation occurs due to the presence of biopolymers that can adsorb to the droplet surfaces.⁷¹⁻⁷⁴ When sufficient attractive forces exist between these biopolymer molecules, the formation of bridges between two or more droplets is induced, promoting bridging flocculation. Depletion flocculation occurs due to the presence of colloidal particles in the continuous phase, such as biopolymers and surfactant micelles.^{73, 75-77} Due to steric constraints, these particles are excluded from the narrow gap between emulsion droplets, which creates an osmotic pressure gradient as these particles draw water from the narrow gap into the continuous phase to decrease the high local concentration of these particles. This osmotic effect manifests itself as an attractive force, causing depletion flocculation.

1.2.3.3 Coalescence

Coalescence refers to the process whereby two or more droplets merge together to form a single larger droplet and generally occurs in creamed and/or flocculated emulsions (Figure 1.5). In an emulsion, coalescence accelerates creaming of the oil droplets and eventually leads to a visible oil layer on top of the liquid, which is sometimes called 'oiling off'. Coalescence is an irreversible process, which drives an emulsion toward its thermodynamically stable state due to the reduction in the contact area between oil and water.

Our understanding of the rate and mechanism of coalescence is much less developed compared to gravitational separations and flocculation because coalescence is highly dependent on the nature of the emulsifier used to stabilize the emulsion. In general, coalescence occurs when the

thin liquid film separating the droplets in creamed and/or flocculated emulsions becomes thinner and eventually ruptures. The stability of the thin liquid film depends on the following factors:

- 1) The capillary pressure, which causes drainage, thinning and eventual rupture of the liquid film. The capillary pressure arises from the interfacial tension and the interfacial curvature of the droplets. Lowering the interfacial tension and increasing the droplet size destabilizes the thin liquid film.¹²
- 2) Colloidal interactions between emulsion droplets, which are controlled by the properties of the interfacial layer as well as the prevailing environmental condition (temperature, pH and ionic strength).¹⁹ Major interactions contributing to the rate of coalescence include van der Waals interactions (negative contribution), electrostatic and steric interactions (positive contribution) between emulsion droplets (Section 1.2.2).
- 3) Hydrodynamic interactions between emulsion droplets, which are controlled by rheological properties of the continuous phase and viscoelastic properties of the interfacial layer.^{12, 19} The rheology of the continuous phase influences the rate of the thin liquid film drainage. When the liquid film drains below a critical thickness, hydrodynamic forces can cause ripples in the film, leading to formation of holes and eventual rupture of the film. A highly viscoelastic and thick interfacial layer formed by adsorption of proteins rather than small-molecule surfactants as the emulsifier can highly resist the formation of ripples and holes and thus film rupture.
- 4) Viscosity of the continuous phase, which can influence the collision frequency of the droplets (Section 1.2.3.2). Increasing the viscosity of the continuous phase retards droplet movement and thus the rate of coalescence.

There are many strategies that can control droplet coalescence, such as varying aqueous phase conditions to prevent the droplets from approaching each other, lowering the interfacial tension and increasing the thickness and viscoelasticity of the interfacial layer. Milk proteins adsorbed at oil-water interfaces of emulsions are good examples of emulsifiers used to resist droplet coalescence. For instance, certain segments of β -casein adsorbed at the surface of the oil droplet can protrude into the aqueous phase and impart steric stability by increasing the thickness of the interfacial layer (Section 1.4.3), thereby slowing droplet coalescence considerably.

1.3 Protein adsorption at oil-water interfaces of emulsions

Many proteins are surface-active molecules due to their amphiphilic nature. They can adsorb to oil-water interfaces of emulsions, reduce the interfacial tension and provide repulsive interactions by forming an interfacial layer at the droplet surface.^{12, 13, 53} Repulsive interactions between the interfacial layers (Section 1.2.2) play a major role in controlling the physical stability

of an emulsion (Section 1.2.3). Therefore, understanding the properties of the interfacial layers of proteins at the droplet surfaces is a major focus in emulsion science. The purpose of this section is to give an overview of the molecular forces and structures of proteins in solution and proteins adsorbed at oil-water interfaces, with a focus on the characterization of the interfacial structure.

1.3.1 Molecular forces and structures of proteins in solution

Proteins have unique three-dimensional (3D) structures dictated by their amino acid sequences. The process of folding from an initially unfolded chain of amino acids (the primary structure) into a well-defined 3D structure (the tertiary structure) is called protein folding.⁷⁸⁻⁸¹ This defined 3D structure, i.e. the native structure of a protein, generally corresponds to the global minimum state of free energy. The native structure of a protein is a consequence of a delicate balance between all driving and opposing molecular forces, including electrostatic forces, ion-pairing, van der Waals interactions, hydrogen bonding, the hydrophobic effect and the conformational entropy.⁷⁸⁻⁸⁰ Studies over the last few decades have identified the dominant driving and opposing forces in protein folding.⁷⁸⁻⁸⁰

The hydrophobic effect is the dominant driving force in protein folding.^{52, 78, 82} The hydrophobic effect, in the context of protein folding, refers to the tendency of the non-polar regions of a protein to come together so that the thermodynamically unfavourable contact with water is decreased. One of the most prominent manifestations of the hydrophobic effect is the hydrophobic core present in globular proteins where the non-polar residues are clustered and buried away from water. This core is the thermodynamic consequence of the hydrophobic effect. Most of the polar and charged residues are located at the surface of the protein and are exposed to water. The hydrophobic effect drives the initial step of the folding of a protein, resulting in a relatively compact state.⁷⁸ This initial collapse of the chain into compactness strongly favours internal organization, i.e. the formation of secondary structures,⁷⁸ which are regularly repeating structures. Three major secondary structures are the α -helix, the β -sheet and the β -turns. The α -helix is a coiled structure stabilized by hydrogen bonding between the CO group of each amino acid and the NH group of the amino acid that is situated four residues ahead in the sequence (Figure 1.6). The β -sheet is a pleated structure formed by hydrogen bonding between the NH group and the CO groups on adjacent β -strands (Figure 1.6). Hydrogen bonding among the backbone amide and carbonyl groups plays an important role in the formation of the α -helix and the β -sheet (Figure 1.6).^{78, 83}

Conformational entropy is the dominant opposing force in protein folding.^{78, 84} Conformational entropy is related to the number of possible conformations that the polypeptide chain can adopt in solution. There is local entropy (translational, rotational, vibrational) and non-local entropy (the excluded volume effect).⁷⁸ The excluded volume effect refers to the impossibility that two chain segments can simultaneously occupy the same volume of space.⁸⁴ After the initial

folding of a protein which is driven by the hydrophobic effect, many segments of the amino acid side chains and the backbone become extremely compact and have limited volume of space to occupy.⁸⁵ Therefore, there are relatively few ways the chain can adopt in its folded state due to severe steric constraints. While the hydrophobic effect leads to the compactness of a globular protein with the hydrophobic core, the severe steric constraints and the hydrogen bonding are largely responsible for its unique internal organization comprised of a combination of secondary structures. The two dominant forces, i.e. the hydrophobic effect and the conformational entropy, eliminate a considerable amount of conformational possibilities and together with all the other types of interactions give a protein its defined native structure.

Understanding the dominant molecular forces in protein folding facilitates the explanation of denaturation mechanisms. Protein denaturation is a process of conformational change at quaternary, tertiary and secondary structure levels by application of external stresses or denaturants.⁸⁶ There are many denaturing conditions that can induce protein conformational change to various degrees, such as high and low temperatures, high pressure and high concentrations of urea and guanidine hydrochloride.^{87, 88} The unfolding mechanism associated with each denaturing condition can be explained by the relative contribution of each of the molecular forces involved in protein folding. Denaturation at high temperatures occurs due to the large gain of conformational entropy so that the hydrogen bonding and hydrophobic interaction are disrupted.^{78, 87, 88} The consequence is the unfolding of the tertiary structure and the loss of the secondary structure with exposure of the hydrophobic regions of the protein, which drives protein aggregation to avoid contact with water. Cold denaturation of proteins occurs because the hydrophobic interaction is weakened with decreased temperatures.^{89, 90} Denaturants such as urea and guanidine hydrochloride cause protein denaturation by forming hydrogen bonds with polar residues, thus destroying the secondary and tertiary structure.^{78, 91}

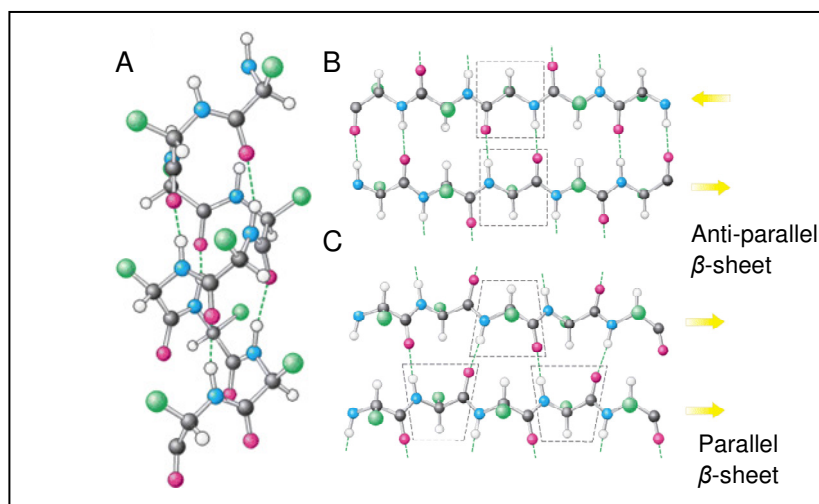


Figure 1.6: A ball-and-stick representation of secondary structures. (A) α -helix; (B) anti-parallel β -sheet; (C) parallel β -sheet. The dashed, green lines depict hydrogen bonds between the backbone NH and CO groups. Adapted from⁹²

1.3.2 Interfacial properties of proteins

Protein adsorption at oil-water interfaces results in an interfacial layer, which is the narrow region that separates the oil phase from the aqueous phase (Figure 1.1). In protein-stabilized model emulsions, the interfacial layer consists only of the protein molecules and its properties determine the physicochemical and the stability characteristics of the emulsions.^{16, 19} These interfacial properties include:

- 1) The interfacial tension (γ), which is related to the free energy stored in an oil-water interface.¹⁹ Reducing the interfacial tension is crucial for emulsion formation and can be achieved by adsorption of proteins as emulsifiers (Section 1.2.1). The rate of reduction in the interfacial tension is related to the molecular flexibility and hydrophobicity of a protein. Proteins that are more flexible and hydrophobic can change their structures and conformations more readily and reduce the interfacial tension more rapidly than more rigid and polar proteins.⁹³⁻⁹⁸
- 2) Interfacial electrical characteristics, such as the surface charge density and the surface potential, which play an important role in the electrostatic interactions (Section 1.2.2.3). Many proteins change their surface charge density and potential once they adsorb and reorientate their charged residues at oil-water interfaces under the right environmental condition, which then determines the strength of the electrostatic interactions in emulsions.
- 3) Interfacial rheological properties, such as the interfacial elasticity and the interfacial viscosity. The interfacial rheology describes the behaviour of mechanical and flow properties of the interfacial layer. The rheological properties of the interfacial layer influence the formation and the physicochemical characteristics of emulsions.^{13, 28, 99-102} The interfacial rheology is governed by the interfacial structure of the protein layer. Generally, globular proteins upon adsorption to oil-water interfaces form an interfacial layer with high elasticity and viscosity.^{13, 28, 99-102}

A very important interfacial property of the adsorbed protein layer is the interfacial structure. In this thesis, the interfacial structure of a protein adsorbed at the oil-water interface of emulsions refers to the thickness and density of the adsorbed layer and the molecular conformation (the secondary and the tertiary structure). The interfacial structure of proteins determines other interfacial properties, the colloidal interactions and the physicochemical and stability characteristics of emulsions.^{13, 15, 19, 100}

The interfacial structure of a protein differs largely from its native structure. In solution, a protein rotates freely and has a characteristic native structure determined by all molecular forces (Section 1.3.1). At oil-water interfaces of emulsions, it is widely thought that a protein rearranges

its structure to facilitate thermodynamically favourable interactions between the hydrophobic regions of the protein and the interface and to reorientate the hydrophilic regions toward the aqueous phase. The major driving force of adsorption-induced structural changes in proteins is therefore the hydrophobic effect. The intrinsic property of a protein, such as its sequence, size, molecular flexibility and surface hydrophobicity can influence the interfacial structure.^{13, 103-105} For example, flexible proteins such as caseins tend to form a thick interfacial layer with long hydrophilic regions protruding to the aqueous phase (the so-called ‘tail’ and ‘loop’) and the hydrophobic regions located at the interface (the so-called ‘train’) (Figure 1.7).¹³ In contrast, rigid globular proteins tend to form a thin and compact interfacial layer (Figure 1.7).¹³ A more detailed review of the interfacial structure of three milk proteins is given below (Section 1.4)

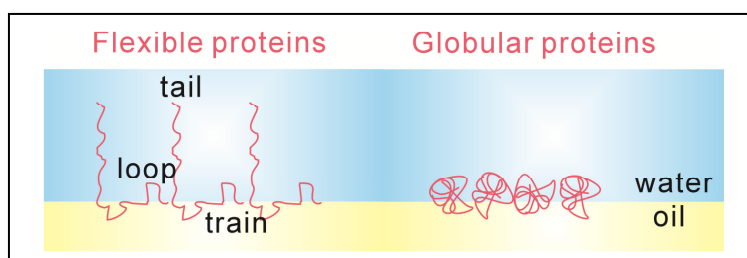


Figure 1.7: A schematic representation of the interfacial structure of flexible and globular proteins at the oil-water interface. Adapted from¹⁹

1.3.3 Characterization of protein interfacial structure

The interfacial structure of proteins adsorbed at oil-water interfaces of emulsions has drawn much attention over the last couple of decades. However, some colloidal properties of an emulsion system, such as the light absorbance and scattering, can prevent biophysical characterization, particularly with spectroscopic techniques. Therefore, many studies characterize protein interfacial structure using model hydrophobic interfaces including lipid-water interfaces of liposomes, solid-liquid interfaces and air-liquid interfaces. Biophysical techniques employed for characterization of protein interfacial structure include scattering techniques for thickness measurements, ellipsometry and reflectometry for thickness and concentration measurements, spectroscopic techniques for conformational change measurements and microscopy for structural organization measurements. This section reviews five major techniques, which are relevant in this thesis, for characterization of the protein interfacial structure at oil-water interfaces and other model hydrophobic interfaces.

1.3.3.1 X-Ray/Neutron reflectometry

X-Ray/Neutron reflectometry is frequently used to measure the thickness and density distribution profile of the protein layer adsorbed at the air-water interface,^{98, 103, 106-110} the oil-water interface^{111, 112} and the solid-water interface.¹¹³⁻¹¹⁶ An X-ray/neutron reflectometry instrument

requires specialized equipment with an X-ray/neutron source. In a reflectometer, a beam of X-rays/neutrons is directed onto and reflected from a layer at low incident angles (Figure 1.8). The reflectivity profile is calculated from the refractive index (n , normal to the interface), which is related to the scattering length density (ρ);

$$n = 1 - \frac{\lambda^2 \rho}{2\pi} \quad (1.4)$$

where λ is the wavelength. The calculated reflectivity profile of the measured surface is then analysed using various computational methods, such as single-layer model fitting and multi-layer model fitting. X-Ray/neutron reflectometry studies have provided valuable information on the thickness and density distribution profile of the adsorbed protein layer (Sections 1.3.2 & 1.4). For example, characteristic interfacial structures formed by flexible proteins and rigid globular proteins have been observed (Figure 1.7).^{103, 109, 112, 114}

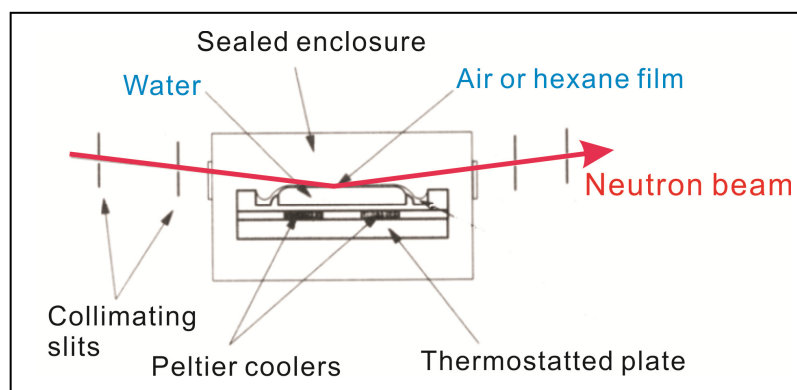


Figure 1.8: A schematic representation of neutron beam passing into a reflectometer cell. Adapted from¹¹²

1.3.3.2 Dual polarization interferometry

Dual polarization interferometry (DPI) is a recently developed optical sensing technique, which allows simultaneous measurements of various structural properties of the protein layer adsorbed at a solid-water interface in real time. DPI technology relies on two polarization modes: the transverse magnetic (TM) and transverse electric (TE) polarization modes. The sensor chip is a dual-slab waveguide, which consists of an upper sensing waveguide and a lower reference waveguide (Figure 1.9). Polarized laser light travels along the sensor chip, generates the evanescent waves in the sensing region or cladding layers and produces interference fringe patterns (Figure 1.9). Using Maxwell's equations, several opto-geometrical properties of the adsorbed protein layer including the refractive index, mass, thickness and density of the adsorbed protein layer are obtained. DPI is emerging as a powerful technique for characterization of protein adsorption to solid-water interfaces¹¹⁷⁻¹²³ as well as protein interactions with solid-supported membrane bilayers.¹²⁴⁻¹²⁸ To date, few studies have employed DPI to study protein adsorption at hydrophobic

solid-water interfaces mimicking oil-water interfaces. With the availability of functionalized hydrocarbon sensing chips, DPI is a bench-top technique to measure the thickness and density of the protein layer adsorbed at hydrophobic solid-water interfaces.

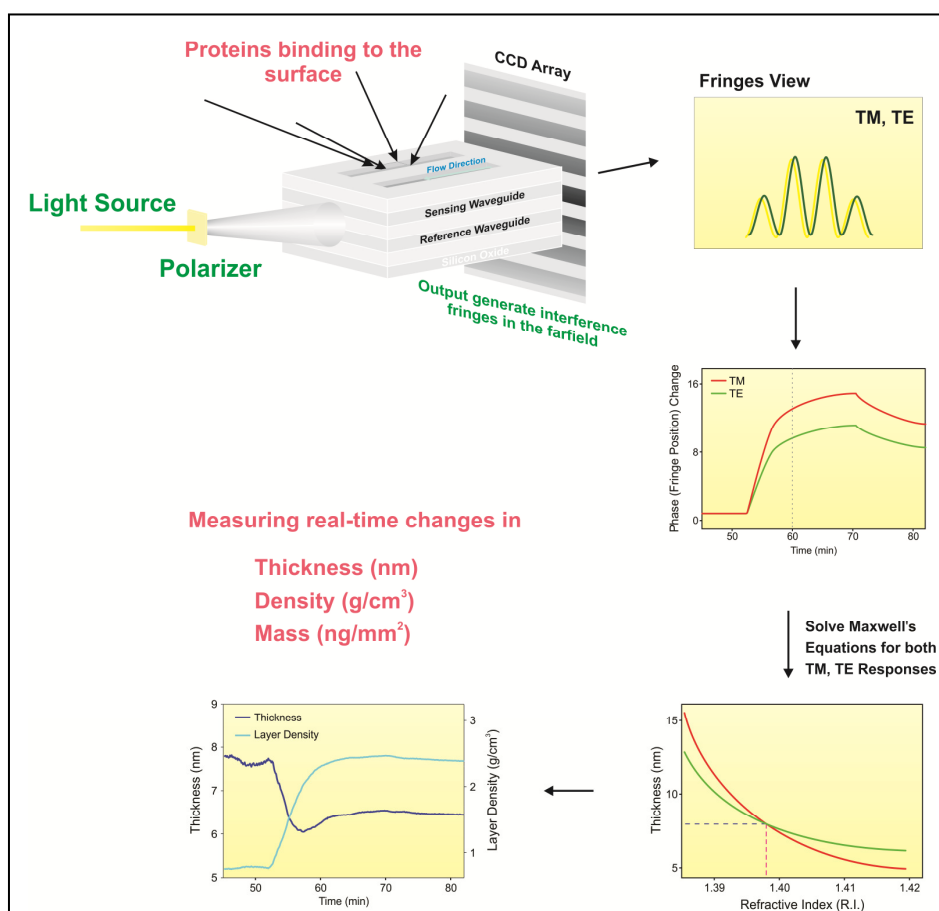


Figure 1.9: A schematic representation of DPI technique. With laser light shines through the waveguide, the protein adsorption event changes the refractive index and influences the positions of interference fringe patterns. The responses of TM and TE give a range of thickness and refractive index values respectively. By overlaying the two calculated ranges, a unique solution for the surface condition is obtained. Adapted from¹²⁴

1.3.3.3 Fourier transform infrared spectroscopy

Fourier transform infrared (FTIR) spectroscopy is an established tool to measure protein secondary structure. FTIR measures the infrared absorption of proteins in the amide I region (1580-1720 cm^{-1}) and amide II region (1510-1580 cm^{-1}), which are sensitive to protein secondary structure motifs. The frequency of the amide I and II absorptions are influenced by the strength of any hydrogen bonds involving the CO and NH groups of proteins. The α -helix and the β -sheet are associated with characteristic hydrogen bonding patterns (Figure 1.6) and therefore give rise to characteristic FTIR spectra. The subsequent data analysis of FTIR spectra thus reveals information about protein secondary structure in a certain environment. Generally, the α -helix absorbs from 1648-1660 and 1545-1551 cm^{-1} in the amide I and II regions respectively; the β -sheet absorbs from

1625-1640 and 1521-1525 cm^{-1} .^{129, 130} In comparison to far-UV circular dichroism (CD) spectroscopy, the major strength of FTIR lies in its ability to allow measurements of protein secondary structure in a variety of environments such as aqueous solution, hydrated films and turbid emulsions. The light scattering arising from emulsions does not cause interference with the FTIR signal and FTIR has thus been used to measure the conformation of proteins adsorbed at oil-water interfaces (Section 1.4).¹³¹⁻¹³⁴ However, one must keep in mind the complexity of the FTIR spectra of proteins, which means that the assignment of the secondary structure content is often an approximation. Unique assignments of individual secondary structures are often difficult because a complex protein structure generally produces an absorption profile of many overlapping peaks and shoulders (Figure 1.10).^{129, 130}

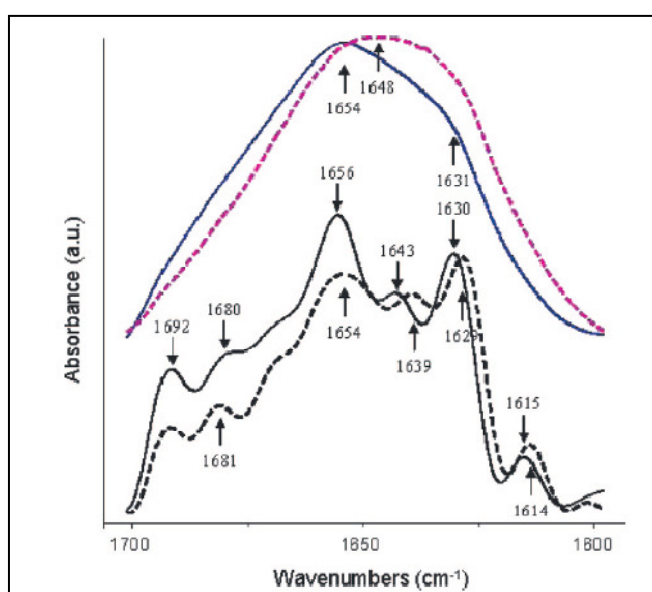


Figure 1.10: An example of original and deconvoluted FTIR spectra of whey proteins in solution (dashed line) and in emulsions (solid line). Reproduced from¹³³

1.3.3.4 Tryptophan emission fluorescence spectroscopy

Tryptophan emission fluorescence spectroscopy is widely used to study protein conformational changes. In a fluorimeter, light excites a sample to a high energy state and then the emission of the absorbed light from the sample is recorded. Aromatic amino acids are intrinsic fluorophores and tryptophan is by far the most useful fluorescent probe for protein folding and conformational change.¹³⁵ The emission energy of tryptophan is highly sensitive to the hydrophobicity of its local environment (Figure 1.11). At an excitation wavelength of around 295 nm, tryptophan buried in the hydrophobic core of a protein or incorporated in a hydrophobic environment emits at wavelengths with a maximum around 335 nm (Figure 1.11).¹³⁵⁻¹³⁹ In comparison, the emission of tryptophan exposed to an aqueous solvent, for example due to denaturation of a globular protein, is red-shifted towards a higher wavelength with a maximum

around 355 nm (Figure 1.11).^{136, 137, 140-143} The emission spectra therefore provide useful information about the local environment of tryptophan, which can reflect protein tertiary structural change.

In normal fluorescence spectroscopy, light excites the sample at an incident angle of 90°. A considerable amount of light is absorbed or scattered by an emulsion sample and thus results in poor signals. In order to study protein conformational change in emulsions, front-face fluorescence spectroscopy has been employed and the results have shown adsorption-induced conformational changes in proteins.¹⁴⁴⁻¹⁴⁶ With the incidence angle set to 56° in a front-face set-up, light does not need to penetrate deeply into the sample and a good signal can be obtained. The advantage of front-face tryptophan fluorescence spectroscopy is that some information about the tertiary folding of proteins adsorbed at oil-water interfaces of emulsions can be obtained in a label-free, non-invasive environment. The major limitation is that fluorescence spectroscopy only reveals information about the local environment surrounding the tryptophan residues of a protein, which is only a small part of the molecule. The interpretation of tryptophan fluorescence signal changes should thus be made carefully in terms of the contribution from molecular conformational changes. It is important to have other spectroscopic techniques for comparison when relating the modifications in the local environment of tryptophan to protein conformational changes at the tertiary structure level.

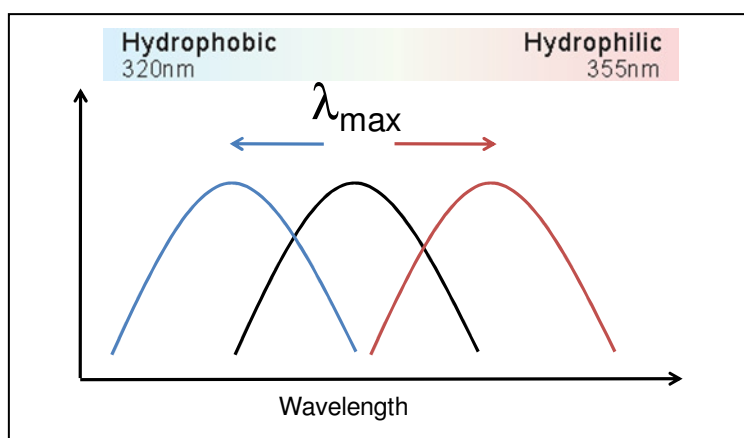


Figure 1.11: A schematic representation of how tryptophan emission (λ_{\max}) could be affected by the hydrophobicity of its immediate environment.

1.3.3.5 Circular dichroism spectroscopy

Circular dichroism (CD) spectroscopy is a spectropolarimetry technique used to measure protein secondary and tertiary structure in solution. A CD instrument measures the difference in the absorbance of left-handed polarized and right-handed polarized light by an optically active substance. Proteins are optically active molecules that can generate CD signals due to the presence of peptide bonds and aromatic amino acids.¹⁴⁷⁻¹⁴⁹ In the far-UV region (170-260 nm), the peptide bond is the major chemical entity contributing to the CD signal and each type of the secondary

structure gives rise to a CD spectrum of a characteristic shape and magnitude (Figure 1.12).¹⁴⁹ The far-UV CD spectrum can be analysed using various mathematical methods, such as SELCON,^{150, 151} CONTIN¹⁵² and CDSSTR,¹⁵³ to obtain quantitative assignment of the secondary structural content in percentage.

The aromatic amino acids contribute to the CD signal in the near-UV region of 260-320 nm (Figure 1.12).^{149, 154} The near-UV CD spectrum depends on the number of aromatic residues present and the nature of their local environments. The major advantage of CD is that one can obtain information about the overall structure of a protein in different UV regions. CD has been used to quantitatively estimate the secondary structure,^{151, 153, 155, 156} to measure the conformational change at the tertiary structural level^{139, 141, 157-159} and to monitor the stability of a protein under defined physical stresses such as extreme pHs and elevated temperatures.^{94, 97, 160}

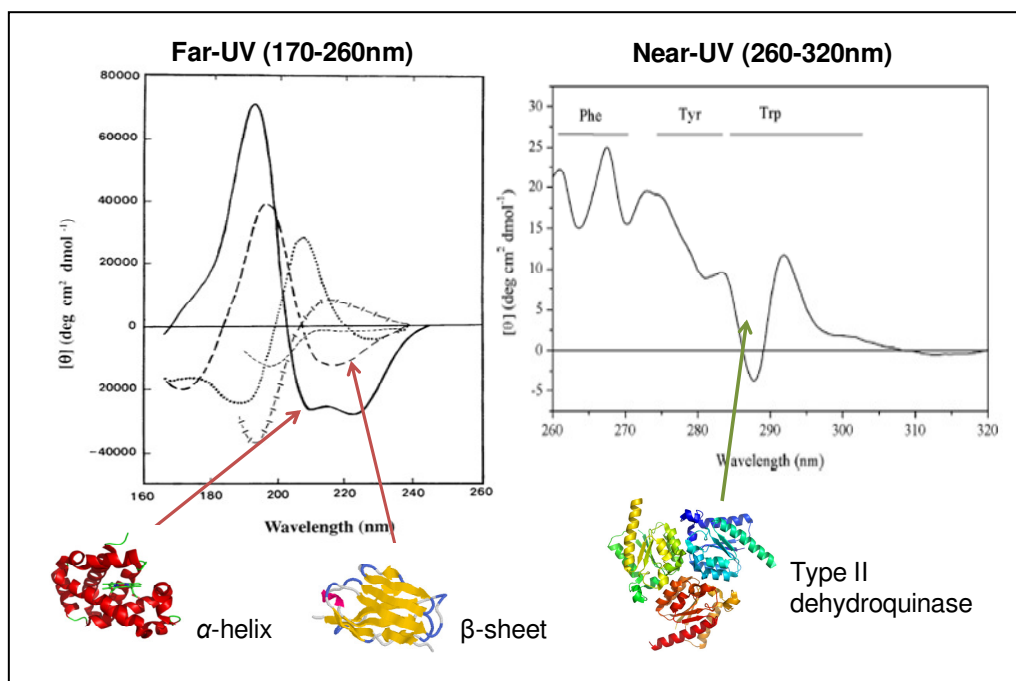


Figure 1.12: An illustration of the information on the secondary and tertiary structure of a protein that can be derived from far-UV and near-UV CD spectra. The far-UV CD spectra can reveal information on the secondary structure of a protein. A certain secondary structure motif, such as the α -helix (solid line in far-UV CD) and the β -sheet (dashed line in far-UV CD), generates a characteristic shape and magnitude of the CD signal in the far-UV region. The near-UV CD spectra can reveal information on the tertiary structure (folding of globular proteins) depending on the number of aromatic residues and their immediate hydrophobic/hydrophilic environments. Adapted from¹⁴⁹ Type II dehydroquinase structure is generated by Pymol based on PDB file 2xd9.¹⁶¹

CD signals can be severely impacted on by light scattering arising from emulsion droplets. When the light passes through an emulsion sample that scatters a large amount of light, there is significant decrease in the intensity of the measured CD spectrum and hence a decrease in the signal-to-noise ratio. As a consequence, there have been relatively few studies that use CD to study

protein conformation at oil-water interfaces of emulsions. However, CD has been used in many studies to characterize the conformation of proteins adsorbed at surfaces of liposomes, latex or teflon beads that mimic oil-water interfaces of emulsions.^{139, 157, 162, 163}

A novel approach was developed to measure the secondary structure of proteins adsorbed at oil-water interfaces of emulsions by Husband et al. (2001).¹⁶⁴ By adding refractive index matching additives such as glycerol to make the refractive index of the aqueous phase the same as that of the oil phase, the resulting matched emulsion became optically transparent and allowed the measurement of emulsion samples using CD. This experiment has demonstrated conformational changes of globular proteins adsorbed at oil-water interfaces (Section 1.4.1).¹⁶⁴ De Jongh and his group have also developed an external reflection CD technique to study the interfacial conformation of proteins, but the technique is limited to planar air-water interfaces.^{105, 165, 166}

Synchrotron radiation circular dichroism (SRCD) spectroscopy has also emerged as a powerful tool which takes advantage of the strong intensity of the light available from synchrotron sources. SRCD produces high signal-to-noise spectra, extends the wavelength region that can be measured down to 160 nm and most importantly enables improved penetration of light into highly absorbing and turbid samples.¹⁶⁷⁻¹⁶⁹ For example, SRCD has been employed to study the secondary structure of membrane proteins in optically turbid media¹⁶⁹ and thus has shown great potential in application to other highly absorbing and turbid samples.

1.4 Interfacial structure and function of milk proteins in emulsions

Bovine milk proteins are widely used in food emulsions because they have excellent emulsifying and stabilizing properties.¹⁹ The two main classes of milk proteins are caseins and whey proteins (Figure 1.13). Caseins contribute approximately 80% total milk proteins and are defined as proteins that precipitate from raw skim milk by acidification to pH 4.6 at 20 °C. Proteins still soluble in the milk serum are referred to as whey proteins.^{170, 171} The heterogeneity of dairy proteins has long been recognized. Caseins are classified into four families, namely, α_1 -caseins, α_2 -caseins, β -caseins and κ -caseins. They vary in many aspects, including the primary structure, degree of phosphorylation, electrophoretic mobility and solubility.^{170, 171} The major components of whey proteins are β -lactoglobulin (β -Lg), α -lactalbumin (α -La), bovine serum albumin (BSA) and immunoglobulins.^{170, 171} Caseins and whey proteins have such different molecular characteristics that they exhibit a range of structural properties when adsorbed at oil-water interfaces of emulsions. This section aims to describe three milk proteins, β -Lg, α -La and β -casein, as examples to provide an overview on the current understanding of the interfacial structure and function of proteins adsorbed at oil-water interfaces of emulsions.

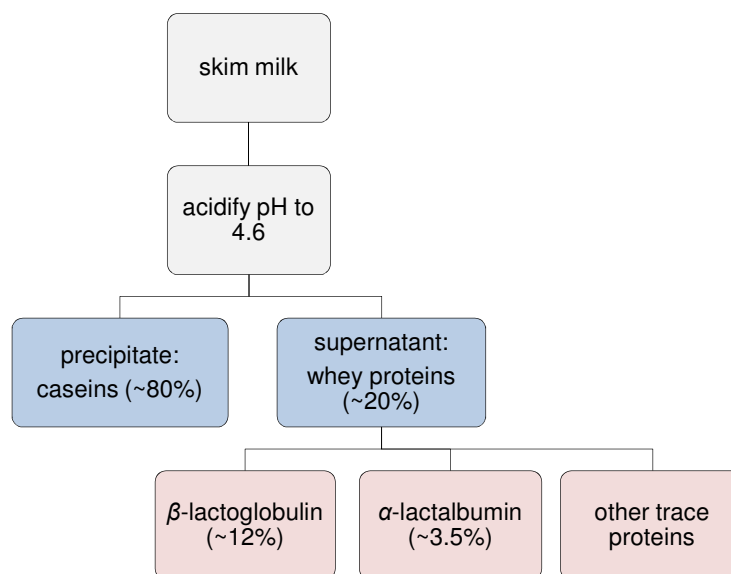


Figure 1.13: Composition of bovine milk proteins. Source from¹⁷¹

1.4.1 β -Lactoglobulin

β -Lactoglobulin (β -Lg) represents about 12% total milk proteins. It consists of 162 amino acids with a molecular mass of approximately 18 kDa. β -Lg exists as dimers of about 36 kDa in natural milk.¹⁷¹ There are two most common genetic variants of β -Lg, A and B, but many others exist.¹⁷¹ β -Lg contains five cysteine residues per monomer; four of the cysteine residues form two intra-molecular disulphide bonds (Cys₆₆-Cys₁₆₀ and Cys₁₀₆-Cys₁₁₉) and one cysteine (Cys₁₂₁) exists as one free thiol. The native structure of β -Lg in solution is well characterized by X-ray crystallography, FTIR and CD spectroscopy.^{131, 160, 163, 172-175} β -Lg is a compact globular protein that consists of nine anti-parallel β -sheets which wrap around to form a hydrophobic β -barrel with one long α -helix and four short 3_{10} helices on the outer surface (Figure 1.14). With respect to the secondary structure, though different methods and algorithms may give rise to a slight variation in the prediction, β -Lg has a very high level of ordered secondary structures with a large amount of the β -sheet structure (40-50%) and a small amount of α -helix (10-15%).^{139, 163, 174}

β -Lg is one of the most extensively studied proteins in the field of denaturation under various conditions. Understanding the effect of thermal treatment is crucial for controlling the interfacial function of β -Lg and the quality of food products containing β -Lg as an ingredient.^{22, 176-178} Thermal denaturation of β -Lg involves two major stages: unfolding and conformational change of the native protein followed by subsequent irreversible aggregation of unfolded molecules (Figure 1.15).¹⁷⁹ In the native state, the disulfide bonds and free thiol group (Cys₁₂₁) of β -Lg are buried and inaccessible to solvents. Subjecting β -Lg to heat at temperatures of 72 °C and above

exposes the free thiol, which can participate in inter-molecular sulfhydryl-disulfide exchange reactions,^{176, 179, 180} which together with hydrophobic interactions are responsible for the irreversible aggregation process. Recent studies on β -Lg thermal denaturation have focused on the early stages of aggregation using size exclusion chromatography and have identified the intermediate oligomers (dimers, trimers, tetramers) on the pathway to larger aggregates (Figure 1.15).^{176, 181-183}

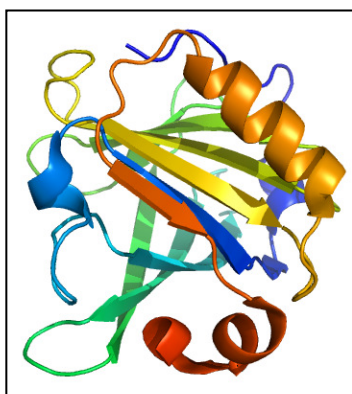


Figure 1.14: A representation of β -Lg crystal structure. Generated by Pymol based on PDB file 1bsy.¹⁷⁵

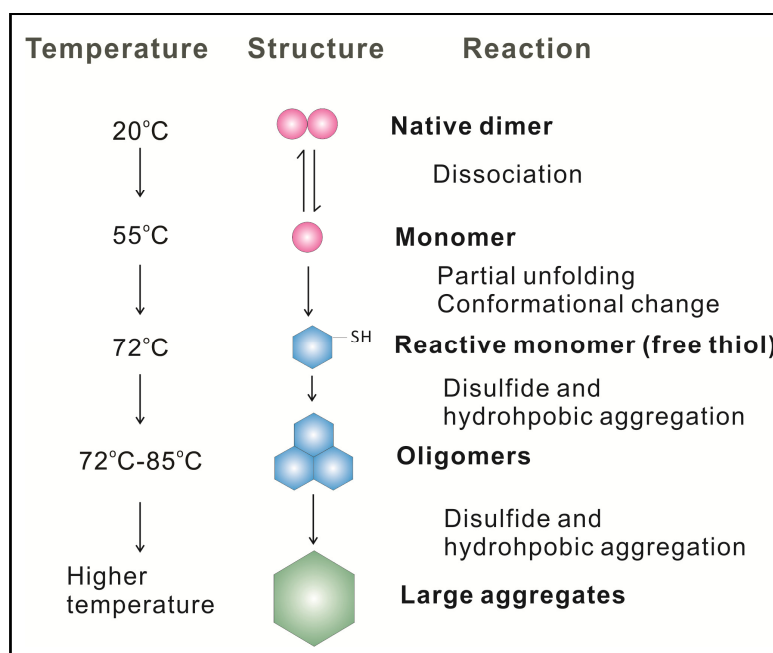


Figure 1.15: A schematic representation of the proposed mechanism of thermal unfolding and aggregation of β -Lg.

β -Lg can act as an emulsifier in reducing the interfacial tension of the oil-water interface and stabilizing the emulsion against droplet flocculation. In comparison to flexible proteins such as β -casein (Section 1.4.3), the rate of adsorption and lowering the interfacial tension by β -Lg is much slower,^{13, 96} which is attributed to the relatively low surface hydrophobicity of β -Lg. In general, β -Lg forms a densely packed thin monolayer of protein molecules adsorbed at the oil-water interface

(Figure 1.7).^{103, 109} Neutron reflectivity studies have revealed that β -Lg adsorbed at the air-water interface may undergo a slow reorientation and the layer thickness and surface coverage may gradually increase with time.^{103, 109} These results showed that following the slow structural reorganization of β -Lg adsorbed at the surface, the initial monolayer converted to a two-dimensional gel-like layer by non-covalent interactions (electrostatic, hydrophobic and hydrogen bonding).^{13, 27, 57, 100, 184-186} The two-dimensional gel-like layer of β -Lg exhibited highly viscoelastic properties which played an important role in emulsion stabilization.⁵⁷

Changes in the tertiary and secondary structure of β -Lg adsorbed at oil-water interfaces of emulsions or other hydrophobic interfaces have been studied using a variety of techniques, such as FTIR, front-face fluorescence and CD spectroscopy.^{131, 146, 163, 164, 187} It is widely considered that upon adsorption to oil-water interfaces, β -Lg undergoes a certain degree of unfolding as well as secondary structural change. However, contradictory results still exist mainly due to the light scattering problem from emulsion droplets. While FTIR studies showed that β -Lg lost some β -sheet structure upon adsorption to oil-water interfaces, the results differed as to whether the loss of the β -sheet structure was accompanied by a concomitant increase in the unordered structure or the ordered α -helical structure.^{131, 133, 146, 164} Attempts to study β -Lg conformation at oil-water interfaces with CD spectroscopy have been undertaken by mimicking oil-water interfaces.^{139, 163} For example, one study examined the conformational change of β -Lg in the presence of anionic dimyristoylphosphatidylglycerol (DMPG) lipid vesicles.¹³⁹ The insertion of β -Lg into the lipid-water interface induced an increase in α -helical structure.¹³⁹ As discussed above (Section 1.3.3.5), Husband et al. (2001) made a considerable advance by developing a refractive index matching method by adding glycerol to the emulsion.¹⁶⁴ They found that when adsorbed at oil-water interfaces β -Lg showed an increase in α -helix.¹⁶⁴ However, parallel FTIR experiments showed no change in α -helix but an increase in β -sheet structure for β -Lg adsorption to oil-water interfaces.¹⁶⁴ Another concern of refractive index matching method is that other reports have shown that a high concentration of glycerol may change the native structure of β -Lg at the first place.¹⁸⁸⁻¹⁹⁰ Overall, the conformation of β -Lg at oil-water interfaces of emulsions needs further examination by more sensitive techniques to achieve a better understanding of the mechanism of adsorption-induced conformational change.

Despite the lack of data on the conformation of β -Lg adsorbed at oil-water interfaces, the influence of heating and moderate ionic strength on β -Lg-stabilized emulsion stability has been well characterized using light scattering techniques and optical microscopy.^{29, 30, 53, 62} The main stabilizing mechanism in β -Lg-stabilized emulsions is electrostatic interactions (Section 1.2.2.3), which are provided by the negatively charged interfacial layer of β -Lg.^{29, 30, 53, 62} In the absence of

salt, β -Lg-stabilized emulsions prepared at neutral pH are resistant to flocculation due to the relatively strong electrostatic repulsion between the droplets.^{29, 30, 53, 62} Addition of NaCl before heating causes electrostatic screening (Section 1.2.2.3) and thus leads to extensive droplet flocculation, particularly when the emulsion is heated above 70 °C.^{29, 30, 62} This phenomenon is related to the combination of increased hydrophobic interactions and inter-molecular disulfide interchanges between β -Lg molecules adsorbed at different droplet surfaces.^{30, 57} In the absence of salt, emulsion droplets are relatively far apart and heating above the thermal denaturation temperature of 70 °C results in inter-molecular disulfide bonding between β -Lg molecules adsorbed on the same droplet. However, in the presence of salt, droplets are close together so that inter-molecular disulfide interchange occurs between β -Lg molecules adsorbed at different droplet surfaces, causing irreversible droplet flocculation.

1.4.2 α -Lactalbumin

α -Lactalbumin (α -La) is the second major whey protein. α -La is an important component of lactose synthase, which catalyses the biosynthesis of lactose.¹⁹¹ It is a small globular protein of 123 amino acids with a molecular mass of 14.2 kDa. X-ray crystallographic studies have shown that α -La is a globular protein with one large domain of three α -helices and one small domain of three anti-parallel β -sheets, which are connected by a calcium binding loop (Figure 1.16).^{192, 193} There are four disulfide bonds stabilizing the tertiary structure of α -La. The two domains are divided by a deep cleft and connected by two disulfide bonds (Cys₆₁-Cys₇₇ and Cys₇₃-Cys₉₁).^{171, 191} The cleft also contains a Ca²⁺ binding site.

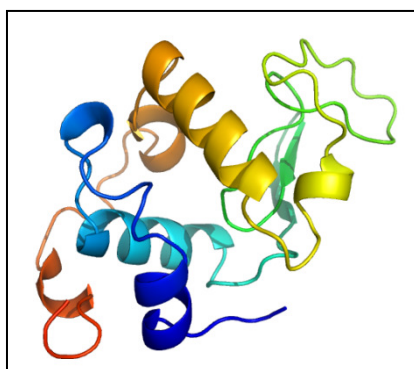


Figure 1.16: A representation of α -La crystal structure. Generated by Pymol based on PDB file 1hfx.¹⁹²

The four disulfide bonds and the lack of a free thiol in native α -La play an important role in the stability of α -La under denaturing conditions. At the secondary structure level, heating α -La can induce a conformational change at a lower temperature (~66 °C) than β -Lg (~73 °C).^{132, 179} However, α -La is more heat stable than β -Lg with respect to protein aggregation and polymerization.^{171, 179} When heated above 70 °C, α -La does not aggregate via the sulfhydryl-

disulfide interchange reaction due to the absence of free thiol.¹⁷⁹ However, α -La becomes more prone to heat denaturation in the presence of β -Lg than when it is heated alone.^{179, 182} The presence of the free thiol group of β -Lg triggers α -La to aggregate via sulfhydryl-disulfide interchange and to a lesser extent via hydrophobic interactions.^{179, 182}

α -La has attracted considerable attention as a classical example of a protein that adopts the molten globule state under certain conditions.^{137, 194-197} The molten globule state of a globular protein is an intermediate physical state on the folding pathway and can be defined as a protein conformational state with native-like secondary structure but lacking any defined tertiary structure.^{197, 198} α -La has the ability to form a molten globule state under a variety of conditions, such as at low pHs, at high temperatures, at a moderate concentration of denaturants and in its Apo (non-calcium bound) form.¹⁹⁷ Measurements of the environment of the buried aromatic residues in native α -La have revealed that α -La in its molten globule state is partially unfolded,^{94, 194, 197, 199} while CD spectroscopy has showed that the partially unfolded α -La still exhibits a significant amount of α -helical content present in the native state.^{97, 199}

α -La adsorbed at oil-water interfaces of emulsions is less well-characterized in comparison to β -Lg (Section 1.4.1) and β -casein (Section 1.4.3). One FTIR study on α -La adsorbed at the soy bean oil-water interface found that adsorption induced additional β -sheet structure at the expense of the α -helical structure.¹³² Another study explored the tertiary conformation of α -La bound to liposomes composed of egg lecithin and dimyristoylphosphatidylcholine (DMPC).¹³⁷ Liposome-bound α -La exposed its deeply buried tryptophan residues, indicating partial unfolding.¹³⁷ A CD study on α -La bound to DMPC vesicles reported an increase in the non-native α -helical structure especially at low pH 2 and 4.²⁰⁰ Despite these studies, the interfacial structure of α -La adsorbed at oil-water interfaces remains poorly understood. Moreover, the physical stability of model emulsions containing α -La as sole emulsifiers has not been extensively studied, likely due to the fact that the concentration of α -La in milk is relatively small.

1.4.3 β -Casein

β -Casein is the major casein protein in milk.¹⁴⁰ β -Casein is a flexible, linear protein, which lacks a well-defined tertiary structure and does not contain a significant amount of secondary structures.¹⁴⁰ Of the 209 amino acids in β -casein, 35 are prolines, the cyclic structure of which accounts for the low amount of the α -helix and β -sheet structures. β -Casein is very amphiphilic containing a highly charged N-terminal domain (0-40 residues) and a long hydrophobic C-terminal domain (Figure 1.17).¹⁷¹ In order to avoid the unfavourable contact between the hydrophobic domain and water, in solution, β -casein molecules self-associate into micelles. In fact, 95% of

caseins in milk associate into micelles, which are large colloidal particles with complex structures.¹⁷¹ In a simplistic view, a micelle consists of a core with buried hydrophobic regions of casein molecules and a ‘hairy’-like surface with protruding hydrophilic regions as well as charged molecules and ions.

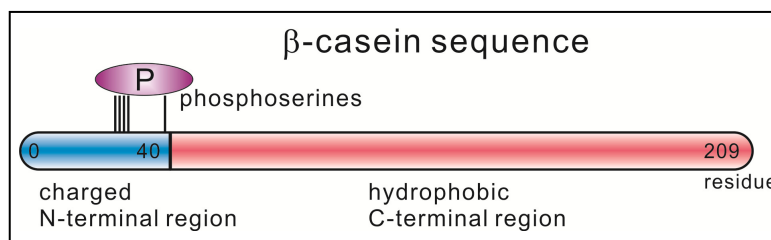


Figure 1.17: A schematic representation of the distribution of the hydrophilic and the hydrophobic regions along the β -casein sequence.

β -Casein has a high surface activity and stabilizing ability due to its characteristic interfacial structure. Experimental studies including neutron reflectivity, dynamic light scattering and molecular modelling have been used to characterize the interfacial structure of β -casein adsorbed at oil-water or air-water interfaces.^{21, 103, 114, 157, 201-204} Results from these studies have shown that β -casein adsorbed at oil-water and air-water interfaces form two distinctive layers: a dense inner layer of 1-2 nm thick and 80-90% protein volume fraction; and an extended outer layer of 5-10 nm thick and less than 20% protein volume fraction.^{103, 112, 114, 205} Modelling and ³¹P nuclear magnetic resonance studies have identified the highly charged N-terminal (1-40 residues) as the protruding region into the aqueous phase.^{205, 206} The so-called ‘train-loop-tail’ model has been proposed to describe the interfacial structural organization of β -casein (Figure 1.7).¹³ When β -casein adsorbs to oil-water or air-water interfaces, the hydrophobic region of β -casein is anchored at the interface (the ‘train’ regions) and the hydrophilic region extensively protrudes into the aqueous phase (the ‘loop’ and ‘tail’ regions) (Figure 1.7). Compared to the current knowledge on the thickness and density profile of the adsorbed β -casein layer, less information is known about the secondary structure of β -casein adsorbed at oil-water interfaces. However, one study on the secondary structure of β -casein adsorbed at the surface of teflon spheres using CD spectroscopy observed an increase in the α -helical content.¹⁵⁷

The interfacial structure of β -casein determines its interfacial activity as an emulsifier and a stabilizer. The hydrophobic region allows the favourable interactions between the protein and the oil phase, facilitating adsorption to the oil-water interface. The charged and long hydrophilic region then provides both electrostatic and steric stabilizing mechanisms (Sections 1.2.2.3 & 1.2.2.4) to emulsion droplets.^{21, 57} Therefore, β -casein-stabilized emulsions have excellent resistance to droplet flocculation upon heating and NaCl addition.^{21, 65}

1.5 Lipid liquid crystalline nanostructured particles

Lipid liquid crystalline nanostructured particles are a colloidal system containing sub-micron lipid particles dispersed in an aqueous environment. These lipid particles contain the internal nanostructures of the lipid liquid crystalline phases and hence are called lipid liquid crystalline nanostructured particles. This section gives an introduction to the liquid crystalline phases of lipids in excess water and how these bulk liquid crystalline phases can be dispersed into sub-micrometer particles.

Polar lipids in excess water can spontaneously self-assemble to form remarkable structures with long-range three-dimensional periodicity but short-range disorder at atomic distances, and these systems are called lyotropic liquid crystalline phases. Glycerol monooleate (GMO) and phytantriol (PHYT) are two examples of such polar lipids, which are amphiphilic and contain a polar head group and non-polar fatty acyl chains. The self-assembling process of these lipids in excess water is driven by the hydrophobic effect, which is the self-association of the non-polar acyl chains to minimize the contact with water.

The liquid crystalline phase behaviour of GMO and PHYT in excess water has been well studied over the last few decades.^{34, 39, 44, 207-218} The chemical structures of GMO and PHYT and a schematic illustration of their phase behaviour in excess water are given in Figure 1.18. Studies have shown that both GMO and PHYT exhibit similar liquid crystalline phase behaviour in excess water.^{34, 219} GMO and PHYT in excess water can form an inverse bicontinuous cubic (V_2) phase at ambient temperatures, an inverse hexagonal (H_2) phase and an inverse micellar (L_2) phase at higher temperatures (Figure 1.18).^{34, 39, 219} A consequence of the thermodynamic stability of these liquid crystalline phases when prepared using lipids such as GMO and PHYT in excess water is that they can be mechanically dispersed in the presence of stabilizers to form sub-micron particles that retain the internal nanostructure of the 'parent' lipid liquid crystalline phase in an aqueous environment. Dispersions of cubic and hexagonal phases into lipid particles with the internal phase structure have been termed 'cubosomes' and 'hexosomes' respectively.

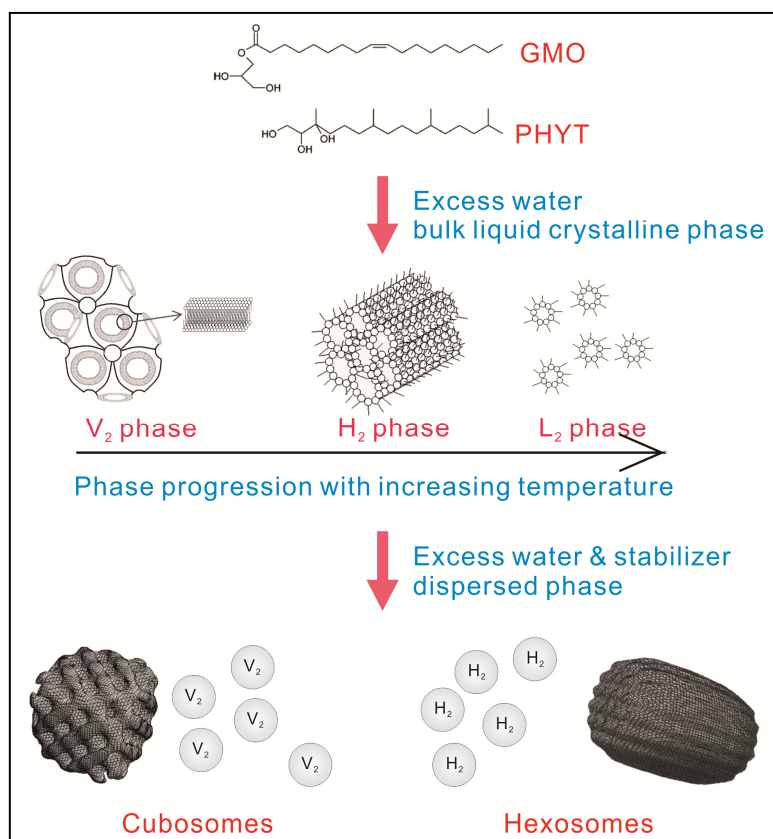


Figure 1.18: Chemical structures of GMO and PHYT and various liquid crystalline phases they form in excess water. Dispersions of the bulk liquid crystalline phases can be achieved with the aid of stabilizers. The calculated surface representations of a hexosome and a cubosome are reproduced from^{40,220} respectively.

Each of the liquid crystalline phases has a unique nanostructure. The V_2 phase consists of a network of two non-intersecting water channels separated by a single continuous lipid bilayer (Figure 1.18). There are three different types of V_2 phases, and they are infinite periodic minimal surfaces (IPMS) of primitive, gyroid and diamond types with an $Im3m$, $Ia3d$ and $Pn3m$ space group respectively (Figure 1.19). The H_2 phase consists of infinite cylinders of water molecules in a continuous medium of the lipid bilayer and the cylinders are arranged in a hexagonal array (Figure 1.18). The L_2 phase consists of water-in-oil micelles with head groups sequestered in the micelle core and the hydrocarbon chains extend towards the exterior (Figure 1.18). One of the commonly used techniques to identify liquid crystalline phases is small angle X-ray scattering (SAXS). SAXS measures the scattered intensity of X-rays from a sample at a small angle. The unique SAXS profile of the scattering intensity versus the scattering vector (q) allows the determination of the nanostructure of the liquid crystalline phases (Figure 1.20). In particular, the position of peaks (q values) allows the calculation of the space group and the lattice parameter for the unit cell of the liquid crystalline phase. SAXS has therefore been widely used in many studies on the temperature-dependent liquid crystalline phase behaviour of GMO and PHYT.^{33, 42, 43, 221}

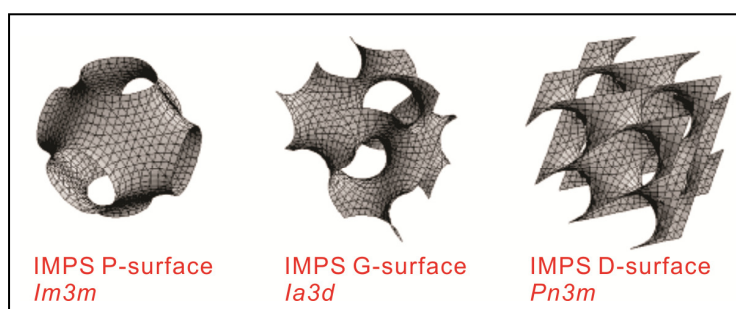


Figure 1.19: Unit cells of the IMPS P-surface (*Im3m* space group), G-surface (*Ia3d* space group) and D-surface (*Pn3m* space group). Reproduced from²²⁰

The cubic and hexagonal phases can be mechanically agitated to form cubosomes and hexosomes, which retain the internal structures of the bulk liquid crystalline phases (Figure 1.18). Mechanical forces that can be used to form cubosomes and hexosomes include high-pressure homogenization, ultrasonication and high shear microfluidization. As is the case for oil-in-water emulsions (Section 1.2.1), stabilizers are required to make kinetically stable dispersions of cubosomes and hexosomes.^{37, 38, 219, 222, 223} One of the commonly used polymers is Pluronic F127 (F127), a commercially available triblock copolymer composed of a polypropylene oxide (PPO) block in the middle and two polyethylene oxide (PEO) blocks capped on both ends. It is believed that when F127 encounters the liquid crystalline phase, the PPO block locates at the hydrophobic lipid bilayer whereas the PEO tails protrude into the aqueous environment.^{37, 38} Such an arrangement provides steric repulsion between adjacent particles to oppose van der Waals and hydrophobic interactions, preventing particles from flocculation and coalescence. Many experimental studies of cubosomes and hexosomes employ cryo-transmission electron microscopy (cryo-TEM) which allows the visualization of these particles and their lattice symmetry (Figure 1.20).^{37, 38, 225}

Both the non-dispersed liquid crystalline phases and the dispersed cubosomes and hexosomes are of particular interest to the pharmaceutical and food industries due to their potential to protect and control the release of cargo molecules.^{31, 32, 36, 41-47} The discovery of biocompatible stabilizers is therefore important for the application of cubosomes and hexosomes in oral drug and nutrient delivery. Peptides and proteins appear to be a logical choice as biocompatible stabilizers. Larsson first described studies using β -casein as a stabilizer for GMO dispersions.^{39, 224} Since the discovery of Pluronic F127, the use of proteins such as β -casein to stabilize cubosomes and hexosomes does not however appear to have been further explored using standard techniques such as SAXS and cryo-TEM. Given the potential of milk proteins as biocompatible stabilizers, it is therefore timely to study the use of proteins to stabilize cubosomes and hexosomes.

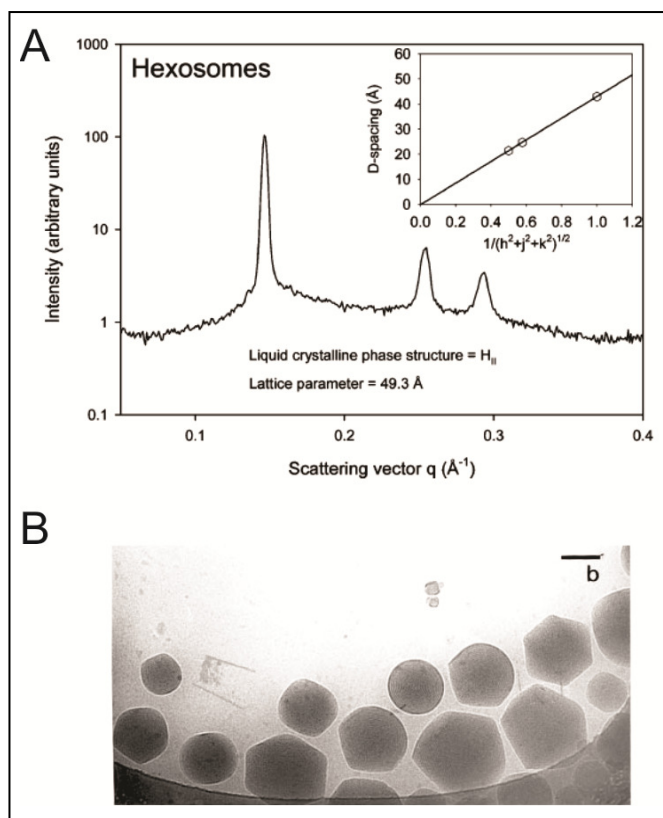


Figure 1.20: (A) A representative SAXS pattern of PHYT hexosomes. Reproduced from²²⁵
 (B) A cryo-TEM image of GMO hexosomes. Reproduced from³⁸

1.6 Project aims and thesis outline

This chapter provides a review of the current understanding of the interfacial structure of milk proteins at oil-water interfaces of emulsions and the relationship between the interfacial structure and the physical stability of protein-stabilized emulsions. Due to the high light scattering and absorbing nature of emulsions, direct measurements of protein structure adsorbed at oil-water interfaces remain a challenge, resulting in a poor understanding of the interfacial structure, particularly at the secondary and tertiary structure level. There is therefore a strong need to determine the interfacial structure of proteins adsorbed at oil-water interfaces to fully understand the relationship between protein interfacial structure and protein function in stabilizing emulsions. The major aims of this PhD project are therefore:

- 1) To develop new approaches for measurement of the interfacial structure of milk proteins in light scattering and absorbing colloidal systems at a molecular level.
- 2) To systematically characterize the interfacial structure of milk proteins adsorbed at oil-water interfaces of emulsions.
- 3) To understand the interplay between milk protein interfacial structure and the emulsion stability under heating and moderate ionic strength conditions.

- 4) Based on the understanding of the interfacial structure of proteins at oil-water interfaces determined in this PhD project, to explore the adsorption of milk proteins at lipid-water interfaces of lipid liquid crystalline nanostructured particles and the potential of milk proteins as stabilizers.

The rest of the thesis consists of five result chapters and one discussion/conclusion chapter. Chapter 2 describes the development of a novel approach using SRCD spectroscopy to directly measure the secondary structure of β -Lg adsorbed at oil-water interfaces of emulsions, which is presented as a published paper. Chapter 3 describes using three biophysical techniques, a study on the structure of β -Lg adsorbed at different oil-water interfaces and the structural relationship to emulsion stability, which is also presented as a published paper. Chapter 4 describes a comparative study of α -La to the previous β -Lg study and is presented as a submitted manuscript. Chapter 5 follows the β -Lg and α -La chapters and describes a systematic study on the interfacial structure of β -casein and its relationship to emulsion stability. Chapter 6 describes an investigation of β -casein as a biocompatible stabilizer for the formation of lipid liquid crystalline nanostructured particles, and is presented as a submitted manuscript. Chapter 7 is the final chapter which summarizes and discusses all results of this project. Overall, the theme of thesis is the adsorption of milk proteins to oil-water and lipid-water interfaces and how the adsorption-induced structural change can influence the function of proteins in stabilizing oil droplets and lipid particles.

References

- (1) Bowie, J.U. *Solving the membrane protein folding problem. Nature* **2005**, *438*, 581-589.
- (2) Langosch, D.; Arkin, I.T. *Interaction and conformational dynamics of membrane-spanning protein helices. Protein Sci.* **2009**, *18*, 1343-1358.
- (3) Levental, I.; Grzybek, M.; Simons, K. *Greasing their way: Lipid modifications determine protein association with membrane rafts. Biochemistry* **2010**, *49*, 6305-6316.
- (4) Mackenzie, K.R. *Folding and stability of α -helical integral membrane proteins. Chem. Rev.* **2006**, *106*, 1931-1977.
- (5) Nath, A.; Atkins, W.M.; Sligar, S.G. *Applications of phospholipid bilayer nanodiscs in the study of membranes and membrane proteins. Biochemistry* **2007**, *46*, 2059-2069.
- (6) Feiler, A.A.; Sahlholm, A.; Sandberg, T.; Caldwell, K.D. *Adsorption and viscoelastic properties of fractionated mucin (BSM) and bovine serum albumin (BSA) studied with quartz crystal microbalance (QCM-D). J. Colloid Interface Sci.* **2007**, *315*, 475-481.
- (7) Marchesseau, S.; Mani, J.C.; Martineau, P.; Roquet, F.; Cuq, J.L.; Pugniere, M. *Casein interactions studied by the surface plasmon resonance technique. J. Dairy Sci.* **2002**, *85*, 2711-2721.
- (8) Rabe, M.; Verdes, D.; Seeger, S. *Understanding protein adsorption phenomena at solid surfaces. Adv. Colloid Interface Sci.* **2011**, *162*, 87-106.
- (9) Swann, M.J.; Peel, L.L.; Carrington, S.; Freeman, N.J. *Dual-polarization interferometry: An analytical technique to measure changes in protein structure in real time, to determine the stoichiometry of binding events, and to differentiate between specific and nonspecific interactions. Anal. Biochem.* **2004**, *329*, 190-198.
- (10) Sonesson, A.W.; Callisen, T.H.; Brismar, H.; Elofsson, U.M. *A comparison between dual polarization interferometry (DPI) and surface plasmon resonance (SPR) for protein adsorption studies. Colloids Surf., B* **2007**, *54*, 236-240.
- (11) Clarkson, J.R.; Cui, Z.F.; Darton, R.C. *Protein denaturation in foam: I. Mechanism study. J. Colloid Interface Sci.* **1999**, *215*, 323-332.
- (12) Damodaran, S. *Protein stabilization of emulsions and foams. J. Food Sci.* **2005**, *70*, R54-R66.
- (13) Dickinson, E. *Milk protein interfacial layers and the relationship to emulsion stability and rheology. Colloids Surf., B* **2001**, *20*, 197-210.
- (14) Foegeding, E.A.; Luck, P.J.; Davis, J.P. *Factors determining the physical properties of protein foams. Food Hydrocolloids* **2006**, *20*, 284-292.
- (15) Wilde, P.J. *Interfaces: Their role in foam and emulsion behaviour. Curr. Opin. Colloid Interface Sci.* **2000**, *5*, 176-181.

- (16) Friberg, S.E.; Larsson, K.; Johan, S. *Food emulsions*, 4th ed.; Marcel Dekker: New York, 2004.
- (17) Dalgleish, D.G. *Food emulsions stabilized by proteins. Curr. Opin. Colloid Interface Sci.* **1997**, *2*, 573-577.
- (18) Dalgleish, D.G. *Food emulsions - their structures and structure-forming properties. Food Hydrocolloids* **2006**, *20*, 415-422.
- (19) McClements, D.J. *Food emulsions: Principles, practices, and techniques*, 2nd ed.; CRC Press: Boca Raton, 2005.
- (20) Nielloud, F.; Marti-Mestres, G. *Pharmaceutical emulsions and suspensions*; Marcel Dekker, Inc.: New York, 2000.
- (21) Dickinson, E. *Caseins in emulsions: Interfacial properties and interactions. Int. Dairy J.* **1999**, *9*, 305-312.
- (22) Euston, S.R.; Finnigan, S.R.; Hirst, R.L. *Aggregation kinetics of heated whey protein-stabilized emulsions. Food Hydrocolloids* **2000**, *14*, 155-161.
- (23) Foegeding, E.A.; Davis, J.P.; Doucet, D.; McGuffey, M.K. *Advances in modifying and understanding whey protein functionality. Trends Food Sci. Technol.* **2002**, *13*, 151-159.
- (24) Hunt, J.A.; Dalgleish, D.G. *Adsorption behaviour of whey protein isolate and caseinate in soya oil-in-water emulsions. Food Hydrocolloids* **1994**, *8*, 175-187.
- (25) Ye, A. *Interfacial composition and stability of emulsions made with mixtures of commercial sodium caseinate and whey protein concentrate. Food Chem.* **2008**, *110*, 946-952.
- (26) Dalgleish, D.G. *Adsorption of protein and the stability of emulsions. Trends Food Sci. Technol.* **1997**, *8*, 1-6.
- (27) Dickinson, E. *Properties of emulsions stabilized with milk proteins: Overview of some recent developments. J. Dairy Sci.* **1997**, *80*, 2607-2619.
- (28) Dickinson, E. *Proteins at interfaces and in emulsions - stability, rheology and interactions. J. Chem. Soc., Faraday Trans.* **1998**, *94*, 1657-1669.
- (29) Kim, H.-J.; Decker, E.A.; McClements, D.J. *Impact of protein surface denaturation on droplet flocculation in hexadecane oil-in-water emulsions stabilized by β -lactoglobulin. J. Agric. Food Chem.* **2002**, *50*, 7131-7137.
- (30) Kim, H.-J.; Decker, E.A.; McClements, D.J. *Role of postadsorption conformation changes of β -lactoglobulin on its ability to stabilize oil droplets against flocculation during heating at neutral pH. Langmuir* **2002**, *18*, 7577-7583.
- (31) Amar-Zrihen, N.; Aserin, A.; Garti, N. *Food volatile compounds facilitating H_{ii} mesophase formation: Solubilization and stability. J. Agric. Food Chem.* **2011**, *59*, 5554-5564.
- (32) Augustin, M.A.; Hemar, Y. *Nano- and micro-structured assemblies for encapsulation of food ingredients. Chem. Soc. Rev.* **2009**, *38*, 902-912.

- (33) Barauskas, J.; Johnsson, M.; Joabsson, F.; Tiberg, F. *Cubic phase nanoparticles (cubosome): Principles for controlling size, structure, and stability*. *Langmuir* **2005**, *21*, 2569-2577.
- (34) Barauskas, J.; Landh, T. *Phase behavior of the phytantriol/water system*. *Langmuir* **2003**, *19*, 9562-9565.
- (35) Ericsson, B.; Eriksson, P.O.; Löfroth, J.E.; Engström, S. *Cubic phases as delivery systems for peptide drugs*, in *Polymeric drugs and drug delivery systems*, Dunn R. L., Ottenbrite, R. M.; American Chemical Society: Washington, 1991. p.251-265.
- (36) Fong, W.-K.; Hanley, T.; Boyd, B.J. *Stimuli responsive liquid crystals provide 'on-demand' drug delivery in vitro and in vivo*. *J. Controlled Release* **2009**, *135*, 218-226.
- (37) Gustafsson, J.; Ljusberg-Wahren, H.; Almgren, M.; Larsson, K. *Cubic lipid-water phase dispersed into submicron particles*. *Langmuir* **1996**, *12*, 4611-4613.
- (38) Gustafsson, J.; Ljusberg-Wahren, H.; Almgren, M.; Larsson, K. *Submicron particles of reversed lipid phases in water stabilized by a nonionic amphiphilic polymer*. *Langmuir* **1997**, *13*, 6964-6971.
- (39) Larsson, K. *Cubic lipid-water phases: Structures and biomembrane aspects*. *J. Phys. Chem.* **1989**, *93*, 7304-7314.
- (40) Larsson, K. *Colloidal dispersions of ordered lipid-water phases*. *J. Dispersion Sci. Technol.* **1999**, *20*, 27-34.
- (41) Libster, D.; Aserin, A.; Garti, N. *Interactions of biomacromolecules with reverse hexagonal liquid crystals: Drug delivery and crystallization applications*. *J. Colloid Interface Sci.* **2011**, *356*, 375-386.
- (42) Nguyen, T.-H.; Hanley, T.; Porter, C.J.H.; Larson, I.; Boyd, B.J. *Phytantriol and glyceryl monooleate cubic liquid crystalline phases as sustained-release oral drug delivery systems for poorly water soluble drugs I. Phase behaviour in physiologically-relevant media*. *J. Pharm. Pharmacol.* **2010**, *62*, 844-855.
- (43) Nguyen, T.-H.; Hanley, T.; Porter, C.J.H.; Larson, I.; Boyd, B.J. *Phytantriol and glyceryl monooleate cubic liquid crystalline phases as sustained-release oral drug delivery systems for poorly water-soluble drugs II. In-vivo evaluation*. *J. Pharm. Pharmacol.* **2010**, *62*, 856-865.
- (44) Sagalowicz, L.; Leser, M.E.; Watzke, H.J.; Michel, M. *Monoglyceride self-assembly structures as delivery vehicles*. *Trends Food Sci. Technol.* **2006**, *17*, 204-214.
- (45) Solaro, R.; Chiellini, F.; Battisti, A. *Targeted delivery of protein drugs by nanocarriers*. *Materials* **2010**, *3*, 1928-1980.
- (46) Yagmur, A.; Glatter, O. *Characterization and potential applications of nanostructured aqueous dispersions*. *Adv. Colloid Interface Sci.* **2009**, *147-148*, 333-342.

- (47) Zhang, L.; Pornpattananangku, D.; Hu, C.M.; Huang, C.M. *Development of nanoparticles for antimicrobial drug delivery*. *Curr. Med. Chem.* **2010**, *17*, 585-594.
- (48) Hiemenz, P.C.; Rajagopalan, R. *Principles of colloid and surface chemistry*, 3rd ed.; Marcel Dekker: New York, 1997.
- (49) Hunter, R.J. *Foundations of colloid science I*, 2nd ed.; Oxford University Press; Oxford, 2001.
- (50) Israelachvili, J.N. *Intermolecular and surface forces*, 3rd ed.; Academic Press: Amsterdam, 1991.
- (51) Chandler, D. *Interfaces and the driving force of hydrophobic assembly*. *Nature* **2005**, *437*, 640-647.
- (52) Tanford, C. *The hydrophobic effect: Formation of micelles and biological membranes*, 2nd ed.; Wiley: New York, 1980.
- (53) McClements, D.J. *Protein-stabilized emulsions*. *Curr. Opin. Colloid Interface Sci.* **2004**, *9*, 305-313.
- (54) Tcholakova, S.; Denkov, N.D.; Ivanov, I.B.; Campbell, B. *Coalescence in β -lactoglobulin-stabilized emulsions: Effects of protein adsorption and drop size*. *Langmuir* **2002**, *18*, 8960-8971.
- (55) Demetriades, K.; Coupland, J.N.; McClements, D.J. *Physicochemical properties of whey protein-stabilized emulsions as affected by heating and ionic strength*. *J. Food Sci.* **1997**, *62*, 462-467.
- (56) Israelachvili, J.; Wennerstrom, H. *Role of hydration and water structure in biological and colloidal interactions*. *Nature* **1996**, *379*, 219-225.
- (57) Dickinson, E. *Flocculation of protein-stabilized oil-in-water emulsions*. *Colloids Surf., B* **2010**, *81*, 130-140.
- (58) Kim, H.-J.; Decker, E.A.; McClements, D.J. *Comparison of droplet flocculation in hexadecane oil-in-water emulsions stabilized by β -lactoglobulin at pH 3 and 7*. *Langmuir* **2004**, *20*, 5753-5758.
- (59) Wooster, T.J.; Augustin, M.A. *β -Lactoglobulin-dextran maillard conjugates: Their effect on interfacial thickness and emulsion stability*. *J. Colloid Interface Sci.* **2006**, *303*, 564-572.
- (60) Wooster, T.J.; Augustin, M.A. *The emulsion flocculation stability of protein-carbohydrate diblock copolymers*. *J. Colloid Interface Sci.* **2007**, *313*, 665-675.
- (61) Zhao, Y.; Turay, R.; Hundley, L. *Monitoring and predicting emulsion stability of metalworking fluids by salt titration and laser light scattering method*. *Tribol. Trans.* **2006**, *49*, 117-123.
- (62) Day, L.; Xu, M.; Lundin, L.; Wooster, T.J. *Interfacial properties of deamidated wheat protein in relation to its ability to stabilise oil-in-water emulsions*. *Food Hydrocolloids* **2009**, *23*, 2158-2167.

- (63) Dauphas, S.; Amestoy, M.; Llamas, G.; Anton, M.; Riaublanc, A. *Modification of the interactions between β -casein stabilised oil droplets with calcium addition and temperature changing. Food Hydrocolloids* **2008**, *22*, 231-238.
- (64) Dickinson, E.; Hunt, J.A.; Horne, D.S. *Calcium induced flocculation of emulsions containing adsorbed β -casein or phosphatidylcholine. Food Hydrocolloids* **1992**, *6*, 359-370.
- (65) Dickinson, E.; Semenova, M.G.; Antipova, A.S. *Salt stability of casein emulsions. Food Hydrocolloids* **1998**, *12*, 227-235.
- (66) Bouyer, E.; Mekhloufi, G.; Potier, I.L.; Kerdaniel, T.D.F.D.; Grossiord, J.L.; Rosilio, V.; Agnely, F. *Stabilization mechanism of oil-in-water emulsions by β -lactoglobulin and gum arabic. J. Colloid Interface Sci.* **2011**, *354*, 467-477.
- (67) Cao, Y.; Dickinson, E.; Wedlock, D.J. *Creaming and flocculation in emulsions containing polysaccharide. Food Hydrocolloids* **1990**, *4*, 185-195.
- (68) Cao, Y.; Dickinson, E.; Wedlock, D.J. *Influence of polysaccharides on the creaming of casein-stabilized emulsions. Food Hydrocolloids* **1991**, *5*, 443-454.
- (69) Dickinson, E. *Hydrocolloids at interfaces and the influence on the properties of dispersed systems. Food Hydrocolloids* **2003**, *17*, 25-39.
- (70) Wang, Y.; Li, D.; Wang, L.J.; Adhikari, B. *The effect of addition of flaxseed gum on the emulsion properties of soybean protein isolate (SPI). J. Food Eng.* **2011**, *104*, 56-62.
- (71) Dickinson, E.; Flint, F.O.; Hunt, J.A. *Bridging flocculation in binary protein stabilized emulsions. Food Hydrocolloids* **1989**, *3*, 389-397.
- (72) Singh, H.; Tamehana, M.; Hemar, Y.; Munro, P.A. *Interfacial compositions, microstructures and properties of oil-in-water emulsions formed with mixtures of milk proteins and κ -carrageenan: 1. Sodium caseinate. Food Hydrocolloids* **2003**, *17*, 539-548.
- (73) Syrbe, A.; Bauer, W.J.; Klostermeyer, H. *Polymer science concepts in dairy systems - an overview of milk protein and food hydrocolloid interaction. Int. Dairy J.* **1998**, *8*, 179-193.
- (74) van Aken, G.A.; Blijdenstein, T.B.J.; Hotrum, N.E. *Colloidal destabilisation mechanisms in protein-stabilised emulsions. Curr. Opin. Colloid Interface Sci.* **2003**, *8*, 371-379.
- (75) Radford, S.J.; Dickinson, E. *Depletion flocculation of caseinate-stabilised emulsions: What is the optimum size of the non-adsorbed protein nano-particles? Colloids Surf. Physicochem. Eng. Aspects* **2004**, *238*, 71-81.
- (76) Reiffers-Magnani, C.K.; Cuq, J.L.; Watzke, H.J. *Depletion flocculation and thermodynamic incompatibility in whey protein stabilised O/W emulsions. Food Hydrocolloids* **2000**, *14*, 521-530.
- (77) Singh, H.; Tamehana, M.; Hemar, Y.; Munro, P.A. *Interfacial compositions, microstructure and stability of oil-in-water emulsions formed with mixtures of milk proteins and κ -carrageenan: 2. Whey protein isolate (WPI). Food Hydrocolloids* **2003**, *17*, 549-561.
- (78) Dill, K.A. *Dominant forces in protein folding. Biochemistry* **1990**, *29*, 7133-7155.

- (79) Dill, K.A.; Ozkan, S.B.; Shell, M.S.; Weikl, T.R. *The protein folding problem. Annu. Rev. Biophys.* **2008**, *37*, 289-316.
- (80) Finkelstein, A.V.; Galzitskaya, O.V. *Physics of protein folding. Phys. Life Rev.* **2004**, *1*, 23-56.
- (81) Jaenicke, R. *Protein folding: Local structures, domains, subunits, and assemblies. Biochemistry* **1991**, *30*, 3147-3161.
- (82) Ha, J.-H.; Spolar, R.S.; Record Jr, M.T. *Role of the hydrophobic effect in stability of site-specific protein-DNA complexes. J. Mol. Biol.* **1989**, *209*, 801-816.
- (83) Kabsch, W.; Sander, C. *Dictionary of protein secondary structure: Pattern recognition of hydrogen-bonded and geometrical features. Biopolymers* **1983**, *22*, 2577-2637.
- (84) Flory, P.J. *Principles of polymer chemistry I*; Cornell University Press: Ithaca, 1953.
- (85) Richards, F.M. *Areas, volumes, packing, and protein structure. Annu. Rev. Biophys. Bioeng.* **1977**, *6*, 151-176.
- (86) Lumry, R.; Eyring, H. *Conformation changes of proteins. J. Phys. Chem.* **1954**, *58*, 110-120.
- (87) Chi, E.Y.; Krishnan, S.; Randolph, T.W.; Carpenter, J.F. *Physical stability of proteins in aqueous solution: Mechanism and driving forces in nonnative protein aggregation. Pharm. Res.* **2003**, *20*, 1325-1336.
- (88) Scharnagl, C.; Reif, M.; Friedrich, J. *Stability of proteins: Temperature, pressure and the role of the solvent. Biochim. Biophys. Acta: Proteins Proteom.* **2005**, *1749*, 187-213.
- (89) Privalov, P.L. *Cold denaturation of proteins. Crit. Rev. Biochem. Mol. Biol.* **1990**, *25*, 281-305.
- (90) Tsai, C.J.; Maizel, J.V., Jr.; Nussinov, R. *The hydrophobic effect: A new insight from cold denaturation and a two-state water structure. Crit. Rev. Biochem. Mol. Biol.* **2002**, *37*, 55-69.
- (91) Almarza, J.; Rincon, L.; Bahsas, A.; Brito, F. *Molecular mechanism for the denaturation of proteins by urea. Biochemistry* **2009**, *48*, 7608-7613.
- (92) Berg, J.M.; Tymoczko, J., L; Stryer, L. *Biochemistry*, 5th ed.; W.H. Freeman: New York, 2002.
- (93) Alexander, M.; Dalglish, D.G. *Dynamic light scattering techniques and their applications in food science. Food Biophysics* **2006**, *1*, 2-13.
- (94) Gao, C.; Wijesinha-Bettoni, R.; Wilde, P.J.; Mills, E.N.C.; Smith, L.J.; Mackie, A.R. *Surface properties are highly sensitive to small pH induced changes in the 3-D structure of α -lactalbumin. Biochemistry* **2008**, *47*, 1659-1666.
- (95) Kato, A.; Nakai, S. *Hydrophobicity determined by a fluorescence probe method and its correlation with surface properties of proteins. Biochim. Biophys. Acta: Protein Struct.* **1980**, *624*, 13-20.

- (96) Razumovsky, L.; Damodaran, S. *Surface activity-compressibility relationship of proteins at the air-water interface. Langmuir* **1999**, *15*, 1392-1399.
- (97) Wijesinha-Bettoni, R.; Gao, C.; Jenkins, J.A.; Mackie, A.R.; Wilde, P.J.; Mills, E.N.C.; Smith, L.J. *Heat treatment of bovine α -lactalbumin results in partially folded, disulfide bond shuffled states with enhanced surface activity. Biochemistry* **2007**, *46*, 9774-9784.
- (98) Yano, Y.F.; Uruga, T.; Tanida, H.; Toyokawa, H.; Terada, Y.; Takagaki, M.; Yamada, H. *Driving force behind adsorption-induced protein unfolding: A time-resolved X-ray reflectivity study on lysozyme adsorbed at an air/water interface. Langmuir* **2009**, *25*, 32-35.
- (99) Bos, M.A.; van Vliet, T. *Interfacial rheological properties of adsorbed protein layers and surfactants: A review. Adv. Colloid Interface Sci.* **2001**, *91*, 437-471.
- (100) Dickinson, E. *Adsorbed protein layers at fluid interfaces: Interactions, structure and surface rheology. Colloids Surf., B* **1999**, *15*, 161-176.
- (101) Lucassen-Reynders, E.H.; Benjamins, J.; Fainerman, V.B. *Dilational rheology of protein films adsorbed at fluid interfaces. Curr. Opin. Colloid Interface Sci.* **2010**, *15*, 264-270.
- (102) Murray, B.S.; Dickinson, E. *Interfacial rheology and the dynamic properties of adsorbed films of food proteins and surfactants. Food Sci. Technol. Int., Tokyo* **1996**, *2*, 131-145.
- (103) Atkinson, P.J.; Dickinson, E.; Horne, D.S.; Richardson, R.M. *Neutron reflectivity of adsorbed β -casein and β -lactoglobulin at the air/water interface. J. Chem. Soc., Faraday Trans.* **1995**, *91*, 2847-2854.
- (104) Matsumura, Y.; Mitsui, S.; Dickinson, E.; Mori, T. *Competitive adsorption of α -lactalbumin in the molten globule state. Food Hydrocolloids* **1994**, *8*, 555-566.
- (105) Meinders, M.B.J.; De Jongh, H.H.J. *Limited conformational change of β -lactoglobulin when adsorbed at the air-water interface. Biopolymers (Biospectrosc.)* **2002**, *67*, 319-322.
- (106) Harzallah, B.; Aguié-Béghin, V.; Douillard, R.; Bosio, L. *A structural study of β -casein adsorbed layers at the air-water interface using X-ray and neutron reflectivity. Int. J. Biol. Macromol.* **1998**, *23*, 73-84.
- (107) Liz, C.C.C.; Petkova, V.; Benattar, J.J.; Michel, M.; Leser, M.E.; Miller, R. *X-ray reflectivity studies of liquid films stabilized by mixed β -lactoglobulin-acacia gum systems. Colloids Surf. Physicochem. Eng. Aspects* **2006**, *282-283*, 109-117.
- (108) Miller, C.E.; Majewski, J.; Kjær, K.; Weygand, M.; Faller, R.; Satija, S.; Kuhl, T.L. *Neutron and X-ray scattering studies of cholera toxin interactions with lipid monolayers at the air-liquid interface. Colloids Surf., B* **2005**, *40*, 159-163.
- (109) Perriman, A.W.; Henderson, M.J.; Holt, S.A.; White, J.W. *Effect of the air-water interface on the stability of β -lactoglobulin. J. Phys. Chem. B* **2007**, *111*, 13527-13537.

- (110) Vierl, U.; Cevc, G. *Time-resolved X-ray reflectivity measurements of protein binding onto model lipid membranes at the air-water interface. Biochim. Biophys. Acta: Biomembr.* **1997**, *1325*, 165-177.
- (111) Cosgrove, T.; Phipps, J.S.; Richardson, R.M. *Neutron reflection from a liquid/liquid interface. Colloids Surf.* **1992**, *62*, 199-206.
- (112) Dickinson, E.; Horne, D.S.; Phipps, J.S.; Richardson, R.M. *A neutron reflectivity study of the adsorption of β -casein at fluid interfaces. Langmuir* **1993**, *9*, 242-248.
- (113) Fragneto, G.; Bellet-Amalric, E.; Charitat, T.; Dubos, P.; Graner, F.; Perino-Galice, L. *Neutron and X-ray reflectivity studies at solid-liquid interfaces: The interaction of a peptide with model membranes. Physica B: Condens. Matter* **2000**, *276-278*, 501-502.
- (114) Fragneto, G.; Thomas, R.K.; Rennie, A.R.; Penfold, J. *Neutron reflection study of bovine β -casein adsorbed on OTS self-assembled monolayers. Science* **1995**, *267*, 657-660.
- (115) Lu, J.R.; Zhao, X.; Yaseen, M. *Protein adsorption studied by neutron reflection. Curr. Opin. Colloid Interface Sci.* **2007**, *12*, 9-16.
- (116) Marsh, R.J.; Jones, R.A.L.; Sferrazza, M.; Penfold, J. *Neutron reflectivity study of the adsorption of β -lactoglobulin at a hydrophilic solid/liquid interface. J. Colloid Interface Sci.* **1999**, *218*, 347-349.
- (117) Cross, G.H.; Reeves, A.A.; Brand, S.; Popplewell, J.F.; Peel, L.L.; Swann, M.J.; Freeman, N.J. *A new quantitative optical biosensor for protein characterisation. Biosens. Bioelectron.* **2003**, *19*, 383-390.
- (118) Freeman, N.J.; Peel, L.L.; Swann, M.J.; Cross, G.H.; Reeves, A.; Brand, S.; Lu, J.R. *Real time, high resolution studies of protein adsorption and structure at the solid-liquid interface using dual polarization interferometry. J. Phys.: Condens. Matter* **2004**, *16*, S2493-S2496.
- (119) Lin, S.; Lee, C.-K.; Wang, Y.-M.; Huang, L.-S.; Lin, Y.-H.; Lee, S.-Y.; Sheu, B.-C.; Hsu, S.-M. *Measurement of dimensions of pentagonal doughnut-shaped C-reactive protein using an atomic force microscope and a dual polarisation interferometric biosensor. Biosens. Bioelectron.* **2006**, *22*, 323-327.
- (120) Lundin, M.; Sandberg, T.; Caldwell, K.D.; Blomberg, E. *Comparison of the adsorption kinetics and surface arrangement of "as received" and purified bovine submaxillary gland mucin (BSM) on hydrophilic surfaces. J. Colloid Interface Sci.* **2009**, *336*, 30-39.
- (121) Ricard-Blum, S.; Peel, L.L.; Ruggiero, F.; Freeman, N.J. *Dual polarization interferometry characterization of carbohydrate-protein interactions. Anal. Biochem.* **2006**, *352*, 252-259.
- (122) Sheu, B.C.; Lin, Y.H.; Lin, C.C.; Lee, A.S.; Chang, W.C.; Wu, J.H.; Tsai, J.C.; Lin, S. *Significance of the pH-induced conformational changes in the structure of C-reactive protein measured by dual polarization interferometry. Biosens. Bioelectron.* **2010**, *26*, 822-827.

- (123) Sonesson, A.W.; Callisen, T.H.; Brismar, H.; Elofsson, U.M. *Adsorption and activity of thermomyces lanuginosus lipase on hydrophobic and hydrophilic surfaces measured with dual polarization interferometry (DPI) and confocal microscopy. Colloids Surf., B* **2008**, *61*, 208-215.
- (124) Lee, T.-H.; Hall, K.N.; Swann, M.J.; Popplewell, J.F.; Unabia, S.; Park, Y.; Hahm, K.S.; Aguilar, M.-I. *The membrane insertion of helical antimicrobial peptides from the N-terminus of helicobacter pylori ribosomal protein L1. Biochim. Biophys. Acta: Biomembr.* **2010**, *1798*, 544-557.
- (125) Lee, T.-H.; Heng, C.; Swann, M.J.; Gehman, J.D.; Separovic, F.; Aguilar, M.-I. *Real-time quantitative analysis of lipid disordering by Aurein 1.2 during membrane adsorption, destabilisation and lysis. Biochim. Biophys. Acta: Biomembr.* **2010**, *1798*, 1977-1986.
- (126) Nielsen, S.B.; Otzen, D.E. *Impact of the antimicrobial peptide novicidin on membrane structure and integrity. J. Colloid Interface Sci.* **2010**, *345*, 248-256.
- (127) Sanghera, N.; Swann, M.J.; Ronan, G.; Pinheiro, T.J.T. *Insight into early events in the aggregation of the prion protein on lipid membranes. Biochim. Biophys. Acta: Biomembr.* **2009**, *1788*, 2245-2251.
- (128) Yu, L.; Guo, L.; Ding, J.L.; Ho, B.; Feng, S.-S.; Popplewell, J.; Swann, M.; Wohland, T. *Interaction of an artificial antimicrobial peptide with lipid membranes. Biochim. Biophys. Acta: Biomembr.* **2009**, *1788*, 333-344.
- (129) Jackson, M.; Mantsch, H.H. *The use and misuse of FTIR spectroscopy in the determination of protein structure. Crit. Rev. Biochem. Mol. Biol.* **1995**, *30*, 95-120.
- (130) Kong, J.; Yu, S. *Fourier transform infrared spectroscopic analysis of protein secondary structures. Acta Biochim. Biophys. Sinica* **2007**, *39*, 549-559.
- (131) Fang, Y.; Dalgleish, D.G. *Conformation of β -lactoglobulin studied by FTIR: Effect of pH, temperature, and adsorption to the oil-water interface. J. Colloid Interface Sci.* **1997**, *196*, 292-298.
- (132) Fang, Y.; Dalgleish, D.G. *The conformation of α -lactalbumin as a function of pH, heat treatment and adsorption at hydrophobic surfaces studied by FTIR. Food Hydrocolloids* **1998**, *12*, 121-126.
- (133) Lee, S.-H.; Lefèvre, T.; Subirade, M.; Paquin, P. *Changes and roles of secondary structures of whey protein for the formation of protein membrane at soy oil/water interface under high-pressure homogenization. J. Agric. Food Chem.* **2007**, *55*, 10924-10931.
- (134) Lee, S.-H.; Lefèvre, T.; Subirade, M.; Paquin, P. *Effects of ultra-high pressure homogenization on the properties and structure of interfacial protein layer in whey protein-stabilized emulsion. Food Chem.* **2009**, *113*, 191-195.

- (135) Royer, C.A. *Probing protein folding and conformational transitions with fluorescence. Chem. Rev.* **2006**, *106*, 1769-1784.
- (136) Casterlain, C.; Genot, C. *Conformational changes of bovine serum albumin upon its adsorption in dodecane-in-water emulsions as revealed by front-face steady-state fluorescence. Biochim. Biophys. Acta: Gen. Subjects* **1994**, *1199*, 59-64.
- (137) Cawthern, K.M.; Permyakov, E.; Berliner, L.J. *Membrane-bound states of α -lactalbumin: Implications for the protein stability and conformation. Protein Sci.* **1996**, *5*, 1394-1405.
- (138) Royer, C.A.; Hinck, A.P.; Loh, S.N.; Prehoda, K.E.; Peng, X.; Jonas, J.; Markley, J.L. *Effects of amino acid substitutions on the pressure denaturation of staphylococcal nuclease as monitored by fluorescence and nuclear magnetic resonance spectroscopy. Biochemistry* **1993**, *32*, 5222-5232.
- (139) Zhang, X.Q.; Keiderling, T.A. *Lipid-induced conformational transitions of β -lactoglobulin. Biochemistry* **2006**, *45*, 8444-8452.
- (140) Creamer, L.K. *Effect of sodium dodecyl-sulfate and palmitic acid on the equilibrium unfolding of bovine β -lactoglobulin. Biochemistry* **1995**, *34*, 7170-7176.
- (141) Halskau, O.; Underhaug, J.; Froystein, N.A.; Martinez, A. *Conformational flexibility of α -lactalbumin related to its membrane binding capacity. J. Mol. Biol.* **2005**, *349*, 1072-1086.
- (142) Roumestand, C.; Boyer, M.; Guignard, L.; Barthe, P.; Royer, C.A. *Characterization of the folding and unfolding reactions of a small β -barrel protein of novel topology, the MTCPL oncogene product P13. J. Mol. Biol.* **2001**, *312*, 247-259.
- (143) Vidugiris, G.J.A.; Markley, J.L.; Royer, C.A. *Evidence for a molten globule-like transition state in protein folding from determination of activation volumes. Biochemistry* **1995**, *34*, 4909-4912.
- (144) Rampon, V.; Genot, C.; Riaublanc, A.; Anton, M.; Axelos, M.A.V.; McClements, D.J. *Front-face fluorescence spectroscopy study of globular proteins in emulsions: Displacement of BSA by a nonionic surfactant. J. Agric. Food Chem.* **2003**, *51*, 2482-2489.
- (145) Rampon, V.; Riaublanc, A.; Anton, M.; Genot, C.; McClements, D.J. *Evidence that homogenization of BSA-stabilized hexadecane-in-water emulsions induces structure modification of the nonadsorbed protein. J. Agric. Food Chem.* **2003**, *51*, 5900-5905.
- (146) Sakuno, M.M.; Matsumoto, S.; Kawai, S.; Taihei, K.; Matsumura, Y. *Adsorption and structural change of β -lactoglobulin at the diacylglycerol/water interface. Langmuir* **2008**, *24*, 11483-11488.
- (147) Bannister, W.H.; Bannister, J.V. *Circular dichroism and protein structure. Int. J. Biochem.* **5**, 673-677.
- (148) Keiderling, T.A. *Protein and peptide secondary structure and conformational determination with vibrational circular dichroism. Curr. Opin. Chem. Biol.* **2002**, *6*, 682-688.

- (149) Kelly, S.M.; Jess, T.J.; Price, N.C. *How to study proteins by circular dichroism. Biochim. Biophys. Acta: Proteins Proteom.* **2005**, *1751*, 119-139.
- (150) Sreerama, N.; Venyaminov, S.Y.; Woody, R.W. *Estimation of the number of α -helical and β -strand segments in proteins using circular dichroism spectroscopy. Protein Sci.* **1999**, *8*, 370-380.
- (151) Sreerama, N.; Woody, R.W. *Estimation of protein secondary structure from circular dichroism spectra: Comparison of CONTIN, SELCON, and CDSSTR methods with an expanded reference set. Anal. Biochem.* **2000**, *287*, 252-260.
- (152) Provencher, S.W.; Glockner, J. *Estimation of globular protein secondary structure from circular dichroism. Biochemistry* **1981**, *20*, 33-37.
- (153) Johnson, W.C. *Analyzing protein circular dichroism spectra for accurate secondary structures. Proteins: Struct. Funct. Genetics* **1999**, *35*, 307-312.
- (154) Rogers, D.M.; Hirst, J.D. *First-principles calculations of protein circular dichroism in the near ultraviolet. Biochemistry* **2004**, *43*, 11092-11102.
- (155) Hoagland, P.D.; Unruh, J.J.; Wickham, E.D.; Farrell, H.M., Jr. *Secondary structure of bovine α_2 -casein: Theoretical and experimental approaches. J. Dairy Sci.* **2001**, *84*, 1944-1949.
- (156) van Stokkum, I.H.; Spoelder, H.J.; Bloemendal, M.; van Grondelle, R.; Groen, F.C. *Estimation of protein secondary structure and error analysis from circular dichroism spectra. Anal. Biochem.* **1990**, *191*, 110-118.
- (157) Caessens, P.W.J.R.; De Jongh, H.H.J.; Norde, W.; Gruppen, H. *The adsorption-induced secondary structure of β -casein and of distinct parts of its sequence in relation to foam and emulsion properties. Biochim. Biophys. Acta* **1999**, *1430*, 73-83.
- (158) Takeda, K.; Ogawa, K.; Ohara, M.; Hamada, S.; Moriyama, Y. *Conformational changes of α -lactalbumin induced by the stepwise reduction of its disulfide bridges: The effect of the disulfide bridges on the structural stability of the protein in sodium dodecyl sulfate solution. J. Protein Chem.* **1995**, *14*, 679-684.
- (159) Viseu, M.I.; Carvalho, T.I.; Costa, S.M.B. *Conformational transitions in β -lactoglobulin induced by cationic amphiphiles: Equilibrium studies. Biophys. J.* **2004**, *86*, 2392-2402.
- (160) El-Zahar, K.; Sitohy, M.; Dalgalarondo, M.; Choiset, Y.; Metro, F.; Haertle, T.; Chobert, J.-M. *Purification and physicochemical characterization of ovine β -lactoglobulin and α -lactalbumin. Nahrung - Food* **2004**, *48*, 177-183.
- (161) Paz, S.; Tizón, L.; Otero, J.M.; Llamas-Saiz, A.L.; Fox, G.C.; van Raaij, M.J.; Lamb, H.; Hawkins, A.R.; Laphorn, A.J.; Castedo, L.; González-Bello, C. *Tetrahydrobenzothiophene derivatives: Conformationally restricted inhibitors of Type II dehydroquinase. ChemMedChem* **2011**, *6*, 266-272.

- (162) Dalgleish, D.G.; Leaver, J. *The possible conformations of milk proteins adsorbed on oil/water interfaces. J. Colloid Interface Sci.* **1991**, *141*, 288-294.
- (163) Wu, X.; Narsimhan, G. *Characterization of secondary and tertiary conformational changes of β -lactoglobulin adsorbed on silica nanoparticle surfaces. Langmuir* **2008**, *24*, 4989-4998.
- (164) Husband, F.A.; Garrod, M.J.; Mackie, A.R.; Burnett, G.R.; Wilde, P.J. *Adsorbed protein secondary and tertiary structures by circular dichroism and infrared spectroscopy with refractive index matched emulsions. J. Agric. Food Chem.* **2001**, *49*, 859-866.
- (165) de Jongh, H.H.J.; Meinders, M.B.J. *Proteins at air-water interfaces studied using external reflection circular dichroism. Spectrochim. Acta Part A* **2002**, *58*, 3197-3204.
- (166) Meinders, M.B.J.; van den Bosch, G.G.M.; de Jongh, H.H.J. *IRRAS, a new tool in food science. Trends Food Sci. Technol.* **2000**, *11*, 218-225.
- (167) Wallace, B.A. *Synchrotron radiation circular-dichroism spectroscopy as a tool for investigating protein structures. J. Synchrotron Radiat.* **2000**, *7*, 289-295.
- (168) Wallace, B.A.; Janes, R.W. *Synchrotron radiation circular dichroism spectroscopy of proteins: Secondary structure, fold recognition and structural genomics. Curr. Opin. Chem. Biol.* **2001**, *5*, 567-571.
- (169) Wallace, B.A.; Lees, J.G.; Orry, A.J.W.; Lobley, A.; Janes, R.W. *Analysis of circular dichroism spectra of membrane proteins. Protein Sci.* **2003**, *12*, 875-884.
- (170) Farrell, H.M., Jr.; Jimenez-Flores, R.; Bleck, G.T.; Brown, E.M.; Butler, J.E.; Creamer, L.K.; Hicks, C.L.; Hollar, C.M.; Ng-Kwai-Hang, K.F.; Swaisgood, H.E. *Nomenclature of the proteins of cows' milk - sixth revision. J. Dairy Sci.* **2004**, *87*, 1641-1674.
- (171) Fox, P.F.; McSweeney, P.L.H. *Advanced dairy chemistry Volume I Proteins*, 3rd ed.; Kluwer Academic/Plenum: New York, 2003.
- (172) Brownlow, S.; Cabral, J.H.M.; Cooper, R.; Flower, D.R.; Yewdall, S.J.; Polikarpov, I.; North, A.C.; Sawyer, L. *Bovine β -lactoglobulin at 1.8 Å resolution - still an enigmatic lipocalin. Structure* **1997**, *5*, 481-495.
- (173) Kontopidis, G.; Holt, C.; Sawyer, L. *The ligand-binding site of bovine β -lactoglobulin: Evidence for a function? J. Mol. Biol.* **2002**, *318*, 1043-1055.
- (174) Mousavi, S.H.-A.; Chobert, J.-M.; Bordbar, A.-K.; Haertle, T. *Ethanol effect on the structure of β -lactoglobulin B and its ligand binding. J. Agric. Food Chem.* **2008**.
- (175) Qin, B.Y.; Bewley, M.C.; Creamer, L.K.; Baker, H.M.; Baker, E.N.; Jameson, G.B. *Structural basis of the tanford transition of bovine β -lactoglobulin. Biochemistry* **1998**, *37*, 14014-14023.
- (176) de la Fuente, M.A.; Singh, H.; Hemar, Y. *Recent advances in the characterisation of heat-induced aggregates and intermediates of whey proteins. Trends Food Sci. Technol.* **2002**, *13*, 262-274.

- (177) Kim, D.A.; Corneç, M.; Narsimhan, G. *Effect of thermal treatment on interfacial properties of β -lactoglobulin*. *J. Colloid Interface Sci.* **2005**, *285*, 100-109.
- (178) Livney, Y.D.; Corredig, M.; Dalgleish, D.G. *Influence of thermal processing on the properties of dairy colloids*. *Curr. Opin. Colloid Interface Sci.* **2003**, *8*, 359-364.
- (179) Considine, T.; Patel, H.A.; Anema, S.G.; Singh, H.; Creamer, L.K. *Interactions of milk proteins during heat and high hydrostatic pressure treatments - a review*. *Innov. Food Sci. Emerg. Technol.* **2007**, *8*, 1-23.
- (180) de Wit, J.N. *Thermal behaviour of bovine β -lactoglobulin at temperatures up to 150 °C. A review*. *Trends Food Sci. Technol.* **2009**, *20*, 27-34.
- (181) Croguennec, T.; O'Kennedy, B.T.; Mehra, R. *Heat-induced denaturation/aggregation of β -lactoglobulin A and B: Kinetics of the first intermediates formed*. *Int. Dairy J.* **2004**, *14*, 399-409.
- (182) Schokker, E.P.; Singh, H.; Creamer, L.K. *Heat-induced aggregation of β -lactoglobulin A and B with α -lactalbumin*. *Int. Dairy J.* **2000**, *10*, 843-853.
- (183) Schokker, E.P.; Singh, H.; Pinder, D.N.; Norris, G.E.; Creamer, L.K. *Characterization of intermediates formed during heat-induced aggregation of β -lactoglobulin AB at neutral pH*. *Int. Dairy J.* **1999**, *9*, 791-800.
- (184) Dickinson, E.; Matsumura, Y. *Time-dependent polymerization of β -lactoglobulin through disulphide bonds at the oil-water interface in emulsions*. *Int. J. Biol. Macromol.* **1991**, *13*, 26-30.
- (185) Floris, R.; Bodnar, I.; Weinbreck, F.; Alting, A.C. *Dynamic rearrangement of disulfide bridges influences solubility of whey protein coatings*. *Int. Dairy J.* **2008**, *18*, 566-573.
- (186) Xu, R.; Dickinson, E.; Murray, B.S. *Morphological changes in adsorbed protein films at the oil-water interface subjected to compression, expansion, and heat processing*. *Langmuir* **2008**, *24*, 1979-1988.
- (187) Corredig, M.; Dalgleish, D.G. *A differential microcalorimetric study of whey proteins and their behaviour in oil-in-water emulsions*. *Colloids Surf., B* **1995**, *4*, 411-422.
- (188) Chanasattru, W.; Decker, E.A.; McClements, D.J. *Physicochemical basis for cosolvent modulation of β -lactoglobulin functionality: Interfacial tension study*. *Food Res. Int.* **2007**, *40*, 1098-1105.
- (189) Chanasattru, W.; Decker, E.A.; McClements, D.J. *Influence of glycerol and sorbitol on thermally induced droplet aggregation in oil-in-water emulsions stabilized by β -lactoglobulin*. *Food Hydrocolloids* **2009**, *23*, 253-261.
- (190) McClements, D.J. *Modulation of globular protein functionality by weakly interacting cosolvents*. *Crit. Rev. Food Sci. Nutr.* **2002**, *42*, 417 - 471.

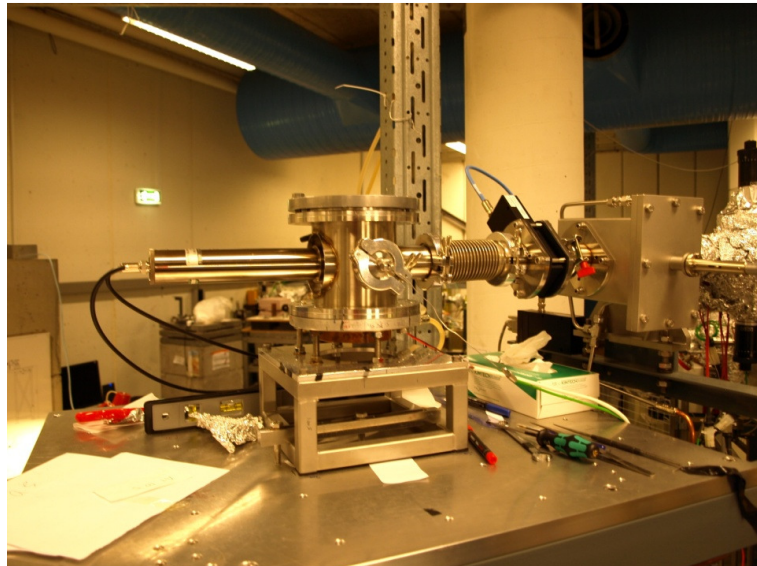
- (191) Permyakov, E.A.; Berliner, L.J. *α -Lactalbumin: Structure and function. FEBS Lett.* **2000**, *473*, 269-274.
- (192) Pike, A.C.W.; Brew, K.; Acharya, K.R. *Crystal structures of guinea-pig, goat and bovine α -lactalbumin highlight the enhanced conformational flexibility of regions that are significant for its action in lactose synthase. Structure* **1996**, *4*, 691-703.
- (193) Chrysina, E.D.; Brew, K.; Acharya, K.R. *Crystal structures of apo- and holo-bovine α -lactalbumin at 2.2-Å resolution reveal an effect of calcium on inter-lobe interactions. J. Biol. Chem.* **2000**, *275*, 37021-37029.
- (194) Farrell, H.M., Jr.; Qi, P.X.; Brown, E.M.; Cooke, P.H.; Tunick, M.H.; Wickham, E.D.; Unruh, J.J. *Molten globule structures in milk proteins: Implications for potential new structure-function relationships. J. Dairy Sci.* **2002**, *85*, 459-471.
- (195) Griko, Y.V. *Energetic basis of structural stability in the molten globule state: α -Lactalbumin. J. Mol. Biol.* **2000**, *297*, 1259-1268.
- (196) Ikeguchi, M.; Kato, S.; Shimizu, A.; Sugai, S. *Molten globule state of equine β -lactoglobulin. Proteins: Struct. Funct. Genetics* **1997**, *27*, 567-575.
- (197) Kunihiro, K. *The molten globule state as a clue for understanding the folding and cooperativity of globular-protein structure. Proteins: Struct. Funct. Genetics* **1989**, *6*, 87-103.
- (198) Ptitsyn, O.B. *The molten globule state*, in *Protein folding*, Creighton, T.E.; W.H. Freeman and Company: New York, 1992. p.243-300
- (199) Dickinson, E.; Matsumura, Y. *Proteins at liquid interfaces: Role of the molten globule state. Colloids Surf., B* **1994**, *3*, 1-17.
- (200) Hanssens, I.; van Ceunbroeck, J.-C.; Pottel, H.; Preaux, G.; van Cauwelaert, F. *Influence of the protein conformation on the interaction between α -lactalbumin and dimyristoylphosphatidylcholine vesicles. Biochim. Biophys. Acta: Biomembr.* **1985**, *817*, 154-164.
- (201) Dalgleish, D.G. *The conformations of proteins on solid/water interfaces - caseins and phosvitin on polystyrene latices. Colloids Surf.* **1990**, *46*, 141-155.
- (202) Dalgleish, D.G. *The size and conformations of the proteins in adsorbed layers of individual caseins on latices and in oil-in-water emulsions. Colloids Surf., B* **1993**, *1*, 1-8.
- (203) Dalgleish, D.G. *Conformations and structures of milk proteins adsorbed to oil-water interfaces. Food Res. Int.* **1996**, *29*, 541-547.
- (204) Fang, Y.; Dalgleish, D.G. *Dimensions of the adsorbed layers in oil-in-water emulsions stabilized by caseins. J. Colloid Interface Sci.* **1993**, *156*, 329-334.

- (205) Leermakers, F.A.M.; Atkinson, P.J.; Dickinson, E.; Horne, D.S. *Self-consistent-field modeling of adsorbed β -casein: Effects of pH and ionic strength on surface coverage and density profile. J. Colloid Interface Sci.* **1996**, *178*, 681-693.
- (206) ter Beek. *Nuclear magnetic resonance study of the conformation and dynamics of β -casein at the oil/water interface in emulsions.* **1996**.
- (207) Boyd, B.J.; Drummond, C.J.; Krodkiewska, I.; Grieser, F. *How chain length, headgroup polymerization, and anomeric configuration govern the thermotropic and lyotropic liquid crystalline phase behavior and the air-water interfacial adsorption of glucose-based surfactants. Langmuir* **2000**, *16*, 7359-7367.
- (208) Clogston, J.; Rathman, J.; Tomasko, D.; Walker, H.; Caffrey, M. *Phase behavior of a monoacylglycerol: (Myverol 18-99K)/water system. Chem. Phys. Lipids* **2000**, *107*, 191-220.
- (209) de Campo, L.; Yaghmur, A.; Sagalowicz, L.; Leser, M.E.; Watzke, H.; Glatter, O. *Reversible phase transitions in emulsified nanostructured lipid systems. Langmuir* **2004**, *20*, 5254-5261.
- (210) Dong, Y.-D.; Dong, A.W.; Larson, I.; Rappolt, M.; Amenitsch, H.; Hanley, T.; Boyd, B.J. *Impurities in commercial phytantriol significantly alter its lyotropic liquid-crystalline phase behavior. Langmuir* **2008**, *24*, 6998-7003.
- (211) Hyde, S. *Identification of lyotropic liquid crystalline mesophases*, in *Handbook of applied surface and colloid chemistry*, Holmberg, K.; John Wiley & Sons: Chichester, 2002. p.299-320.
- (212) Hyde, S.; Andersso, S.; Larsson, K.; Blum, Z.; Landh, T.; Lidin, S.; Ninham, B.W. *The language of shape: The role of curvature in condensed matter: Physics, chemistry and biology*; Elsevier B.V.: New York, 1997. p.199-235.
- (213) Israelachvili, J.N.; Mitchell, D.J.; Ninham, B.W. *Theory of self-assembly of hydrocarbon amphiphiles into micelles and bilayers. J. Chem. Soc., Faraday Trans. 2* **1976**, *72*, 1525-1568.
- (214) Johnsson, M.; Barauskas, J.; Tiberg, F. *Cubic phases and cubic phase dispersions in a phospholipid-based system. J. Am. Chem. Soc.* **2005**, *127*, 1076-1077.
- (215) Larsson, K.; Lindblom, G. *Molecular amphiphile bilayers forming a cubic phase in amphiphile-water systems. J. Dispersion Sci. Technol.* **1982**, *3*, 61-66.
- (216) Qiu, H.; Caffrey, M. *The phase diagram of the monoolein/water system: Metastability and equilibrium aspects. Biomaterials* **2000**, *21*, 223-234.
- (217) Sagalowicz, L.; Mezzenga, R.; Leser, M.E. *Investigating reversed liquid crystalline mesophases. Curr. Opin. Colloid Interface Sci.* **2006**, *11*, 224-229.
- (218) Templer, R.H.; Seddon, J.M.; Duesing, P.M.; Winter, R.; Erbes, J. *Modeling the phase behavior of the inverse hexagonal and inverse bicontinuous cubic phases in 2:1 fatty acid/phosphatidylcholine mixtures. J. Phys. Chem. B* **1998**, *102*, 7262-7271.

- (219) Dong, Y.-D.; Larson, I.; Hanley, T.; Boyd, B.J. *Bulk and dispersed aqueous phase behavior of phytantriol: Effect of vitamin E acetate and F127 polymer on liquid crystal nanostructure. Langmuir* **2006**, *22*, 9512-9518.
- (220) Spicer, P.T. *Cubosomes: Bicontinuous cubic liquid crystalline nanostructured particles*, in *Dekker encyclopedia of nanoscience and nanotechnology*, Schwarz A., Contescu, C. I.; CRC Press: New York, 2004.
- (221) Dong, Y.-D.; Tilley, A.J.; Larson, I.; Lawrence, M.J.; Amenitsch, H.; Rappolt, M.; Hanley, T.; Boyd, B.J. *Nonequilibrium effects in self-assembled mesophase materials: Unexpected supercooling effects for cubosomes and hexosomes. Langmuir* **2010**, *26*, 9000-9010.
- (222) Abraham, T.; Hato, M.; Hirai, M. *Polymer-dispersed bicontinuous cubic glycolipid nanoparticles. Biotechnol. Prog.* **2005**, *21*, 255-262.
- (223) Almgren, M.; Borne, J.; Feitosa, E.; Khan, A.; Lindman, B. *Dispersed lipid liquid crystalline phases stabilized by a hydrophobically modified cellulose. Langmuir* **2007**, *23*, 2768-2777.
- (224) Buchheim, W.; Larsson, K. *Cubic lipid-protein-water phases. J. Colloid Interface Sci.* **1987**, *117*, 582-583.
- (225) Boyd, B.J.; Rizwan, S.B.; Dong, Y.-D.; Hook, S.; Rades, T. *Self-assembled geometric liquid-crystalline nanoparticles imaged in three dimensions: Hexosomes are not necessarily flat hexagonal prisms. Langmuir* **2007**, *23*, 12461-12464.

Chapter 2

Changes in β -lactoglobulin conformation at the oil-water interface of emulsions studied by synchrotron radiation circular dichroism spectroscopy



The SRCD set-up at ISA-ASTRID, Aarhus, Denmark

Changes in β -Lactoglobulin Conformation at the Oil/Water Interface of Emulsions Studied by Synchrotron Radiation Circular Dichroism Spectroscopy

Jiali Zhai,^{†,‡} Andrew J. Miles,[§] Leonard Keith Pattenden,^{||} Tzong-Hsien Lee,[†]
Mary Ann Augustin,[‡] B. A. Wallace,[§] Marie-Isabel Aguilar,^{*,†} and Tim J. Wooster^{*,‡}

Department of Biochemistry and Molecular Biology, Monash University, Clayton, Victoria 3800, Australia, CSIRO Food and Nutritional Sciences, Sneydes Road, Werribee, Victoria 3030, Australia, Department of Crystallography, Birkbeck College, University of London, London, WC1E 7HX, United Kingdom, and Health Innovations Research Institute, School of Medical Sciences, RMIT University, Bundoora, Victoria 3083, Australia

Received May 9, 2010; Revised Manuscript Received July 5, 2010

The structure of proteins at interfaces is a key factor determining the stability as well as organoleptic properties of food emulsions. While it is widely believed that proteins undergo conformational changes at interfaces, the measurement of these structural changes remains a significant challenge. In this study, the conformational changes of β -lactoglobulin (β -Lg) upon adsorption to the interface of hexadecane oil-in-water emulsions were investigated using synchrotron radiation circular dichroism (SRCD) spectroscopy. Far-UV SRCD spectra showed that adsorption of β -Lg to the O/W interface caused a significant increase in non-native α -helix structure, accompanied by a concomitant loss of β -sheet structure. Near-UV SRCD spectra revealed that a considerable disruption of β -Lg tertiary structure occurred upon adsorption. Moreover, heat-induced changes to the non-native β -Lg conformation at the oil/water interface were very small compared to the dramatic loss of β -Lg secondary structure that occurred during heating in solution, suggesting that the interface has a stabilizing effect on the structure of non-native β -Lg. Overall, our findings provide insight into the conformational behavior of proteins at oil/water interfaces and demonstrate the applicability of SRCD spectroscopy for measuring the conformation of adsorbed proteins in optically turbid emulsions.

Introduction

Emulsions are frequently used in the food and pharmaceutical industries and there is currently significant focus on the properties of the molecules that facilitate their formation and control their physical stability.^{1–4} Proteins are common emulsifiers and their structure at oil/water (O/W) interfaces is a key factor determining the stability as well as organoleptic properties of food emulsions.^{5–7} Milk proteins are frequently used as emulsifiers because their natural amphiphilicity promotes emulsification and their polymeric structure aids droplet stabilization.^{8–10} The two main classes of milk proteins are the caseins and whey proteins.¹¹ β -Lactoglobulin (β -Lg) constitutes around 80% of whey protein and is among the most studied milk protein.¹¹ The native conformation of β -Lg consists of nine antiparallel β -strands, eight of which form a hydrophobic β -barrel with one long α -helix and four short 3_{10} helices on the outer surface.^{12,13} In comparison, the conformation of β -Lg adsorbed at emulsion interfaces is thought to differ from the native conformation in aqueous solution.¹⁴

The structure and denaturation of β -Lg has been extensively studied in solution, both in the presence of chemical denaturants (alcohols,^{15,16} ligands,^{17,18} and surfactants^{19,20}) and physical denaturants (heat and pressure).²¹ In the presence of chemical denaturants, it is well-known that β -Lg converts from its native

β -sheet rich conformation into one with a high proportion of non-native α -helix.^{15,20} In contrast, only a few studies have examined protein conformation at O/W interfaces, and their results are contradictory in the case of β -Lg. While Fourier transform infrared spectroscopy (FTIR) studies indicate that β -Lg loses some β -sheet structure upon adsorption to O/W interfaces, the results differ as to whether the loss of β -sheet structure is accompanied by a concomitant increase in unordered structure or ordered α -helical structure.^{22–25} Moreover, Husband et al.²³ obtained conflicting results when studying the conformation of β -Lg in refractive index matched emulsions (RIME) using FTIR and circular dichroism (CD). FTIR measurements showed no change in α -helix and an increase in β -sheet content, while CD indicated there was an increase in α -helix content upon β -Lg adsorption to emulsion interfaces.²³ These differences may be due to the difficulty in obtaining CD spectra of proteins in emulsions, where light scattering arising from the emulsion droplets and high sample absorbance leads to very weak CD signals.

Attempts to study protein conformation at emulsion interfaces with CD have been undertaken by mimicking the O/W interface encountered in emulsions.^{20,23,26} Zhang and Keiderling²⁰ examined the conformational changes of β -Lg in the presence of lipid vesicles. The insertion of β -Lg into this particular lipid–water interface induced an increase in α -helix in β -Lg.²⁰ Husband et al.²³ made a considerable advance by developing a refractive index (RI) matching method which enabled CD measurements of protein conformation at O/W interfaces. However, adding glycerol or polyethylene glycol can change the hydration environment around the protein, thereby changing

* To whom correspondence should be addressed. E-mail: mibel.aguilar@med.monash.edu.au (M.-I.A.); timothy.wooster@csiro.au (T.J.W.).

[†] Monash University.

[‡] CSIRO Food and Nutritional Sciences.

[§] University of London.

^{||} RMIT University.

its conformation.^{27–29} Furthermore, the RI of the triglyceride oils conventionally used in food is much higher (1.46–1.47) than hexadecane (1.434) and would require almost pure glycerol to match the RI.

Despite these previous FTIR and CD studies, the conformation of β -Lg at the interface of oil-in-water emulsions remains poorly understood. Furthermore, there has been little examination of protein thermal stability at emulsion interfaces. Since emulsions are frequently exposed to heat during food processing, it is important to understand how heat affects the conformation of proteins adsorbed at their interface. Therefore, alternative CD methods are needed to overcome light scattering effects to allow direct measurement of protein structure at emulsion interfaces as a function of temperature. In the present study, we developed a new approach, based on synchrotron radiation circular dichroism (SRCD) spectroscopy, to investigate the adsorption-induced changes and thermal stability of β -Lg in a model oil-in-water emulsion. This is the first SRCD spectroscopy study of proteins at emulsion interfaces and provides new insight into surface-mediated conformational changes.

Materials and Methods

Materials. Fresh bovine milk was obtained from Tatura Milk Industries Limited (Tatura, Vic, Australia). The milk was skimmed at the pilot plant of the CSIRO Division of Food and Nutritional Sciences (Werribee, Vic, Australia). β -Lg was then purified from the freshly skimmed milk following the method developed by de Jongh et al.,³⁰ with some modifications. The purity and molecular mass of the isolated β -Lg variants were confirmed using a reversed phase HPLC-MS system (Agilent Technologies, Santa Clara, CA). For detailed experimental methods, see Supporting Information.

Tris(hydroxymethyl)aminomethane (Tris), sodium chloride (NaCl), sodium phosphate (monobasic and dibasic), hexadecane, glycerol, and sodium dodecyl sulfate (SDS) were purchased from Sigma-Aldrich (St. Louis, MO). All chemicals and solvents were of analytical grade. The Ultra pure water was prepared by a Purelab Ultra Genetic purification system (ELGA LabWater) and used for all the experiments.

Emulsion Preparation. Solutions of purified β -Lg were prepared in 10 mM sodium phosphate buffer, pH 7. Protein concentration was calculated from solution absorbance measured at 280 nm (the molar absorption coefficient of β -Lg was $0.96 \text{ mL mg}^{-1} \text{ cm}^{-1}$).¹¹ A series of 20% (v/v) hexadecane oil-in-water emulsions stabilized by 1–10 mg/mL β -Lg were prepared by homogenization at room temperature. Hexadecane and the required amount of protein solution were blended at 8000 r/min for 2 min using a high-speed mixer (Ultra Turrax, Janke and Kunkel, Germany) and then passed through a high-pressure valve homogenizer twice at approximately 500 bar (EmulsiFlex C5, Avestin, Canada). To prepare the emulsion baseline, 0.3% (w/w) SDS-stabilized emulsions containing 20% (v/v) hexadecane were prepared using identical conditions to those used for the preparation of β -Lg-stabilized emulsions. All emulsions were freshly prepared on site at the ISA-synchrotron where the UV1 SRCD beamline is located (Institute for Storage Ring Facilities, Aarhus University)³¹ and experiments were performed within 24 h of preparation.

Particle Size Determination. Commercial β -Lg (Sigma-Aldrich, St. Louis, MO) was used in experiments to determine the relationship between β -Lg concentration and the average emulsion particle size. Purified genetic variants were used to prepare emulsions at 0.3% (w/w) protein concentration and were examined for particle size and the surface coverage. The particle size distribution of the emulsions was measured using laser light diffraction (Malvern Mastersizer 2000, Worcestershire, U.K.) equipped with a Hydro SM small volume sample dispersion unit. The emulsion droplet size distribution was calculated from a best fit between the measured scattering pattern and a model scattering pattern of equivalent polydisperse spheres (Mie theory). A differential refractive index of 1.079 (1.435 for hexadecane and 1.33

for water) and an absorbance of 0.001 were used as optical properties of the dispersed hexadecane droplets. The particle size was reported as the surface area moment mean diameter $d_{3,2}$ ($= \sum n_i d_i^3 / \sum n_i d_i^2$, where n_i is the number of particles with diameter d_i) and the weight average mean diameter $d_{4,3}$ ($= \sum n_i d_i^4 / \sum n_i d_i^3$). For each emulsion, five individual measurements were made and reported as the average.

Determination of the Adsorbed Amount of Protein. Fresh emulsions were centrifuged at $11600 \times g$ for 15 min to separate the oil droplets (the cream layer) and the supernatant phase containing unadsorbed protein. The concentration of unadsorbed protein in the supernatant was obtained by measuring absorbance at 280 nm. The adsorbed amount of protein was calculated from the specific surface area of the emulsion droplets ($\propto d_{3,2}^{-1}$) and is reported as the surface coverage (weight of protein per unit of surface area).

SRCD Measurements. All SRCD measurements were performed on the UV1 beamline of the SRCD station at the ISA.³¹ The SRCD beamline was calibrated using camphorsulfonic acid for optical rotation and wavelength at the beginning of every beam fill.³² A circular demountable quartz cell (Hellma GmbH and Co., Germany) of 0.01 cm path length was used for far-UV SRCD measurements at 20 °C. The operating conditions were 1 nm bandwidth, 2.69 s averaging time, 3 scans for solution sample, or 8 scans for emulsion sample. The spectra were truncated at the low wavelength as defined in Miles and Wallace.³² For the RI-matched emulsion, 58% (v/v) glycerol was added to freshly prepared emulsions. Unless otherwise noted, all measurements were made at 20 °C in a temperature-controlled sample holder. For thermal denaturation studies, an enclosed quartz cell (0.01 cm path length; Hellma GmbH and Co., Germany) was used instead of the demountable quartz plates. The temperatures examined were 20, 50, and 81 °C. For each case, the first and third spectra were compared to ensure the sample had reached equilibrium at that temperature. The near-UV SRCD spectra were collected under similar conditions to those used for far-UV SRCD, except that an enclosed quartz cell (Hellma GmbH and Co., Germany) with a path length of 0.5 cm was used.

SRCD Data Analysis and Secondary Structure Calculations. All spectra were processed using CDtool software.³³ The spectra were calibrated, averaged, smoothed, and baseline-subtracted. All spectra presented were truncated at a low wavelength defined by the linearity of the detection, as described in Miles and Wallace.³² The far-UV SRCD spectra were converted to mean residue ellipticity [θ] units, using a mean residue weight of 113 for β -Lg. Secondary structural content calculations were performed using DICHROWEB, an interactive Web server that incorporates various methods and a wide range of protein spectral databases.³⁴ The three methods used in this study were SELCON3,³⁵ CONTINLL,³⁶ and CDSSTR.³⁷ The reference set SP175 (optimized for 190–240 nm) was used in the spectral analysis.³⁸ A goodness-of-fit parameter (the NRMSD) was calculated for all methods.³⁹

Results and Discussion

Design of Emulsion Systems. The aim of this work was to study the conformation of β -Lg adsorbed at the interface of oil-in-water emulsions using SRCD spectroscopy. The purification protocol yielded genetic variants of β -Lg with a very high purity (>98%) for the investigation of β -Lg structures (see Supporting Information, Figure 1). Both β -Lg A and β -Lg B have the same near and far-UV SRCD spectra in solution (data not shown). Therefore, the current study only focused on the structure of β -Lg A adsorbed at the interface of hexadecane oil-in-water emulsions.

Two experimental approaches were used in this work (see Supporting Information, Figure 2). In the first approach, glycerol (58% v/v) was added to the aqueous phase of the emulsion to match the RI of the two phases, effectively making the emulsion translucent and measurable using SRCD spectroscopy. In a second approach, a novel method was developed to measure

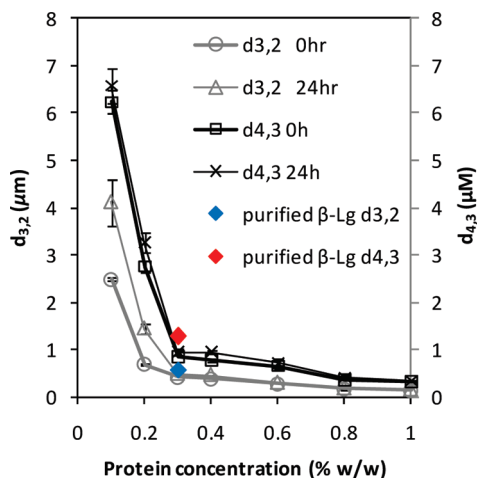


Figure 1. Mean particle diameter ($d_{3,2}$ and $d_{4,3}$) of 20% v/v hexadecane oil-in-water emulsions stabilized by a range of commercial β -Lg concentrations (0.1–1.0% w/w). Measurements were made immediately after emulsion preparation and after aging for 24 h. Values are the average of five individual measurements and the standard deviations are shown. Single dots represent the particle size of emulsions prepared using 0.3% (w/w) purified β -Lg A.

the conformation of β -Lg adsorbed at the interface of O/W emulsions without the need for RI matching. In this emulsion, light scattering from oil droplets generated a significant background in the far-UV region. To eliminate these light scattering effects, a baseline spectrum of an emulsion having similar light scattering properties as the protein stabilized emulsion was subtracted from the protein emulsion's SRCD spectrum. Specifically, SDS, which is a nonchiral surfactant frequently used in the formation of oil-in-water emulsions, was used to generate the hexadecane oil-in-water emulsion.

Particle Size Determination of β -Lg Stabilized Emulsions.

The SRCD spectrum of an emulsion can be confounded by signals from protein both in solution and adsorbed at the interface. Therefore, it is important to design emulsions where there is a minimum of unadsorbed protein. To determine the optimum protein concentration for emulsion preparation, the influence of protein concentration on emulsion particle size was examined (Figure 1). Figure 1 shows that the particle diameter $d_{3,2}$ was significantly reduced from 2.5 to 0.4 μm as protein concentration increased from 0.1 to 0.3% (w/w). Further increases in protein concentration greater than 0.3% (w/w) resulted in a gradual decrease in average particle diameter, reaching 0.15 μm at 1.0% (w/w) protein concentration. The decrease in the particle diameter of emulsions stabilized by high protein concentrations suggests that most of the protein should be adsorbed at the O/W interface at 0.3% (w/w). Measurements made after 24 h showed that the particle diameter of emulsions made with 0.3–1.0% (w/w) β -Lg remained fairly constant. A similar trend was also seen with $d_{4,3}$. In the case of 0.1 and 0.2% (w/w) β -Lg stabilized emulsions, an appreciable amount of creaming was observed. Creaming arose because emulsion droplets of this size have sufficient buoyancy in the aqueous continuous phase to undergo physical separation under gravity over this time period.

The amount of adsorbed β -Lg was assayed by centrifuging the emulsion and measuring the unadsorbed protein content in the supernatant. Protein surface coverage was only assessed after one centrifugation, which does not account for protein trapped between droplets in the cream layer. The results showed that approximately 90% of the protein was at the interface of the emulsion stabilized by 0.3% (w/w) β -Lg, which corresponds

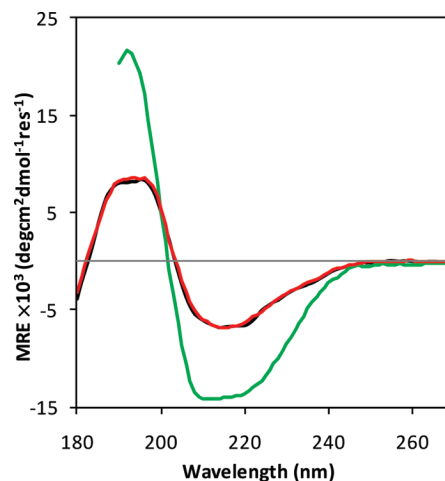


Figure 2. Far-UV SRCD spectra of β -Lg in 10 mM sodium phosphate buffer pH 7 (black line), in 58% (v/v) glycerol/10 mM phosphate buffer (red line), and in the RI-matched emulsion with 58% glycerol (green line). The spectra were measured in situ at 20 °C.

to a surface coverage (Γ) of 1.29 mg/m². This value is slightly less than a densely packed monolayer of adsorbed β -Lg ($\Gamma = 1.65 \text{ mg/m}^2$)⁴⁰ and indicates that β -Lg probably forms a slightly expanded monolayer at the oil droplet interface. Consequently, 0.3% (w/w) β -Lg stabilized emulsions were considered to be relatively stable, to have almost all of the protein adsorbed at the interface and to have a monolayer of adsorbed protein allowing conformational change. Therefore, a 20% (v/v) hexadecane oil-in-water emulsion stabilized by 0.3% (w/w) β -Lg was chosen for subsequent analysis of adsorbed protein conformation.

Secondary Structure of β -Lg Adsorbed at the O/W Interface. The conformation of β -Lg in solution and at the interface of oil-in-water emulsions was measured using SRCD spectroscopy. Figure 2 shows the far-UV CD profiles of β -Lg in solution, in 58% glycerol, and at the O/W interface of the RI-matched emulsion. In the far-UV region, β -Lg in solution exhibited a minimum at around 216 nm, a zero-crossing at 203 nm and a maximum at 195 nm, indicating high β -sheet content. However, the spectrum of β -Lg adsorbed at the interface of the RI-matched emulsion had two negative minima at 219 and 209 nm and a zero crossing at 201 nm. Moreover, the magnitudes of the positive and negative CD signals of β -Lg in the RI-matched emulsion increased considerably. In comparison to the protein in solution, the overall shape and magnitude of the adsorbed β -Lg spectrum indicated a considerable increase in α -helical content.

Because a large amount of glycerol (58% v/v) was added to the emulsion to match the RI, the effect of glycerol on protein conformation was also investigated. The results indicate that the amount of glycerol used in this study only had a small impact on β -Lg secondary structure in solution as shown in Figure 2. However, previous studies have shown that higher glycerol concentrations can affect the secondary structure of globular proteins in solution, due to the preferential interactions that occur between the protein hydration surface and the cosolvent and solvent molecules.^{27–29} Furthermore, β -Lg is thought to unfold to some extent at emulsion interfaces, exposing nonpolar groups to the cosolvent, which may increase the preferential interaction between β -Lg and glycerol. This may result in a larger effect of glycerol on the secondary structure of the adsorbed protein compared to the native protein in solution.

To avoid the possible negative effect of glycerol on protein conformation, the unmatched emulsion was examined directly

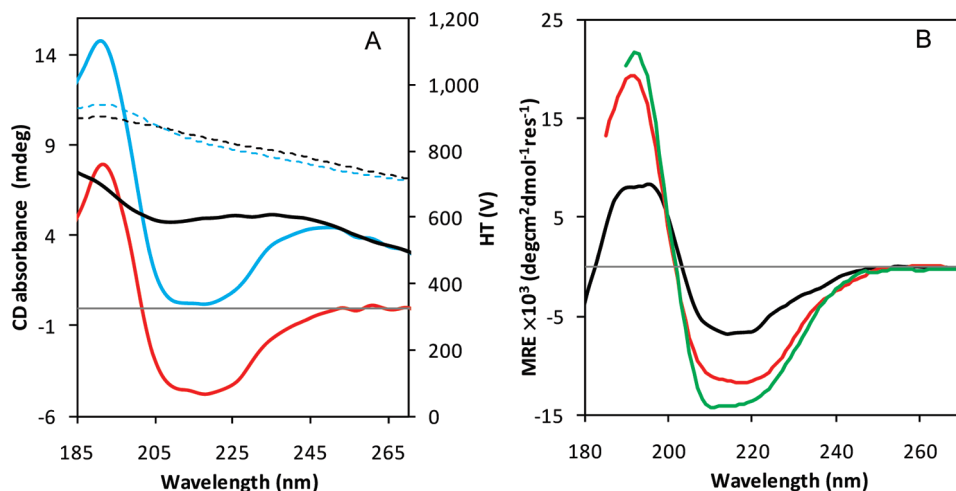


Figure 3. (A) Far-UV SRCD spectra of the unmatched SDS stabilized emulsion (black line), the unmatched β -Lg stabilized emulsion (red line) and the baseline corrected β -Lg stabilized emulsion (blue line). HT signals are represented in dashed line (black for SDS emulsion and blue for β -Lg emulsion). (B) Far-UV SRCD spectra of β -Lg in 10 mM phosphate buffer (black line), the RI-matched emulsion (green line), and the unmatched emulsion (red line). The spectra were measured in situ at 20 °C.

using SRCD spectroscopy. As a result of the high intensity of the synchrotron photon flux, the spectrum of the unmatched emulsion (Figure 3A) exhibited a dramatically higher signal-to-noise ratio compared to that measured using conventional CD reported elsewhere.²³ However, light scattering from the emulsion droplets caused the spectrum to be positively displaced from the x -axis, particularly over the region of 255–270 nm. To account for this background signal, an emulsion that had similar light scattering properties as the protein stabilized emulsion, but also did not absorb the circularly polarized light was prepared. Figure 3A shows that the high tension (HT) voltage signals of the two emulsions were similar, suggesting that the SDS stabilized emulsion had similar light scattering properties as the protein stabilized emulsion. Moreover, the SRCD spectrum of the SDS (nonchiral) stabilized emulsion replicated the positive displacement seen in the β -Lg stabilized emulsion and allowed the positive background signal to be quantitatively offset. The subtracted spectrum of the β -Lg stabilized emulsion was then compared with the spectrum of the β -Lg stabilized RI-matched emulsion as shown in Figure 3B. The spectra of adsorbed β -Lg in the RI-matched emulsion and in the unmatched emulsion were very similar, validating this new approach for measuring protein structures at emulsion O/W interfaces in situ using SRCD spectroscopy.

To obtain an estimate of the secondary structure content, all far-UV SRCD spectra were analyzed using the SELCON3 method in combination with reference set SP175 via the Dichroweb online server (see Supporting Information, Table 1). The solution structure of β -Lg was calculated to be comprised of 36% β -sheet and 14% α -helix, which is consistent with the proportion determined from the β -Lg crystal structure (PDB: 1bsy)⁴¹ by the DSSP program (40.1% β -sheet and 16.7% α -helix).⁴² The presence of 58% (v/v) glycerol in buffer caused minimal change in β -Lg secondary structural content. However, upon adsorption to the O/W interface, the α -helical content of β -Lg increased from 14% in solution to 35% in the matched emulsion, whereas the β -sheet content decreased from 36 to 20%. Adsorbed β -Lg was 35% α -helical in the RI-matched emulsion, whereas there was only 30% α -helix in β -Lg in the unmatched emulsion. This difference in helical content may be due to the effects of glycerol. The presence of glycerol in the aqueous phase changes solvent properties which may alter protein conformation at emulsion interfaces. Nevertheless, the

results of the RI-matched and the unmatched emulsions were in broad agreement in terms of the adsorption-induced structural change of β -Lg.

Fitting the spectra of β -Lg in the emulsion environment must be carefully interpreted because the available reference databases mostly contain spectra of known proteins in solution rather than in emulsions with 20% (v/v) oil. For comparison, two other algorithms, CONTIN and CDSSTR, were also used to calculate the secondary structures (see Supporting Information, Table 1). For the adsorbed β -Lg in emulsions, the various methods yielded relatively consistent results in terms of the α -helix and β -sheet content. Therefore, it can be concluded that adsorption to the O/W interface induces an increase in the α -helix content in adsorbed β -Lg secondary structure at the expense of β -sheet structure. Previous CD and FTIR studies produced contradictory results in terms of secondary structural changes of β -Lg upon adsorption to the O/W interface.^{22–25} While some studies reported a small increase in α -helix with little or no change in β -sheet structure, others found a significant increase in unordered secondary structure. In particular, our results differ to those of Husband et al., the only other study to use CD to measure β -Lg conformation at emulsion interfaces.²³ The difference between the two studies most likely arises because different β -Lg concentrations were examined, which alters protein surface coverage and the amount of protein in the continuous phase. In this study, we have used a novel approach to correct for light scattering effects and together with the application of SRCD spectroscopy, have improved the signal-to-noise of the spectra and the wavelength down to which spectra can be collected.

Tertiary Structure of β -Lg Adsorbed at the O/W Interface. To study the tertiary structural changes of β -Lg upon adsorption to O/W interfaces, near-UV SRCD spectra of β -Lg in solution and in emulsions were recorded. In the near-UV region of 260–340 nm, aromatic residues in proteins give characteristic CD signals depending on their number, mobility, and local environment. Figure 4 shows the near-UV SRCD profiles of β -Lg in solution and in the RI-matched emulsion. The measurement of near-UV CD spectra of β -Lg adsorbed at emulsion interfaces can only be made in RI-matched emulsions because near-UV CD signals are much weaker than those in the far-UV region. The spectrum of native β -Lg in solution shows a profile of two sharp negative peaks at 285 and 293 nm arising from tryptophan residues, and two shallow minima at

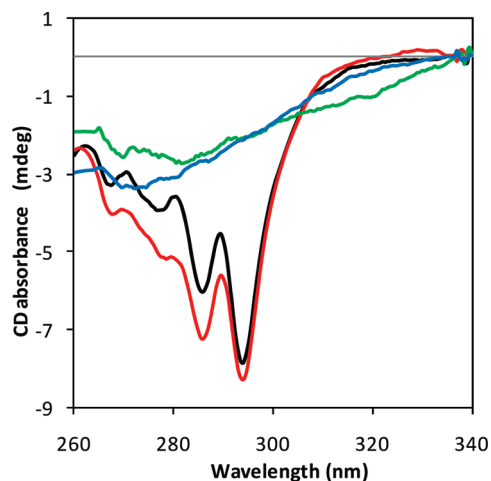


Figure 4. Near-UV SRCD spectra of β -Lg in 10 mM sodium phosphate buffer pH 7 at 20 °C (black line) and at 81 °C (blue line), in 58% (v/v) glycerol/10 mM phosphate buffer at 20 °C (red line), and in the R.I. matched emulsion with 58% glycerol at 20 °C (green line).

266 and 277 nm originating from phenylalanine and tyrosine residues.⁴³ In the native structure of β -Lg, Trp-19 is located inside the hydrophobic β -barrel and has a much lower solvent accessibility than Trp-61, which is partially exposed to water. It has been reported that the two peaks at 285 and 293 nm largely reflect the environment around Trp-19.^{18,44–46} The presence of glycerol had little effect on the near-UV SRCD spectrum of β -Lg in solution (Figure 4).

Upon β -Lg adsorption to the O/W interface, the characteristic peaks at 285 and 293 nm disappeared and collapsed into a broad negative band with few features. The lack of definition in the Near-UV CD spectrum of β -Lg adsorbed at the O/W interface indicates a significant change in the environment of aromatic residues, which could be due to overall loss of tertiary structure or to the binding of hexadecane molecules inside the hydrophobic β -barrel. However, several studies have shown that the two peaks at 285 and 293 nm are strongly retained upon ligand (retinol and SDS) binding to the β -barrel of β -Lg.^{17,18} To assess if the spectral changes were due to the loss of tertiary structure, β -Lg in solution was heated to 81 °C (9 °C above its thermal denaturation temperature of 72 °C). The near-UV SRCD spectrum of thermally denatured β -Lg in solution gave a profile with a broad and shallow negative band similar to that of β -Lg adsorbed at the interface of the O/W emulsion. Therefore, it can be concluded that adsorption of β -Lg to the interface of O/W emulsions results in considerable loss of tertiary structure, which if analogous to thermal denaturation may correspond to the collapse of the β -barrel.

Thermal Stability of β -Lg in Solution and Adsorbed at the O/W Interface. To compare the thermal stability of β -Lg in solution and at the O/W interface, far-UV SRCD spectra were recorded at room temperature (20 °C), 50 and 81 °C. In the solution spectra (Figure 5), a small decrease in the negative peak and a slight shift in the zero-crossing occurred at 50 °C, indicating a small change in the secondary structure at 50 °C. At 81 °C, the characteristic CD profile of β -Lg was completely lost, indicating an appreciable loss of native secondary structure and a shift toward a random coil conformation. This result agrees with many studies of the thermal behavior of β -Lg in solution, which show that the native dimer of β -Lg dissociates to the monomer and small conformational changes may occur at temperatures below the denaturation point.²¹ Above the thermal

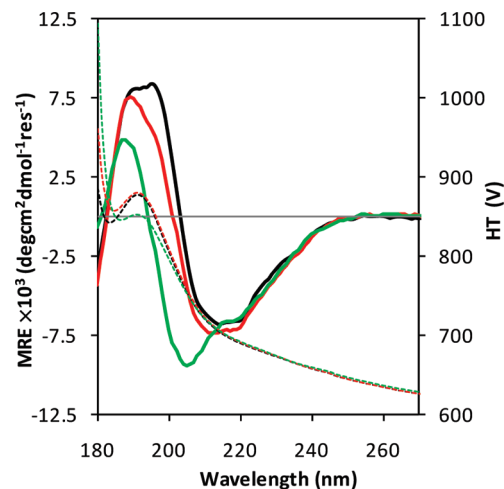


Figure 5. Far-UV SRCD spectra of β -Lg in 10 mM sodium phosphate buffer pH 7 measured in situ at 20 °C (black line), 50 °C (red line), and 81 °C (green line). Dashed lines represent HT of the corresponding spectra.

denaturation temperature, β -Lg unfolds and exposes reactive thiol groups, resulting in an irreversible conformational change due to disulfide exchange.²¹

The far-UV SRCD spectra of β -Lg in the RI-matched emulsion and in the unmatched emulsion are presented in Figure 6A and B, respectively. In both cases, the spectral peak positions and zero-crossing points remain relatively constant upon heating to various temperatures. In comparison to the thermal denaturation of β -Lg in solution, the results in the emulsions indicate considerably less change in secondary structure of β -Lg at the O/W interface at higher temperatures. However, increasing temperature resulted in a decrease in the intensity of the CD signals. To determine whether the signal decrease was due to a conformational change, the concentration-dependent HT voltage values were examined, as they are proportional to the absorbance of the sample. Figure 6A and B show that the HT values of the emulsion sample (dashed lines) also decreased with the decrease in CD signals as the temperature increased. This suggests that the loss in the SRCD signal may be due to a decrease in protein concentration as well as some conformational change as a result of temperature-induced emulsion creaming (see Supporting Information, Figure 3). Heating the emulsion generally accelerates creaming, where buoyant emulsion droplets rise to the top of the sample over time causing an increase in sample concentration at the top and a decrease in sample concentration at the bottom. Because the SRCD instrument only detects the sample in the central area of the cell, if creaming occurs, the protein concentration in the detection area will decrease and lead to an overall loss in SRCD signal. Therefore, the results suggest that the O/W interface not only induces an increased α -helical content in β -Lg but also stabilizes this non-native secondary structure against thermal denaturation.

In summary, this study has developed a new SRCD spectroscopy method for the measurement of protein structure at emulsion interfaces. Our results provide high quality data which permit further insight into the conformational rearrangement of β -Lg at emulsion interfaces upon adsorption and during heating. Like several other denaturants (alcohols, ligands/surfactants, and phospholipids), the hydrophobic O/W interface triggers the conversion from the native β -sheet structure of β -Lg to a conformation with a high proportion of non-native α -helix.^{15,20} There are certainly common features between O/W interfaces and solution-based denaturants, such as the role of hydrophobic

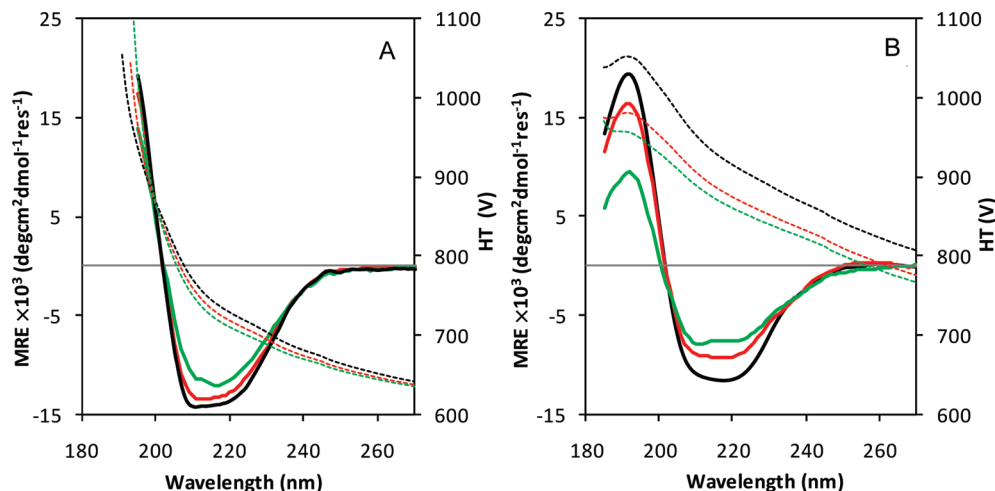


Figure 6. Far-UV SRCD spectra of (A) β -Lg in the RI-matched emulsion and (B) β -Lg in the unmatched emulsion. Both spectra were measured in situ at 20 °C (black line), 50 °C (red line), and 81 °C (green line). Dashed lines represent HT of the corresponding spectra.

interactions in driving conformational change. However, the mechanism of protein unfolding and stabilization in emulsions is likely to differ from that in solution since the defined interface found in emulsions provides a unique molecular environment. The approach developed in this study now provides the basis for future detailed thermodynamic analysis of this unfolding phenomenon.

Conclusion

This study represents the first report of high signal-to-noise SRCD spectra of proteins at the O/W interface of emulsions. The adsorption of β -Lg to the O/W interface induced a significant amount of non-native α -helix, accompanied by the loss of the well-defined tertiary structure. In addition, the non-native α -helical-rich secondary structure of adsorbed β -Lg was significantly stabilized at the interface against heating. The results suggest that the unfolding of β -Lg and the non-native α -helical-rich structure are important in establishing the hydrophobic interactions with the oil phase. The present study has also provided new insight into the conformational stability of β -Lg adsorbed to emulsion interfaces during heating, which has important implications for improving emulsion properties under thermal processing in industry. It has also demonstrated that the high photon intensity of the SRCD beamline allows the in situ measurement of the structure of adsorbed protein in highly absorbing and optically turbid emulsion systems. Thus, we have established a new method for studying protein conformation at various interfaces, which has revealed new insight into the effects of surface-mediated stresses on protein structure.

Acknowledgment. The authors would like to sincerely thank Dr. Søren Vørnning Hoffman and Dr. Nykola Jones for helpful advice and assistance, the Institute for Storage Ring Facilities in Aarhus (ISA), Denmark, for provision of beamtime (under the EU Integrated Infrastructure Initiative (I3), Integrated Activity on Synchrotron, and Free Electron Laser Science (IA-SFS), Contract No. RII3-CT-2004-506008), the AMFRP for travel funding (Grant No. 08/09-s-14), and the Australian Research Council, Dairy Innovation Australia Limited, and the Australian National University for financial support through ARC Linkage Grant No. LP0774909 and by grants from the U.K. Biotechnology and Biological Science Research Council (to B.A.W.).

Supporting Information Available. The detailed experimental method for purification of β -Lg genetic variants and the chromatographic data are included in this section. The secondary structural component analysis is included in Table 1. A schematic of the emulsion design and pictures of SRCD cells with fresh emulsion and heated emulsion (creaming) are also included. This material is available free of charge via the Internet at <http://pubs.acs.org>.

References and Notes

- (1) Dalgleish, D. G. *Food Res. Int.* **1996**, *29*, 541–547.
- (2) Damodaran, S. *J. Food Sci.* **2005**, *70*, R54–R66.
- (3) Dickinson, E. *Colloids Surf., B.* **1999**, *15*, 161–176.
- (4) Wilde, P. J. *Curr. Opin. Colloid Interface Sci.* **2000**, *5*, 176–181.
- (5) Dalgleish, D. G. *Food Hydrocolloids* **2006**, *20*, 415–422.
- (6) Kim, H.-J.; Decker, E. A.; McClements, D. J. *Langmuir* **2002**, *18*, 7577–7583.
- (7) Kim, H.-J.; Decker, E. A.; McClements, D. J. *J. Agric. Food Chem.* **2002**, *50*, 7131–7137.
- (8) Dickinson, E. *J. Dairy Sci.* **1997**, *80*, 2607–2619.
- (9) Dickinson, E. *Colloids Surf., B.* **2001**, *20*, 197–210.
- (10) Fragneto, G.; Thomas, R. K.; Rennie, A. R.; Penfold, J. *Science* **1995**, *267*, 657–660.
- (11) Farrell, H. M., Jr.; Jimenez-Flores, R.; Bleck, G. T.; Brown, E. M.; Butler, J. E.; Creamer, L. K.; Hicks, C. L.; Hollar, C. M.; Ng-Kwai-Hang, K. F.; Swaisgood, H. E. *J. Dairy Sci.* **2004**, *87*, 1641–1674.
- (12) Brownlow, S.; Cabral, J. H. M.; Cooper, R.; Flower, D. R.; Yewdall, S. J.; Polikarpov, I.; North, A. C.; Sawyer, L. *Structure* **1997**, *5*, 481–495.
- (13) Kontopidis, G.; Holt, C.; Sawyer, L. *J. Mol. Biol.* **2002**, *318*, 1043–1055.
- (14) Dalgleish, D. G.; Leaver, J. J. *Colloid Interface Sci.* **1991**, *141*, 288–294.
- (15) Mendieta, J.; Folqué, H.; Tauler, R. *Biophys. J.* **1999**, *76*, 451–457.
- (16) Kauffmann, E.; Darnton, N. C.; Austin, R. H.; Batt, C.; Gerwert, K. *Proc. Natl. Acad. Sci. U.S.A.* **2001**, *98*, 6646–6649.
- (17) Creamer, L. K. *Biochemistry* **1995**, *34*, 7170–7176.
- (18) Considine, T.; Singh, H.; Patel, H. A.; Creamer, L. K. *J. Agric. Food Chem.* **2005**, *53*, 8010–8018.
- (19) Viseu, M. I.; Melo, E. P.; Carvalho, T. I.; Correia, R. F.; Costa, S. M. B. *Biophys. J.* **2007**, *93*, 3601–3612.
- (20) Zhang, X. Q.; Keiderling, T. A. *Biochemistry* **2006**, *45*, 8444–8452.
- (21) Considine, T.; Patel, H. A.; Anema, S. G.; Singh, H.; Creamer, L. K. *Innovative Food Sci. Emerging Technol.* **2007**, *8*, 1–23.
- (22) Fang, Y.; Dalgleish, D. G. *J. Colloid Interface Sci.* **1997**, *196*, 292–298.
- (23) Husband, F. A.; Garrod, M. J.; Mackie, A. R.; Burnett, G. R.; Wilde, P. J. *J. Agric. Food Chem.* **2001**, *49*, 859–866.
- (24) Lee, S.-H.; Lefèvre, T.; Subirade, M.; Paquin, P. *J. Agric. Food Chem.* **2007**, *55*, 10924–10931.

- (25) Sakuno, M. M.; Matsumoto, S.; Kawai, S.; Taihei, K.; Matsumura, Y. *Langmuir* **2008**, *24*, 11483–11488.
- (26) Wu, X.; Narsimhan, G.; Narsimhan, G. *Langmuir* **2008**, *24*, 4989–4998.
- (27) McClements, D. J. *Crit. Rev. Food Sci. Nutr.* **2002**, *42*, 417–471.
- (28) Chanasattru, W.; Decker, E. A.; McClements, D. J. *Food Res. Int.* **2007**, *40*, 1098–1105.
- (29) Chanasattru, W.; Decker, E. A.; McClements, D. J. *Food Hydrocolloids* **2009**, *23*, 253–261.
- (30) de Jongh, H. H. J.; Groneveld, T.; de Groot, J. J. *Dairy Sci.* **2001**, *84*, 562–571.
- (31) Eden, S.; Limão-Vieira, P.; Hoffmann, S. V.; Mason, N. *J. Chem. Phys.* **2006**, *323*, 313–333.
- (32) Miles, A. J.; Wallace, B. A. *Chem. Soc. Rev.* **2006**, *35*, 39–51.
- (33) Lees, J. G.; Smith, B. R.; Wien, F.; Miles, A. J.; Wallace, B. A. *Anal. Biochem.* **2004**, *332*, 285–289.
- (34) Whitmore, L.; Wallace, B. A. *Biopolymers* **2008**, *89*, 392–400.
- (35) Sreerama, N.; Woody, R. W. *Anal. Biochem.* **2000**, *287*, 252–260.
- (36) Provencher, S. W.; Glockner, J. *Biochemistry* **1981**, *20*, 33–37.
- (37) Johnson, W. C. *Proteins: Struct., Funct., Genet.* **1999**, *35*, 307–312.
- (38) Lees, J. G.; Miles, A. J.; Wien, F.; Wallace, B. A. *Bioinformatics* **2006**, *22*, 1955–1962.
- (39) Miles, A. J.; Whitmore, L.; Wallace, B. A. *Protein Sci.* **2005**, *14*, 368–374.
- (40) Tcholakova, S.; Denkov, N. D.; Ivanov, I. B.; Campbell, B. *Langmuir* **2002**, *18*, 8960–8971.
- (41) Qin, B. Y.; Bewley, M. C.; Creamer, L. K.; Baker, H. M.; Baker, E. N.; Jameson, G. B. *Biochemistry* **1998**, *37*, 14014–14023.
- (42) Wolfgang, K.; Christian, S. *Biopolymers* **1983**, *22*, 2577–2637.
- (43) Kelly, S. M.; Jess, T. J.; Price, N. C. *Biochim. Biophys. Acta* **2005**, *1751*, 119–139.
- (44) Viseu, M. I.; Carvalho, T. I.; Costa, S. M. B. *Biophys. J.* **2004**, *86*, 2392–2402.
- (45) Cho, Y. J.; Batt, C. A.; Sawyer, L. *J. Biol. Chem.* **1994**, *269*, 11102–11107.
- (46) Ikeguchi, M.; Kato, S.; Shimizu, A.; Sugai, S. *Proteins: Struct., Funct., Genet.* **1997**, *27*, 567–575.

BM100510J

Appendix 2.1: Supporting information

Purification of β -Lg genetic variants

The skim milk was acidified to pH 4.4 to 4.5 with 5 M HCl. The casein precipitates were removed by centrifugation for 35 min at 10 °C and 6000 \times g (Beckman J2-MC, JA-10 rotor). The supernatant was poured over glass wool and the pH of the supernatant was raised to pH 7.2 with 1 M NaOH. The residual precipitates were subsequently removed by centrifugation for 20 min at 10 °C and 12000 \times g. The supernatant was pooled and was referred to as the acid whey, which was dialyzed using 10 kDa molecular weight cut-off dialysis tubing for 24 h at 4 °C against Milli-Q water (Millipore, Billerica, MA). Whey preteins were then separated using a Pharmacia fast protein liquid chromatography system (Pharmacia, Uppsala, Sweden) on a Q-Sepharose column (height: 9 cm, diameter: 4.45 cm). The system was equilibrated with 20 mM Tris buffer, pH 7, and run at 7 mL/min. The elution was carried out using a 0-0.4 M NaCl linear gradient. The pooled fractions corresponding to β -Lg A and β -Lg B from multiple runs were concentrated and clarified by ultra-filtration at 4 °C using the regenerated cellulose membrane with a 10 kDa molecular weight cut-off (Millipore, Billerica, MA). The samples were then frozen and lyophilized and stored at -20 °C.

Liquid chromatography-mass spectrometry (LC-MS)

Lyophilized β -Lg obtained from anion-exchange chromatography was dissolved in Milli-Q water at a concentration of 1 mg/mL. The reversed phase-high performance liquid chromatography system with a C18 column was operated at 5 μ L/min in solvent A (0.1% (v/v) formic acid/Milli-Q water). The elution of β -Lg was achieved by a linear gradient from 10% to 100% solvent B (0.09% (v/v) formic acid/acetonitrile) in 30 min. The mass spectrometer was operated in a positive ion mode of electrospray ionization at a temperature of 325 °C. Nitrogen gas was used as drying and nebulising gas. The capillary exit was set at 88.3 V. The scan range of ions was from 150 m/z to 2200 m/z . All spectra were obtained as an average of 5 scans. The LC-MS system was controlled by Agilent Chemstation software allowing the data acquisition and data analysis.

Table S1: Calculated secondary structure of β -Lg under various conditions.

Method	α -helix %	β -sheet %	NRMSD	α -helix %	β -sheet %	NRMSD
	in phosphate buffer			in glycerol/phosphate buffer		
DSSP	16.7	40.1	-	-	-	-
SELCON3	14	36	0.129	14	36	0.128
CONTIN	16	34	0.137	15	35	0.038
CDSSTR	16	35	0.052	15	35	0.047
SD	1.2	1.0	-	0.6	0.6	-
	in the matched emulsion			in the unmatched emulsion		
SELCON3	35	20	0.057	30	22	0.065
CONTIN	34	20	0.022	23	28	0.052
CDSSTR	38	18	0.024	30	23	0.026
SD	2.1	1.2	-	4.0	0.6	-

Note: DSSP calculates the secondary structure from the crystal structure of β -Lg (the PDB file used: 1bsy). SELCON3, CONTIN, and CDSSTR are the programs used to calculate the secondary structure from SRCD spectra based on the reference set SP175 (optimized for 190-240 nm) provided in the Dichroweb online server. The NRMSD is the normalized root-mean-square deviation parameter (goodness of fit). Standard deviations (SD) are also presented.

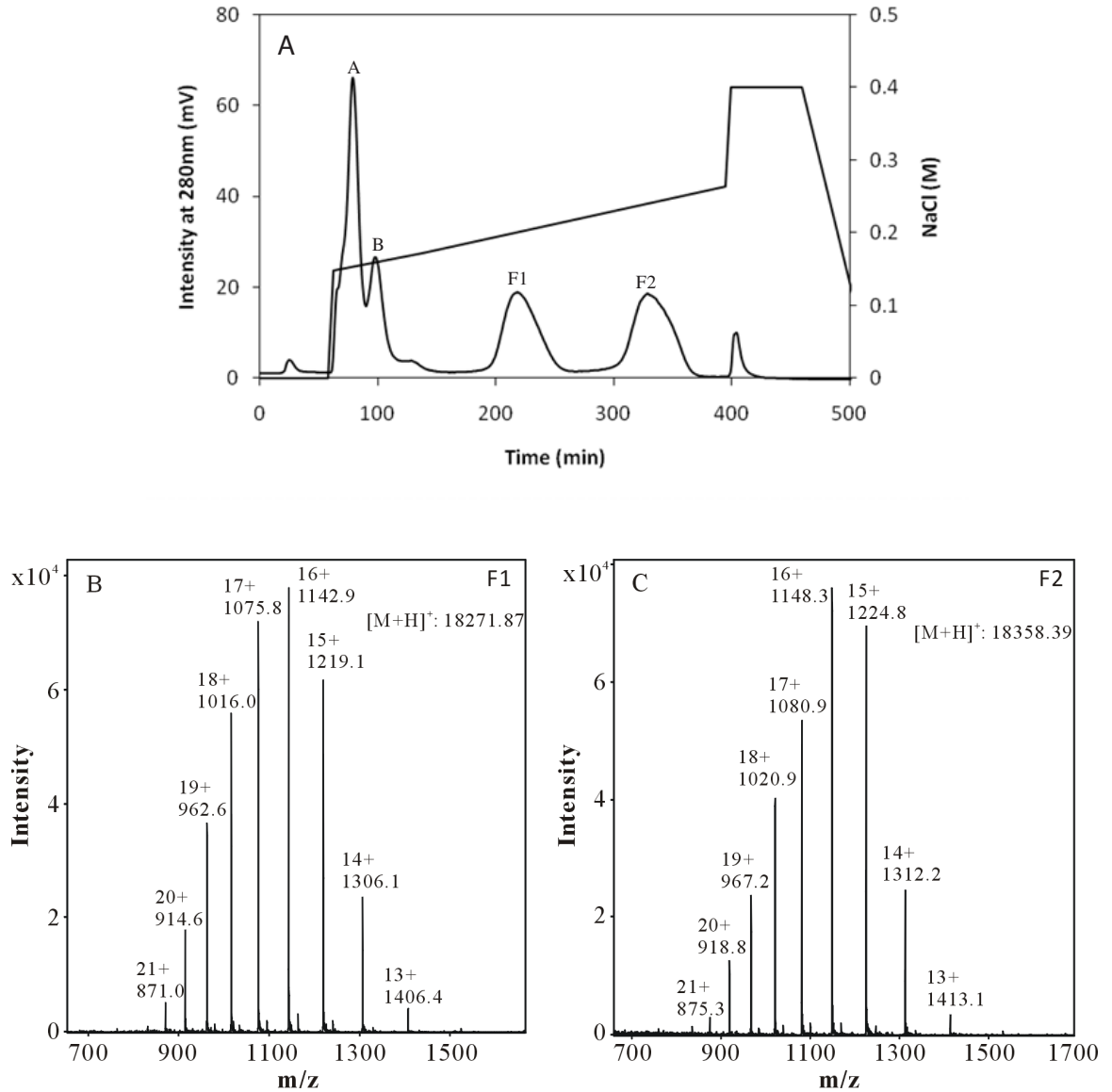


Figure S1: (A) Anion exchange chromatography of dialyzed acid whey on a Q-Sepharose column equilibrated in 20 mM Tris buffer pH 7 with a linear gradient of 0-0.4 M NaCl. Peak A and Peak B are a mixture of whey proteins, mainly α -lactalbumin and bovine serum albumin. Peak F1 is β -Lg B. Peak F2 is β -Lg A. (B) (C) Positive ion electrospray mass spectra of β -Lg B fraction (F1) and β -Lg A fraction (F2) obtained from the Pharmacia anion exchange chromatography. The multiple charge states and the deconvoluted masses are shown.

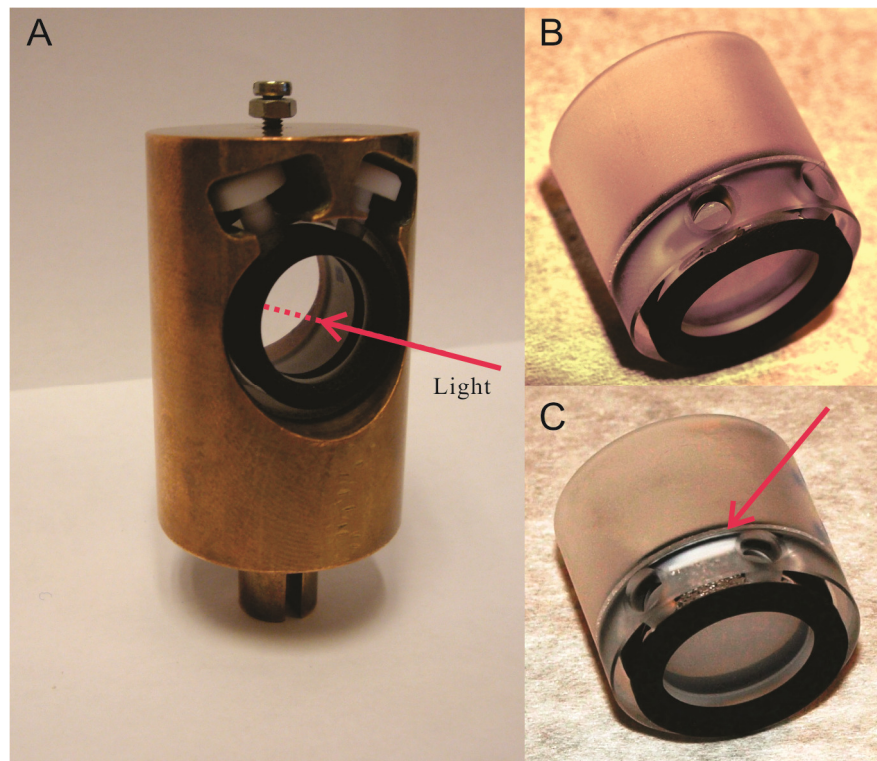
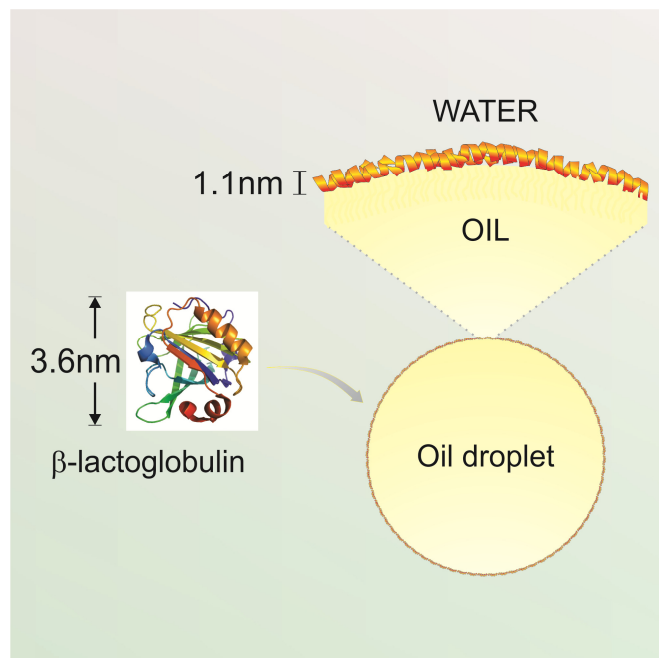


Figure S2: (A) The SRCD cell used for the thermal study sitting in the bronze cell holder which can be temperature controlled in the cell chamber. Arrow indicates the synchrotron light passing through the sample. (B) The SRCD cell (without stoppers) with a freshly loaded emulsion sample ready for measurement. (C) The SRCD cell with the same emulsion sample as in (B) after the heat treatment. Arrow indicates the white cream layer.

Chapter 3

Structural rearrangement of β -lactoglobulin at different oil-water interfaces and its effect on emulsion stability



A schematic model of β -lactoglobulin adsorption to the oil-water interface

Structural Rearrangement of β -Lactoglobulin at Different Oil–Water Interfaces and Its Effect on Emulsion Stability

Jiali Zhai,^{†,‡} Tim J. Wooster,^{*,‡,||} Søren V. Hoffmann,[§] Tzong-Hsien Lee,[†] Mary Ann Augustin,[‡] and Marie-Isabel Aguilar^{*,†}

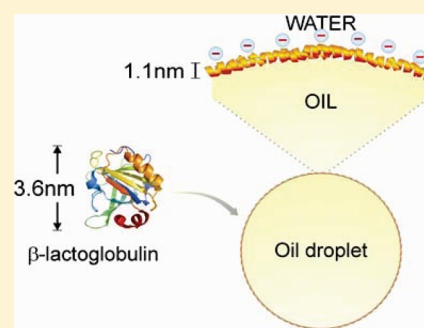
[†]Department of Biochemistry and Molecular Biology, Monash University, Clayton, Victoria 3800, Australia

[‡]CSIRO Food and Nutritional Sciences, Sneydes Road, Werribee, Victoria 3030, Australia

[§]Institute for Storage Ring Facilities (ISA), Aarhus University, Ny Munkegade 120, DK-8000 Aarhus C, Denmark

S Supporting Information

ABSTRACT: Understanding the factors that control protein structure and stability at the oil–water interface continues to be a major focus to optimize the formulation of protein-stabilized emulsions. In this study, a combination of synchrotron radiation circular dichroism spectroscopy, front-face fluorescence spectroscopy, and dual polarization interferometry (DPI) was used to characterize the conformation and geometric structure of β -lactoglobulin (β -Lg) upon adsorption to two oil–water interfaces: a hexadecane–water interface and a tricaprolylin–water interface. The results show that, upon adsorption to both oil–water interfaces, β -Lg went through a β -sheet to α -helix transition with a corresponding loss of its globular tertiary structure. The degree of conformational change was also a function of the oil phase polarity. The hexadecane oil induced a much higher degree of non-native α -helix compared to the tricaprolylin oil. In contrast to the β -Lg conformation in solution, the non-native α -helical-rich conformation of β -Lg at the interface was resistant to further conformational change upon heating. DPI measurements suggest that β -Lg formed a thin dense layer at emulsion droplet surfaces. The effects of high temperature and the presence of salt on these β -Lg emulsions were then investigated by monitoring changes in the ζ -potential and particle size. In the absence of salt, high electrostatic repulsion meant β -Lg-stabilized emulsions were resistant to heating to 90 °C. Adding salt (120 mM NaCl) before or after heating led to emulsion flocculation due to the screening of the electrostatic repulsion between colloidal particles. This study has provided insight into the structural properties of proteins adsorbed at the oil–water interface and has implications in the formulation and production of emulsions stabilized by globular proteins.



INTRODUCTION

Proteins are widely used in the food and pharmaceutical industries for the formulation of emulsions owing to their natural amphiphilicity.^{1–3} When they adsorb to oil–water interfaces in emulsions, proteins form an interfacial layer which stabilizes emulsions against flocculation via electrostatic and/or steric repulsions.^{4–7} The structural properties of proteins adsorbed at oil–water interfaces are key factors determining the stability and other physicochemical properties, such as viscosity and texture, of emulsions.^{8–11} Therefore, understanding the structure and stability of proteins adsorbed at oil–water interfaces has been a major focus for researchers to improve the formulation of emulsion-based products. However, despite considerable research, we still have an incomplete understanding of the geometric structure and conformation of proteins adsorbed at emulsion oil–water interfaces and the specific effect of the protein conformation on emulsion stability. While it is widely accepted that proteins undergo some degree of conformational change upon adsorption, the extent of the change and the subsequent impact on emulsion stability remains unclear due to limitations in measurement techniques. New approaches are

therefore needed to characterize the protein geometric structure and conformation in situ at oil–water interfaces at the molecular level.

A number of spectroscopic techniques have been used to characterize the conformation of proteins adsorbed at oil–water interfaces.^{12–15} Fourier transform infrared (FTIR) spectroscopy, circular dichroism spectroscopy coupled with the refractive index matching method, and tryptophan fluorescence spectroscopy have all shown that proteins undergo some degree of conformational change upon adsorption to oil–water interfaces.^{12–15} We recently reported the development of a new approach using synchrotron radiation circular dichroism (SRCD) which allows the direct measurement of the conformation of proteins adsorbed at oil–water interfaces in emulsions.¹⁶ This SRCD method differentiates the signal arising solely from the protein in the emulsion from the signal arising from droplet light scattering. β -Lactoglobulin (β -Lg) has served as a model globular

Received: April 22, 2011

Revised: June 11, 2011

Published: June 13, 2011

protein in many studies on protein structures both in solution and at emulsion interfaces,^{17–22} and we recently applied our new SRCD technique to the study of the β -Lg conformation in emulsions.¹⁶ With the strong light intensity from the synchrotron source, this method allowed the conformation of β -Lg adsorbed at the oil–water interface to be measured in situ without the need for additional sample preparation.¹⁶

There is also limited molecular understanding of the geometric structure of proteins in terms of their molecular dimensions when adsorbed at oil–water interfaces. While the adsorption of proteins to a number of interfaces has been studied using a range of techniques, including X-ray/neutron reflectivity,^{23–25} ellipsometry,^{26,27} interfacial rheology,^{28–31} and scattering techniques such as small-angle X-ray scattering (SAXS) and dynamic light scattering (DLS),^{32–34} most of these techniques have focused on either air–water interfaces (reflectivity) or particle surfaces (SAXS/DLS). Measurements using DLS and X-ray/neutron reflectivity have shown that whey proteins adsorbed at oil–water interfaces form interfacial layers around 2–3 nm thick.³⁵ Unlike the whey proteins, the caseins form a thick interfacial layer which protrudes more than 10 nm into the bulk aqueous phase.³⁶ Interfacial rheology studies may provide some information on the unfolded state of adsorbed protein molecules by examining the variability of the molecular areas and viscoelasticity of films at oil–water or air–water interfaces.^{28–31} However, it is not possible to obtain higher resolution structural information on proteins at oil–water interfaces using these techniques. More recently, dual polarization interferometry (DPI) has been used to characterize the geometric dimensions of surface-adsorbed proteins and lipid layers.^{37–41} DPI is an optical biosensing technique that analyzes thin layers adsorbed to planar surfaces within aqueous environments. The dual optical waveguide interferometer also allows the simultaneous measurement of both the thickness and the density of adsorbed protein monolayers in real time as has been demonstrated for bovine serum albumin adsorbed to a silicon oxynitride sensor surface.³⁸

Despite the lack of high-resolution data on the structure of proteins in emulsions, the stability of protein-stabilized emulsions has been studied extensively for both globular proteins and naturally unfolded proteins.^{4,42–45} In the case of β -Lg, emulsion colloidal stability is primarily governed by the balance between van der Waals attraction and electrostatic repulsion.^{4,10,44} It is well-known that β -Lg-stabilized emulsions become unstable when exposed to sufficiently high concentrations of salt (100 mM NaCl or 10 mM CaCl₂) due to screening of the electrostatic repulsion between the droplets.^{10,42,45} β -Lg-stabilized emulsions are also sensitive to heat. Free cysteine residues undergo disulfide exchange reactions as the emulsions are heated past the solution denaturation temperature.^{4,10,44} In the absence of salt, disulfide exchange is thought to result in protein cross-linking within the interfacial layer, but in the presence of salt, it is thought that cross-linking occurs between interfacial layers on neighboring droplets.^{4,10,44} This sensitivity to heat suggests that conformational changes at the interface contribute to emulsion instability, but to date it has been technically difficult to investigate these effects.

In the present study, we have employed several new complementary approaches to characterize the geometric structure and conformation of β -Lg adsorbed at the oil–water interface in emulsions. To characterize the adsorbed structure of β -Lg, we utilized DPI to measure the geometric dimensions of the adsorbed protein monolayer and combined these data with

conformational analysis by SRCD and front-face tryptophan fluorescence spectroscopy. Specifically we have studied the thermal stability of β -Lg upon adsorption to two oil–water interfaces: the tricaprilyn–water interface and the more hydrophobic hexadecane–water interface. We also examined the role that the emulsion oil phase polarity has in the protein structure and how this impacts emulsion stability. We sought to use the novel information we obtained on the structural changes of β -Lg at different emulsion oil–water interfaces to provide a more detailed understanding of the mechanism by which protein adsorption influences emulsion colloidal stability.

MATERIALS AND METHODS

Materials. β -Lg, sodium chloride (NaCl), sodium phosphate (monobasic and dibasic), hexadecane, tricaprilyn, glycerol, urea, and sodium dodecyl sulfate (SDS) were purchased from Sigma-Aldrich Company (St. Louis, MO). All chemicals and solvents were of analytical grade. The ultrapure water was prepared by a Purelab Ultra Genetic purification system (ELGA LabWater) and used for all the experiments.

DPI Measurements and Data Analysis. The geometric dimensions of β -Lg adsorbed to the oil–water interface were determined by measuring the thickness and refractive index (RI) of the β -Lg layer adsorbed on a C18 hydrocarbon–water interface, which mimics the oil–water interface. The thickness and RI of the β -Lg layer adsorbed on the immobilized C18 hydrocarbon AnaChip (Farfield Group, United Kingdom) were analyzed using an Anaght Bio2000 DPI instrument (Farfield Group) equipped with an independent Harvard Apparatus PHD2000 programmable syringe pump. DPI measures the phase changes of two orthogonal polarization modes of light, namely, the transverse magnetic (TM) mode and transverse electric (TE) mode, traveling through a silicon oxynitride waveguide.^{37,38} The deposition of molecules and the formation of layers on the planar surface of the waveguide lead to a change in the responses of the TM and TE polarizations. The thickness and refractive index of the layer structure are obtained by solving Maxwell's equations of electromagnetic radiation for both TM and TE polarizations for every time point. It is assumed for the purposes of calculation that the layers are isotropic in nature. The mathematical model for the conversion of thickness and RI data into the layer mass and density is described below and in detail elsewhere.^{37,46,47}

The C18 AnaChip surface and the bulk buffer (10 mM sodium phosphate buffer, pH 7) were calibrated at 20 °C with 80% (w/w) ethanol and water. The adsorption of β -Lg onto the immobilized C18 hydrocarbon–water interface was conducted in bulk buffer at 20 °C. Freshly prepared 10 μ M β -Lg solution in 10 mM sodium phosphate buffer, pH 7, was injected at 10 μ L/min for 15 min and followed by a dissociation phase with the bulk buffer flowing over the layer for another 15 min. The obtained TM and TE phase change signals were resolved into the thickness, the RI, and the mass of the β -Lg layer. Maxwell's standard equations of electromagnetic radiation were used to resolve the experimentally obtained phase changes of TM and TE polarizations into the thickness and the RI of the β -Lg layer. The density and mass of the β -Lg layer were calculated using the following equations:

$$\text{layerdensity (g/cm}^3\text{)} = \frac{D_a(RI - RI_b)}{RI_a - RI_b}$$

$$\text{mass (ng/mm}^2\text{)} = \text{layerdensity (g/cm}^3\text{)} \times \text{thickness (nm)}$$

where D_a is the density of the protein (0.71 g/cm³), RI is the absolute RI value of the layer, RI_a is the RI of the analyte (1.465 for protein), and RI_b is the bulk RI (1.3332 for 10 mM sodium phosphate buffer).

A reference study was also performed by adsorbing β -Lg to a hydrophilic silicon oxynitride Anachip (Farfield Group). The bulk buffer

used for the reference study was 10 mM sodium phosphate buffer, pH 3, in which β -Lg became positively charged to enable physical adsorption onto the negatively charged silicon oxynitride Anachip surface. A 100 μ M β -Lg solution in 10 mM sodium phosphate buffer, pH 3, was used for the adsorption to the silicon surface. Since the physical adsorption is a weak event, a high concentration (100 μ M) of β -Lg solution was needed to provide an amount of mass deposition similar to that of the C18 Anachip experiment. All other experimental conditions were the same as those in the C18 surface adsorption experiment.

Emulsion Preparation. Protein-stabilized emulsions (0.3%, w/w) containing 20% (v/v) hexadecane or tricaprilyn were used for the study. Our previous study has shown that, at a final protein concentration of 0.3% (w/w) in emulsions, greater than 90% of the protein was adsorbed to the interface.¹⁶ The protein concentration in buffer was determined by an absorbance reading at 280 nm using a ThermoSpectronic UV-vis spectrophotometer (Thermo, Wilmington, DE). The extinction coefficient used for β -Lg was 0.96 mL mg⁻¹ cm⁻¹.⁴⁸ The emulsions were prepared by blending the protein solution with hexadecane or tricaprilyn (20%, v/v) at 8000 rpm for 2 min using a high-speed blender (Ultra Turrax, Janke & Kunkel, Germany) and then passing the mixtures through a high-pressure valve homogenizer twice at approximately 700 bar (EmulsiFlex C5, Avestin, Canada). All emulsions used for SRCD and fluorescence studies were freshly prepared on site at the ISA-synchrotron where the CD1 beamline is located (Institute for Storage Ring Facilities, Aarhus University, Denmark), and experiments were performed within 24 h of preparation.

SRCD Measurements and Data Analysis. All SRCD measurements were performed on the CD1 beamline of the SRCD station at the ASTRID storage ring.^{49,50} A Suprasil cell (Hellma GmbH & Co., Germany) of 0.01 cm path length was used for far-UV SRCD measurements at 20 °C. The operating conditions were 1 nm bandwidth, 2.15 s averaging time, and three scans for a solution sample or eight scans for an emulsion sample. Spectra for baseline subtraction were recorded in 10 mM sodium phosphate buffer for a solution sample or in 1% (w/w) SDS-stabilized emulsions for emulsion samples. The SDS-stabilized emulsion has been shown in a previous study to be a valid baseline which gives light scattering background but no protein signal by SRCD.¹⁶ The temperatures examined for the heat treatment study were 20, 34, 48, 62, and 76 °C, and the SRCD cell containing the sample was heated in situ in a temperature-controlled chamber. All spectra were processed using CDtool software,⁵¹ as described in our previous study. The far-UV SRCD spectra are presented as mean residue ellipticity [θ] based on a mean residue weight of 113 for β -Lg calculated from its sequence. Secondary structural content calculations were performed by fitting the spectra to the reference set SP175 (optimized for 190–240 nm) in DICHROWEB⁵² using the SELCON3 method.^{53,54}

Near-UV SRCD analysis was carried out under SRCD conditions similar to those used for far-UV SRCD, except that a circular quartz cell (Hellma GmbH & Co., Germany) with a path length of 0.5 cm was used. Emulsion samples for near-UV SRCD measurements were RI matched using 58% (v/v) glycerol for hexadecane and 63% (v/v) for tricaprilyn. Our previous study showed no significant influence of glycerol addition on the β -Lg native structure in the near-UV region. The near-UV SRCD spectra were presented in the original unit of SRCD (mdeg).

Front-Face Fluorescence Spectroscopy Measurements. Front-face fluorescence spectra were obtained with a luminescence spectrometer (PerkinElmer LS50B, Waltham, MA) equipped with a front surface accessory (PerkinElmer part no. S212 3130), which allows measurements of turbid samples. Fresh solution samples or emulsion samples were poured into a quartz cell of 10 mm path length (Hellma GmbH & Co.). The cell was then mounted behind the mounting bracket and clamped with a plunger. The excitation wavelength was set at 290 nm. The emission fluorescence spectra were collected in the wavelength range of 300–450 nm with a scan speed of 100 nm/min.

Excitation and emission slits were set at 10 nm. Each individual emission spectrum was the average of three runs. All data were collected at room temperature.

Treatment of Emulsions under High Temperatures and Salt Addition. Emulsions were prepared as described above and were then treated under three different conditions involving high temperatures and/or salt addition. The first two treatments involved heating aliquots of freshly prepared emulsions in a water bath at selected temperatures (ranging from 20 to 90 °C) for 20 min. These emulsions were then cooled to room temperature, diluted (1:5) with 10 mM sodium phosphate buffer containing either 0 or 150 mM NaCl. The third treatment involved diluting the freshly prepared emulsions with 10 mM sodium phosphate buffer containing 150 mM NaCl first and then heating these diluted emulsions as described above. The final concentration of NaCl in the diluted emulsion samples was 120 mM. This concentration of 120 mM NaCl was chosen because it has been shown to provide sufficient electrostatic screening to permit droplet flocculation, but is not excessive as to create large aggregates at room temperature before the heating treatment.^{10,42,43} Once the treatments were finished, all aliquots of emulsions were stored at 20 °C for 24 h in a temperature-controlled room, after which their ζ -potential and droplet size were measured.

Emulsion ζ -Potential Measurements. The ζ -potential of the emulsions was measured using laser Doppler velocimetry (Malvern Zetasizer Nano ZS, Worcestershire, U.K.). The emulsion samples stored for 24 h after various treatments were diluted (2 μ L in 30 mL of 10 mM sodium phosphate buffer, pH 7) and injected into a folded capillary cell with electrodes at either end to which a potential was applied. The cell was placed in a cell chamber controlled at 20 °C, and the velocity of the charged droplet movement toward the oppositely charged electrode was measured. The ζ -potential was then calculated from the droplet velocity. The results were reported as the average of at least three individual measurements, and the standard deviation was given in the plot.

Emulsion Droplet Size Measurements. The droplet size of the emulsions was measured using laser light diffraction (Malvern Mastersizer 2000) equipped with a Hydro SM small-volume sample dispersion unit. The emulsion samples stored for 24 h after various treatments were dispersed in circulating buffer in the Hydro SM unit. Differential refractive indexes of 1.079 and 1.101 were used for the hexadecane emulsion and the tricaprilyn emulsion, respectively. The emulsion droplet size was calculated from a best fit between the measured scattering pattern and a model scattering pattern of equivalent polydisperse spheres (Mie theory). The volume-weighted average mean diameter $D_{4,3}$ ($= \sum n_i d_i^4 / \sum n_i d_i^3$, where n_i is the number of particles with diameter d_i) was reported as the average of at least three individual measurements, and the standard deviation was given in the plot.

RESULTS

Geometric Dimensions of β -Lg Adsorbed at the Oil–Water Interface. Defining the geometric dimensions of the adsorbed protein layer is important for understanding protein structural rearrangement and assembly at oil–water interfaces and elucidating the mechanisms of emulsion droplet stability. In this study, DPI was used to investigate the geometric dimensions of β -Lg adsorbed to a C18 hydrocarbon–water interface as a model oil–water interface. A solution of β -Lg was passed over the C18 chip surface, and the resulting TM and TE phase changes were converted to real-time changes in mass, thickness, and RI upon β -Lg adsorption to the C18 surface, which are plotted in Figure 1A. There was a rapid adsorption of β -Lg onto the C18 hydrocarbon–water interface, resulting in a protein layer with a mass of 1.25 ng/mm², a thickness of 1.1 nm, and a

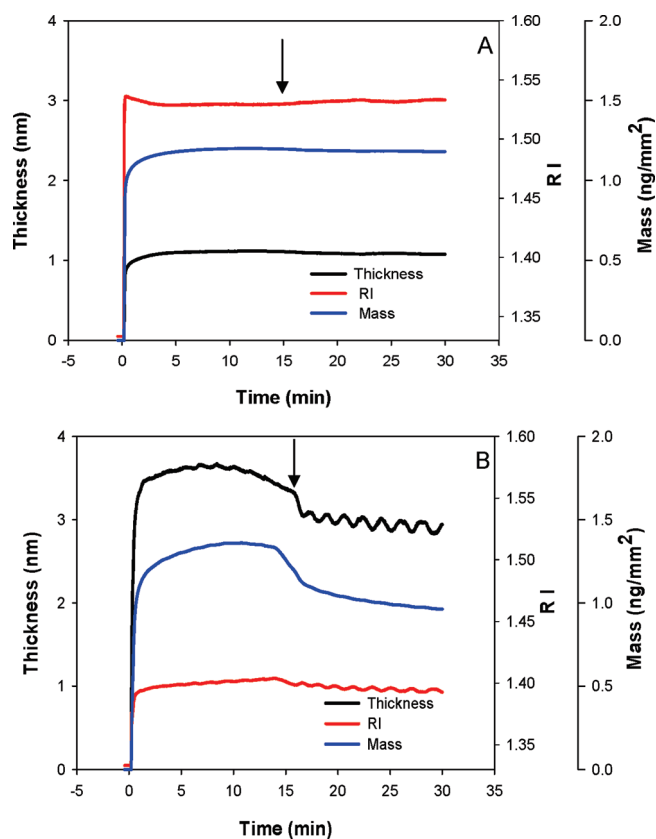


Figure 1. Dual polarization interferometry sensorgrams of real-time changes in the mass, thickness, and refractive index of β -Lg binding to a C18 hydrocarbon surface (A) and a silicon oxynitride surface (B). β -Lg was injected to the surface at $10 \mu\text{L}/\text{min}$ for 15 min (association phase), followed by a 15 min buffer wash (dissociation phase). The arrow indicates the time when the dissociation phase began.

density of $0.98 \text{ g}/\text{cm}^3$ (derived from a layer RI of 1.53). These values were recorded at the end of protein adsorption to the interface (indicated by the arrow in Figure 1A). This result shows that β -Lg formed a thin and dense protein layer upon adsorption to the oil–water interface. This is consistent with previous studies on β -Lg adsorption to the air–water interface using reflectometry measurements, which indicated the adsorbed monolayer to be dense and 1–3 nm thick.^{23–25} Recent interfacial rheology studies also generally agree with the DPI result. For example, Pradines et al. examined the adsorption behavior of β -Lg at the hexane–water interface and found a significantly decreased molar area, indicating the unfolding state of the protein and the strong affinity to the hydrophobic surface.³⁰ The molecular dimensions of β -Lg molecules adsorbed at hydrophobic surfaces measured using DPI help to expand our understanding of how the changes in molecular surface area observed by Pradines et al. impact the overall structure of β -Lg at interfaces. However, the thickness (1.1 nm) of the adsorbed β -Lg layer obtained from our DPI experiments was less than that (3 nm) obtained from DLS measurements,¹⁸ as DPI measured the actual thickness of the protein layer adsorbed on top of the hydrophobic surface rather than the hydrodynamic diameter of the emulsion droplet reported by the DLS technique. The subsequent dissociation phase indicated no dissociation of β -Lg from the C18 surface (Figure 1A), suggesting a strong hydrophobic interaction between the protein and the C18 surface.

The dimensions of the β -Lg layer adsorbed to an unmodified silicon oxynitride surface were also measured as a reference, and the results are shown in Figure 1B. The positively charged β -Lg (in 10 mM sodium phosphate buffer of pH 3) adsorbed to the negatively charged silicon surface, causing a rapid increase in the mass of the adsorbed layer to $1.35 \text{ ng}/\text{mm}^2$. At the end point of protein adsorption, physical adsorption via electrostatic attraction generated a β -Lg layer with a thickness of 3.6 nm and a layer density of $0.37 \text{ g}/\text{cm}^3$ (derived using a layer RI of 1.4), which is consistent with the crystal structure of β -Lg (approximately 3.6 nm in diameter).^{55,56} The layer density at the silicon oxynitride surface was also found to be lower than that at the C18 surface. Overall, the DPI results suggest that the protein maintained its native globular structure at the silicon oxynitride surface while adsorption to the C18 surface induced the denaturation of β -Lg into a flat and dense structure.

Secondary and Tertiary Structures of β -Lg at the Oil–Water Interface. The secondary structure of β -Lg adsorbed to the tricaprylin–water interface and the hexadecane–water interface was investigated using SRCD, and the resulting far-UV spectra are shown in Figure 2A. The SRCD spectrum of β -Lg in 10 mM sodium phosphate buffer (black line) shows a single minimum at 217 nm, a zero-crossing at 203 nm, and a maximum at 193 nm which is characteristic of a β -sheet-rich structure. The β -Lg solution spectrum was deconvoluted to yield 33% β -sheet and 16% α -helix and the remaining unordered structure and is consistent with our previous results as well as the calculated secondary structure contents from the β -Lg crystal structure.^{16,55} In comparison to the solution spectrum, the spectra of β -Lg adsorbed at both oil–water interfaces is characteristic of an α -helical-rich structure with the appearance of double minima at 220 and 209 nm, a blue shifting of the zero crossing, and a general increase in the dichroism signal. Moreover, the extent of these spectral changes depends on the polarity of the oil phase, with a larger change observed with the more nonpolar hexadecane. Table 1 summarizes the secondary structural content of β -Lg in solution and at different oil–water interfaces. The α -helical content of β -Lg increased from 16% in buffer to 24% in the case of the tricaprylin–water interface and to 50% at the hexadecane–water interface. At the same time, the percentage of β -sheet conformation decreased from 33% in buffer to 28% and 15% for β -Lg adsorbed at the tricaprylin–water and hexadecane–water interfaces, respectively.

To gain further insight into the changes in tertiary structure, near-UV SRCD spectra of β -Lg adsorbed at the tricaprylin–water interface and the hexadecane–water interface were also examined (Figure 2B). The native tertiary structure of β -Lg in solution gave a distinct profile of two sharp minima at 285 and 293 nm arising from tryptophan residues and two shallow minima at 266 and 277 nm originating from phenylalanine and tyrosine residues. In comparison, β -Lg adsorbed at both the tricaprylin and the hexadecane oil–water interfaces yielded broad and shallow spectra without distinctive peaks. The results are consistent with our previous SRCD study¹⁶ and suggest a loss of nativelike environment around the aromatic residues and in turn a lack of well-defined native tertiary structure due to adsorption-induced protein structural change at the hydrophobic interface.

Tryptophan emission fluorescence spectroscopy in its front-face mode was also used to further investigate the changes in the conformation of β -Lg adsorbed at oil–water interfaces. The fluorescence spectra of β -Lg in solution and in each emulsion are shown in Figure 3. β -Lg in its native state in solution gave rise to a

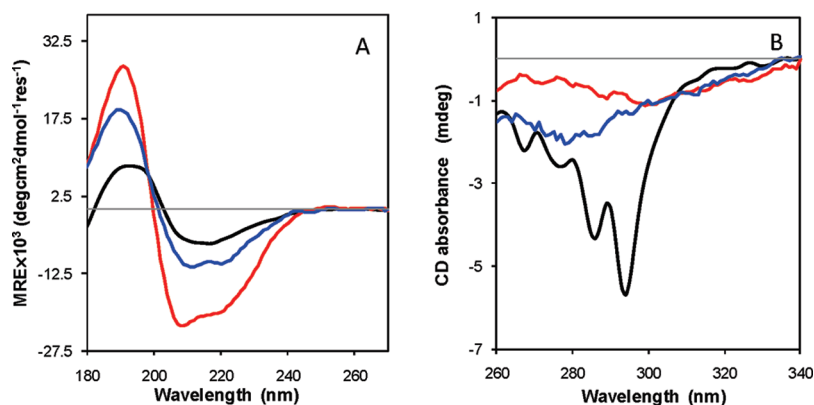


Figure 2. Far-UV SRCD spectra (A) and near-UV SRCD spectra (B) of β -Lg in 10 mM sodium phosphate buffer, pH 7 (black line), at the tricaprylin–water interface (blue line), and at the hexadecane–water interface (red line). All spectra were measured at 20 °C.

Table 1. Secondary Structural Content (%) of β -Lg in Different Environments Derived from Far-UV SRCD Spectra

	α -helix	β -sheet
in solution	16	33
at tricaprylin–water interface	24	28
at hexadecane–water interface	50	15

λ_{\max} at 335 nm due to the two tryptophan residues Trp19 and Trp61, with the former buried in the hydrophobic core and the latter partially exposed to solvent in aqueous solution. The solvent accessibilities of Trp19 and Trp61 relative to the fully exposed state were calculated on the β -Lg crystal structure (PDB ID 1bsy)⁵⁵ by the DSSP program⁵⁷ and were 1.7% and 20.8%, respectively. β -Lg adsorbed to both oil–water interfaces showed a blue shift of 4.5 nm to give λ_{\max} values of 330.5 nm at the tricaprylin–water interface and 328.5 nm (6.5 nm shift) at the hexadecane–water interface. The blue shifting of λ_{\max} of β -Lg at both oil–water interfaces indicates that the tryptophan residues move to a more hydrophobic environment. It is not possible to differentiate the relative contribution of each Trp residue to the fluorescence change. However, given that the SRCD results indicate a significant conformational change, these fluorescent results suggest that this conformational change is associated with an increase in the hydrophobic environment of the two Trp residues. This blue shift was also previously observed upon adsorption of β -Lg to a diacylglycerol–water and a triacylglycerol–water interface.²¹ In comparison, urea denaturation of β -Lg in solution showed a red shift of λ_{\max} to 353 nm originating from the two tryptophan residues which are fully exposed to the aqueous solvent.

Effect of Temperature on the Stability of the β -Lg Conformation at the Oil–Water Interface. To assess the effect of temperature on the conformation of β -Lg, far-UV SRCD spectra of β -Lg in solution and at both oil–water interfaces were measured at temperatures ranging from 20 to 76 °C (Figure 4). In solution, increasing the temperature caused a gradual decrease in the β -Lg spectral intensity and a shift in the spectral maximum at 195 nm toward lower wavelengths, with the largest change observed at 76 °C (Figure 4A). These changes in β -Lg SRCD spectra indicate the heat-induced denaturation of β -Lg secondary structure. In comparison, high temperatures had much less effect on the SRCD spectra of β -Lg adsorbed at both oil–water

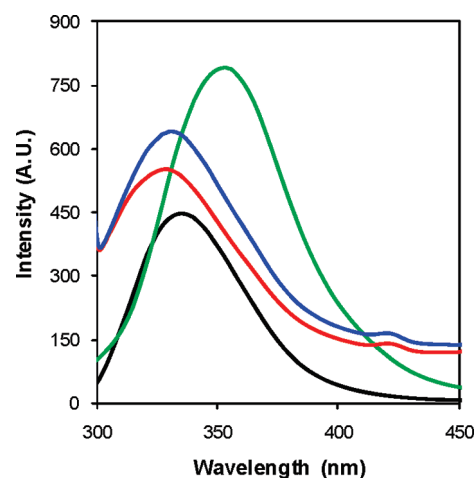


Figure 3. Tryptophan front-face fluorescence spectra of β -Lg in 10 mM sodium phosphate buffer, pH 7 (black line), in 6 M urea/phosphate buffer (green line), at the tricaprylin–water interface (blue line), and at the hexadecane–water interface (red line). All spectra were measured at 20 °C.

interfaces. In the case of β -Lg adsorbed at the tricaprylin–water interface, the spectra remained relatively constant at temperatures up to 62 °C, apart from a moderate decrease in the intensity of the peak at 195 nm (Figure 4B). The spectra for β -Lg adsorbed at the hexadecane–water interface remained constant at all temperatures up to 76 °C, with little change in the double minima region of 207 and 220 nm (Figure 4C). Thus, the secondary structure of β -Lg was more resistant to heat treatment at the more nonpolar hexadecane–water interface than at the tricaprylin–water interface.

Effect of Temperature and Salt on the ζ -Potential and Droplet size of β -Lg Oil-in-Water Emulsions. To investigate the effect of protein conformational change on emulsion physical stability, the ζ -potential and particle size of emulsions stabilized by β -Lg heated to different temperatures (20–90 °C) in the absence/presence of salt (120 mM NaCl) were characterized. Figure 5 shows changes in the ζ -potential measured at 20 °C 24 h after heating in the absence/presence of salt. The β -Lg-stabilized tricaprylin-in-water emulsion had a ζ -potential of -66 ± 1 mV, which remained constant with temperature up to 90 °C in the absence of salt (Figure 5A). On the other hand, the ζ -potential

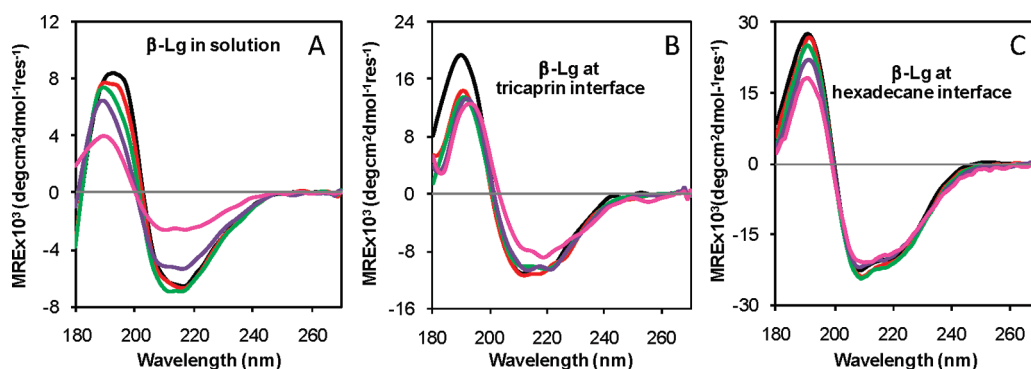


Figure 4. Far-UV SRCD spectra showing the effect of high temperatures on the conformation of β -Lg in 10 mM sodium phosphate buffer, pH 7 (A), at the tricaprillin–water interface (B), and at the hexadecane–water interface (C). Spectra were recorded at various temperatures: 20 °C (black line), 34 °C (red line), 48 °C (green line), 62 °C (purple line), and 76 °C (pink line).

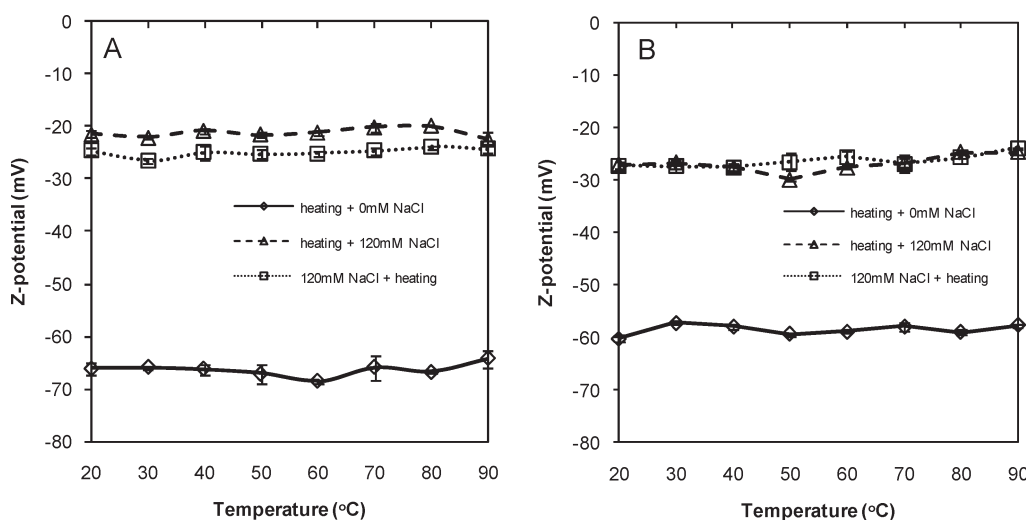


Figure 5. Effect of high temperatures and high ionic strengths on the ζ -potentials of the β -Lg-stabilized tricaprillin oil-in-water emulsion (A) and β -Lg-stabilized hexadecane oil-in-water emulsion (B). Note that “heating + 0 mM NaCl” indicates no salt addition after heating, “heating + 120 mM NaCl” indicates salt addition after heating, and “120 mM NaCl + heating” indicates salt addition before heating.

was strongly affected by the presence of salt, decreasing to -21 ± 0.6 mV (20 °C) when salt was added after heating and -24 ± 0.6 mV when salt was added prior to heating. This reduction in the emulsion ζ -potential was observed at increased temperatures irrespective of whether the salt was added before or after heating. The hexadecane-in-water emulsion had a ζ -potential of -60 ± 0.6 mV at 20 °C, which decreased to -27 ± 0.8 mV with the addition of salt before/after heating (Figure 5B). Both types of emulsions had no change in the ζ -potential as a function of the temperature of heat treatment. Overall, the results show that the emulsion ζ -potential is affected by the presence of salt, confirming that the addition of salt leads to a loss of emulsion surface charge via electrostatic screening.

The stability of β -Lg-stabilized emulsions was further assessed by measuring the particle size at 20 °C 24 h after heating in the absence/presence of 120 mM NaCl. The effects of temperature and the presence of salt on the β -Lg-stabilized tricaprillin-in-water emulsion particle size are shown in Figure 6A. The mean particle size ($D_{4/3}$) in the absence of salt was 1.8 ± 0.09 μm at 20 °C and was relatively stable against increased temperatures up to 90 °C. Adding 120 mM NaCl after heating resulted in an increase in the

mean droplet size from 3.6 ± 0.2 μm at 20 °C to 10.5 ± 1.5 μm at 90 °C. When salt was added prior to high-temperature treatment, a gradual increase in the mean particle size was observed from 20 to 80 °C but with a larger increase up to 28.7 ± 4.7 μm at 90 °C.

Figure 6B shows the mean particle size of β -Lg-stabilized hexadecane-in-water emulsions in response to heating at different temperatures in the absence/presence of salt (120 mM NaCl). The untreated β -Lg hexadecane-in-water emulsion had a mean particle size ($D_{4/3}$) of 1.1 ± 0.01 μm at 20 °C, which remained constant when heated at temperatures ranging from 30 to 90 °C in the absence of salt. When the exposure to high temperature was followed by the addition of salt, the mean particle size of the emulsion was still relatively stable with a slight increase to 1.8 ± 0.05 μm when treated at 90 °C. On the other hand, when salt was added to the emulsion prior to heating, there was a substantial increase in the mean particle size from 2.2 ± 0.03 μm at 50 °C to 26.5 ± 1.7 μm at 90 °C. The confocal images of both tricaprillin-in-water and hexadecane-in-water emulsions (see the Supporting Information) are consistent with the particle size measurements, and the result demonstrated that the increase in the particle size was largely due to flocculation rather than

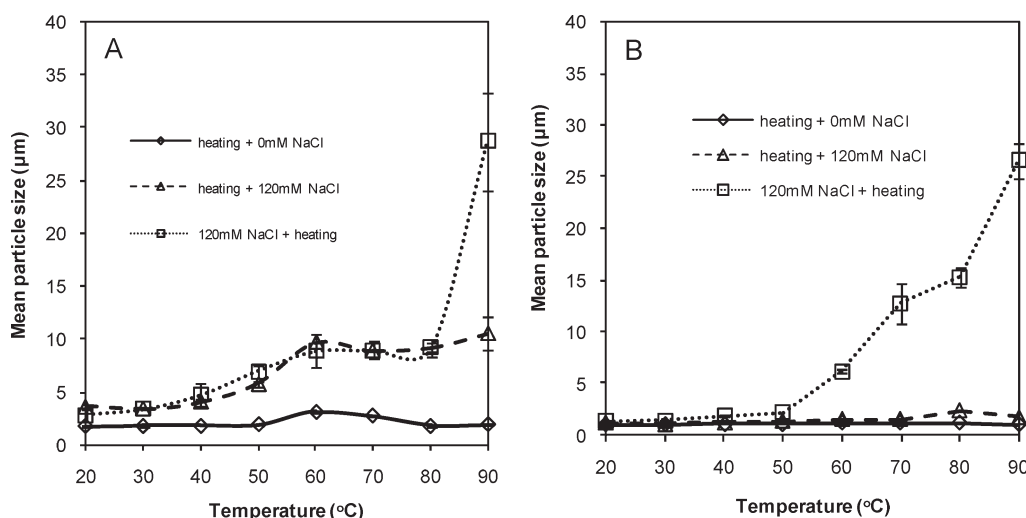


Figure 6. Effect of high temperatures and high ionic strengths on the mean particle diameter $D_{4,3}$ of the β -Lg-stabilized tricaprolylin oil-in-water emulsion (A) and β -Lg-stabilized hexadecane oil-in-water emulsion (B). Note that “heating + 0 mM NaCl” indicates no salt addition after heating, “heating + 120 mM NaCl” indicates salt addition after heating, and “120 mM NaCl + heating” indicates salt addition before heating.

coalescence. However, it is hard to entirely exclude the coalescence destabilization from the confocal images as they only represent a fraction of the emulsion samples, in particular when emulsions were heated to high temperatures in the presence of 120 mM NaCl.

DISCUSSION

The structural properties of the protein layer adsorbed at oil–water interfaces in emulsions have long been recognized as a major factor controlling the colloidal stability and the quality of emulsion-based products.^{8,9} It is necessary, therefore, to characterize the structures of adsorbed proteins, which are thought to be largely different from the solution structures of proteins due to the hydrophobic environment of oil–water interfaces. In the current study, we have examined the structural rearrangement of β -Lg at two different oil–water interfaces and the effect of these structural changes on emulsion stability. Specifically, we have used a combination of DPI, SRCD, and front-face fluorescence spectroscopy to measure, in situ, the dimensions and the conformation of β -Lg adsorbed at oil–water interfaces in emulsions. The impact of these structural changes on emulsion stability was then determined through measurements of the emulsion ζ -potential and particle size.

The geometric dimensions, in terms of the thickness and density of β -Lg adsorbed to an oil–water interface, were determined using DPI. β -Lg adsorbed onto the silicon oxynitride surface had a layer thickness of 3.6 nm of moderate density (0.37 g/cm^3) (Figure 1B), which agrees with the crystal structure dimensions reported (approximately 3.6 nm in diameter).^{55,56} This result suggests that the β -Lg tertiary structure remained intact upon adsorption to this surface. In contrast, adsorption of β -Lg to the C18 surface yielded a denser (0.98 g/cm^3) protein layer with a thickness of 1.1 nm (Figure 1A). Thus, β -Lg undergoes a significant change from a native globular shape to an open flat structure at the hydrocarbon surface, forming a dense protein layer.

The DPI results are consistent with the conformational change of β -Lg at oil–water interfaces measured using SRCD

and front-face fluorescence spectroscopy. The near-UV SRCD results show that adsorption of β -Lg to oil–water interfaces induces protein unfolding with a loss of the globular tertiary structure (Figure 2B), which was confirmed by fluorescence measurements (Figure 3). This change in conformation was associated with a large change in the secondary structure of β -Lg adsorbed at both oil–water interfaces, resulting in a significant increase in α -helical structure and some loss of β -sheet structure (Figure 2A). Thus, adsorption of the protein at the hydrophobic interface leads to the unfolding of the tertiary structure, and the native β -sheet structure converts to an α -helical structure. This interconversion essentially allows the reorientation of nonpolar side chains toward the hydrophobic oil phase and enhances the interaction with the hydrophobic interface. This modified bound conformation was also significantly stabilized at the surface since this secondary structure was highly resistant to thermal denaturation (Figure 4).

The effect of the oil phase polarity on the β -Lg structural change at the interface, and in turn on emulsion stability, was also evaluated. Of the two oil phases investigated (hexadecane and tricaprolylin), hexadecane is the least polar because of its *n*-alkane structure and lack of a polar glycerol headgroup. The difference in oil phase polarity had a distinct impact on the β -Lg conformation. The degree of β -Lg conformational rearrangement at the hexadecane–water interface was more than 3.5 times larger than that at the tricaprolylin–water interface. This considerable impact of the oil phase polarity on the degree of structural change indicates that solvation in the oil phase plays a key role in determining the preferred conformation of the protein. In fact, adsorption of β -Lg to either oil–water interface considerably increases its resistance to thermal unfolding. In solution the balance between the folded and unfolded states is governed by a number of interactions, including hydrogen bonding, ion pair, van der Waals, hydrophobic, and configurational entropy.^{58–60} The two dominant forces are the hydrophobic effect (the energy penalty associated with exposing buried hydrophobic residues as a result of unfolding) and configurational entropy.^{58–60} Since the main thermodynamic driving force for protein adsorption at the oil–water interface is the reorientation of nonpolar side chains toward the

hydrophobic oil phase, it is clear that the non-native α -helical structure plays an important role in the free energy of the protein. The interaction between the hydrophobic residues of the protein and the oil phase stabilizes the protein structure and increases its resistance to thermal denaturation (Figure 4). Moreover, β -Lg adsorbed at the hexadecane–water interface was more stable to heating than at the tricaprylin–water interface (Figure 4B,C). This tends to suggest that there is a more favorable interaction between β -Lg and the hexadecane oil phase than with the tricaprylin oil phase.

The question now remains as to the influence that the changes in the β -Lg structure upon adsorption have on emulsion colloidal stability, which was investigated by heating the emulsions in the absence or presence of salt. Three stress conditions were utilized, namely, (i) heating in the absence of salt, (ii) adding salt (120 mM NaCl) to an emulsion which has been heated in the absence of salt, (iii) heating in the presence of salt (120 mM NaCl). Measurements of the emulsion ζ -potential and particle size were conducted in each case to assess physical stability. When the two β -Lg-stabilized emulsions were heated in the absence of salt, there was no change in the measured ζ -potential or particle size, which is consistent with previous studies.^{5,10,34,42} These emulsions were thus stable to heat-induced aggregation because their high surface charge (-66 ± 1 mV for the tricaprylin-in-water emulsions and -60 ± 0.6 mV for the hexadecane-in-water emulsions) provides strong electrostatic repulsion. In general, once an emulsion droplet has a ζ -potential larger than ± 30 mV, the net colloidal interaction energy is sufficient to overcome the thermal energy of the emulsion droplets. Compared to the ζ -potential of β -Lg in solution, which was measured to be -21 ± 1.7 mV, these results indicate that the structural change from a compact β -sheet structure to a partially extended α -helical layer at the oil–water interface exposes a net increase in negatively charged amino acids to the aqueous phase. This negatively charged protein layer stabilizes the emulsion through electrostatic repulsion between the droplets. Thus, adsorption of β -Lg at the oil–water interface imparts a significant structural stability to the emulsion droplets by preventing flocculation under thermal stress via electrostatic repulsions.

When salt was added to each emulsion after the heat treatment, the ζ -potential was reduced due to electrostatic screening. However, the effect on the emulsion particle size was different depending on the oil phase. Adding salt after heating did not affect the particle size of the hexadecane-in-water emulsion, but resulted in a moderate increase in the particle size of the tricaprylin-in-water emulsion. This difference in emulsion stability arises because the two emulsions have different net colloidal interaction energies, possibly as a result of the difference in the β -Lg conformation at each interface. The colloidal stability of β -Lg-stabilized emulsions is primarily governed by the balance between van der Waals attractive forces and electrostatic repulsive forces.^{4,10,45} Of the two emulsions studied, the hexadecane-in-water emulsion (-27 ± 0.8 mV) has a slightly higher ζ -potential compared to the tricaprylin-in-water emulsion (-21 ± 0.6 mV), probably as a result of the more helical conformation adopted by β -Lg. Furthermore, it is likely that the van der Waals attractions of the hexadecane-in-water emulsion are weaker than those of the tricaprylin-in-water emulsion. The strength of van der Waals attractions is in part a function of the difference in the RI of the oil and water phases.^{61,62} Hexadecane has an RI of 1.435 and tricaprylin an RI of 1.449, and hence, there is a smaller difference in RI between hexadecane and water ($\Delta RI = 0.102$) in the

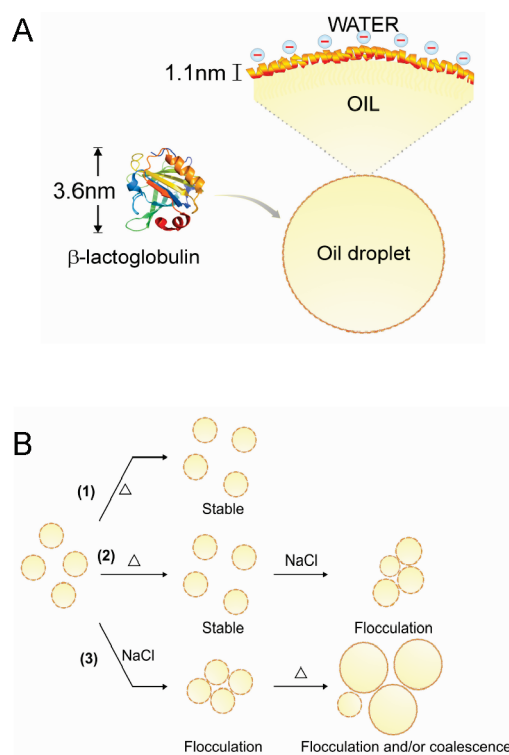


Figure 7. (A) Schematic representation of β -Lg structural rearrangement upon adsorption to the oil–water interface. (B) Influence of high temperatures and high ionic strengths on emulsion droplet stability against flocculation. Emulsions were treated as follows: (1) heated alone; (2) heated at high temperatures and then salt added; (3) salt added and then heated at high temperatures.

emulsion compared to tricaprylin and water ($\Delta RI = 0.116$). The combination of stronger electrostatic repulsion and weaker van der Waals attractions makes the hexadecane-in-water emulsion more stable to salt addition after heating.

Finally, when salt was added to each emulsion before heating, the combined effect of electrostatic screening and high thermal energy resulted in a significant increase in the particle size of both emulsions at high temperatures (Figure 6). The results are once again consistent with previous studies showing the emulsion instability under both heating and salt presence.^{5,10,34,42} The emulsions become unstable because the presence of salt reduces the surface charge and permits the droplets to be in close contact, as seen in flocculation at room temperature. Heating then causes further emulsion flocculation due to interdroplet protein–protein interactions. Especially in the case of β -Lg, disulfide interchange between the free cysteine residue and disulfide bonds can result in intermolecular and hence interdroplet bridges. Comparison of the two different emulsions reveals that the tricaprylin-in-water emulsion starts to undergo flocculation at a lower temperature than the hexadecane-in-water emulsion. Moreover, the changes in particle diameter between 40 and 80 °C follow a different trend for the two oil-in-water emulsions. However, there was little difference in the final particle diameter at 90 °C. One possible explanation for the differences between 40 and 80 °C is that the surface charge of the hexadecane-in-water emulsion (-27 mV) corresponds to that of a stable colloid (> -30 mV). As the treatment temperature is increased, the droplets gain thermal energy, the electrostatic repulsion is no longer larger than the

van der Waals attractions, and the droplets flocculate. Finally, once the emulsions are heated, small conformational changes as detected by SRCD (i.e., the systematic decrease in the helical content) decrease the net colloidal repulsion and the droplets flocculate.

In summary, we have measured the globular protein structural rearrangement upon adsorption to oil–water interfaces (Figure 7A). Under homogenizing conditions, β -Lg adsorbs to oil–water interfaces and changes from a globular structure rich in β -sheet into an open flat structure with a large amount of non-native α -helix. This structural change establishes the interaction between the protein hydrophobic region and the oil phase and also exposes the negatively charged protein region to the aqueous phase. Overall this results in a thin, dense protein layer, which is highly negatively charged at the droplet surface. This emulsion is then resistant to flocculation at high temperatures (Figure 7B1), but once exposed to salt, the electrostatic repulsion between the droplets is reduced and different flocculation and/or coalescence may occur as discussed above (Figure 7B2,3). Our study now provides a more detailed molecular explanation for protein-stabilized emulsion colloidal stability and enhances our understanding of the mechanism of protein denaturation at oil–water interfaces.

CONCLUSION

In this study, the conformation and structural dimensions of β -Lg at oil–water interfaces in emulsions were characterized using a combination of SRCD, front-face fluorescence spectroscopy, and DPI biosensing techniques. The impact of these structural changes on the emulsion stability was then assessed via changes in the particle size and ζ -potential. Upon adsorption to the oil–water interface, β -Lg, a well-defined globular protein rich in β -sheet structure, converts to a conformation containing a large amount of non-native α -helix and opens to form a thin dense protein layer around the emulsion droplet surface. This resultant negatively charged protein layer prevents droplet interactions even under high thermal energy conditions via electrostatic repulsion. β -Lg-stabilized emulsions become unstable in the presence of salt because of the reduction in electrostatic repulsion. Heating then causes further emulsion flocculation due to interdroplet protein–protein interactions. Previously it has been widely suggested that β -Lg emulsion thermal instability was in part a result of protein surface denaturation as the temperature passed through the solution denaturation temperature.^{4,10,11} What our new SRCD results indicate is that most of the change in β -Lg conformation occurs as a result of emulsion formation and that there is only a minor change in protein structure as the emulsions are heated past the solution denaturation temperature, where cysteine residues become capable of disulfide interchange. Overall, this study significantly improves our current understanding of interface-mediated protein denaturation mechanisms and reveals a molecular detail not hitherto possible, the importance of protein structural change and the oil phase polarity on the physical stability of β -Lg-stabilized emulsions.

ASSOCIATED CONTENT

S Supporting Information. Confocal images of β -Lg emulsion under a few representative conditions after the treatment of heating and salt addition. This material is available free of charge via the Internet at <http://pubs.acs.org/>.

AUTHOR INFORMATION

Corresponding Author

*E-mail: mibel.aguilar@monash.edu (M.-I.A.); timothyjames.wooster@rdls.nestle.com (T.J.W.). Phone: +61-3-9905-3723 (M.-I.A.). Fax: +61-3-9902-9500 (M.-I.A.).

Present Addresses

[†]Nestlé Research Centre, Lausanne, Switzerland.

ACKNOWLEDGMENT

We sincerely thank Dr. Nykola Jones for her assistance with the experimental technique, the Institute for Storage Ring Facilities in Aarhus (ISA), Denmark, for provision of beam time, and the Australian Research Council and Dairy Innovation Australia Ltd. (through ARC Linkage Grant No. LP0774909).

REFERENCES

- Dalgleish, D. G. *Trends Food Sci. Technol.* **1997**, *8*, 1–6.
- Damodaran, S. *J. Food Sci.* **2005**, *70*, R54–R66.
- Dickinson, E. *Colloids Surf., B* **1999**, *15*, 161–176.
- Dickinson, E. *Colloids Surf., B* **2010**, *81*, 130–140.
- McClements, D. J. *Curr. Opin. Colloid Interface Sci.* **2004**, *9*, 305–313.
- Wilde, P.; Mackie, A.; Husband, F.; Gunning, P.; Morris, V. *Adv. Colloid Interface Sci.* **2004**, *108–109*, 63–71.
- Wilde, P. J. *Curr. Opin. Colloid Interface Sci.* **2000**, *5*, 176–181.
- Dalgleish, D. G. *Food Hydrocolloids* **2006**, *20*, 415–422.
- Dickinson, E. *Colloids Surf., B* **2001**, *20*, 197–210.
- Kim, H. J.; Decker, E. A.; McClements, D. J. *Langmuir* **2002**, *18*, 7577–7583.
- Kim, H. J.; Decker, E. A.; McClements, D. J. *J. Agric. Food Chem.* **2002**, *50*, 7131–7137.
- Fang, Y.; Dalgleish, D. G. *J. Colloid Interface Sci.* **1997**, *196*, 292–298.
- Husband, F. A.; Garrood, M. J.; Mackie, A. R.; Burnett, G. R.; Wilde, P. J. *J. Agric. Food Chem.* **2001**, *49*, 859–866.
- Rampon, V.; Genot, C.; Riaublanc, A.; Anton, M.; Axelos, M. A. V.; McClements, D. J. *J. Agric. Food Chem.* **2003**, *51*, 2482–2489.
- Wu, X.; Narsimhan, G. *Langmuir* **2008**, *24*, 4989–4998.
- Zhai, J.; Miles, A. J.; Pattenden, L. K.; Lee, T. H.; Augustin, M. A.; Wallace, B. A.; Aguilar, M. I.; Wooster, T. J. *Biomacromolecules* **2010**, *11*, 2136–42.
- Croguennec, T.; O’Kennedy, B. T.; Mehra, R. *Int. Dairy J.* **2004**, *14*, 399–409.
- Hagiwara, T.; Sakiyama, T.; Watanabe, H. *Langmuir* **2009**, *25*, 226–234.
- Keiderling, T. A. *Biochemistry* **2006**, *45*, 8444–8452.
- Lee, S.-H.; Lefevre, T.; Subirade, M.; Paquin, P. *J. Agric. Food Chem.* **2007**, *55*, 10924–10931.
- Sakuno, M. M.; Matsumoto, S.; Kawai, S.; Taihei, K.; Matsumura, Y. *Langmuir* **2008**, *24*, 11483–11488.
- Tcholakova, S.; Denkov, N. D.; Ivanov, I. B.; Campbell, B. *Langmuir* **2002**, *18*, 8960–8971.
- Atkinson, P. J.; Dickinson, E.; Horne, D. S.; Richardson, R. M. *J. Chem. Soc., Faraday Trans.* **1995**, *91*, 2847–54.
- Fragneto, G.; Thomas, R. K.; Rennie, A. R.; Penfold, J. *Science* **1995**, *267*, 657–60.
- Holt, S. A.; White, J. W. *Phys. Chem. Chem. Phys.* **1999**, *1*, 5139–5145.
- Murray, B. S. *Prog. Colloid Polym. Sci.* **1997**, *103*, 41–50.
- Noskov, B. A.; Mikhailovskaya, A. A.; Lin, S. Y.; Loglio, G.; Miller, R. *Langmuir* **2010**, *26*, 17225–17231.
- Benjamins, J.; Lyklema, J.; Lucassen-Reynders, E. H. *Langmuir* **2006**, *22*, 6181–6188.

- (29) Miller, R.; Leser, M. E.; Michel, M.; Fainerman, V. B. *J. Phys. Chem. B* **2005**, *109*, 13327–13331.
- (30) Pradines, V.; Krägel, J. r.; Fainerman, V. B.; Miller, R. *J. Phys. Chem. B* **2008**, *113*, 745–751.
- (31) Maldonado-Valderrama, J.; Miller, R.; Fainerman, V. B.; Wilde, P. J.; Morris, V. J. *Langmuir* **2010**, *26*, 15901–8.
- (32) Hemar, Y.; Horne, D. S. *J. Colloid Interface Sci.* **1998**, *206*, 138–145.
- (33) Mackie, A. R.; Mingins, J.; North, A. N. *J. Chem. Soc., Faraday Trans.* **1991**, *87*, 3043–9.
- (34) Wooster, T. J.; Augustin, M. A. *J. Colloid Interface Sci.* **2006**, *303*, 564–572.
- (35) Friberg, S. E.; Larsson, K.; Johan, S. *Food Emulsions*, 4th ed.; Marcel Dekker: New York, 2004.
- (36) Dickinson, E. *J. Dairy Sci.* **1997**, *80*, 2607–2619.
- (37) Cross, G. H.; Reeves, A. A.; Brand, S.; Popplewell, J. F.; Peel, L. L.; Swann, M. J.; Freeman, N. J. *Biosens. Bioelectron.* **2003**, *19*, 383–90.
- (38) Freeman, N. J.; Peel, L. L.; Swann, M. J.; Cross, G. H.; Reeves, A.; Brand, S.; Lu, J. R. *J. Phys.: Condens. Matter* **2004**, *16*, S2493–S2496.
- (39) Lee, T. H.; Hall, K. N.; Swann, M. J.; Popplewell, J. F.; Unabia, S.; Park, Y.; Hahm, K. S.; Aguilar, M. I. *Biochim. Biophys. Acta* **2010**, *1798*, 544–57.
- (40) Lee, T. H.; Heng, C.; Swann, M. J.; Gehman, J. D.; Separovic, F.; Aguilar, M. I. *Biochim. Biophys. Acta* **2010**, *1798*, 1977–86.
- (41) Sheu, B. C.; Lin, Y. H.; Lin, C. C.; Lee, A. S.; Chang, W. C.; Wu, J. H.; Tsai, J. C.; Lin, S. *Biosens. Bioelectron.* **2010**, *26*, 822–7.
- (42) Day, L.; Xu, M.; Lundin, L.; Wooster, T. J. *Food Hydrocolloids* **2009**, *23*, 2158–2167.
- (43) Gu, Y. S.; Regnier, L.; McClements, D. J. *J. Colloid Interface Sci.* **2005**, *286*, 551–558.
- (44) Kim, H. J.; Decker, E. A.; McClements, D. J. *Langmuir* **2004**, *20*, 5753–5758.
- (45) Wooster, T. J.; Augustin, M. A. *J. Colloid Interface Sci.* **2007**, *313*, 665–675.
- (46) Ricard-Blum, S.; Peel, L. L.; Ruggiero, F.; Freeman, N. J. *Anal. Biochem.* **2006**, *352*, 252–9.
- (47) Swann, M. J.; Peel, L. L.; Carrington, S.; Freeman, N. J. *Anal. Biochem.* **2004**, *329*, 190–8.
- (48) Farrell, H. M., Jr.; Jimenez-Flores, R.; Bleck, G. T.; Brown, E. M.; Butler, J. E.; Creamer, L. K.; Hicks, C. L.; Hollar, C. M.; Ng-Kwai-Hang, K. F.; Swaisgood, H. E. *J. Dairy Sci.* **2004**, *87*, 1641–1674.
- (49) Eden, S.; Lim o-Vieira, P.; Hoffmann, S. V.; Mason, N. J. *Chem. Phys.* **2006**, *323*, 313–333.
- (50) Miles, A. J.; Janes, R. W.; Brown, A.; Clarke, D. T.; Sutherland, J. C.; Tao, Y.; Wallace, B. A.; Hoffmann, S. V. *J. Synchrotron Radiat.* **2008**, *15*, 420–422.
- (51) Lees, J. G.; Smith, B. R.; Wien, F.; Miles, A. J.; Wallace, B. A. *Anal. Biochem.* **2004**, *332*, 285–289.
- (52) Whitmore, L.; Wallace, B. A. *Nucleic Acids Res.* **2004**, *32*, W668–673.
- (53) Sreerama, N.; Woody, R. W. *Anal. Biochem.* **1993**, *209*, 32–44.
- (54) Sreerama, N.; Venyaminov, S. Y.; Woody, R. W. *Protein Sci.* **1999**, *8*, 370–80.
- (55) Bewley, M. C.; Creamer, L. K.; Baker, H. M.; Baker, E. N.; Jameson, G. B. *Biochemistry* **1998**, *37*, 14014–14023.
- (56) Kontopidis, G.; Holt, C.; Sawyer, L. *J. Mol. Biol.* **2002**, *318*, 1043–1055.
- (57) Kabsch, W.; Sander, C. *Biopolymers* **1983**, *22*, 2577–2637.
- (58) Bowie, J. U. *Nature* **2005**, *438*, 581–589.
- (59) Dill, K. A. *Biochemistry* **1990**, *29*, 7133–55.
- (60) Dill, K. A.; Ozkan, S. B.; Shell, M. S.; Weikl, T. R. *Annu. Rev. Biophys.* **2008**, *37*, 289–316.
- (61) Hunter, R. J. *Foundations of Colloid Science*; Clarendon Press: Oxford, U.K., 1986; Vol. 1.
- (62) Israelachvili, J. N. *Intermolecular and Surface Forces*; Academic Press: New York, 1991.

Appendix 3.1: Supporting Information

Emulsion visualization by confocal microscopy

The β -Lg-stabilized emulsions after the treatment of heating and/or salt addition were examined using a Leica SP5 Confocal Laser Scanning Microscope equipped with an argon ion laser (Leica Microsystems, Wetzlar, Germany). One drop of fluorescence dye Nile Red (0.025% dissolved in 0.1% dimethyl sulfoxide/99.9% ethanol) was added to the emulsion sample (1 mL) which was gently mixed by inversion. The sample was then observed under the microscope and the images were exported in a scale of 25 μ m.

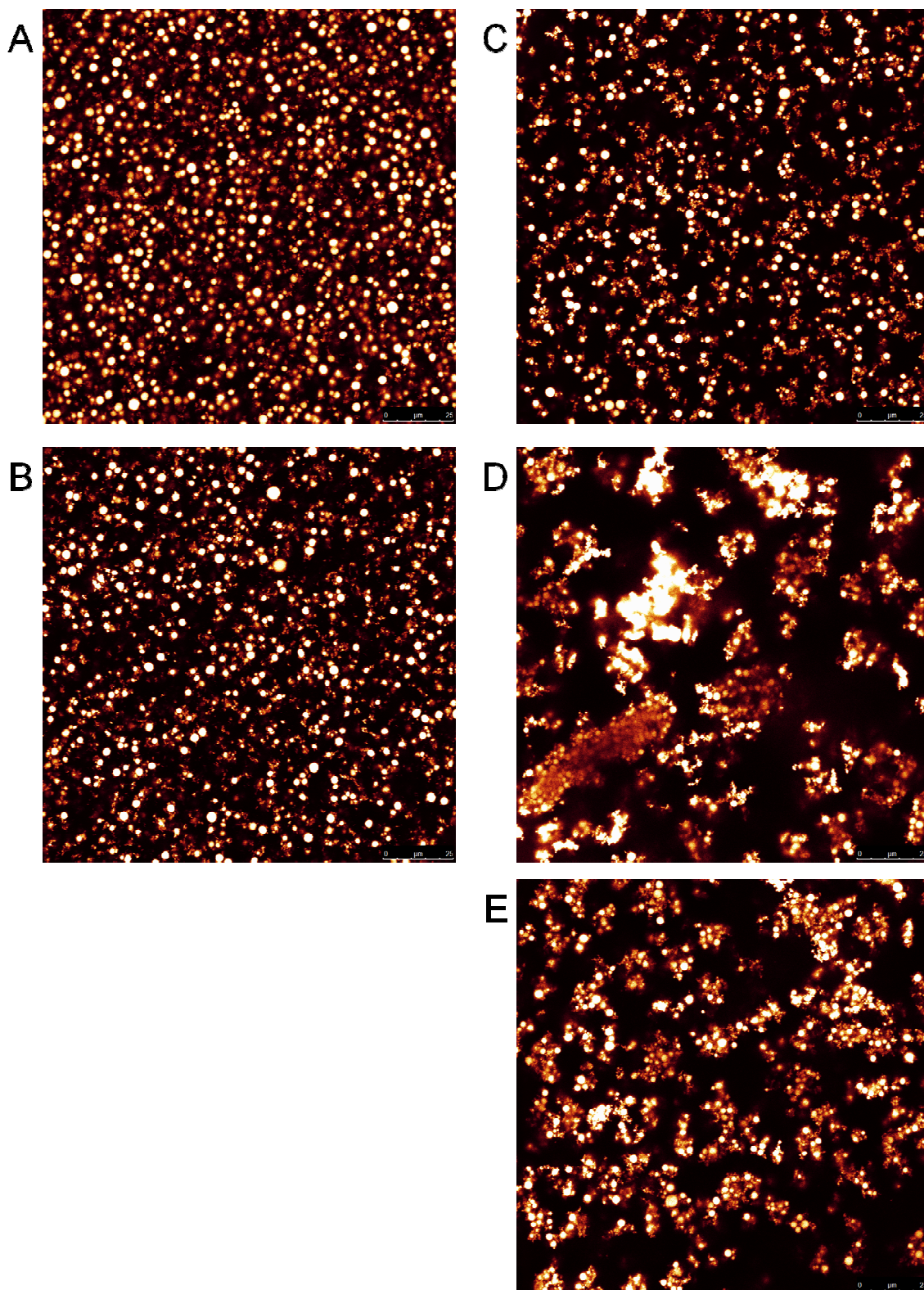


Figure S1: Confocal images of β -Lg-stabilized tricaprylin-in-water emulsions 24 h after the treatment of (A) 20 °C + 0 mM NaCl; (B) 90 °C + 0 mM NaCl; (C) 20 °C + 120 mM NaCl; (D) 120 mM NaCl + 90 °C; (E) 90 °C + 120 mM NaCl.

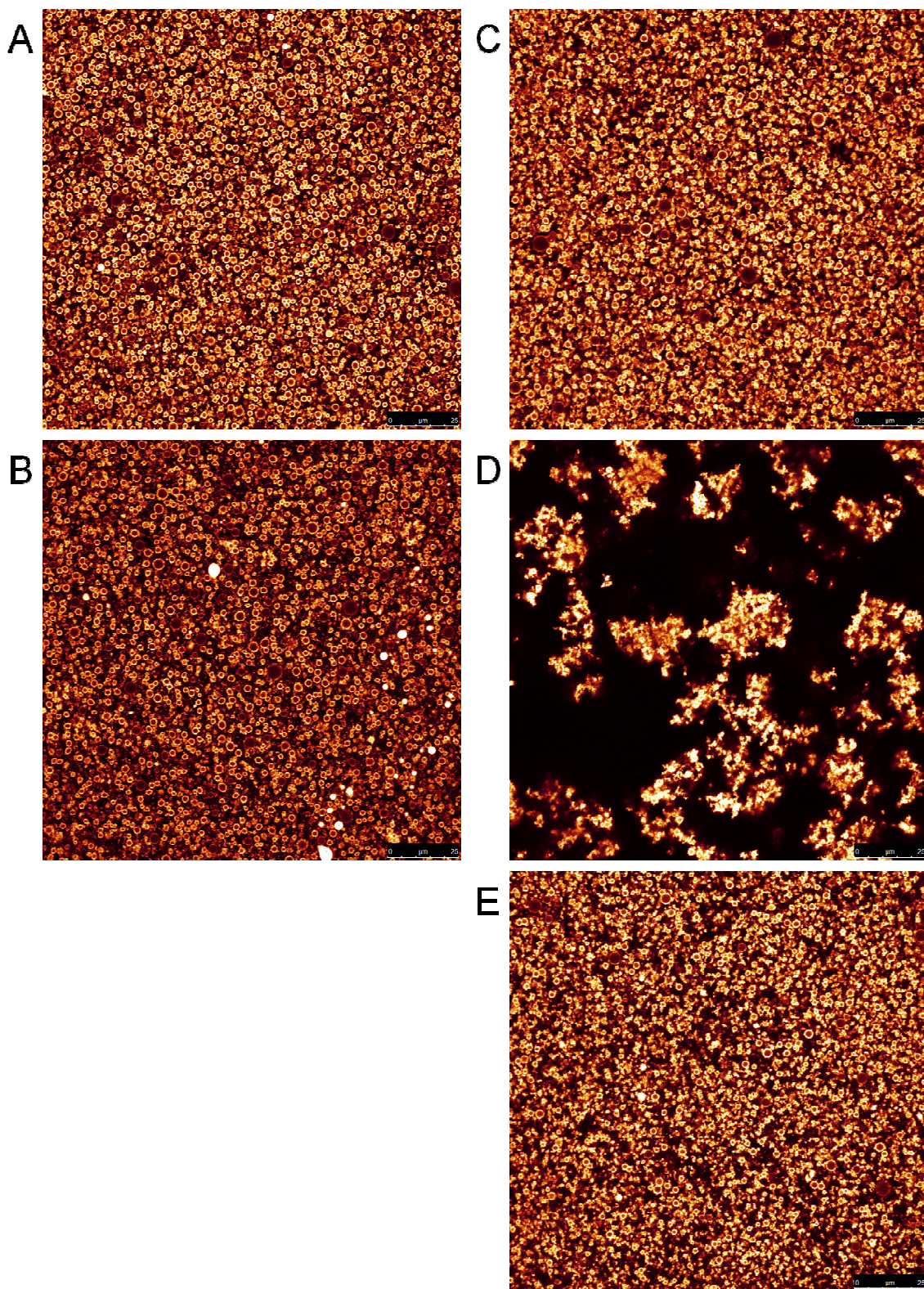
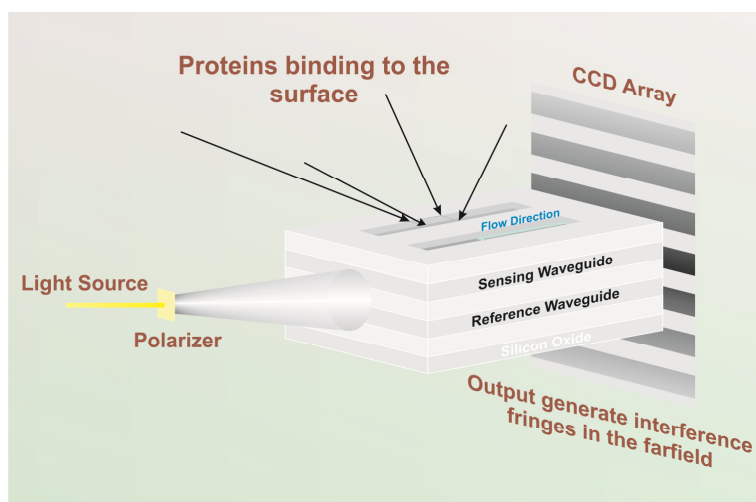


Figure S2: Confocal images of β -Lg-stabilized hexadecane-in-water emulsions 24 h after the treatment of (A) 20 °C + 0 mM NaCl; (B) 90 °C + 0 mM NaCl; (C) 20 °C + 120 mM NaCl; (D) 120 mM NaCl + 90 °C; (E) 90 °C + 120 mM NaCl.

Chapter 4

Conformational changes of α -lactalbumin adsorbed at oil-water interfaces: Interplay between protein structure and emulsion stability



A schematic representation of dual polarization interferometry

**Conformational changes of α -lactalbumin adsorbed at oil-water
interfaces: Interplay between protein structure and emulsion
stability**

Jiali Zhai^{1,2}, Søren V. Hoffmann³, Li Day², Tzong-Hsien Lee¹, Mary Ann Augustin²,
Marie-Isabel Aguilar^{1,*} and Tim J. Wooster^{2,#,*}

¹ Department of Biochemistry and Molecular Biology, Monash University, Clayton, VIC 3800, Australia

² CSIRO Food and Nutritional Sciences, 671 Sneydes Road, Werribee, VIC 3030, Australia

³Institute for Storage Ring Facilities (ISA), Aarhus University, Ny Munkegade 120, DK-8000 Aarhus C,
Denmark

#Present Address: Nestlé Research Centre, CH-1000 Lausanne 26, Switzerland

*Corresponding author:

Dr. Tim J. Wooster,
CSIRO Food and Nutritional Sciences,
671 Sneydes Rd, Werribee, VIC 3030, Australia
Present Address: Nestlé Research Centre, Lausanne, Switzerland.
timothyjames.wooster@rdls.nestle.com

Prof. Marie-Isabel Aguilar,
Department of Biochemistry & Molecular Biology,
Monash University, Clayton, Vic 3800, Australia
mibel.aguilar@monash.edu
Ph: +61-3-9905-3723
Fx: +61-3-9902-9500

Abstract

The conformation and structural dimensions of α -lactalbumin (α -La) both in solution and adsorbed at oil-water interfaces of emulsions were investigated using synchrotron radiation circular dichroism (SRCD) spectroscopy, front-face tryptophan fluorescence (FFTF) spectroscopy and dual polarization interferometry (DPI). The near-UV SRCD and the FFTF results demonstrated that the hydrophobic environment of the aromatic residues located in the hydrophobic core of native α -La was significantly altered upon adsorption, indicating the unfolding of the hydrophobic core of α -La upon adsorption. The far-UV SRCD results showed that adsorption of α -La at oil-water interfaces created a new non-native secondary structure that was more stable to thermally-induced conformational changes. Specifically, the α -helical conformation increased from 29.9% in solution to 45.8% at the tricaprylin-water interface and to 58.5% at the hexadecane-water interface. However, the β -sheet structure decreased from 18.0% in solution to less than 10% at both oil-water interfaces. The DPI study showed that adsorption of α -La to a hydrophobic C18-water surface caused a change in the dimensions of α -La from the native globule-like particle (2.5-3.7 nm) to a thin flat layer approximately 1.1 nm thick. Analysis of the colloidal stability of α -La-stabilized emulsions showed that these emulsions were physically stable against droplet flocculation at elevated temperatures both in the absence and presence of 120 mM NaCl. In the absence of salt, the thermal stability of emulsions was due to the strong electrostatic repulsion provided by the adsorbed α -La layer, which was formed after the adsorption and structural rearrangement. In the presence of salt, although the electrostatic repulsion was reduced via electrostatic screening, heating did not induce strong and permanent droplet flocculation. The thermal stability of α -La-stabilized emulsions in the presence of salt is a combined effect of the electrostatic repulsion and the lack of covalent disulfide interchange reactions. This study reported how the interfacial structure of α -La adsorbed at oil-water interfaces played an active role in controlling the physical stability of α -La-stabilized oil-in-water emulsions under heating and moderate ionic strength (120 mM NaCl) conditions.

Introduction

Many studies in the food emulsion field have focused on investigating the physical stability of protein-stabilized emulsions.¹⁻⁶ Proteins are surface active molecules and are commonly used as emulsifying agents in the food industry.^{5, 7-11} Proteins stabilize oil-in-water emulsions by adsorbing at the oil-water interface, forming a protein layer around the droplet surface that provides electrostatic and/or steric repulsive forces between emulsion droplets.^{2, 5, 11-13} The physical stability of protein-stabilized emulsions is governed by the balance between van der Waals attractive forces and electrostatic and/or steric repulsive forces. The type of stabilization mechanism in a protein-stabilized emulsion depends on the interfacial structure of the protein layer at the droplet surface. For example, emulsions stabilized by flexible proteins or protein-polysaccharide conjugates are more stable against flocculation in the presence of salt due to the protrusion of long segments into the aqueous phase, which provides excellent steric repulsion between the droplets.^{5, 6, 12, 14} In contrast, emulsions stabilized by globular proteins have thin interfacial layers and hence are prone to flocculation in the presence of salt because they only have electrostatic repulsion between the droplets, which can be easily screened.^{3-5, 12}

Compared to our knowledge on the physical stability of protein-stabilized emulsions, the understanding of the structure of proteins adsorbed at oil-water interfaces of emulsions remains poor.^{10, 13, 15-17} Previous studies using Fourier transform infrared (FTIR) spectroscopy have given some limited information on the change in secondary structure of globular proteins such as β -lactoglobulin (β -Lg), bovine serum albumin (BSA) and α -lactalbumin (α -La) upon adsorption at oil-water interfaces of model emulsions.¹⁸⁻²² However, the complexity of FTIR spectra arising from the overlapping peaks of the secondary structure of proteins can affect the accuracy of the results in terms of the structural change upon adsorption. For example, three FTIR studies have demonstrated that the β -sheet structure of β -Lg underwent changes upon protein adsorption to oil-water interfaces; however changes in other secondary structures such as the α -helix were not reported, most likely due to the difficulties associated with deconvolution of the FTIR spectra. Front-face tryptophan fluorescence (FFTF) spectroscopy studies on globular proteins adsorbed at oil-water interfaces have demonstrated changes in the maximum emission wavelengths of tryptophan residues in proteins upon adsorption, suggesting the unfolding of the globular structure of proteins.²³⁻²⁵ Neutron reflectometry²⁶⁻³¹ studies on proteins adsorbed at planar hydrophobic surfaces and dynamic light scattering studies on proteins adsorbed at surfaces of model emulsions containing latex or silica beads³²⁻³⁴ have given some information on the thickness and density distribution of the adsorbed protein layers. These studies have advanced our understanding of the adsorption-induced structural change of proteins by showing that proteins change their structure and form an interfacial layer at the droplet surfaces with a certain thickness and density distribution

profile. However, the molecular conformation, in particular at the secondary and tertiary structure level, of proteins adsorbed at oil-water interfaces has yet to be clearly elucidated.

We have recently employed two biophysical methods, i.e. synchrotron radiation circular dichroism (SRCD) spectroscopy and dual polarization interferometry (DPI) to study the conformation and geometric dimensions of β -Lg adsorbed at oil-water interfaces of emulsions.^{35, 36} The SRCD method measured the conformation of β -Lg at oil-water interfaces in freshly made emulsions without further sample preparation and allowed the secondary and tertiary structure of β -Lg adsorbed at oil-water interfaces to be characterized. The DPI method was used to measure the thickness and density of the protein layer adsorbed at solid-water interfaces containing different hydrophobic properties. The results showed that β -Lg, a well-defined globular protein rich in β -sheet structure in solution, unfolded to form a thin dense layer around the droplet surface and converted to a conformation with α -helical-rich and heat-resistant characteristics.

To extend our knowledge on protein structural behaviour upon adsorption at oil-water interfaces, the biophysical methods in the β -Lg study can be employed to study a wider range of proteins. α -La, a major component of whey protein isolates derived from milk, is also an important protein for providing emulsion colloidal stability. While the structure of α -La in solution has been well characterized,³⁷ its structure at oil-water interfaces and ability to stabilize emulsions has not been extensively studied. α -La is similar to β -Lg in that they are both small globular proteins with a large amount of ordered secondary structure. X-ray crystallographic studies reveal that α -La is a protein with one large domain of three α -helices and one sub-domain of three small anti-parallel β -sheets, which are connected by a calcium binding loop.^{38, 39} However, unlike β -Lg which has two disulfide bonds and one free thiol group, α -La contains four disulfide bonds and does not contain a free thiol group. Moreover, α -La contains more α -helical structure than β -Lg. Heating α -La in solution induces a conformational transition at a lower temperature (~ 66 °C) than β -Lg (~ 73 °C).⁴⁰⁻
⁴² However, in contrast to β -Lg, heating α -La results in very little protein polymerization and aggregation due to the lack of the free thiol in α -La.⁴⁰⁻⁴²

An important feature of α -La is its ability to adopt the molten globule state under various conditions such as at low pHs, high temperatures, at moderate concentration of denaturant or in its Apo (non-calcium bound) form.⁴³⁻⁴⁶ The molten globule state of a globular protein is an intermediate or ensemble of physical states on the folding pathway and is defined as containing native-like secondary structure but no stabilized tertiary structure.^{43, 44} With limited understanding of the structure of proteins adsorbed at oil-water interfaces in the past decades, it was proposed that the concept of the molten globule state might be applied to describe proteins adsorbed at oil-water interfaces.⁴⁴ Moreover, it was suggested that α -La, in its molten globule state, resulted in improved surface activities.^{47, 48} For example, under conditions which were considered to induce a molten

globule structure, α -La reduced the surface tension of the air-water interface and the *n*-tetradecane-water interface more rapidly than in its native state.^{47, 48} The putative molten globule form of α -La has also been shown to displace β -Lg adsorbed at oil-water interfaces whereas no such ability was observed for native α -La.⁴⁹ This enhanced surface activity of α -La is attributable to the increased exposure of the hydrophobic groups and increased molecular flexibility.^{47, 48} Although the concept of the molten globule structure of α -La provided a mechanism to explain enhanced surface activity, none of these studies unequivocally confirmed the presence of molten globule structures of α -La once it was adsorbed at oil-water interfaces. Moreover, an FTIR study showed that the adsorption of α -La to oil-water interfaces induced a decrease in α -helix and an increase in β -sheet structure,¹⁹ which was inconsistent with a native-like molten globule structure.

To understand the geometric dimensions and conformation of α -La adsorbed at oil-water interfaces and the potential role of the molten globule state, direct measurements of the secondary and tertiary structure are thus required. Moreover, although it is hypothesized that the mechanism by which α -La stabilizes emulsions is similar to other globular proteins, the physical stability of emulsions stabilized by α -La alone has not been studied in detail. In this study, DPI, SRCD and FFTF methods were used to investigate the geometric dimensions and conformation of α -La adsorbed at oil-water interfaces. The ζ -potential and the particle size of α -La-stabilized emulsions under the conditions of heating and salt addition were also examined. Moreover, the effect of oil polarity on protein structure at oil-water interfaces and the physical stability of emulsions was investigated using two model oils, i.e. *n*-hexadecane (more non-polar) and tricaprylin (more polar). This study aimed to broaden our understanding of how the structure of α -La adsorbed at oil-water interfaces can be related to its function of controlling emulsion physical stability.

Materials and Methods

Materials

α -La (Type 1, calcium-bound, $\geq 85\%$ α -La PAGE) was purchased from Sigma-Aldrich Company (St Louis, MO) and used without further preparation. Sodium chloride (NaCl), sodium phosphate (monobasic and dibasic), *n*-hexadecane, tricaprylin (glyceryl trioctanoate, $>99\%$), glycerol, urea and sodium dodecyl sulphate (SDS) were purchased from Sigma-Aldrich Company (St Louis, MO). All chemicals and solvents were of analytical grade. The ultrapure water was prepared by a Purelab Ultra Genetic purification system (ELGA LabWater) and used for all experiments.

DPI measurements

The geometric dimensions of α -La adsorbed at model hydrophobic interfaces was determined by measuring the thickness and refractive index (RI) of the α -La layer adsorbed at a C18 hydrocarbon AnaChip immobilized on an *Analight* Bio2000 DPI instrument (Farfield Group, UK). The detailed instrumental set-up and calibration procedure using 80% (w/w) EtOH have been previously described.³⁶ The C18 hydrocarbon chip surface with bulk buffer flowing over the top served as a model planar oil-water interface for protein adsorption studies. Freshly prepared 10 μ M α -La solution in 10 mM sodium phosphate buffer pH 7 was injected for adsorption at a flow rate of 10 μ L/min for 15 min and followed by a dissociation phase with the buffer flowing over the surface of the adsorbed layer for another 15 min. In comparison, a reference study was also performed by adsorbing α -La to a hydrophilic silicon oxynitride Anachip (Farfield Group, UK). α -La was injected over the silicon Anachip in a similar experimental condition as in the C18 Anachip study except that a higher concentration (100 μ M) and a lower pH buffer (10 mM sodium phosphate, pH 3) were used. This was to ensure that the positively charged α -La at pH 3 adsorbed to the hydrophilic silicon chip via weak polar interactions between the protein surface and the silicon surface, rather than the strong hydrophobic force encountered in the C18 surface. The conversion of transverse magnetic (TM) and transverse electric (TE) data into layer mass, thickness, RI and density used the mathematical model as previously described.³⁶

Emulsion preparation and centrifugation assay

α -La-stabilized emulsions (0.3% w/w) containing 20% (v/v) hexadecane or tricaprylin were used for the study. The emulsions were prepared following the method previously described.³⁶ Briefly, the oil phase was added to protein solution by weight. The mixture was then blended using an Ultra-turrax rotor stator homogenizer at 8000 rpm for 2 min and then passed through an Avestin C5 high-pressure valve homogenizer twice at approximately 700 bar. All emulsions used for SRCD

and fluorescence studies were freshly prepared on site at the ASTRID-synchrotron where the CD1 beam line is located (Institute for Storage Ring Facilities, Aarhus University, Denmark) and experiments were performed within 24 h of preparation.

To determine the amount of α -La adsorbed at the oil-water interface, emulsions were centrifuged in 30 kDa centrifuge tubes (Pall, Port Washington, NY) at $11600 \times g$ for 15 min. The concentration of the protein in the aqueous phase (supernatant) was obtained by measuring absorbance at 280 nm and using an extinction coefficient of $2.01 \text{ mLmg}^{-1}\text{cm}^{-1}$.⁵⁰ The amount of protein adsorbed at oil-water interfaces of emulsions was then estimated from the specific surface area of the emulsion droplets as previously described and reported as the surface coverage.³⁵ An average of 12 aliquots of each emulsion sample was reported.

Front-face tryptophan fluorescence (FFTF) measurements

FFTF spectra of fresh α -La solution and emulsions were obtained with a Luminescence Spectrometer (PerkinElmer LS50B, Massachusetts) in its front face mode, using the methods previously described.³⁶ The excitation wavelength was set at 290 nm and the emission spectra were collected in the range of 300 nm to 450 nm with a scanning speed of 100 nm/min. Excitation and emission slit widths were set at 10 nm. Each individual emission spectrum was the average of three runs. All data were collected at room temperature, $\sim 20 \text{ }^\circ\text{C}$.

SRCD measurements and data analysis

All far-UV and near-UV SRCD measurements of α -La in solution and in emulsions were performed on the CD1 beam line of the SRCD station at the ASTRID storage ring.^{51, 52} The operating conditions and the data analysis followed the method previously described.³⁶ Suprasil cells (Hellma GmbH & Co., Germany) with 0.01 cm and 0.5 cm path lengths were used for the far-UV and the near-UV SRCD measurements respectively. The operating conditions were: 1 nm bandwidth, 2.15 s averaging time, 3 scans for a solution sample and 8 scans for an emulsion sample. An SDS-stabilized emulsion was used as a baseline to correct for the light scattering background of the emulsion spectra as previously described.³⁶ The thermal stability study of the secondary structure of α -La in solution and in emulsions was carried out by heating in situ in a temperature-controlled chamber of the SRCD instrument. A mean residue weight of 115 for α -La was used to convert the unit of milli-degrees in SRCD to the standard unit of mean residue ellipticity $[\theta]$. The secondary structural content was calculated using the SELCON3 method⁵³ and the reference set SP175 in DICHROWEB⁵⁴ as previously described.³⁶

Treatment of emulsions under high temperatures and salt addition

α -La-stabilized emulsions were prepared as described above and were then treated under three different conditions involving high temperatures and/or salt addition. The experimental procedures used were similar to those previously described for the study of β -Lg-stabilized emulsions.³⁶ Briefly, the first condition involved heating the freshly made emulsions in the absence of NaCl from 20 °C to 90 °C for 20 min. The second condition involved heating the freshly made emulsions in the presence of NaCl (120 mM). The third condition involved firstly heating the emulsions in the absence of NaCl and then adding 120 mM NaCl to the emulsions after cooling to room temperature. The ζ -potential and particle size measurements were taken after 24 h storage.

Measurements of the ζ -potential and average particle size of α -La-stabilized emulsions

The ζ -potential of emulsions was measured using laser doppler velocimetry (Malvern Zetasizer Nano ZS, Worcestershire, UK). The emulsion samples stored for 24 h after various treatments were diluted (2 μ L in 30 mL of the corresponding buffer, 10 mM sodium phosphate buffer, pH 7, with 0 mM or 120 mM NaCl) and injected into a folded capillary cell with electrodes for measurements. The ζ -potential was calculated from the direction and velocity of the droplet movement when subjected to an alternating electric field.

The average particle size of the emulsions was measured using laser light diffraction (Malvern Mastersizer 2000, Worcestershire, U.K.) equipped with a Hydro SM small volume sample dispersion unit. The emulsion samples were dispersed in buffer (same composition as test conditions) circulating in the Hydro SM unit and the average particle size was calculated from a best fit between the measured scattering pattern and a model scattering pattern of equivalent polydisperse spheres (Mie theory). The volume-weighted average mean diameter $D_{4,3}$ ($=\sum n_i d_{i4} / \sum n_i d_{i3}$, where n_i is the number of particles with diameter d_i) was reported. All measurements of the ζ -potential and particle size were an average of at least three individual samples and the standard deviations are included in Figure 5 and 6 respectively. Detailed experimental procedures and operating conditions were previously described.³⁶

Results

Geometric dimensions of α -La adsorbed at hydrophobic and hydrophilic surfaces

A DPI biosensor equipped with chips containing different surface properties was used to investigate the geometric dimensions of α -La adsorbed at planar solid-water interfaces. Freshly prepared α -La solution was passed over either a hydrophobic C18 surface or a hydrophilic silicon oxynitride surface and the resulting sensorgrams showed real-time changes in the thickness, RI, and mass of the adsorbed layer of α -La (Figure 1). The adsorption of α -La to the hydrophobic C18 surface revealed a strong interaction between the surface and protein with the adsorbed protein layer achieving a mass of 1.2 ng/mm^2 ($= \text{mg/m}^2$) at the end of the 15 min association time and remained at the same value during the following 15 min of the dissociation phase (Figure 1A). The thickness and the density, which were derived from the RI value, of the adsorbed layer at the end of the association phase were determined to be 1.1 nm and 1.1 g/cm^3 respectively. This geometric property of α -La adsorbed at the C18 hydrocarbon-water interface was very similar to that of β -Lg adsorbed at the same surface.³⁶ Together the results indicate that a strong hydrophobic attraction exists during the adsorption of globular proteins to this particular planar hydrocarbon-water interface and results in a thin dense protein layer at the surface.

In the reference study where α -La was passed over the hydrophilic silicon oxynitride surface at a lower pH and a higher concentration, a very different layer of α -La was observed (Figure 1B). A maximum mass of only 0.55 ng/mm^2 ($= \text{mg/m}^2$) was found during the association phase (at 11 min) and from that point onward, the mass steadily decreased and levelled out at 0.3 ng/mm^2 ($= \text{mg/m}^2$) at the end of the dissociation phase. The adsorption also resulted in a much lower density of the adsorbed α -La layer at the silicon surface (0.18 g/cm^3 at the end of association) compared to the C18 surface (1.1 g/cm^3) as revealed by the RI values. The real-time changes in thickness provided further information on the dimension of the α -La layer adsorbed at the silicon surface. Specifically, the thickness varied from 2.3 nm to 3.2 nm during the association phase which is relatively consistent with the crystal structure of α -La ($2.5 \text{ nm} \times 3.2 \text{ nm} \times 3.7 \text{ nm}$).^{38, 55} In the dissociation phase, the thickness was found to be generally lower than the association phase as more and more weakly adsorbed α -La was washed off the surface, which influenced the average thickness value across the whole chip surface. The results demonstrated that the positively charged α -La at pH 3 was adsorbed at the hydrophilic silicon oxynitride surface via weak polar interactions, so that it was in a relatively native state compared to the structure on the C18 surface.

Tertiary structure of α -La adsorbed at oil-water interfaces

The conformation of α -La adsorbed at oil-water interfaces of emulsions was investigated by FFTF spectroscopy and SRCD spectroscopy. Prior to these measurements, it was necessary to

create emulsions where most of the α -La in the emulsions was adsorbed at the interface rather than remaining in the bulk solution. To confirm this, the protein remaining in the bulk solution was measured using the centrifugation assay. The results indicated that compared to the initial protein concentration (3 mg/mL) used to make the emulsion, less than 0.027 ± 0.005 mg/mL of α -La remained in the bulk solution of the hexadecane-in-water emulsion and even less (0.015 ± 0.008 mg/mL) was found in the bulk solution of the tricaprylin-in-water emulsion. A calculated surface coverage (Γ) of 0.87 mg/m² and 1.01 mg/m² was found for the hexadecane-in-water and the tricaprylin-in-water emulsions respectively. Compared to previous reports, these values indicated that an expanded monolayer of α -La was formed at oil-water interfaces of emulsions in this study.^{56, 57}

FFTF spectroscopy was used to probe changes in the environment of the Trp residues of α -La. Figure 2 shows the fluorescence spectra of α -La in solution and at two oil-water interfaces (tricaprylin-water and hexadecane-water). In its native state, α -La gave rise to a λ_{max} at 328.5 nm, which was attributable to the deeply buried four Trp residues (W26, W60, W104, W118) in α -La and was consistent with previous studies.^{47, 48, 58} Dissolving α -La in 6 M urea caused a red shift (21.5 nm) in λ_{max} to 350 nm, indicating the exposure of Trp residues to a more aqueous environment and the unfolding of the protein. Adsorption of α -La to oil-water interfaces resulted in a 6.5 nm red shift of λ_{max} to 335 nm at the tricaprylin-water interface and a 12 nm red shift to 340.5 nm at the hexadecane-water interface respectively. These results demonstrated the movement of the four Trp residues to a more hydrophilic environment when α -La adsorbed at oil-water interfaces, suggesting a perturbation in the native tertiary structure. Moreover, the red-shift of λ_{max} was larger for α -La adsorbed at the hexadecane-water interface than at the tricaprylin-water interface, indicating that the more hydrophobic oil induced a larger conformational change.

Further information on the tertiary structure of α -La adsorbed at the two oil-water interfaces was obtained using near-UV SRCD spectroscopy (Figure 3A). α -La is a globular protein with a well-defined tertiary structure. The near-UV CD spectrum for α -La in solution exhibited a deep broad minimum in the region of 260-290 nm, which arose from tyrosine residues and disulfide bonds, and a small peak at 295 nm arising from Trp residues. This near-UV SRCD spectrum of α -La in solution was consistent with many previous studies.^{45, 47-49, 59} In the emulsion samples, the broad absorption bands were totally lost and inverted to be slightly positive in the region of 260-300 nm, suggesting unfolding/loss of the globular structure of α -La upon adsorption to both the hexadecane-water and the tricaprylin-water interfaces. The near-UV spectra of α -La at oil-water interfaces were also very similar to that previously obtained for the pH 2-induced molten globule state of α -La, which was in an unfolded state, i.e. loss of globular tertiary structure in solution.^{45, 49, 59}

Secondary structure of α -La adsorbed at oil-water interfaces and its stability against heating

The secondary structure of α -La adsorbed at the tricaprylin-water interface and the hexadecane-water interface was measured using far-UV SRCD spectroscopy. Figure 3B shows that in 10 mM sodium phosphate buffer, the far-UV SRCD spectrum for α -La in solution contained double minima at 208 nm and 222 nm and a peak at 188 nm, which was characteristic of α -helical-containing secondary structure. The quantitative analysis of secondary structural content yielded 29.9% α -helix and 18.0% β -sheet. Although the secondary structure content arising from SRCD data were found to be different from those determined from the α -La crystal structure (45% α -helix and 9% β -sheet), the spectrum of α -La in solution was consistent with many previous CD studies of α -La in solution.^{45, 47-49, 59} Adsorption of α -La to the oil-water interface of both emulsions (tricaprylin-in-water and hexadecane-in-water emulsions) resulted in a significant increase in the CD intensities with the appearance of clear double minima at 208 nm and 222 nm. The deconvolution of the secondary structure content indicated a significant increase in α -helical content of α -La from 29.9% in buffer environment to 45.8% at the tricaprylin-water interface and to 58.5% at the hexadecane-water interface (Table 1). In comparison, the β -sheet content decreased from 18.0% in buffer environment to 8.3% for α -La at the tricaprylin-water interface and 9.9% at the hexadecane-water interface (Table 1). Overall therefore, both the far-UV SRCD results (greater change in the secondary structural content) and the FFTF results (the greater red-shift) confirmed a greater effect on changes of the secondary and tertiary structure when α -La was adsorbed at the more hydrophobic hexadecane-water interface than the tricaprylin-water interface.

Since α -La adopted a non-native conformation at oil-water interfaces upon adsorption, the stability of this interfacial secondary structure against heating was further investigated. Five different temperatures ranging from 20 °C to 76 °C were examined and the far-UV SRCD spectra are shown in Figure 4. The SRCD spectra of α -La in solution remained unchanged at temperatures up to 48 °C but at higher temperatures, heating resulted in a significant loss of α -helical intensities (Figure 4A). Indeed, quantitative analysis of α -La secondary structure as summarized in Table 1 revealed that the change was only seen at 62 °C and 76 °C. For example, the α -helix decreased from 29.9 % at 20 °C to 16.9% at 76 °C. The β -sheet increased from 18.0 % at 20 °C to 30.6% at 76 °C. In comparison, heating had much less of an effect on the secondary structure of α -La adsorbed at oil-water interfaces than in solution. The SRCD spectra of α -La at both oil-water interfaces remained relatively stable, particularly in the α -helical region, but some loss of intensities at the positive peak was observed with increasing temperature (Figure 4 B and C). Compared to 20 °C, α -La at the tricaprylin-water interface showed a 5.4% decrease in α -helix and 3.3% increase in β -sheet at 76 °C; α -La at the hexadecane-water interface showed a 10.5% decrease in α -helix and 3.3% increase in β -sheet at 76 °C.

Effect of heating and salt on the ζ -potential and average particle size of α -La-stabilized oil-in-water emulsions

The stability of α -La-stabilized emulsions against heating and moderate ionic strength was further assessed by measuring the ζ -potential and average particle size at room temperature, 24 h after the emulsions were heated for 20 minutes at temperatures ranging from 20 °C to 90 °C in the absence or presence of 120 mM NaCl. α -La-stabilized tricaprylin-in-water emulsions and hexadecane-in-water emulsions had a ζ -potential of approximately -49 ± 2 mV, which remained very stable with increased temperatures (Figure 5A and 5B). Addition of 120 mM NaCl reduced the ζ -potential of both emulsions to approximately -19 ± 2 mV, which also remained stable at high temperatures (Figure 5A and 5B). This trend of reduction in the ζ -potential of emulsions with addition of salt was irrespective of whether the salt was added before or after heating. The addition of salt reduced the surface charge of the protein layer via electrostatic screening.

The change in the average particle size ($D_{4,3}$) of α -La-stabilized emulsions in response to heating and/or salt addition is shown in Figure 6. In the absence of salt, the tricaprylin-in-water emulsion had an average particle size of 0.60 ± 0.01 μm at 20 °C and 0.59 ± 0.01 μm after heating up to 90 °C, meaning that heating had no effect on the emulsion particle size (Figure 6A, solid line). The hexadecane-in-water emulsion had an average particle size of 0.69 ± 0.01 μm at 20 °C and 0.71 ± 0.01 μm at 90 °C, clearly demonstrating particle size stability against heating (Figure 6B, solid line).

When 120 mM NaCl was added to the emulsion prior to heating, the particle size of the tricaprylin-in-water emulsion increased slightly to 0.85 ± 0.01 μm at 20 °C compared to 0.60 ± 0.01 μm at 20 °C in the absence of salt. (Figure 6A, dotted line). The hexadecane-in-water emulsion also had an increase in particle size at 20 °C, increasing from 0.69 ± 0.01 μm in the absence of salt to 0.79 ± 0.01 μm in the presence of salt (Figure 6B, dotted line). When heating the tricaprylin-in-water emulsions in the presence of salt, the initial particle size at 20 °C (0.85 ± 0.01 μm) remained relatively stable up to 80 °C (0.93 ± 0.01 μm) but underwent a moderate increase at 90 °C (1.71 ± 0.03 μm). However, heating the hexadecane-in-water emulsion in the presence of salt had no significant effect on the particle size (0.79 ± 0.01 at 20 °C to 0.81 ± 0.01 μm at 90 °C), suggesting a higher physical stability compared to the tricaprylin-in-water emulsion.

In the treatment where the emulsion was heated prior to salt addition, the tricaprylin-in-water emulsion had an average particle size of 0.87 ± 0.01 μm at 20 °C. Heating the tricaprylin-in-water emulsion then adding salt gradually increased the particle size from 0.87 ± 0.01 μm at 20 °C to 1.21 ± 0.02 μm at 80 °C, which rose up to 15.56 ± 2.59 μm at 90 °C (Figure 6A, dashed line). A similar trend was observed for the hexadecane-in-water emulsion under the condition of heating

prior to adding salt. The average particle size of the hexadecane-in-water emulsion increased from $0.77 \pm 0.01 \mu\text{m}$ at 20 °C to $1.43 \pm 0.06 \mu\text{m}$ at 90 °C (Figure 6B, dashed line). In comparison to the tricaprylin-in-water emulsion, the particle size increase in the hexadecane-in-water emulsion was much smaller under the condition of adding salt after heating. Overall, adding salt after heating destabilized α -La-stabilized emulsions to the greatest extent compared to the other two conditions (heating in the absence of salt and heating in the presence of salt) investigated in this study, particularly at high temperatures (80 and 90 °C). Furthermore, the hexadecane-in-water emulsion was generally more stable than the tricaprylin-in-water emulsion.

The confocal images of α -La-stabilized emulsions under the conditions of heating and moderate ionic strength conditions were also consistent with the particle size measurements (See the Supporting Information). The results showed that the increase in the particle size of emulsions in this study was largely due to droplet flocculation rather than coalescence. However, it is hard to entirely exclude the coalescence destabilization from the confocal images as they only represent a fraction of the emulsion samples.

Discussion

Adsorption-induced α -La structural change

This study characterized the geometrical dimensions and conformation of α -La adsorbed at oil-water interfaces of emulsions using the complementary techniques of DPI, FFTF and SRCD. Overall, the results showed that adsorption of the small globular protein α -La to oil-water interfaces induced a significant change in both the secondary and the tertiary structure. The geometric data for α -La adsorbed at surfaces containing different properties clearly demonstrated the strong effect of the hydrophobic force on perturbing protein structure (Figure 1). α -La adsorbed at the C18-water interface resulted in a layer which was thinner (1.1 nm) and with higher mass (1.2 mg/m²) and higher density (1.1 g/cm³) with respect to the layer adsorbed at a hydrophilic silicon surface, indicating unfolding of the native globular shape into an open flat structure (Figure 1). A similar structural change at the C18 surface was also observed for the globular protein β -Lg in a previous study.³⁶ The structural change of α -La and β -Lg occurs upon adsorption at the C18-water interface, where the hydrophobic region of proteins interacts with the hydrophobic C18 surface and the hydrophilic region of proteins remains exposed to the aqueous environment. At pH 3 below its *pI* of 4.2, α -La was adsorbed at the hydrophilic silicon oxynitride surface via weak polar interactions so that its crystal structure-like dimensions were retained. This study demonstrated that DPI is a sensitive technique to investigate the mechanism of protein adsorption at solid-fluid interfaces.

The λ_{\max} in FFTF spectra of α -La adsorbed at two oil-water interfaces of emulsions (tricaprylin-water and hexadecane-water) were red-shifted with respect to that of native protein in solution (Figure 2), suggesting a change in protein globular structure with increased solvent exposure of Trp residues. It is generally difficult to differentiate the contribution of individual Trp residues to the emission signal for a multi-tryptophan protein. In the case of α -La, all four Trp (W26, W60, W104, W118) lie in the hydrophobic cluster of the protein and hence are deeply buried.^{38, 39} The increased solvent exposure of these Trp residues upon α -La adsorption to oil-water interfaces clearly indicated the disruption of the hydrophobic cluster of native α -La. The near-UV SRCD spectra confirmed this conclusion by showing a complete disappearance of the characteristic profile of native α -La in solution. Low positive signals for α -La adsorbed at both oil-water interfaces were seen in the region of 260-300 nm versus the deep negative peaks from Tyr, Phe and Trp for native α -La in solution (Figure 3A). Such a dramatic spectral change strongly suggests that the hydrophobic cluster of native α -La has been significantly perturbed upon adsorption to oil-water interfaces.

To define the α -La structure at oil-water interfaces in the context of the molten globule state, detailed characterization of the secondary structure is needed. This study reported for the first

time the far-UV SRCD spectra of α -La in emulsions (Figure 3B) and found that the secondary structure of α -La adsorbed at oil-water interfaces to be largely different from the structure of α -La in solution. Although native α -La contained a relatively large amount of α -helix, adsorption to oil-water interfaces induced even more α -helix structure with a concomitant loss of β -sheet structure (Figure 3B and Table 1). Overall, α -La adsorbed at oil-water interfaces became partially unfolded and expanded with a highly ordered non-native secondary structure with a large amount of α -helix structure. While the loss of the tertiary structure of α -La upon adsorption to oil-water interfaces is a hallmark of a molten globule structure,^{45, 47, 48, 58, 60} the secondary structural change demonstrates that it is most unlikely that a molten globule structure exists for α -La adsorbed at oil-water interfaces of emulsions.

Both the FFTF and the far-UV SRCD results showed that the more hydrophobic (non-polar) hexadecane-water interface induced a greater degree of conformational change in α -La compared to the tricaprylin-water interface (Figure 2 and 3B). This effect of oil polarity on the structural change of proteins adsorbed at oil-water interfaces was also seen in a previous study on β -Lg.³⁶ Protein structural change upon adsorption to oil-water interfaces of emulsions is largely driven by the hydrophobic effect, i.e. the reorientation and solvation of the hydrophobic region of proteins toward the oil phase. The more hydrophobic hexadecane therefore requires a greater structural change for the solvation of the hydrophobic regions of proteins, which minimizes the thermodynamically unfavourable contact with water.

The thermal stability study using far-UV SRCD on α -La adsorbed at oil-water interfaces showed that the non-native secondary structure exhibited a higher thermal stability compared to the native structure in solution (Figure 4 and Table 1). This result was consistent with a previous study on β -Lg adsorbed at oil-water interfaces, which was also stable against thermally-induced secondary structural change. Globular proteins such as β -Lg and α -La in solution can undergo significant conformational changes upon heating due to the large gain of conformational entropy, so that the hydrogen bonding and hydrophobic interactions in the native structure are disrupted. When adsorbed at oil-water interfaces, the conformation of proteins becomes more stable to heating due to two effects: the hydrophobic interactions between unfolded proteins and the oil phase and the steric constraints of proteins anchored at the oil-water interface.

Physical stability of α -La-stabilized oil-in-water emulsions

Creation of emulsions with desirable stability and physicochemical properties relies on the understanding of the relationship between protein interfacial structure and the bulk properties of emulsions. This study investigated the physical stability of α -La-stabilized emulsions by monitoring the ζ -potential and particle size under heating and moderate ionic strength conditions.

The structural change of α -La adsorbed at two oil-water interfaces of emulsions (tricaprylin-water and hexadecane-water) exposed charged side chains to the aqueous phase and resulted in adsorbed protein layers at the droplet surfaces with increased surface charge (-49 ± 2 mV) (Figure 5) in comparison to the ζ -potential of free α -La in solution (-14 ± 2 mV). With the addition of 120 mM NaCl, the ζ -potential of both emulsions decreased to -19 ± 2 mV although they were stable against heating. The reduction of the ζ -potential of α -La-stabilized emulsions with the addition of salt was consistent with results obtained from emulsions stabilized by many other proteins including β -Lg, β -casein and deamidated wheat protein.^{1-4, 36} This phenomenon is known as electrostatic screening, where positively charged Na^+ ions act as counter-ions to the negative charges of the adsorbed protein layer, decreasing the net effective charge.

In the absence of 120 mM NaCl, the highly charged layer of α -La provided excellent physical stability for both emulsions against heating up to 90 °C for 20 min, as there was no considerable change in the average particle size (Figure 6, solid line). The major stabilization mechanism is electrostatic repulsion between the droplets, which at -49 ± 2 mV is sufficient to oppose the attractive van der Waals forces.

Compared to the experiments in the absence of salt, addition of 120 mM NaCl caused a small increase in the average particle size at 20 °C for both the tricaprylin-in-water emulsion ($\Delta D_{4,3} = 0.25 \mu\text{m}$) and the hexadecane-in-water emulsion ($\Delta D_{4,3} = 0.10 \mu\text{m}$) (Figure 6). The average particle size of the tricaprylin-in-water emulsion remained relatively stable up to 80 °C but had a moderate increase of approximately $0.7 \mu\text{m}$ at 90 °C versus 20 °C (Figure 6A, dotted line). Heating the hexadecane-in-water emulsion in the presence of 120 mM NaCl did not cause any further increase in the particle size up to 90 °C (Figure 6B, dotted line). The minor increase in the average particle size of α -La-stabilized emulsions when heating in the presence of salt compared to heating in the absence of salt is due to the reduction in the electrostatic repulsion to a point where the emulsion droplet may become weakly flocculated. Weakly flocculated emulsions may be disrupted upon sample dilution and stirring when measured in the circulating buffer in the sample unit of a laser diffraction instrument.

The stability of α -La-stabilized emulsions under the condition of heating in the presence of 120 mM NaCl (Figure 6, dotted lines) was in sharp contrast to the same oil-in-water emulsions stabilized by β -Lg as shown in previous studies.^{1, 3, 36} The α -La-stabilized emulsions were more stable to extensive droplet flocculation than the β -Lg-stabilized emulsions, which showed a considerable increase in the average particle size when heating in the presence of salt.³⁶ This is despite the fact that the ζ -potential of α -La-stabilized emulsions (-19 ± 2 mV) was lower than that of β -Lg-stabilized emulsions (-21 to -24 mV). β -Lg-stabilized emulsions are susceptible to more extensive droplet flocculation when heated above 60 °C in the presence of salt, which can be due to

the exposure of a free thiol group in β -Lg, which can participate in a sulfydryl-disulfide interchange reaction at high temperatures. When salt is added to the emulsion and the effective electrostatic repulsive force is reduced, the emulsion droplets come together and the chance of the inter-droplet sulfydryl-disulfide interchange reaction is largely increased. The sulfydryl-disulfide interchange reaction promotes the formation of covalent links between droplets and hence permanent droplet flocculation. The strong flocculation of β -Lg-stabilized emulsions upon heating above 60 °C can also be due to the increased hydrophobicity of β -Lg adsorbed at the droplet surfaces and the subsequent increase in the attractive hydrophobic interactions between emulsion droplets.⁴ In contrast, α -La has no free thiol group to participate in sulfydryl-disulfide interchange and hence resulting in a higher thermal stability of emulsions in terms of permanent droplet flocculation.

In the final condition, addition of 120 mM NaCl after heating, the α -La-stabilized hexadecane-in-water emulsion underwent a moderate increase in the average particle size from 0.77 μm at 20 °C to 1.43 μm at 90 °C (Figure 6B, dashed line). In contrast, the α -La-stabilized tricaprylin-in-water emulsion remained relatively stable in the region of 60 °C to 80 °C, but had a larger increase in the particle size to approximately 15.5 μm at 90 °C. In a previous study on β -Lg, it was also seen that the β -Lg-stabilized tricaprylin-in-water emulsion was more prone to droplet flocculation than the hexadecane-in-water emulsion when salt was added after heating.³⁶ Together these results demonstrate the influence of the oil phase on colloidal stability. Colloidal stability of globular protein-stabilized emulsions is mainly governed by the balance between van der Waals attractive forces and electrostatic repulsive forces. The RI of the oil phase can affect the strength of van der Waals attractive forces through the Hamaker function.^{4,61} The smaller difference in the RI between hexadecane and water ($\Delta\text{RI} = 0.102$) results in a weaker van der Waals attraction between the hexadecane-in-water emulsion droplets as compared to that of the tricaprylin-in-water emulsion ($\Delta\text{RI} = 0.116$), further contributing to the higher stability of the hexadecane-in-water emulsion compared to the tricaprylin-in-water emulsion.

It is not yet clear whether addition of salt after heating destabilized α -La-stabilized emulsions more than addition of salt prior to heating. To date, there are relatively few studies on the colloidal stability of α -La-stabilized oil-in-water emulsions and even less on the characterization of α -La interfacial structure. It would be interesting to explore the interfacial properties of α -La by techniques such as rheology or reflectivity under different conditions.

Conclusion

The structural dimensions and conformation of α -La adsorbed at oil-water interfaces were investigated using SRCD, FFTF and DPI. The compact globular structure of α -La was disrupted and the secondary structure underwent a change with a significant increase in the α -helical content. The impact of oil phase polarity was also investigated, confirming our previous observations with β -Lg that a more hydrophobic environment induced a larger degree of conformational change. This structural rearrangement resulted in a protein layer around the oil droplet surface, which resulted in excellent thermal stability of α -La emulsions when heated in the absence of NaCl via electrostatic repulsion. Furthermore, the lack of free thiol groups made the α -La emulsion droplets, which were already close to each other by adding salt, resistant to permanent droplet flocculation upon further heat treatment. Overall, this study has added to our current understanding of α -La structural rearrangement upon adsorption to oil-water interfaces of emulsions by demonstrating the formation of a characteristic conformation different from both the native α -La and the molten globule α -La in solution. Moreover, this study provides further information on the mechanism by which the interfacial structure of proteins can affect the physical stability of the emulsion under heating and moderate ionic strength conditions.

Acknowledgements

The authors would like to sincerely thank Dr. Nykola Jones for her assistance with the experimental technique, the Institute for Storage Ring Facilities in Aarhus (ISA), Denmark for provision of beam time, the Australian Synchrotron for provision of a travel grant and the Australian Research Council and Dairy Innovation Australia Limited for funding (through ARC Linkage Grant No. LP0774909).

Supporting Information available

The confocal images of α -La emulsions under representative conditions after the treatment of heating and salt addition are included in this section. This information is available free of charge via the Internet at <http://pubs.acs.org/>.

References

- (1) Day, L.; Xu, M.; Lundin, L.; Wooster, T.J. *Interfacial properties of deamidated wheat protein in relation to its ability to stabilise oil-in-water emulsions. Food Hydrocolloids* **2009**, *23*, 2158-2167.
- (2) Dickinson, E. *Flocculation of protein-stabilized oil-in-water emulsions. Colloids Surf., B* **2010**, *81*, 130-140.
- (3) Kim, H.-J.; Decker, E.A.; McClements, D.J. *Role of postadsorption conformation changes of β -lactoglobulin on its ability to stabilize oil droplets against flocculation during heating at neutral pH. Langmuir* **2002**, *18*, 7577-7583.
- (4) Kim, H.-J.; Decker, E.A.; McClements, D.J. *Impact of protein surface denaturation on droplet flocculation in hexadecane oil-in-water emulsions stabilized by β -lactoglobulin. J. Agric. Food Chem.* **2002**, *50*, 7131-7137.
- (5) McClements, D.J. *Protein-stabilized emulsions. Curr. Opin. Colloid Interface Sci.* **2004**, *9*, 305-313.
- (6) Wooster, T.J.; Augustin, M.A. *β -Lactoglobulin-dextran maillard conjugates: Their effect on interfacial thickness and emulsion stability. J. Colloid Interface Sci.* **2006**, *303*, 564-572.
- (7) Dalgleish, D.G. *Adsorption of protein and the stability of emulsions. Trends Food Sci. Technol.* **1997**, *8*, 1-6.
- (8) Dalgleish, D.G. *Food emulsions stabilized by proteins. Curr. Opin. Colloid Interface Sci.* **1997**, *2*, 573-577.
- (9) Dickinson, E. *Proteins at interfaces and in emulsions - stability, rheology and interactions. J. Chem. Soc., Faraday Trans.* **1998**, *94*, 1657-1669.
- (10) Dickinson, E. *Adsorbed protein layers at fluid interfaces: Interactions, structure and surface rheology. Colloids Surf., B* **1999**, *15*, 161-176.
- (11) Wilde, P.; Mackie, A.; Husband, F.; Gunning, P.; Morris, V. *Proteins and emulsifiers at liquid interfaces. Adv. Colloid Interface Sci.* **2004**, *108-109*, 63-71.
- (12) Damodaran, S. *Protein stabilization of emulsions and foams. J. Food Sci.* **2005**, *70*, R54-R66.
- (13) Dickinson, E. *Milk protein interfacial layers and the relationship to emulsion stability and rheology. Colloids Surf., B* **2001**, *20*, 197-210.
- (14) Dickinson, E. *Caseins in emulsions: Interfacial properties and interactions. Int. Dairy J.* **1999**, *9*, 305-312.
- (15) Dalgleish, D.G. *Conformations and structures of milk proteins adsorbed to oil-water interfaces. Food Res. Int.* **1996**, *29*, 541-547.
- (16) Dalgleish, D.G.; Hallett, F.R. *Dynamic light scattering: Applications to food systems. Food Res. Int.* **1995**, *28*, 181-193.

- (17) Dalgleish, D.G.; Leaver, J. *The possible conformations of milk proteins adsorbed on oil/water interfaces. J Colloid Interface Sci.* **1991**, *141*, 288-294.
- (18) Fang, Y.; Dalgleish, D.G. *Conformation of β -lactoglobulin studied by FTIR: Effect of pH, temperature, and adsorption to the oil-water interface. J. Colloid Interface Sci.* **1997**, *196*, 292-298.
- (19) Fang, Y.; Dalgleish, D.G. *The conformation of α -lactalbumin as a function of pH, heat treatment and adsorption at hydrophobic surfaces studied by FTIR. Food Hydrocolloids* **1998**, *12*, 121-126.
- (20) Husband, F.A.; Garrood, M.J.; Mackie, A.R.; Burnett, G.R.; Wilde, P.J. *Adsorbed protein secondary and tertiary structures by circular dichroism and infrared spectroscopy with refractive index matched emulsions. J. Agric. Food Chem.* **2001**, *49*, 859-866.
- (21) Lee, S.-H.; Lefèvre, T.; Subirade, M.; Paquin, P. *Changes and roles of secondary structures of whey protein for the formation of protein membrane at soy oil/water interface under high-pressure homogenization. J. Agric. Food Chem.* **2007**, *55*, 10924-10931.
- (22) Lefèvre, T.; Subirade, M. *Formation of intermolecular β -sheet structures: A phenomenon relevant to protein film structure at oil-water interfaces of emulsions. J. Colloid Interface Sci.* **2003**, *263*, 59-67.
- (23) Rampon, V.; Genot, C.; Riaublanc, A.; Anton, M.; Axelos, M.A.V.; McClements, D.J. *Front-face fluorescence spectroscopy study of globular proteins in emulsions: Displacement of BSA by a nonionic surfactant. J. Agric. Food Chem.* **2003**, *51*, 2482-2489.
- (24) Rampon, V.; Riaublanc, A.; Anton, M.; Genot, C.; McClements, D.J. *Evidence that homogenization of BSA-stabilized hexadecane-in-water emulsions induces structure modification of the nonadsorbed protein. J. Agric. Food Chem.* **2003**, *51*, 5900-5905.
- (25) Sakuno, M.M.; Matsumoto, S.; Kawai, S.; Taihei, K.; Matsumura, Y. *Adsorption and structural change of β -lactoglobulin at the diacylglycerol/water interface. Langmuir* **2008**, *24*, 11483-11488.
- (26) Atkinson, P.J.; Dickinson, E.; Horne, D.S.; Richardson, R.M. *Neutron reflectivity of adsorbed β -casein and β -lactoglobulin at the air/water interface. J. Chem. Soc., Faraday Trans.* **1995**, *91*, 2847-2854.
- (27) Dickinson, E.; Horne, D.S.; Phipps, J.S.; Richardson, R.M. *A neutron reflectivity study of the adsorption of β -casein at fluid interfaces. Langmuir* **1993**, *9*, 242-248.
- (28) Fragneto, G.; Thomas, R.K.; Rennie, A.R.; Penfold, J. *Neutron reflection study of bovine β -casein adsorbed on OTS self-assembled monolayers. Science* **1995**, *267*, 657-660.
- (29) Junghans, A.; Champagne, C.; Cayot, P.; Loupiac, C.; Köper, I. *Probing protein-membrane interactions using solid supported membranes. Langmuir* **2011**, *27*, 2709-2716.

- (30) Perriman, A.W.; Henderson, M.J.; Holt, S.A.; White, J.W. *Effect of the air-water interface on the stability of β -lactoglobulin*. *J. Phys. Chem. B* **2007**, *111*, 13527-13537.
- (31) Yano, Y.F.; Uruga, T.; Tanida, H.; Toyokawa, H.; Terada, Y.; Takagaki, M.; Yamada, H. *Driving force behind adsorption-induced protein unfolding: A time-resolved X-ray reflectivity study on lysozyme adsorbed at an air/water interface*. *Langmuir* **2009**, *25*, 32-35.
- (32) Caessens, P.W.J.R.; De Jongh, H.H.J.; Norde, W.; Gruppen, H. *The adsorption-induced secondary structure of β -casein and of distinct parts of its sequence in relation to foam and emulsion properties*. *Biochim. Biophys. Acta* **1999**, *1430*, 73-83.
- (33) Dalgleish, D.G. *The conformations of proteins on solid/water interfaces - caseins and phosphovitin on polystyrene latices*. *Colloids Surf.* **1990**, *46*, 141-155.
- (34) Wu, X.; Narsimhan, G. *Characterization of secondary and tertiary conformational changes of β -lactoglobulin adsorbed on silica nanoparticle surfaces*. *Langmuir* **2008**, *24*, 4989-4998.
- (35) Zhai, J.; Miles, A.J.; Pattenden, L.K.; Lee, T.-H.; Augustin, M.A.; Wallace, B.A.; Aguilar, M.-I.; Wooster, T.J. *Changes in β -lactoglobulin conformation at the oil/water interface of emulsions studied by synchrotron radiation circular dichroism spectroscopy*. *Biomacromolecules* **2010**, *11*, 2136-2142.
- (36) Zhai, J.; Wooster, T.J.; Hoffmann, S.V.; Lee, T.-H.; Augustin, M.A.; Aguilar, M.-I. *Structural rearrangement of β -lactoglobulin at different oil-water interfaces and its effect on emulsion stability*. *Langmuir* **2011**, *27*, 9227-9236.
- (37) Permyakov, E.A.; Berliner, L.J. *α -Lactalbumin: Structure and function*. *FEBS Lett.* **2000**, *473*, 269-274.
- (38) Chrysina, E.D.; Brew, K.; Acharya, K.R. *Crystal structures of apo- and holo-bovine α -lactalbumin at 2.2-Å resolution reveal an effect of calcium on inter-lobe interactions*. *J. Biol. Chem.* **2000**, *275*, 37021-37029.
- (39) Pike, A.C.W.; Brew, K.; Acharya, K.R. *Crystal structures of guinea-pig, goat and bovine α -lactalbumin highlight the enhanced conformational flexibility of regions that are significant for its action in lactose synthase*. *Structure* **1996**, *4*, 691-703.
- (40) Considine, T.; Patel, H.A.; Anema, S.G.; Singh, H.; Creamer, L.K. *Interactions of milk proteins during heat and high hydrostatic pressure treatments - a review*. *Innov. Food Sci. Emerg. Technol.* **2007**, *8*, 1-23.
- (41) Dalgleish, D.G.; Senaratne, V.; Francois, S. *Interactions between α -lactalbumin and β -lactoglobulin in the early stages of heat denaturation*. *J. Agric. Food Chem.* **1997**, *45*, 3459-3464.
- (42) Schokker, E.P.; Singh, H.; Creamer, L.K. *Heat-induced aggregation of β -lactoglobulin A and B with α -lactalbumin*. *Int. Dairy J.* **2000**, *10*, 843-853.

- (43) Kunihiro, K. *The molten globule state as a clue for understanding the folding and cooperativity of globular-protein structure. Proteins: Struct. Funct. Genetics* **1989**, *6*, 87-103.
- (44) Dickinson, E.; Matsumura, Y. *Proteins at liquid interfaces: Role of the molten globule state. Colloids Surf., B* **1994**, *3*, 1-17.
- (45) Chyan, C.L.; Wormald, C.; Dobson, C.M.; Evans, P.A.; Baum, J. *Structure and stability of the molten globule state of guinea pig α -lactalbumin: A hydrogen exchange study. Biochemistry* **1993**, *32*, 5681-5691.
- (46) Alexandrescu, A.T.; Evans, P.A.; Pitkeathly, M.; Baum, J.; Dobson, C.M. *Structure and dynamics of the acid-denatured molten globule state of α -lactalbumin: A two-dimensional nmr study. Biochemistry* **1993**, *32*, 1707-1718.
- (47) Gao, C.; Wijesinha-Bettoni, R.; Wilde, P.J.; Mills, E.N.C.; Smith, L.J.; Mackie, A.R. *Surface properties are highly sensitive to small pH induced changes in the 3-D structure of α -lactalbumin. Biochemistry* **2008**, *47*, 1659-1666.
- (48) Wijesinha-Bettoni, R.; Gao, C.; Jenkins, J.A.; Mackie, A.R.; Wilde, P.J.; Mills, E.N.C.; Smith, L.J. *Heat treatment of bovine α -lactalbumin results in partially folded, disulfide bond shuffled states with enhanced surface activity. Biochemistry* **2007**, *46*, 9774-9784.
- (49) Matsumura, Y.; Mitsui, S.; Dickinson, E.; Mori, T. *Competitive adsorption of α -lactalbumin in the molten globule state. Food Hydrocolloids* **1994**, *8*, 555-566.
- (50) Farrell, H.M., Jr.; Jimenez-Flores, R.; Bleck, G.T.; Brown, E.M.; Butler, J.E.; Creamer, L.K.; Hicks, C.L.; Hollar, C.M.; Ng-Kwai-Hang, K.F.; Swaisgood, H.E. *Nomenclature of the proteins of cows' milk - sixth revision. J. Dairy Sci.* **2004**, *87*, 1641-1674.
- (51) Miles, A.J.; Hoffmann, S.V.; Tao, Y.; Janes, R.W.; Wallace, B.A. *Synchrotron radiation circular dichroism (SRCD) spectroscopy: New beamlines and new applications in biology. Spectroscopy* **2007**, *21*, 245-255.
- (52) Miles, A.J.; Janes, R.W.; Brown, A.; Clarke, D.T.; Sutherland, J.C.; Tao, Y.; Wallace, B.A.; Hoffmann, S.V. *Light flux density threshold at which protein denaturation is induced by synchrotron radiation circular dichroism beamlines. J. Synchrotron Radiat.* **2008**, *15*, 420-422.
- (53) Sreerama, N.; Venyaminov, S.Y.; Woody, R.W. *Estimation of the number of α -helical and β -strand segments in proteins using circular dichroism spectroscopy. Protein Sci.* **1999**, *8*, 370-380.
- (54) Whitmore, L.; Wallace, B.A. *Dichroweb, an online server for protein secondary structure analyses from circular dichroism spectroscopic data. Nucl. Acids Res.* **2004**, *32*, W668-673.
- (55) Fox, P.F.; McSweeney, P.L.H. *Advanced dairy chemistry Volume I Proteins*, 3rd ed.; Kluwer Academic/Plenum: New York, 2003.

- (56) Razumovsky, L.; Damodaran, S. *Surface activity–compressibility relationship of proteins at the air–water interface. Langmuir* **1999**, *15*, 1392-1399.
- (57) Tcholakova, S.; Denkov, N.D.; Ivanov, I.B.; Campbell, B. *Coalescence in β -lactoglobulin-stabilized emulsions: Effects of protein adsorption and drop size. Langmuir* **2002**, *18*, 8960-8971.
- (58) Cawthorn, K.M.; Permyakov, E.; Berliner, L.J. *Membrane-bound states of α -lactalbumin: Implications for the protein stability and conformation. Protein Sci.* **1996**, *5*, 1394-1405.
- (59) El-Zahar, K.; Sitothy, M.; Dalgarrondo, M.; Choiset, Y.; Metro, F.; Haertle, T.; Chobert, J.-M. *Purification and physicochemical characterization of ovine β -lactoglobulin and α -lactalbumin. Nahrung - Food* **2004**, *48*, 177-183.
- (60) Halskau, O.; Underhaug, J.; Froystein, N.A.; Martinez, A. *Conformational flexibility of α -lactalbumin related to its membrane binding capacity. J. Mol. Biol.* **2005**, *349*, 1072-1086.
- (61) Israelachvili, J.N. *Intermolecular and surface forces*, 3rd ed.; Academic Press: Amsterdam, 1991. p.253-289.

Table 1: Secondary structural content of α -La in different environments derived from the SRCD spectra.

	α -La in solution		α -La at tricaprylin-water		α -La at hexadecane-water	
	α -helix (%)	β -sheet (%)	α -helix (%)	β -sheet (%)	α -helix (%)	β -sheet (%)
20 °C	29.9	18.0	45.8	8.3	58.5	9.9
34 °C	29.6	19.0	46.6	5.6	51.0	15.8
48 °C	28.9	19.4	41.9	9.6	51.7	14.2
62 °C	24.7	22.1	45.8	5.5	49.6	16.5
76 °C	16.5	30.6	40.4	11.6	48	15.3

Figure Legends

Figure 1: DPI sensorgrams of real-time changes in mass, thickness and refractive index of (A) α -La (10 μ M, pH 7) binding to a C18 hydrocarbon surface and (B) α -La (100 μ M, pH 3) binding to a silicon oxynitride surface. α -La was injected to the surface at 10 μ L/min for 15 min (association phase), followed by 15 min buffer wash (dissociation phase). Arrow indicates the time when the dissociation phase began.

Figure 2: FFTF spectra of α -La in 10 mM sodium phosphate buffer pH 7 (black line), in 6 M urea/phosphate buffer (green line), at the tricaprylin-water interface (blue line), and at the hexadecane-water interface (red line). All spectra were measured at 20 °C.

Figure 3: (A) Near-UV SRCD spectra and (B) far-UV SRCD spectra of α -La in 10 mM sodium phosphate buffer pH 7 (black line), at the tricaprylin-water interface (blue line) and at the hexadecane-water interface (red line). All spectra were measured at 20 °C.

Figure 4: Effect of temperature on α -La (A) in 10 mM sodium phosphate buffer pH 7, (B) at the tricaprylin-water interface and (C) at the hexadecane-water interface. Spectra were recorded at various temperatures: 20 °C (black line), 34 °C (red line), 48 °C (green line), 62 °C (purple line), and 76 °C (pink line).

Figure 5: Effect of temperature and salt addition on ζ -potential of (A) α -La-stabilized tricaprylin oil-in-water emulsions and (B) α -La-stabilized hexadecane oil-in-water emulsions (B). Note: 'heating + 0mM NaCl' indicates no salt addition after heating; 'heating + 120mM NaCl' indicates salt addition after heating; and '120mM NaCl + heating' indicates salt addition before heating.

Figure 6: Effect of temperature and salt addition on the mean particle diameter $D_{4,3}$ of (A) α -La-stabilized tricaprylin oil-in-water emulsions and (B) α -La-stabilized hexadecane oil-in-water emulsions. Note: 'heating + 0mM NaCl' indicates no salt addition after heating; 'heating + 120mM NaCl' indicates salt addition after heating; and '120mM NaCl + heating' indicates salt addition before heating.

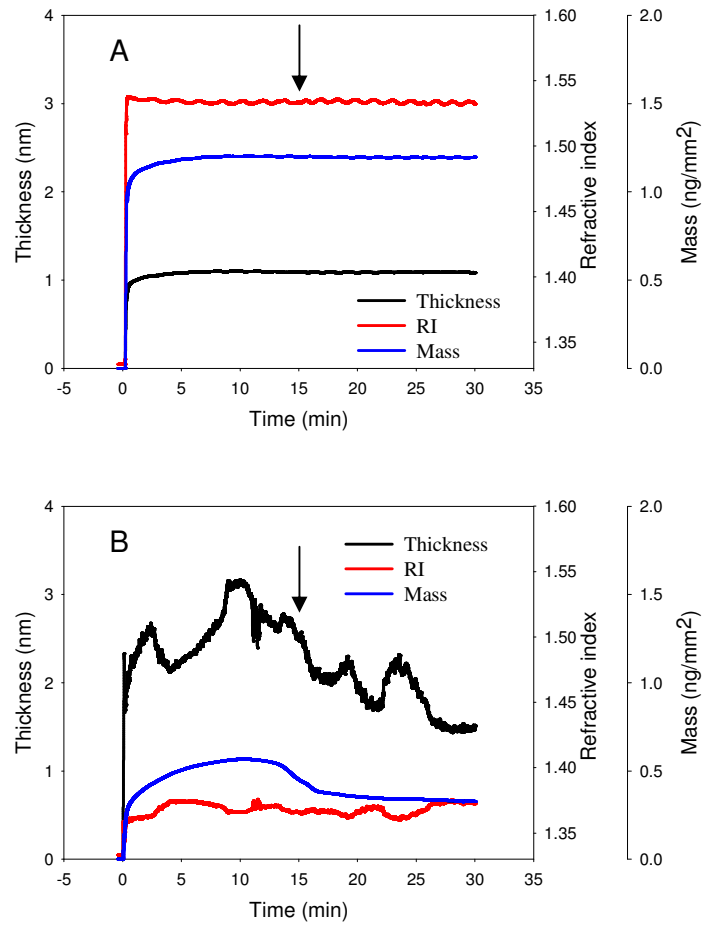


Figure 1

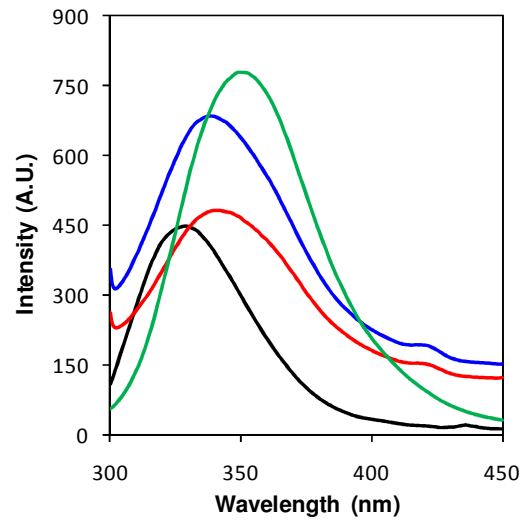


Figure 2

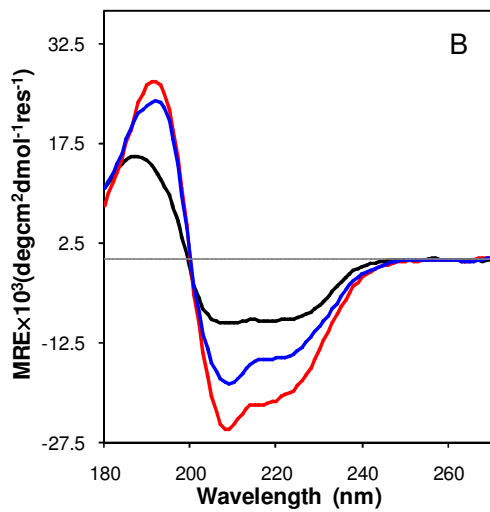
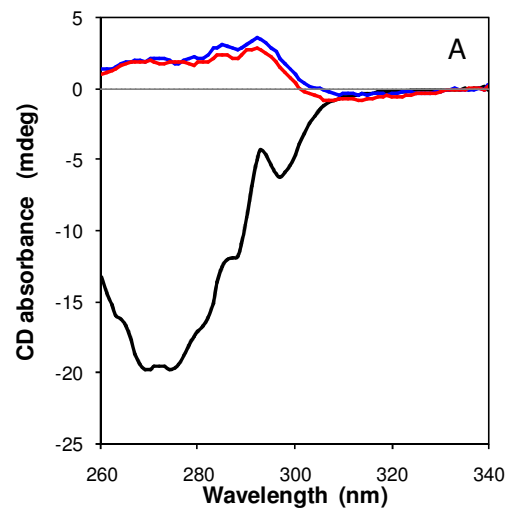


Figure 3

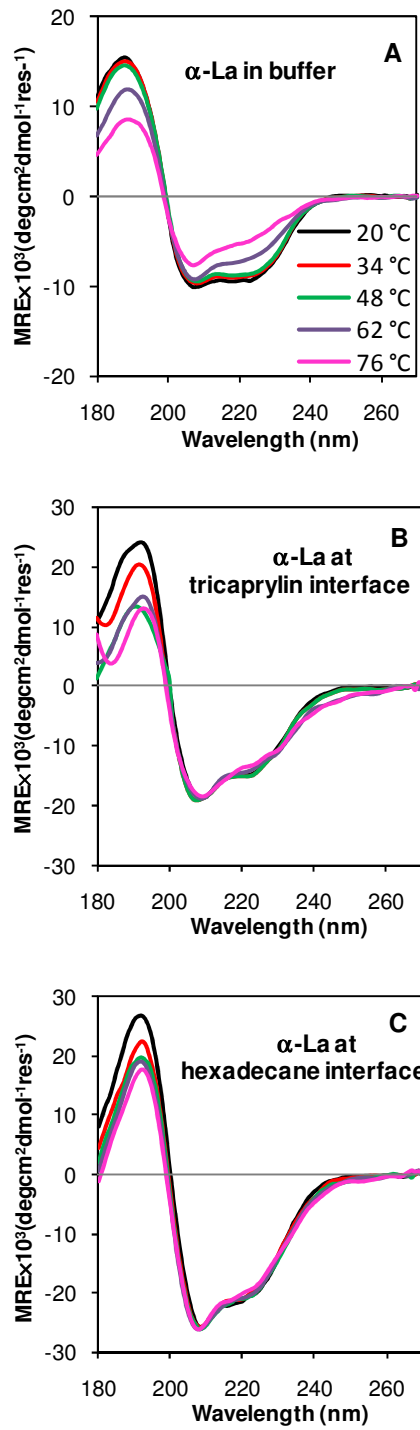


Figure 4

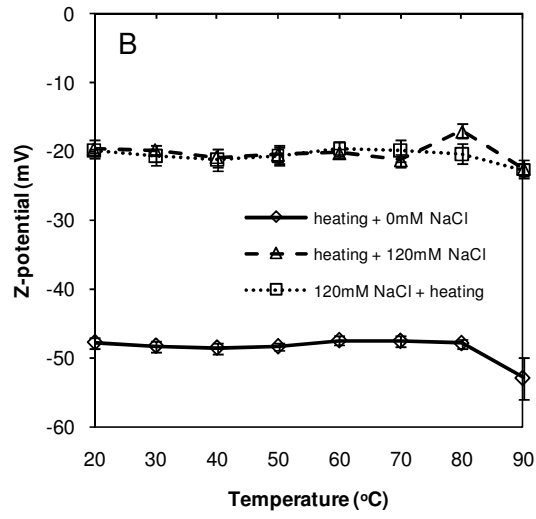
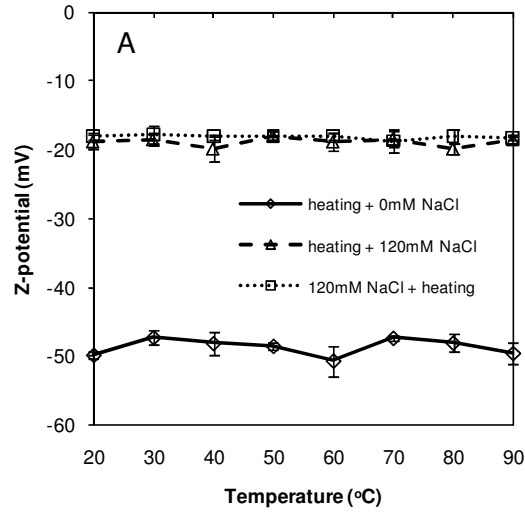


Figure 5

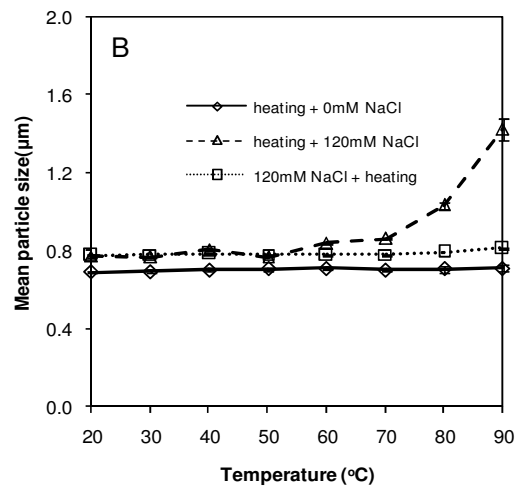
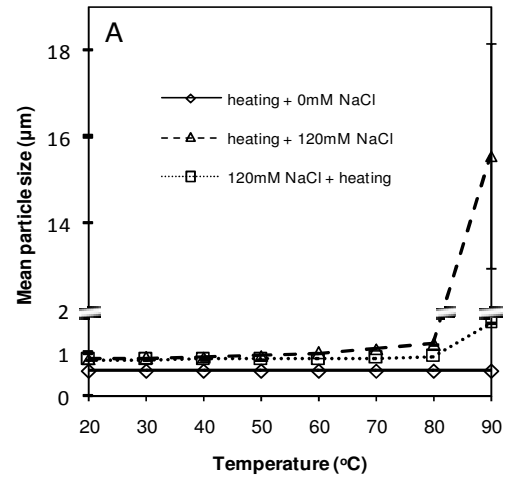


Figure 6

Appendix 4.1: Supporting Information

Emulsion visualization by confocal microscopy

The α -La-stabilized emulsions after the treatment of heating and/or salt addition were examined using a Leica SP5 Confocal Laser Scanning Microscope equipped with an argon ion laser (Leica Microsystems, Wetzlar, Germany). One drop of fluorescence dye Nile Red (0.025% dissolved in 0.1% dimethyl sulfoxide/99.9% ethanol) was added to the emulsion sample (1 mL) which was gently mixed by inversion. The sample was then observed under the microscope and the images were exported in a scale of 25 μm .

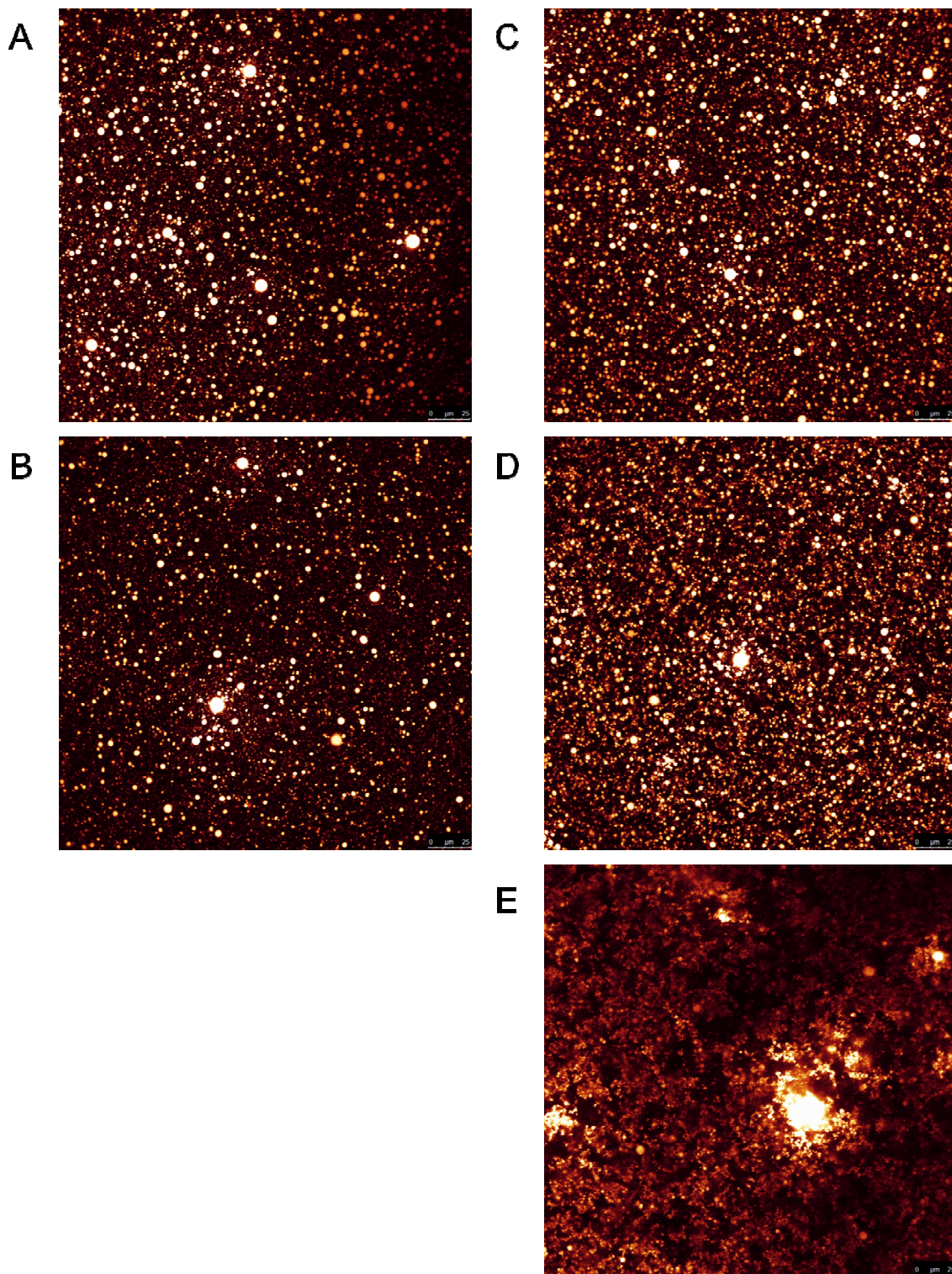


Figure S1: Confocal images of α -La-stabilized tricaprylin-in-water emulsions 24 h after the treatment of (A) 20 °C + 0 mM NaCl; (B) 90 °C + 0 mM NaCl; (C) 20 °C + 120 mM NaCl; (D) 120 mM NaCl + 90 °C; (E) 90 °C + 120 mM NaCl.

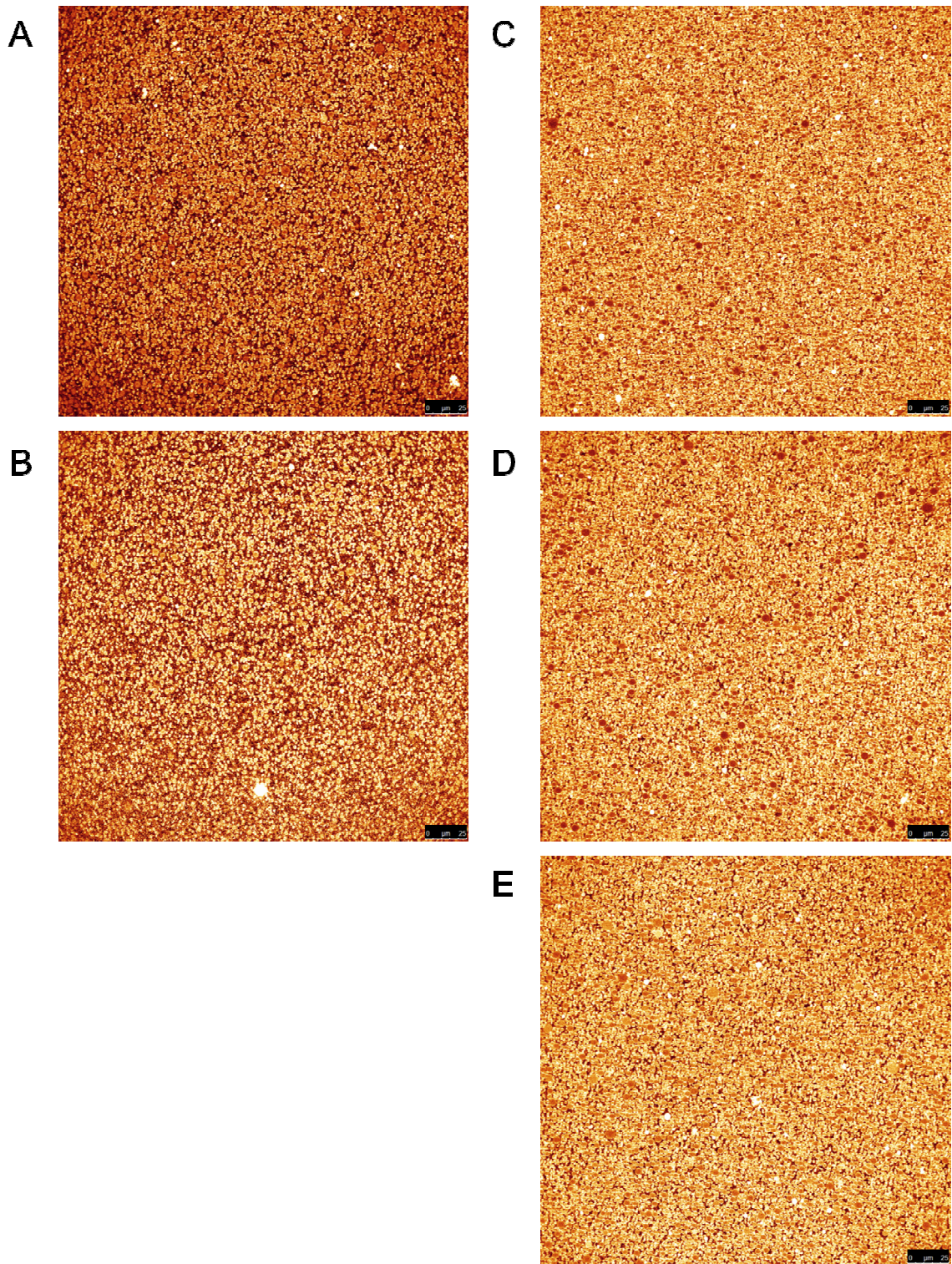
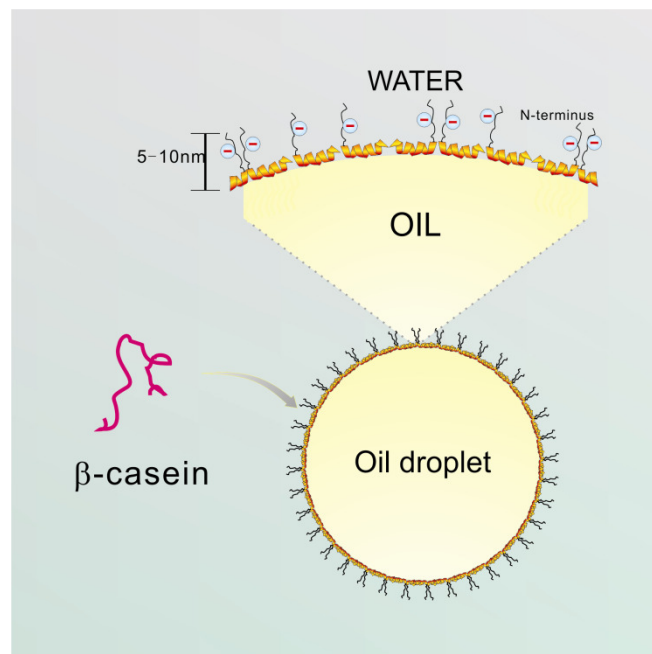


Figure S2: Confocal images of α -La-stabilized hexadecane-in-water emulsions 24 h after the treatment of (A) 20 °C + 0 mM NaCl; (B) 90 °C + 0 mM NaCl; (C) 20 °C + 120 mM NaCl; (D) 120 mM NaCl + 90 °C; (E) 90 °C + 120 mM NaCl.

Chapter 5

Interfacial structure and stabilizing function of β -casein at oil-water interfaces of emulsions



A schematic model of β -casein adsorption to the oil-water interface

5.1 Introduction

Milk proteins are commonly used as emulsifiers in the food industry due to their excellent surface-active and emulsion-stabilizing characteristics (Chapter 1 Section 1.4).¹⁻³ The properties of milk protein-stabilized oil-in-water emulsions are determined by the interfacial structure of the adsorbed protein layer at droplet surfaces.⁴⁻⁹ It is widely thought that milk proteins change their structure upon adsorption to oil-water interfaces of emulsions.¹⁰⁻¹³ However, detailed characterization of the structure of proteins adsorbed at oil-water interfaces has long been difficult (Chapter 1 Section 1.3.3). Standard methods of structural analysis, such as circular dichroism (CD) spectroscopy and Fourier transform infrared (FTIR) spectroscopy are either impossible to use on emulsions or provide limited information. Indirect methods such as dynamic light scattering (DLS) and neutron reflectivity are used to study the thickness and density distribution of the adsorbed protein layer but they do not provide information on protein conformation at a molecular level.

Previous chapters (Chapters 2-4) outlined studies that employed a range of biophysical methods including synchrotron radiation circular dichroism (SRCD) spectroscopy, front-face tryptophan fluorescence (FFTF) spectroscopy and dual polarization interferometry (DPI) to study the adsorption-induced structural change of globular proteins.^{14, 15} These approaches overcame the issue of high light scattering and absorbance from emulsion droplets and systematically characterized the secondary structure, tertiary structure, and geometric dimensions of β -lactoglobulin (β -Lg) and α -lactalbumin (α -La) adsorbed at oil-water interfaces. The results showed that the process of adsorption to oil-water interfaces caused the unfolding of these two globular proteins and induced a large amount of non-native α -helical conformation.

Although studies in previous chapters significantly improved our understanding on the structural change of proteins upon adsorption to oil-water interfaces, both β -Lg and α -La have compact globular structures and ordered secondary structures in solution. In order to gain a broader insight into protein structural behaviour upon adsorption, it is necessary to investigate a range of proteins with different molecular properties. β -Casein is a good contrast to β -Lg and α -La because it has a very different structure in solution. The current knowledge on the structural property of β -casein in solution and adsorbed at oil-water interfaces has been reviewed (Chapter 1 Section 1.4.3). Briefly, β -casein is a flexible protein with a large amount of unordered secondary structure.¹⁶ β -Casein contains 209 amino acid residues including 35 prolines, the cyclic structure of which accounts for the low amount of the α -helix and the β -sheet. A characteristic feature of the β -casein sequence is that it can be divided into a hydrophilic region of 0-40 residues at the N-terminus and a hydrophobic C-terminus (Chapter 1 Figure 1.17).¹⁶ As a result, β -casein forms micelles in solution to minimize the contact of the hydrophobic C-terminus with water. When it comes to adsorption to oil-water interfaces, the amphiphilic property makes β -casein very surface-active. The structure of

β -casein adsorbed at air-water or oil-water interfaces has been characterized in many experiments using neutron reflectivity, DLS, and molecular modelling.¹⁷⁻²⁵ These studies have shown that the inner layer of β -casein anchored at the surface is dense and thin (1-2 nm) with a large protein mass (80 to 90%) whilst the outer layer exposed in the aqueous phase is diffuse and thick (5-10 nm) with less than 20% protein mass.¹⁷⁻²⁵ These results suggest that β -casein adsorbs to hydrophobic surfaces with its hydrophobic region located at the surface and its hydrophilic region protruding into the aqueous phase, the so called ‘train-loop-tail’ model (Chapter 1 Figure 1.7).^{5, 13} Due to steric repulsion between the droplets provided by the layer of β -casein from its structural change upon adsorption, emulsions stabilized by β -casein have excellent stability against droplet flocculation under conditions of heating and moderate ionic strength from NaCl.²⁶

Previous studies have mainly focused on investigating the mass and density distribution profile of β -casein adsorbed at planar hydrophobic surfaces using neutron reflectivity.^{17, 21} This present study employed DPI to investigate the thickness and density of the β -casein layer adsorbed at a hydrophobic C18 surface and compared the DPI result to that from neutron reflectivity. Moreover, given that β -casein has a very different structure from β -Lg and α -La, this study also investigated the effect of native molecular structure on the adsorption-induced structural change using SRCD for in situ characterization of the secondary structure of β -casein adsorbed at oil-water interfaces.

5.2 Materials and Methods

5.2.1 Materials

β -Casein (BioUltra, $\geq 98\%$ PAGE) was purchased from Sigma-Aldrich Company (St Louis, MO). Sodium chloride (NaCl), sodium phosphate (monobasic and dibasic), hexadecane, tricaprylin and sodium dodecyl sulphate (SDS) were purchased from Sigma-Aldrich Company (St Louis, MO). All chemicals and solvents were of analytical grade. The ultrapure water was prepared by a Purelab Ultra Genetic purification system (ELGA LabWater) and used for all experiments.

5.2.2 DPI measurements and data analysis

The geometric dimensions of β -casein adsorbed at a hydrophobic surface was determined by measuring the thickness and refractive index (RI) of the β -casein layer adsorbed at a C18 hydrocarbon AnaChip immobilized on an Analight Bio2000 DPI instrument (Farfield Group, UK). The detailed instrumental set-up and calibration procedure were previously described (Chapter 3 Materials and Methods).¹⁵ The C18 hydrocarbon chip surface with bulk buffer flowing over the top served as a model planar oil-water interface. Freshly prepared 10 μM β -casein solution in 10 mM sodium phosphate buffer pH 7 was injected onto the C18 surface at 10 $\mu\text{L}/\text{min}$ flow rate for 15 min

during an association phase and followed by a dissociation phase with the bulk buffer flowing over the layer for another 15 min. For comparison, a reference study was also performed by adsorbing β -casein to a hydrophilic silicon oxynitride AnaChip. β -Casein was injected over the silicon oxynitride AnaChip using a similar experimental condition as in the C18 study except that a higher concentration (100 μ M in 10 mM sodium phosphate buffer, pH 7) was used. The mathematical model for the conversion of transverse magnetic (TM) and transverse electric (TE) data into layer mass, thickness, RI and density was previously described (Chapter 3 Materials and Methods).¹⁵ Maxwell's equations of electromagnetic radiation were used to resolve the experimentally obtained phase changes of TM and TE polarizations into the thickness and RI of the adsorbed protein layer. The density and mass of the adsorbed layer were calculated using the thickness and RI values (Chapter 3 Materials and Methods).¹⁵

5.2.3 Emulsion preparation and centrifugation assay

β -Casein-stabilized emulsions (0.3% w/w) containing 20% (v/v) hexadecane or tricaprylin were used for this study. The emulsions were prepared following a method previously described (Chapter 3 Materials and Methods).¹⁵ Briefly, the oil phase was added to protein solution by weight. The mixture was then blended using an Ultra-turrax high-speed blender at 8000 rpm for 2 min and then passed through an Avestin C5 high-pressure homogenizer twice at approximately 700 bar. All emulsions used for SRCD and fluorescence studies were freshly prepared on site at the ISA-synchrotron where the CD1 beam line is located (Institute for Storage Ring Facilities, Aarhus University, Denmark) and experiments were performed within 24 h of preparation.

To determine the amount of β -casein adsorbed at oil-water interfaces, emulsions were centrifuged in 300 kDa centrifuge tubes (Pall, Port Washington, NY) at $11600 \times g$ for 15 min. The concentration of proteins in the aqueous phase (supernatant) was obtained by measuring absorbance at 280 nm and using an extinction coefficient of $0.47 \text{ mLmg}^{-1}\text{cm}^{-1}$.²⁷ The amount of proteins adsorbed at oil-water interfaces was then calculated from the specific surface area of the emulsion droplets and was reported as the surface coverage (weight of protein per unit of surface area). An average of 12 aliquots of each emulsion sample was reported.

5.2.4 SRCD measurements and data analysis

All far-UV and near-UV SRCD measurements of β -casein in solution and emulsions were performed on the CD1 beam line of the SRCD station at the ASTRID storage ring.^{28, 29} The operating conditions and data analysis followed a method previously described (Chapter 3 Materials and Methods).¹⁵ A Suprasil cells (Hellma GmbH & Co., Germany) with a 0.01 cm path length was used for the far-UV SRCD measurement. The operating conditions were: 1 nm bandwidth, 2.15 s averaging time, 3 scans for a solution sample and 8 scans for an emulsion

sample. The SDS-stabilized emulsion was used as a valid baseline to correct light scattering background of the emulsion spectra as previously described.¹⁵ A mean residue weight of 114.9 for β -casein was used to convert the unit of milli-degrees in SRCD to the standard unit of mean residue ellipticity [θ]. The secondary structural content was calculated using the SELCON3 method³⁰ and the reference set SP175 in DICHROWEB³¹ as previously described.¹⁵

5.2.5 Treatment of emulsions under high temperatures and salt addition

β -Casein-stabilized emulsions were prepared as described above and were then treated under three different conditions involving heating and/or salt addition using previously described experimental procedures.¹⁵ Briefly, the first condition involved heating freshly made emulsions in the absence of NaCl from 20 °C to 90 °C for 20 min. The second condition involved heating the freshly made emulsions in the presence of NaCl (120 mM). The third condition involved firstly heating the emulsions in 0 mM NaCl and then adding 120 mM NaCl to the emulsions. ζ -Potential and particle size measurements were made after 24 h storage.

5.2.6 Measurements of emulsion ζ -potential and average particle size

The ζ -potential of β -casein-stabilized emulsions was measured using laser doppler velocimetry (Malvern Zetasizer Nano ZS, Worcestershire, UK). The emulsion samples stored for 24 h after various treatments were diluted (2 μ L in 30 mL of the corresponding buffer, 10 mM sodium phosphate buffer, pH 7, with 0 mM or 120 mM NaCl) and injected into a folded capillary cell with electrodes for measurements. The ζ -potential was calculated from the droplet velocity and direction when subjected to an alternating electric field. The average particle size of emulsions was measured using laser light diffraction (Malvern Mastersizer 2000, Worcestershire, U.K.) equipped with a Hydro SM small volume sample dispersion unit. The emulsion samples were dispersed in circulating buffer in the Hydro SM unit and the average particle size was calculated from a best fit between the measured scattering pattern and a model scattering pattern of equivalent polydisperse spheres (Mie theory). The volume-weighted average mean diameter $D_{4,3}$ ($=\sum n_i d_{i4} / \sum n_i d_{i3}$, where n_i is the number of particles with diameter d_i) was reported. All measurements were an average of at least three individual samples and the standard deviations were given in the plot (Figures 5.3 & 5.4). Detailed experimental procedures and operating conditions were previously described.¹⁵

5.3 Results

5.3.1 Geometric dimensions of β -casein adsorbed at hydrophobic and hydrophilic surfaces

A DPI equipped with chips containing either a hydrophobic C18 surface or a hydrophilic silicon oxynitride surface was employed to study the geometric dimensions of the adsorbed β -

casein layer. Figure 5.1 shows the real-time changes in the thickness, RI and mass of the β -casein layer at the C18 surface as well as the silicon oxynitride surface. Table 5.1 summarizes the experimental values of the layer mass, thickness and density (derived from RI) at three different time intervals, i.e. the moment of adsorption (Time 0 min), the end of the association/adsorption phase (Time 15 min) and the end of the dissociation phase (Time 30 min). β -Casein adsorption to the C18 surface resulted in a deposited mass of 2.0 ng/mm² which gradually decreased before it reached a plateau at 1.4 ng/mm² (Time 30 min) (Figure 5.1A & Table 5.1). The thickness of the adsorbed layer at the C18 surface reduced from 5 nm upon adsorption (Time 0 min) to 2.3 nm after dissociation (Time 30 min). However, the adsorbed layer at the C18 surface became a little denser from 0.41 g/cm³ (Time 0 min) to 0.57 g/cm³ (Time 30 min).

β -Casein adsorption to the silicon oxynitride surface resulted in a protein layer with a similar amount of mass deposited as that at the C18 surface (Figure 5.1 & Table 5.1). However, the adsorbed layer at the silicon oxynitride surface was thicker and less dense than that at the C18 surface, in particular during the association/adsorption phase (Time 0-15 min) (Figure 5.1B). At the end of the dissociation phase (Time 30 min), the adsorbed layer at the silicon oxynitride surface was 0.7 nm thicker and 0.17 g/cm³ less dense than the layer at the C18 surface (Table 5.1).

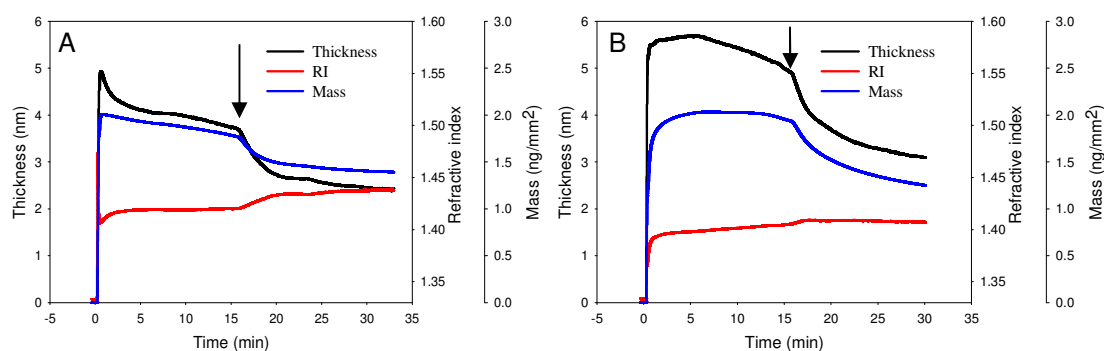


Figure 5.1: DPI sensorgrams of the real-time changes in the mass, thickness and refractive index of the β -casein layer binding to a C18 hydrocarbon surface (A) and a silicon oxynitride surface (B). β -Casein was injected to the surface at 10 μ L/min for 15 min (the association phase), followed by 15 min buffer wash (the dissociation phase). Arrows indicate the time when the dissociation phase began.

Table 5.1: Experimental values of the adsorbed β -casein layer at the C18 and silicon oxynitride surfaces.

Surface	Time (min)	Mass (ng/mm ²)	Thickness (nm)	Density (g/cm ³)
C18 hydrocarbon	0	2.0	5.0	0.41
	15	1.8	3.7	0.47
	30	1.4	2.3	0.57
Silicon oxynitride	0	1.7	5.5	0.15
	15	2.0	5.0	0.40
	30	1.2	3.0	0.40

5.3.2 Secondary structure of β -casein at oil-water interfaces

Before investigating the secondary structure of β -casein adsorbed at oil-water interfaces, it was necessary to create emulsions where most of β -casein in emulsions adsorbed at the interface rather than remaining in the bulk solution. The centrifugation assay found that greater than 95% protein was adsorbed at oil-water interfaces under the homogenization condition. Compared to the initial protein concentration (3 mg/mL), less than 0.13 mg/mL of β -casein remained in the bulk solution of the hexadecane-in-water emulsion and only 0.06 mg/mL was found in the bulk phase of the tricaprylin-in-water emulsion. The adsorbed β -casein layers in the hexadecane-in-water and the tricaprylin-in-water emulsion had a surface coverage of 0.96 mg/m² and 1.05 mg/m² respectively. These values were relatively consistent with previous studies, indicating that an expanded monolayer of β -casein was located at the droplet surfaces.³²⁻³⁴

The secondary structural change of β -casein upon adsorption to two oil-water interfaces (tricaprylin-water and hexadecane-water) was examined by far-UV SRCD and the results are shown in Figure 5.2. β -Casein in solution (10 mM sodium phosphate buffer, pH 7) gave a far-UV SRCD spectrum containing a minimum peak at 200 nm and no zero-crossing, indicating a large amount of unordered structure. Analysis of this solution spectrum revealed that there was 11% α -helix, 25% β -sheet, 16% turn and 47% unordered structure (Table 5.2). The solution spectrum was highly consistent with previous studies.^{18, 35} Upon adsorption to oil-water interfaces, the SRCD spectra of β -casein changed to those characteristic of an α -helical-containing conformation as shown by the appearance of double minima at approximately 208 nm and 222 nm and the increase in signal intensity at 190 nm. Secondary structural analysis confirmed this observation. Table 5.2 shows that the α -helical content rose from 11% in solution to 18% at the tricaprylin-water interface and to 23% at the hexadecane-water interface, accompanied by decreases in the unordered structure and the β -sheet structure.

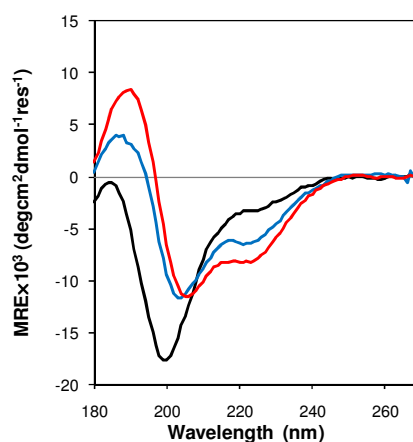


Figure 5.2: Far-UV SRCD spectra of β -casein in 10 mM sodium phosphate buffer pH 7 (black line), at the tricaprylin-water interface (blue line) and at the hexadecane-water interface (red line). All spectra were measured at 20 °C.

Table 5.2: Secondary structural content of β -casein in different environments.

β -casein	α -helix (%)	β -sheet (%)	Turns (%)	Unordered (%)
In solution	11.0	25.2	16.1	46.9
At tricaprylin-water interface	18.1	28.5	15.2	40.6
At hexadecane-water interface	23.0	22.9	14.0	39.4

5.3.3 Effect of temperature and salt on the ζ -potential and particle size of β -casein-stabilized oil-in-water emulsions

The stability of β -casein-stabilized emulsions under conditions of heating and moderate ionic strength (120 mM NaCl) was assessed by monitoring the emulsion ζ -potential and average particle size. Figure 5.3 shows changes in the emulsion ζ -potential in response to heating and 120 mM NaCl addition. Both the tricaprylin-in-water and the hexadecane-in-water emulsions had a ζ -potential of approximately -40 mV which was stable against heating up to 90 °C. Addition of 120 mM NaCl reduced the ζ -potential of both emulsions to -18 ± 1 mV which also remained stable upon heating. These results indicated that in the absence of 120 mM NaCl, the β -casein layer at the droplet surface was highly charged. Addition of 120 mM NaCl reduced the surface charge of the protein layer via the electrostatic screening effect.

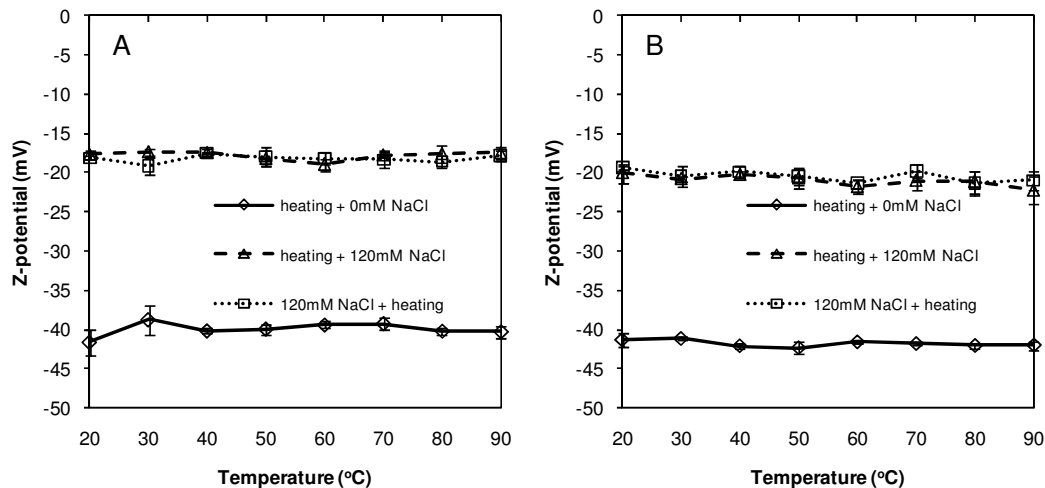


Figure 5.3: Effect of heating and 120 mM NaCl addition on the ζ -potential of β -casein-stabilized tricaprylin-in-water emulsions (A) and β -casein-stabilized hexadecane-in-water emulsions (B). Note: 'heating + 0mM NaCl' indicates no salt addition after heating; 'heating + 120mM NaCl' indicates salt addition after heating; and '120mM NaCl + heating' indicates salt addition before heating.

Figure 5.4 shows changes in the emulsion average particle size as a function of temperature and ionic strength. In the absence of salt, the tricaprylin-in-water emulsion had a mean particle size of $0.61 \pm 0.01 \mu\text{m}$ at 20 °C and increasing temperatures up to 90 °C for 20 min had no effect on

emulsion stability (Figure 5.4A). Addition of 120 mM NaCl to the emulsion, whether before or after heating, caused the mean particle size to increase slightly to around 0.7 μm , which remained stable against droplet flocculation up to 90 $^{\circ}\text{C}$ (Figure 5.4A). This stability against flocculation was also observed in the hexadecane-in-water emulsion which had an initial particle size of $0.54 \pm 0.01 \mu\text{m}$ at 20 $^{\circ}\text{C}$ in the absence of salt (Figure 5.4B). There was no significant change in the mean particle size under heating and salt addition (Figure 5.4B). These results were consistent with previous studies on β -casein-stabilized emulsion stability under heating and moderate ionic strength (NaCl) conditions.²⁶ Together with the structural studies, these results demonstrated that the adsorbed layer of β -casein provided both electrostatic and steric repulsion to emulsion droplets and hence a good stabilization against droplet flocculation and coalescence under the investigated conditions.

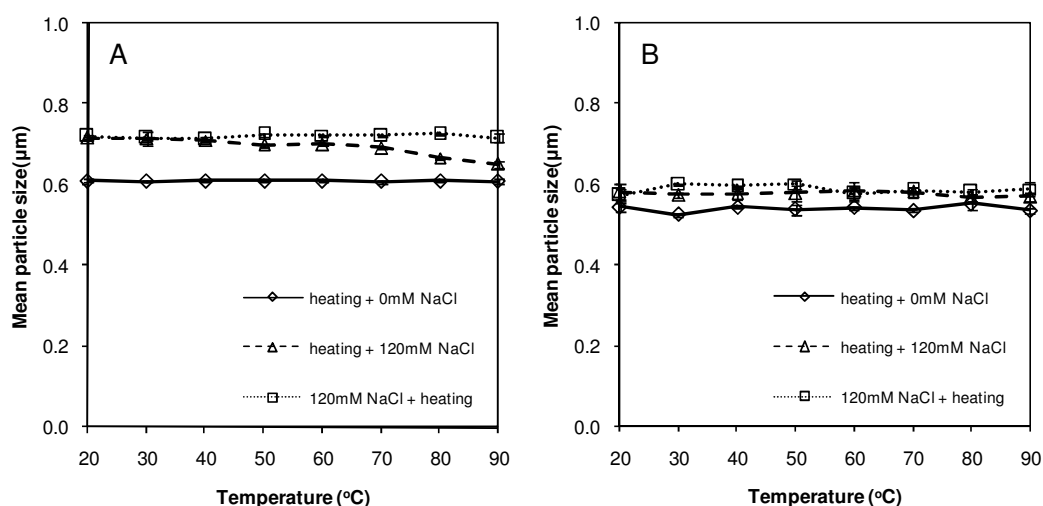


Figure 5.4: Effect of heating and 120 mM NaCl addition on average particle size of β -casein-stabilized tricaprylin-in-water emulsions (A) and β -casein-stabilized hexadecane-in-water emulsions (B). Note: 'heating + 0mM NaCl' indicates no salt addition after heating; 'heating + 120mM NaCl' indicates salt addition after heating; and '120mM NaCl + heating' indicates salt addition before heating.

5.4 Discussion

This is the first study to use DPI and SRCD techniques to characterize the structure of β -casein adsorbed at a planar hydrophobic surface or the oil-water interface of emulsions. Specifically, the DPI study gave information on the geometric dimensions of the β -casein layer adsorbed at a hydrophobic surface. In the DPI study, a C18 planar surface with buffer flowing over was used to mimic the oil-water interface of emulsions and a hydrophilic silicon oxynitride surface was used for comparison. With similar amounts of mass adsorbed at the two surfaces, the protein layer at the C18 surface was 1.1 nm thinner and 0.25 g/cm^3 denser than that at the silicon oxynitride surface at the end of the adsorption phase (Table 5.1). This result can be due to the

influence of the hydrophobic surface on driving the structural rearrangement of β -casein, where its hydrophobic region is located at the surface. The hydrophilic silicon oxynitride surface may not favour the contact between the surface and the hydrophobic region of β -casein and therefore induces a different orientation of β -casein, generating a thicker and more diffuse layer with a larger region of β -casein remaining in the aqueous environment than at the C18 surface.

Previous neutron reflectivity studies on β -casein layers adsorbed at hydrophobic surfaces (air-water and hexane-water) reported thickness values of 5-10 nm,^{17, 21} which are higher than the DPI study (2-5 nm). Another recent study also compared the measured layer thickness of bovine serum albumin (BSA) adsorbed at silicon surfaces in parallel DPI and neutron reflectivity studies.³⁶ The study reported that when a single-layer model was used in neutron reflectivity data analysis, similar layer thickness was observed between the two techniques. However, when a two-layer model was used in neutron reflectivity, a higher layer thickness was detected in neutron reflectivity than DPI. DPI only has a single-layer model assuming a uniform protein layer at the surface. When an adsorbed protein layer is non-uniformly distributed perpendicular to the surface, DPI with the single layer model can be less sensitive to the outer layer of the protein adsorbed at the surface than neutron reflectivity. The two layer model in the neutron reflectivity may deconvolute both the inner layer and the outer layer, giving a higher thickness value than DPI. Moreover, the difference between the thickness values of the adsorbed β -casein layers obtained from DPI and neutron reflectivity can arise from the different physical conditions of the protein layer, which was adsorbed at a C18 solid-water interface in DPI and at an air-water or a hexane-water interface in neutron reflectivity. Nevertheless, DPI can serve as a valuable and sensitive technique for comparing uniform protein layers adsorbed at surfaces of different properties, such as the cases of previous studies on β -Lg and α -La (Chapters 3 & 4).

In the SRCD study, secondary structural change of β -casein was characterized in situ at oil-water interfaces of emulsions. Two phenomena were observed and were consistent with previous β -Lg and α -La studies (Chapters 3 & 4). The first phenomenon was the increase in the non-native α -helical conformation upon adsorption to oil-water interfaces. There was an increase of 7.1% and 12% from the unordered structure to the α -helix upon β -casein adsorption to the tricaprylin-water interface and the hexadecane-water interface respectively (Table 5.2). Considering the high content of proline residues in β -casein, this increase was quite significant and demonstrated once again that the α -helical structure is preferred at oil-water interfaces.

The second phenomenon is the effect of oil hydrophobicity on the extent of structural change upon adsorption to oil-water interfaces. The SRCD results showed that the more hydrophobic hexadecane-water interface induced a larger change in the structure of β -casein than the tricaprylin-water interface (Figure 5.2 & Table 5.2). In a parallel study on the structural change

of β -casein upon adsorption to these two oil-water interfaces, SRCD results were also obtained (Appendix 5.1 Figure 6A) that were consistent with the present study.³⁵ Moreover, that study measured the FFTF spectra of β -casein in solution and adsorbed at the hexadecane-water and the tricaprylin-water interfaces (Appendix 5.1 Figure 6B).³⁵ The results showed a significant shift in λ_{\max} from 349 nm for β -casein in solution to 339.5 nm and 337.5 nm at the tricaprylin-water and the hexadecane-water interfaces respectively. The shift in λ_{\max} indicated that the only Trp residue (at position 143 in the sequence) in β -casein moved from a hydrophilic environment in the native state to a more hydrophobic environment, in this case, the oil-water interface. The larger shift in λ_{\max} when β -casein adsorbed to the hexadecane-water interface than the tricaprylin-water interface also revealed that the more hydrophobic oil induced a greater conformational change. This phenomenon of the effect of oil hydrophobicity reflects the fact that the main thermodynamic driving force of adsorption-induced structural change is the reorientation of a protein to expose its hydrophobic region toward the interface. A more hydrophobic interface thus requires a larger change in structure in order to establish the favourable interaction between the protein and the interface.

Based on previous studies with neutron reflectivity and FFTF and this study with DPI and SRCD, a schematic representation of the adsorbed β -casein layer at the oil-water interface is proposed and shown in Figure 5.5. The layer can be described in two distinct parts: a dense inner layer at the interface and a diffuse outer layer exposed to the aqueous phase. Specifically, the inner layer contains the hydrophobic C-terminus and most of the non-native α -helical conformation, which plays an important role in anchoring the protein at the interface. The outer layer contains the hydrophilic N-terminus that is negatively charged and thick (approximately 5-10 nm), which provides both electrostatic and steric repulsion within emulsions (Chapter 1 Section 1.2.2). Due to this unique structure of β -casein adsorbed at oil-water interfaces, emulsions stabilized by β -casein displayed excellent physical stability under conditions of heating and moderate ionic strength from 120 mM NaCl (Figures 5.3 & 5.4).

5. 5 Conclusion

This study employed DPI and SRCD methods to characterize the structural properties of β -casein adsorbed at a planar hydrophobic surface or the oil-water interface of emulsions. Together with previously studies on β -Lg and α -La (Chapters 3 & 4), the results obtained on β -casein structural behaviour upon adsorption enriched our current understanding in two aspects. First, the SRCD study showed that, at a secondary structural level, the transition from the unordered structure in β -casein to the preferred α -helical conformation at oil-water interfaces despite the high content of proline residues. Second, the structure of the β -casein layer adsorbed at oil-water interfaces was related to the emulsion physical stability under conditions of heating and moderate ionic strength. The combination of steric and electrostatic repulsion between the emulsion droplets

provided by the adsorbed β -casein layer thus explains the excellent functionality of β -casein as an emulsion stabilizer under conditions of heating and ionic strength (120 mM NaCl).

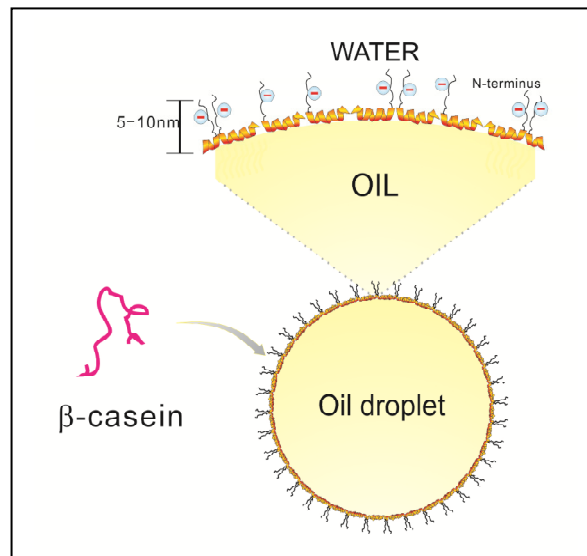


Figure 5.5: A schematic representation of the interfacial structure of β -casein adsorbed at the oil-water interface.

References

- (1) Dalgleish, D.G. *Food emulsions stabilized by proteins. Curr. Opin. Colloid Interface Sci.* **1997**, *2*, 573-577.
- (2) Dalgleish, D.G. *Food emulsions - their structures and structure-forming properties. Food Hydrocolloids* **2006**, *20*, 415-422.
- (3) McClements, D.J. *Food emulsions: Principles, practices, and techniques*, 2nd ed.; CRC Press: Boca Raton, 2005.
- (4) Dalgleish, D.G. *Adsorption of protein and the stability of emulsions. Trends Food Sci. Technol.* **1997**, *8*, 1-6.
- (5) Dickinson, E. *Milk protein interfacial layers and the relationship to emulsion stability and rheology. Colloids Surf., B* **2001**, *20*, 197-210.
- (6) Dickinson, E. *Flocculation of protein-stabilized oil-in-water emulsions. Colloids Surf., B* **2010**, *81*, 130-140.
- (7) Kim, H.-J.; Decker, E.A.; McClements, D.J. *Impact of protein surface denaturation on droplet flocculation in hexadecane oil-in-water emulsions stabilized by β -lactoglobulin. J. Agric. Food Chem.* **2002**, *50*, 7131-7137.
- (8) Kim, H.-J.; Decker, E.A.; McClements, D.J. *Role of postadsorption conformation changes of β -lactoglobulin on its ability to stabilize oil droplets against flocculation during heating at neutral pH. Langmuir* **2002**, *18*, 7577-7583.
- (9) McClements, D.J. *Protein-stabilized emulsions. Curr. Opin. Colloid Interface Sci.* **2004**, *9*, 305-313.
- (10) Dickinson, E. *Adsorbed protein layers at fluid interfaces: Interactions, structure and surface rheology. Colloids Surf., B* **1999**, *15*, 161-176.
- (11) Dickinson, E.; Matsumura, Y. *Proteins at liquid interfaces: Role of the molten globule state. Colloids Surf., B* **1994**, *3*, 1-17.
- (12) Wilde, P.; Mackie, A.; Husband, F.; Gunning, P.; Morris, V. *Proteins and emulsifiers at liquid interfaces. Adv. Colloid Interface Sci.* **2004**, *108-109*, 63-71.
- (13) Dalgleish, D.G. *Conformations and structures of milk proteins adsorbed to oil-water interfaces. Food Res. Int.* **1996**, *29*, 541-547.
- (14) Zhai, J.; Miles, A.J.; Pattenden, L.K.; Lee, T.-H.; Augustin, M.A.; Wallace, B.A.; Aguilar, M.-I.; Wooster, T.J. *Changes in β -lactoglobulin conformation at the oil/water interface of emulsions studied by synchrotron radiation circular dichroism spectroscopy. Biomacromolecules* **2010**, *11*, 2136-2142.
- (15) Zhai, J.; Wooster, T.J.; Hoffmann, S.V.; Lee, T.-H.; Augustin, M.A.; Aguilar, M.-I. *Structural rearrangement of β -lactoglobulin at different oil-water interfaces and its effect on emulsion stability. Langmuir* **2011**, *27*, 9227-9236.

- (16) Fox, P.F.; McSweeney, P.L.H. *Advanced dairy chemistry Volume I Proteins*, 3rd ed.; Kluwer Academic/Plenum: New York, 2003.
- (17) Atkinson, P.J.; Dickinson, E.; Horne, D.S.; Richardson, R.M. *Neutron reflectivity of adsorbed β -casein and β -lactoglobulin at the air/water interface. J. Chem. Soc., Faraday Trans.* **1995**, *91*, 2847-2854.
- (18) Caessens, P.W.J.R.; De Jongh, H.H.J.; Norde, W.; Gruppen, H. *The adsorption-induced secondary structure of β -casein and of distinct parts of its sequence in relation to foam and emulsion properties. Biochim. Biophys. Acta* **1999**, *1430*, 73-83.
- (19) Dalgleish, D.G. *The conformations of proteins on solid/water interfaces - caseins and phosphovitin on polystyrene latices. Colloids Surf.* **1990**, *46*, 141-155.
- (20) Dalgleish, D.G. *The size and conformations of the proteins in adsorbed layers of individual caseins on latices and in oil-in-water emulsions. Colloids Surf., B* **1993**, *1*, 1-8.
- (21) Dickinson, E.; Horne, D.S.; Phipps, J.S.; Richardson, R.M. *A neutron reflectivity study of the adsorption of β -casein at fluid interfaces. Langmuir* **1993**, *9*, 242-248.
- (22) Fang, Y.; Dalgleish, D.G. *Dimensions of the adsorbed layers in oil-in-water emulsions stabilized by caseins. J. Colloid Interface Sci.* **1993**, *156*, 329-334.
- (23) Fragneto, G.; Thomas, R.K.; Rennie, A.R.; Penfold, J. *Neutron reflection study of bovine β -casein adsorbed on OTS self-assembled monolayers. Science* **1995**, *267*, 657-660.
- (24) Leermakers, F.A.M.; Atkinson, P.J.; Dickinson, E.; Horne, D.S. *Self-consistent-field modeling of adsorbed β -casein: Effects of pH and ionic strength on surface coverage and density profile. J. Colloid Interface Sci.* **1996**, *178*, 681-693.
- (25) ter Beek, L.C.; Ketelaars, M.; McCain, D.C.; Smulders, P.E.; Walstra, P.; Hemminga, M.A. *Nuclear magnetic resonance study of the conformation and dynamics of β -casein at the oil/water interface in emulsions. Biophys. J.* **1996**, *70*, 2396-2402.
- (26) Dickinson, E. *Caseins in emulsions: Interfacial properties and interactions. Int. Dairy J.* **1999**, *9*, 305-312.
- (27) Farrell, H.M., Jr.; Jimenez-Flores, R.; Bleck, G.T.; Brown, E.M.; Butler, J.E.; Creamer, L.K.; Hicks, C.L.; Hollar, C.M.; Ng-Kwai-Hang, K.F.; Swaisgood, H.E. *Nomenclature of the proteins of cows' milk - sixth revision. J. Dairy Sci.* **2004**, *87*, 1641-1674.
- (28) Miles, A.J.; Janes, R.W.; Brown, A.; Clarke, D.T.; Sutherland, J.C.; Tao, Y.; Wallace, B.A.; Hoffmann, S.V. *Light flux density threshold at which protein denaturation is induced by synchrotron radiation circular dichroism beamlines. J. Synchrotron Radiat.* **2008**, *15*, 420-422.
- (29) Miles, A.J.; Hoffmann, S.V.; Tao, Y.; Janes, R.W.; Wallace, B.A. *Synchrotron radiation circular dichroism (SRCD) spectroscopy: New beamlines and new applications in biology. Spectroscopy* **2007**, *21*, 245-255.

- (30) Sreerama, N.; Venyaminov, S.Y.; Woody, R.W. *Estimation of the number of α -helical and β -strand segments in proteins using circular dichroism spectroscopy.* *Protein Sci.* **1999**, *8*, 370-380.
- (31) Whitmore, L.; Wallace, B.A. *Dichroweb, an online server for protein secondary structure analyses from circular dichroism spectroscopic data.* *Nucl. Acids Res.* **2004**, *32*, W668-673.
- (32) Graham, D.E.; Phillips, M.C. *Proteins at liquid interfaces: I. Kinetics of adsorption and surface denaturation.* *J. Colloid Interface Sci.* **1979**, *70*, 403-414.
- (33) Singh, H.; Tamehana, M.; Hemar, Y.; Munro, P.A. *Interfacial compositions, microstructures and properties of oil-in-water emulsions formed with mixtures of milk proteins and κ -carrageenan: I. Sodium caseinate.* *Food Hydrocolloids* **2003**, *17*, 539-548.
- (34) Srinivasan, M.; Singh, H.; Munro, P.A. *Sodium caseinate-stabilized emulsions: Factors affecting coverage and composition of surface proteins.* *J. Agric. Food Chem.* **1996**, *44*, 3807-3811.
- (35) Wong, B.T.; Zhai, J.; Hoffmann, S.V.; Aguilar, M.-I.; Augustin, M.A.; Wooster, T.J.; Day, L. *Conformational changes to deamidated wheat gliadins and β -casein upon adsorption to oil-water emulsion interfaces.* *Food Hydrocolloids*, in press.
- (36) Cowsill, B.J.; Coffey, P.D.; Yaseen, M.; Waigh, T.A.; Freeman, N.J.; Lu, J.R. *Measurement of the thickness of ultra-thin adsorbed globular protein layers with dual-polarisation interferometry: A comparison with neutron reflectivity.* *Soft Matter* **2011**, *7*, 7223-7230.

**Conformational changes to deamidated wheat gliadins and β -casein
upon adsorption to oil-water emulsion interfaces**

Benjamin T. Wong^{1,2}, Jiali Zhai^{1,3}, Søren V. Hoffmann⁴, Marie-Isabel Aguilar³,
Mary Ann Augustin¹, Tim J. Wooster^{1,#} and Li Day^{1,*}

¹CSIRO Food and Nutritional Sciences, 671 Sneydes Road, Werribee, VIC 3030, Australia

²School of Chemistry and Centre for Biospectroscopy, Monash University, Clayton, VIC 3800, Australia

³Department of Biochemistry and Molecular Biology, Monash University, Clayton, VIC 3800, Australia

⁴Institute for Storage Ring Facilities (ISA), Aarhus University, Ny Munkegade, DK-8000 Aarhus C,
Denmark

[#]Present Address: Nestlé Research Centre, CH-1000 Lausanne 26, Switzerland

*Corresponding author:

Dr. Li Day,
CSIRO Food and Nutritional Sciences,
671 Sneydes Rd, Werribee, VIC 3030, Australia
li.day@csiro.au;
Ph: +61-3-9731-3233
Fx: +61-3-9731-3250

Abstract

The conformation of deamidated gliadins and β -casein in solution and adsorbed at the interface of oil-in-water emulsions was studied using synchrotron radiation circular dichroism (SRCD) and front face fluorescence spectroscopy. Deamidation led to partial unfolding of gliadins in solution. The α -helix content of the protein decreased from 35% (in the native form) to 16.3% while the percentage of β -sheet and unordered structure increased upon deamidation. The secondary structure of deamidated gliadins was largely unchanged upon adsorption to both tricaprln/water and hexadecane/water interfaces. In contrast, β -casein adopted a more ordered structure upon adsorption to these two oil/water interfaces, the α -helix content increased from 5.5% (solution) to 20% and 22.5% respectively after adsorption to tricaprln/water and hexadecane/water interfaces. Both deamidated gliadins and β -casein have distinctive N-terminal hydrophilic and C-terminal hydrophobic domains. Unlike β -casein which contains no cysteine residue, gliadins have a large number of intramolecular disulphide bonds located in the C-terminal hydrophobic domain which constrains the conformational freedom of this protein upon adsorption to oil/water interfaces. The hydrophobicity of the oil phase also has an impact on the conformation of each protein upon adsorption to the oil/water interfaces – systematic trends were observed between oil phase polarity from: i) tryptophan fluorescence emission maxima, and ii) the α -helix content in the adsorbed state. Our results demonstrate that conformational rearrangement of proteins upon adsorption to emulsion interfaces is dependent not only on the hydrophobicity of the oil phase, but more importantly on the conformational flexibility of the protein.

Introduction

Proteins are widely used to stabilise oil/water and air/water interfaces in emulsion and foam based consumer products. Proteins are excellent emulsifiers because their natural amphiphilicity promotes emulsification and their polymeric structure helps to prevent emulsion structure breakdown via processes such as flocculation and coalescence.^{1, 2} The structural organisation of proteins at oil/water interfaces has long been recognized as a major factor controlling the stability of emulsion-based products.^{3, 4} Extensive effort has been directed at understanding the mechanism and dynamics of protein adsorption, the hierarchical structure of proteins at interfaces and how these relate to emulsion stability.⁴⁻⁶ It is widely thought that upon adsorption to droplet interfaces, proteins tend to unfold and adopt a conformation that maximizes the exposure of their hydrophobic/hydrophilic segments to oil/water phases respectively.^{2-4, 6} What is not well understood is the extent of protein conformational rearrangement that accompanies adsorption and how this is affected by the nature of the protein and the oil phase. Given that the structure and behavior of proteins adsorbed at interfaces play a key role in stabilizing emulsions, a detailed understanding of these conformation rearrangements is of high importance.

Among the most studied protein emulsifiers are those derived from dairy, such as β -lactoglobulin and the caseins.⁷⁻¹⁰ Proteins from plant sources (e.g. wheat, soy and corn, etc.) have not been used extensively as emulsifiers due to their poor water solubility at neutral pH.^{11, 12} Modification of these proteins, either by deamidation and/or enzymatic hydrolysis, is required to enhance their solubility by increasing their polyelectrolyte character.¹³⁻¹⁶ Deamidation using mild acid converts amide groups, primarily from glutamine residues, into carboxyl groups, with minimal protein hydrolysis.¹³ This process results in an increase in the protein charge at neutral pH and a reduction in inter- and intra-molecular hydrogen bonding interactions, which enhances protein solubility by decreasing aggregation.¹⁷

There is increasing interest in the properties of emulsions stabilised by (modified) plant proteins.^{14-16, 18, 19} Studies have shown that emulsions stabilised by deamidated wheat protein have excellent physical stability, particularly against coalescence and thermally induced aggregation.^{16, 20} There is very limited knowledge of the interfacial structure of plant proteins, particularly as to how this structure relates to emulsion stability. Recently we found that deamidated wheat protein forms a relatively thick interfacial layer of ~18 nm upon adsorption to oil/water interfaces.¹⁶ The protein film also has a weak fluid-like interfacial rheology, indicating low friction within the interfacial layer which suggests the protein does not have a highly ordered structure (globular proteins form strong viscoelastic films).^{21, 22} However, whether or not deamidated wheat protein undergoes any conformational change upon adsorption to oil/water interfaces and the mechanism of how this protein stabilises emulsions is not well understood.

Circular dichroism (CD) is used extensively to determine protein secondary and tertiary structures in solution.²³⁻²⁵ However, there have been few studies examining the conformation of proteins at emulsion interfaces using CD as the high absorbance/light scattering of these structures prevents good quality spectra to be obtained using conventional instruments. A few studies have used solid particles or surfaces to mimic oil/water interfaces.^{24, 26-29} Although such studies can provide insight into protein behaviour at hydrophobic surfaces, they do not mimic the physiochemical nature of emulsion oil/water interfaces. The conformation of proteins adsorbed at liquid interfaces, especially oil/water interfaces, may differ from that at solid surfaces or colloidal particles because the protein molecules have much greater mobility at the interface and greater penetration into the non-aqueous phase.³ Attempts to study the structure of proteins adsorbed at emulsion interfaces using CD have been undertaken by matching the refractive index (RI) of the two phases to reduce signal interference.³⁰ The drawback of RI matched emulsions is that the presence of the high levels of glycerol (58% (v/v)) required to achieve RI matching may affect the conformation of the protein. Recently, a method was developed to directly measure the conformation of proteins (β -lactoglobulin) adsorbed at emulsion oil/water interfaces using Synchrotron Radiation Circular Dichroism (SRCD).³¹ The main advantage of SRCD is that the much higher photon flux (which is uniform across the whole wavelength range) enables the measurement of turbid or highly absorbing samples, thereby permitting spectra to be collected at much lower wavelengths, increasing the accuracy of structural assignment.³² In particular, SRCD overcomes the difficulties associated with emulsion turbidity and allows measurement of protein conformation at emulsion oil/water interfaces without the use of RI matched emulsions.³¹

It is known that proteins adopt structures at interfaces different to that in solution and that the structure of proteins at the oil/water interface plays an important role in their ability to stabilise emulsions. However, there is very limited understanding of the exact nature of the conformational changes that proteins undergo upon adsorption to oil/water interfaces, or how their inherent native structure, or hydrophobicity of the oil phase, affects these conformational re-arrangements. Therefore this study sought to investigate the conformational changes of deamidated gliadins upon adsorption to emulsion oil/water interfaces by using SRCD in combination with fluorescence emission spectroscopy. Since the primary structure and conformation of deamidated gliadins are not well known, and the study of protein conformation at emulsion interfaces using SRCD is a relatively new technique, a second protein β -casein was studied as a comparison. β -casein provides a good comparison to deamidated gliadins because it has a largely random coil structure in solution, a similar distribution of hydrophilic/hydrophobic domains and similar interfacial rheological properties.^{13, 16, 33, 34} However β -casein differs from deamidated gliadins in that β -casein has no internal disulfide bonds, whereas deamidated gliadins have up to 4 disulfide bonds, all located in the C-terminal domain. This study seeks to develop further knowledge about

conformational changes of proteins upon adsorption to emulsion interfaces and to understand how they relate to the ability of proteins to stabilise emulsions.

Materials and Methods

Materials

Isolated wheat protein (IWP, 30-35% deamidation, 78% protein (N×6.25) and 6.7% moisture) and vital wheat gluten (VWG, 69% protein (N×5.7) and 7.2% moisture) were obtained from The Manildra Group (Nowra, NSW, Australia). Hexadecane, tricaprin (glyceryl tridecanoate) and camphorsulfonic acid (CSA) were purchased from Sigma-Aldrich (Denmark). Other chemicals and bovine milk β -casein (C6905, minimum 90%) were purchased from Sigma-Aldrich (Sydney, Australia).

Preparation of protein materials

The gliadin-rich fractions were prepared from IWP and VWG using 70% aqueous ethanol. IWP or VWG dispersion (10 wt%) was prepared by dispersing the protein in 70% ethanol and mixed using an Ultra-turrax at 9500 rpm for 1 min. The protein dispersion was then gently stirred for 1 h at room temperature and centrifuged at 10,000 g for 45 min at 10 °C using a Beckman J2-MC centrifuge (Beckman Coulter, Australia). Ammonium chloride solution (1.5 M, 2 × volume of the supernatant) was added to the supernatant to precipitate the protein overnight at 4 °C. Following centrifugation at 10,000 g for 45 min at 10 °C, the precipitate was then washed with deionised water twice to remove residual ammonium chloride. The protein pellet was then freeze-dried. The resulting gliadin-rich fractions were used throughout the study.

A laboratory sample of deamidated gliadins was prepared using the gliadin fraction enriched from VWG. The protein was dispersed in 0.2 M HCl (10 wt%) and heated at 70 °C for 2 h with constant stirring in a sealed glass container. The dispersion was then cooled to room temperature (~22 °C) and adjusted to pH 7 using 1 M NaOH. The dispersion was centrifuged at 10,000 g for 15 min at 10 °C and its supernatant was collected. The supernatant was dialysed (8,000 Da cut off) against deionised water (3 × 5L) at 4 °C overnight and then freeze-dried.

The degree of deamidation was determined using an ammonia test kit (Randox, Crumlin, United Kingdom) and calculated by comparing the ammonia content measured from the sample to that of a totally deamidated gliadins, prepared by heating the protein in 2 M HCl at 98 °C for 3 h.

Size Exclusion – High Performance Liquid Chromatography (SE-HPLC)

SE-HPLC was conducted using a Shimadzu LC-20 HPLC system equipped with a UV-Vis detector. Protein dispersions were prepared in 50 mM sodium phosphate buffer (pH 6.8) containing 0.5 wt% sodium dodecyl sulphate (SDS) and then mixed for 2 h using a vortex mixer. The dispersion of VWG or the insoluble fraction of IWP in buffer was sonicated for 10 min each time

to allow better dispersion of insoluble proteins. The protein dispersions were then centrifuged at 10,000 g for 5 min and filtered through 0.45 μm syringe filters. These samples (20 μL) were then injected into a Phenomenex BIOSEP-SEC-S4000 column and run at 0.5 mL/min in a 50 mM sodium phosphate buffer (pH 6.8). The elution profiles were monitored at 214 nm.

Sodium-dodecyl-sulphate Polyacrylamide Gel Electrophoresis (SDS-PAGE)

SDS-PAGE was performed according to the method of Kasarda et al. (1998) and modified by McCann et al. (2009).^{35, 36} Protein samples (10 μL , 3.8 mg/mL) were dissolved in a sample buffer containing 11.25 mM Tris-HCl, 3.6 wt% SDS, 18 wt% glycerol, at pH 8.6. Electrophoresis was carried out at 100 V for 45 min and then 120 V for 1 h in morpholinoethanesulfonic (MES) running buffer containing 50 mM MES, 50 mM Tris base, 0.1% SDS, 1 mM ethylenediaminetetraacetic acid (EDTA), pH 7.3. After electrophoresis, the gels were stained with 0.1 wt% Coomassie brilliant blue-R250 (in 40 wt%/10 wt% methanol/acetic acid) for 25 min and then de-stained overnight in a solution of 10 wt%/7.5 wt% methanol/acetic acid. The gels were photographed using a Kodak digital camera controlled by Kodak 1D v3.5 software.

Protein solutions for SRCD measurements

The protein solutions (1 wt%) were prepared in 20 mM McIlvaine's buffer (19.45 mL, 20 mM Na_2HPO_4 and 0.55 mL, 0.1 M citric acid, pH 8) and gently stirred for 2 h prior to use for SRCD measurements. Solutions containing non-deamidated gliadin fraction were prepared by constant stirring overnight at 4 °C, followed by centrifugation at 14,000 g using a bench-top centrifuge for 5 min to remove the insoluble protein. The protein concentration in the solution was determined by measuring the absorbance at 280 nm using a 0.1 cm path length quartz cell and calculated using the extinction coefficient of 0.9551 for gliadins or 0.5772 for β -casein.³⁷ The extinction coefficient of gliadins was determined by measuring the absorbance of gliadin fractions in solution whose concentrations have been determined by the Leco total nitrogen method, at 280 nm.

Preparation of emulsions

The optimum amount of protein required to obtain a stable emulsion for 24 h with the majority of proteins adsorbed onto the emulsion interface was determined according to the method of Zhai et al. (2010). Briefly, a series of 20% (v/v) oil-in-water emulsions stabilized by 0.1-1% (w/w) protein were prepared by homogenization at room temperature. The particle size of the emulsions was determined immediately after emulsion preparation, and again after 24 h storage. The residue protein in the aqueous phase was determined by centrifuging the emulsion at 5,000 \times g for 20 min and analysis of nitrogen content in the lower aqueous phase using a LECO[®] FP2000

instrument. In all cases, the optimum protein concentration was 0.3 wt% (protein base) in the final emulsions. This protein concentration was therefore used to prepare emulsions for SRCD measurements. The emulsions were prepared by homogenising 20 wt% hexadecane or tricaprln with 80 wt% aqueous protein solution (pH 8) using an Ultra-turrax mixer at 11,500 rpm for 2 min at room temperature (~22 °C), followed by two passes through a high-pressure valve homogenizer at approximately 500 bar (EmulsiFlex C5, Avestin, Canada). The emulsions were freshly prepared immediately prior to each experiment, stored at 4 °C and measured again after 24 h.

SDS stabilised oil-in-water emulsions were prepared by homogenising 20 wt% hexadecane or tricaprln with 80 wt% aqueous solution (pH 8) at room temperature (~22 °C), under the same conditions as described above for the preparation of protein stabilised oil-in-water emulsions. The emulsion contained 0.45 wt% SDS and was used for SRCD baseline correction. Care was taken so that the SDS stabilized emulsion had similar light scattering properties to the sample protein stabilized emulsion as shown by Zhai et al. (2010).

Particle size determination

Emulsion droplet size was measured by laser light scattering using a Malvern Mastersizer 2000 instrument (Malvern Instruments Ltd, Worcestershire, UK). An aliquot of the emulsion sample was transferred into the recirculating water of a Hydro SM sample dispersion unit until an obscuration rate of 10-20% was obtained. A differential refractive index of 1.078 (1.434 for hexadecane/1.33 for water) or 1.102 (1.466 for tricaprln/1.33 for water) and absorption of 0.001 were used as the optical properties of the emulsion. The droplet size distribution of the emulsion was then obtained via a best fit between light scattering (Mie) theory and the measured light scattering pattern. The mean emulsion droplet size is quoted as the volume-length mean diameter $d_{4,3}$ ($d_{4,3} = \sum n_i d_i^4 / \sum n_i d_i^3$). The results reported are an average of three measurements.

SRCD measurements

SRCD measurements were carried out on the UV-VUV CD1 beamline at the ASTRID synchrotron radiation source, Institute for Storage Ring Facilities (ISA), Aarhus University in Denmark.^{38, 39} The SRCD spectrometer was calibrated daily using camphorsulfonic acid for optical rotation magnitude and wavelength.⁴⁰

A 0.01 cm path length quartz Suprasil cell (Hellma GmbH & Co., Germany) was used for far-UV SRCD measurements at 25 °C and the baseline was corrected using 20 mM McIlvaine's buffer (pH 8) for protein solutions and SDS hexadecane or tricaprln emulsions for protein stabilised oil-in-water emulsions. The far-UV SRCD spectra were recorded at from 270 to 170 nm in 1 nm steps, 2.1 s averaging time, and 3 scans for protein solution sample or 8 scans for emulsion sample.

SRCD data analysis and calculation of protein secondary structure

All spectra were processed using CDtool software.⁴¹ Each spectrum was calibrated, averaged, smoothed using a 7 point Savitzky-Golay smoothing filter and baseline subtracted. All spectra presented were truncated at a certain low wavelength where the high tension (HT) dynode voltage was higher than 1.1 kV, indicating the point of which the transmitted light levels to the detector was too low for accurate measurements. The spectra were converted to mean residue ellipticity (θ) units using a mean residue weight of 110 for gliadins and 114.9 for β -casein.^{42, 43}

The proportions of each secondary structure components were determined using a web-based calculation server DICHROWEB that incorporates various methods and a wide range of protein spectral databases.⁴⁴ The calculation method used in this study was CDSSTR with the reference set SP175 (optimised for 175-240 for protein in solution and 190-240 nm for emulsion).⁴⁵

Front-Face Fluorescence

The tryptophan emission fluorescence spectra were recorded using a Perkin-Elmer LS-55 spectro-fluorophotometer equipped with a front-face-fluorescence accessory. Protein solutions (0.04 mg/mL) were prepared in 20mM McIlvaine's buffer (pH 8) and stirred for 2 h. Protein-stabilized emulsions were freshly prepared as described above. The fluorescence spectra of the samples were all recorded in the front-face configuration using an excitation wavelength of 280 nm, with 1 nm resolution, 10 nm slit width and a scanning speed of 100 nm/min.⁴⁶

Results and Discussion

Secondary structure of deamidated gliadins in solution

Gluten proteins contain a mixture of monomeric gliadins with a molecular weight (MW) between 30,000 and 60,000 Da and glutenins who have the potential to form polymers with a MW ranging from about 80,000 Da to several million.⁴⁷ Gliadin fractions corresponding to the deamidated and native form were enriched from commercial sources of deamidated and native gluten respectively. The protein contents of gliadin-rich fractions, non-deamidated and deamidated, were 85.9% and 79.2% respectively. The SE-HPLC chromatograms in Fig. 1A and 1B demonstrate that there was a significant or complete reduction of the glutenin peak in the enriched gliadin fractions compared to original IWP or VWG respectively. However residual glutenin (likely to the non polymerised low molecular subunits) could be observed in the deamidated gliadin-rich fraction prepared from the commercial deamidated wheat protein (Fig. 1A), but was absent in the laboratory prepared deamidated gliadins (Fig. 1B). The corresponding SDS-PAGE gel images (Fig. 1C and 1D) tend to suggest that the enriched deamidated gliadins and native gliadins were comprised of a significant fraction of gliadins (likely to be α -/ β - and γ -type) in the MW range of 32,000-42,000 Da.^{42, 48}

The deamidated gliadins had a degree of deamidation of approximately 35%, whereas the laboratory prepared deamidated gliadins had a slightly lower degree of deamidation of 29%. The secondary structures of the native gliadins and deamidated gliadins in solution were investigated using far-UV SRCD. Their spectra are shown in Fig. 2. The high signal intensity of SRCD meant that a good quality CD spectra was obtained for the native gliadins even though gliadins are known to have low solubility in aqueous solutions near neutral pH. The protein concentration in solution was determined by UV/Vis spectrometry to be 0.15 mg/mL which was used for SRCD spectra correction. SRCD spectra of gliadins in solution exhibited minima at 222 nm and 208 nm, a peak maximum at 190 nm which is a typical feature of α -helical protein, and a zero-crossing at 198 nm. Secondary structure analysis using CDSSTR and the SP175 reference set showed that gliadins contained 35% α -helix; 16% β -sheet; 14% β -turns and 35% unordered structure (Table 1). The CD spectra of native gliadins and the percentage of its secondary structural components were more similar to those of α - or γ -gliadins solubilised in 70% ethanol than those of the ω -gliadins measured by conventional CD.^{42, 49}

Upon deamidation, the spectra of deamidated gliadins (laboratory-prepared and that enriched from IWP) exhibited a shift in peak minima and zero-crossing towards lower wavelengths and a reduction in mean residue ellipticities (MRE) at 190 nm. The secondary structure analysis showed that deamidated gliadins contain 16-22% α -helical structure, which is lower than that in

native gliadins (Table 1). Conversely deamidated gliadins had higher proportions of β -sheet and unordered structures at 22-26% and 41-42% respectively, compared to 16% β -sheet and 35% unordered structures in native gliadins (Table 1). The retention of a moderate amount of helical structure indicates that the protein did not unfold completely after the deamidation. The differences in the secondary structure between the laboratory-deamidated gliadins (29% deamidation) and the deamidated gliadins prepared from the commercial source (35% deamidation) is likely due to the different degree of deamidation of the protein. A reduction in α -helical content up to 20% as a result of deamidation (40%) has also been reported by Matsudini et al. (1982).

The primary structure of gliadins for α -/ β - and γ -type is divided into two distinct domains, an N-terminal repetitive domain rich in glutamine and proline residues and a C-terminal non-repetitive domain containing several hydrophobic residues and 6-8 cysteines involved in the formation of 3-4 intra-disulphide bonds.^{47, 49, 50} The repetitive and non-repetitive domains of the proteins formed different structures with the former having an extended conformation with an equilibrium between polyproline II-like structure and β -turns, and the latter a more compact globular structure rich in α -helix.⁴⁷ Limited changes in SH- and SS-content during deamidation of wheat gluten have been previously reported.¹³ Partial unfolding of the protein caused by deamidation might be expected to expose hydrophobic patches previously buried within the globular structure of this domain. To assess the hydrophobic environment around the tryptophan residues, the fluorescence emission spectra of the tryptophan residue(s) were measured. Depending on the type of gliadin (α , β or γ), gliadins can contain between 1 and 3 tryptophan residues, at least one of which is located at the C-terminal domain.^{51, 52} Fig. 3 shows that the tryptophan fluorescence emission spectra of gliadins had a λ_{\max} at 351 nm, and that deamidated gliadins had a λ_{\max} at 353 nm, i.e. a small shift towards longer wavelengths. It is known that the polarity of the environment surrounding tryptophan residues affects the fluorescence emission maximum (λ_{\max}).⁵³ This shift towards longer wavelength implies that the tryptophan residue of deamidated gliadins was exposed to a more hydrophilic environment due to the partial unfolding of the protein upon deamidation.

Conformation of deamidated gliadins upon adsorption at oil/water interfaces

In this study, an approach developed by Zhai et al.^{31, 52} for the direct measurement of protein conformation at emulsion interfaces using SRCD was used to investigate the conformational changes of deamidated gliadins upon adsorption to oil/water interfaces. The approach utilises the high intensity of synchrotron radiation, together with appropriate correction for sample light scattering (by subtraction of the CD signals arising from an emulsion stabilised by a non-chiral emulsifier - SDS), to obtain high quality SRCD spectra from the protein in an emulsion system. Un-adsorbed protein in the continuous phase of the emulsion was limited by choosing an appropriate protein concentration to ensure sufficient surface coverage for the

emulsion to be stable within the timeframe of the experiments (Fig. 4). The lowest protein concentration c.a. 0.3 w/w%, at which only limited changes over 24 hr in the particle size was observed was used for the SRCD study. At this protein concentration, surface load measurements indicate that approximately 87% of the total protein was adsorbed at the oil droplets surface. With an average particle size $d_{4,3}$ of $1.2 \pm 0.03 \mu\text{m}$, the amount of protein adsorbed at the interface at this protein concentration equates to a protein surface load of 2.0 mg/m^2 , which is very close to the saturation surface coverage of deamidated wheat protein previously measured by adsorbing the protein to the surface of latex particles which is $2.3 \pm 0.4 \text{ mg/m}^2$.¹⁶

Two emulsions, made from either tricaprins or hexadecane, were used to assess the conformational changes of deamidated gliadins upon adsorption to emulsion interfaces. The two oil phases had different polarities and were used in order to understand if solvation of proteins in the oil phase influences the conformation of proteins at oil/water interfaces. Fig. 5A shows the SRCD spectra of deamidated gliadins adsorbed at the two oil-in-water emulsion interfaces compared to the protein in solution. The secondary structure components derived from these spectra are summarised in Table 2. At the tricaprins/water interface, there was a 3.7% increase in α -helix and a 4.5% reduction in β -sheet content of the protein adsorbed at the emulsion interface compared to its solution conformation. At the hexadecane/water interface, the protein exhibited a 7.2% increase in α -helix and a 7.1% reduction in β -sheet in its conformation compared to its solution conformation. Fig. 5B shows fluorescence emission spectra of deamidated gliadins adsorbed at each emulsion interface compared to in solution. There was a significant shift in λ_{max} towards lower wavelengths of 347.5 nm and 344.5 nm for deamidated gliadins adsorbed at the tricaprins/water or hexadecane/water interface respectively compared to λ_{max} of 353 nm for deamidated gliadins in solution.

Overall, the adsorption of deamidated gliadins to oil/water interfaces caused only subtle changes in protein conformation. However, there was a systematic impact of the oil polarity on secondary structure of adsorbed protein demonstrated by a further increase in the α -helix content and tryptophan λ_{max} shift towards shorter wavelength with the decrease in oil polarity. The shift in λ_{max} suggests that the tryptophan residues located at the C-terminal of deamidated gliadins were in a more hydrophobic environment when the protein was adsorbed at emulsion oil/water interfaces, and further that these residues were in a more hydrophobic environment when at the hexadecane/water interface than at the tricaprins/water interface. This result is consistent with the molecular structure of the two oils, where tricaprins is less hydrophobic because of its glycerol head group and short aliphatic chains. The shift in tryptophan emission signals with oil polarity also supports the conclusion that the C-terminal domain of deamidated gliadins is anchored at the oil/water interface. Other studies have shown that the more hydrophobic C-terminus domain of gliadins was adsorbed to an emulsified oil droplet surface.⁵⁴ There was also little change in the

protein conformation at the emulsion interfaces after 24 h (Table 2), suggesting that adsorption-induced conformational change occurs within a very short period of time. However, it was noted that there was more rearrangement of the protein at the hexadecane/oil interface compared to that of the tricaprln/oil interface over 24 h aging of the emulsions.

Changes (e.g. 3-6% increase in α -helix) in the conformation of deamidation gliadins upon adsorption to oil/water interfaces is small in comparison with many common food proteins studied to date, including lysozyme (~10%) and BSA (~9%), both of which have high internal disulfide cross-links, are known to re-arrange and form re-ordered structures at interfaces.^{26, 30, 31, 55, 56} It could be that the unfolding caused by deamidation (from 35% α -helix in native protein reduced to 16%) means that further refolding is not required upon adsorption to oil/water interfaces because deamidated gliadins in solution are in an optimal, partially unfolded conformation. In order to gain a better understanding of how open unfolded proteins behave upon adsorption to emulsion interfaces the structure of the more well-known dairy protein β -casein, which has a largely random coil structure, was studied using the same methods.

Secondary structure of β -casein upon adsorption to oil/water interfaces

Fig. 6A shows the far-UV SRCD spectra of β -casein in solution and adsorbed at hexadecane/water and tricaprln/water interfaces. The SRCD spectrum of β -casein in solution had a minimum MRE at 200 nm with no zero-crossing in the far UV region, indicating a high degree of unordered structure. Analysis of the solution spectra of β -casein shows the presence of approximately 5.5% α -helix, 34.5% β -sheet, 15% turns, and 44.5% unordered structure (Table 3). This result is similar to that reported by Graham et al. (1984) using conventional CD measurements at 25 °C, pH 6.9, and to that predicted using molecular modeling, but with a slightly lower helical content and unordered structure than that reported by other studies.^{24, 43, 57} This may be due to the use of different mathematical fittings and algorithms to the CD spectra.

Upon adsorption to emulsion oil/water interfaces, the SRCD spectra of β -casein showed significant changes – an increase in the intensity of the peak at 190 nm, a shift of peak minima towards 206 nm and the appearance of a peak at 222 nm. The latter was particularly visible for β -casein at the hexadecane/water interface. The tryptophan fluorescence emission spectra also showed a significant shift in λ_{max} towards lower wavelengths, 339.5 nm and 337.5 nm for β -casein adsorbed at tricaprln/water and hexadecane/water interfaces respectively, compared to 349 nm for β -casein in solution (Fig. 6B). It is well known that casein undergoes structural re-ordering as a consequence of absorption to interfaces. However this is the first time that the structure of β -casein adsorbed at oil-in-water emulsion interfaces has been measured directly.

The dramatic changes in SRCD spectra of β -casein provides direct evidence that adsorption to oil/water interfaces induces a more ordered secondary structure. Secondary structure calculations confirm that there is a significant increase in β -casein α -helix content (rising from 5.5% in solution to 20% and 21.5% after its adsorption at tricaprin/water and hexadecane/water interface respectively), which is accompanied by corresponding decreases in β -sheet and unordered structures (Table 3). Caessens et al. compared β -casein conformation in solution with that at teflon/water interface and showed an increased amount of α -helix (20%) and a decreased amount of random coil structure of β -casein upon adsorption.²⁴

The hydrophobicity of the oil phase clearly had an influence on the conformation of β -casein at the oil/water interfaces, there was an increase in the α -helix content and shifts in λ_{\max} towards shorter wavelength with the decreasing in oil polarity. Given that the only tryptophan residue in β -casein is located towards the C-terminal, the significant shift in tryptophan emission λ_{\max} when β -casein is adsorbed to oil/water interfaces also suggests that the C-terminal of adsorbed β -casein is in contact with the interface. Ageing of the emulsion had little impact on the conformation of adsorbed β -casein at oil/water interfaces. This may be expected because flexible proteins such as β -casein would adopt re-ordered structures in order to lower the interfacial tension at the interface more quickly than globular proteins.^{2, 4, 58}

Comparison of the conformational structure of deamidated gliadins and β -casein at emulsion interfaces

It is known that the conformation of proteins can change upon adsorption to emulsion interfaces. A reduction or increase in α -helix content upon adsorption have been reported for globular proteins such as lysozyme (~10% reduction), BSA (~9% reduction) and β -lactoglobulin (~15% increase), and for more flexible proteins such as casein (~15% increase).^{24, 30, 59-62} A major driving force for protein unfolding or reordering at interfaces is to increase the exposure of non-polar groups to the hydrophobic environment. It would be expected then that adsorption to oil/water interfaces would have an effect on protein conformation and that this effect would be a function of oil phase polarity, particularly in the present case since hexadecane (~ 52.8 mN) and tricaprin (30 mN) have considerably different interfacial tensions.⁶³ Furthermore, in a parallel study, it was found that the degree of β -lactoglobulin conformational rearrangement at emulsion interfaces also scaled with the polarity of the oil phase.⁵² However in the present study, we found that there was little change in the conformation of deamidated gliadins upon its adsorption at oil/water interfaces. A number of factors might explain this lack of conformational re-arrangement upon adsorption. The most likely explanation is that re-ordering of deamidated gliadins is restricted by a number of internal disulphide linkages which constrain molecular mobility. It has been reported that the conformational changes of BSA upon adsorption to solid surfaces and/or emulsion

interfaces are much lower compared to those observed for other globular proteins.^{30, 56} This is thought to be due to the high degree of disulphide cross-links within BSA which constrain structural rearrangement. In the case of deamidated gliadins, the disulphide bonds located at the surface active C-terminus could provide an energy barrier which limits the proteins ability to adopt a more thermodynamically stable conformation upon adsorption to the interface. It is also possible that there is restricted mobility within the interfacial layer because of a high packing density of the protein. There has been extensive study of the rheological characteristics of protein interfaces, and it is increasingly being recognized that protein layers with high packing densities have highly restricted internal mobility.^{4, 64, 65} Restricted mobility within a protein interfacial layer can limit conformational re-arrangement of β -lactoglobulin, for example, as shown recently by Lin and White (2009).⁶⁶ However, deamidated gliadins have a weak fluid interfacial rheology suggesting that there is high mobility within the layer.¹⁶

An alternative, but much less likely, explanation is that the structure of deamidated gliadins may be in a state (i.e. the distribution of hydrophobic/hydrophilic domains, etc.) that requires no further conformational change upon adsorption to oil/water interfaces. Although the deamidation process resulted in only partial unfolding of native gliadins in solution, this partial unfolding, particularly at the C-terminal domain, was crucial as it exposed the hydrophobic residues that favour interaction with the oil phase. A conceptual model of how the structure of gliadins changes upon deamidation and its subsequent adsorption at oil/water interfaces is proposed in Fig. 7A. Deamidation increases the charge of the protein, particularly at the N-terminal domain, and partial unfolding of the C-terminal domain aids its adsorption to interfaces. This distribution of hydrophilic and hydrophobic domains allows the protein to adsorb to emulsion oil/water interfaces with an open structure resembling that of β -casein (Fig. 7B). The C-terminus is anchored into the oil phase and the N-terminus forms a tail which extends considerably (some 18 nm) into the aqueous phase. As a result, the protein forms a thick charged 'hairy' layer at the interface which provides excellent steric and electrostatic stabilisation to emulsion droplets.

There are many similarities between deamidated gliadins and β -casein, the molecular size, and the distinctive distribution of hydrophilic and hydrophobic domains at N- and C-terminals respectively. One important difference between deamidated gliadins and β -casein is that deamidated gliadins have up to 4 intramolecular disulphide bonds at its C-terminal domain, whereas β -casein contains no cysteine residues. The more flexible β -casein undergoes a structural rearrangement upon adsorption (Fig. 7B). Deamidated gliadins on the other hand, undergo minimal re-arrangement upon adsorption to oil/water interfaces, most likely due to the internal disulphide bonds. What is consistent is that both proteins adopt a helical structure upon adsorption to emulsion oil/water interfaces. There is growing evidence from a number of recent studies of other proteins which suggests that there is a preference for the formation of α -helical motifs upon adsorption to

oil/water interfaces.³¹ The preference for this conformation may be governed by the need to form amphipathic moieties, as is the case with membrane proteins which also show a high propensity for α -helical motifs.^{67, 68}

Conclusions

Conformational changes to deamidated gliadins and β -casein upon adsorption to oil/water interfaces were investigated using synchrotron radiation circular dichroism (SRCD) and front face fluorescence spectroscopy. The secondary structure of deamidated gliadins was largely unchanged upon adsorption to both tricaprin oil-in-water and hexadecane oil-in-water interfaces. This is likely due to the high numbers of internal disulphide linkages at the C-terminal domain of gliadins which limited molecular mobility of protein upon adsorption to the interfaces. β -casein, on the other hand, underwent a structure re-ordering with a significant increase in the protein's α -helix content and corresponding decrease in the proportion of un-ordered structure after it was absorbed to the oil/water interfaces. A slight increase in the α -helical content and a shift of tryptophan fluorescence emission maxima towards lower wavelength were observed for both proteins absorbed at hexadecane/water interface compared to tricaprin/water interface. The results demonstrate that conformational rearrangement of proteins upon adsorption to emulsion interfaces is dependent not only on the hydrophobicity of the oil phase, but more importantly on the conformational flexibility of the protein. The results also confirmed that deamidated gliadins underwent limited re-arrangement at the interface upon adsorption and corroborate our previous findings that its ability to provide excellent emulsion stability, particularly against coalescence and thermally induced aggregation, is attributed by its hydrodynamic size and molecular packing at the interface (~18 nm thickness).

Acknowledgement

The authors would like to thank the Manildra Group for kindly donating the protein ingredients used in this study; Dr. Nykola Jones from the Institute for Storage Ring Facilities (ISA, Aarhus University, Denmark) for her technical support during the experiments; the Institute for Storage Ring Facilities in Aarhus (ISA), Denmark, for provision of beamtime (ISA grant No. 09-1015 / 1016). We also acknowledge travel funding for Benjamin T. Wong and Jiali Zhai provided by the International Synchrotron Access Program (ISAP) managed by the Australian Synchrotron and funded by the Australian Government.

References

- (1) Dalgleish, D.G. *Adsorption of protein and the stability of emulsions. Trends Food Sci. Technol.* **1997**, *8*, 1-6.
- (2) Damodaran, S. *Protein stabilization of emulsions and foams. J. Food Sci.* **2005**, *70*, R54-R66.
- (3) Dickinson, E. *Adsorbed protein layers at fluid interfaces: Interactions, structure and surface rheology. Colloids Surf., B* **1999**, *15*, 161-176.
- (4) Wilde, P.J. *Interfaces: Their role in foam and emulsion behaviour. Curr. Opin. Colloid Interface Sci.* **2000**, *5*, 176-181.
- (5) Dalgleish, D.G. *Food emulsions - their structures and structure-forming properties. Food Hydrocolloids* **2006**, *20*, 415-422.
- (6) Dickinson, E. *Milk protein interfacial layers and the relationship to emulsion stability and rheology. Colloids Surf., B* **2001**, *20*, 197-210.
- (7) Dickinson, E. *Caseins in emulsions: Interfacial properties and interactions. Int. Dairy J.* **1999**, *9*, 305-312.
- (8) Dickinson, E.; Golding, M.; Povey, M.J.W. *Creaming and flocculation of oil-in-water emulsions containing sodium caseinate. J. Colloid Interface Sci.* **1997**, *185*, 515-529.
- (9) Dalgleish, D.G. *Conformations and structures of milk proteins adsorbed to oil-water interfaces. Food Res. Int.* **1996**, *29*, 541-547.
- (10) Tcholakova, S.; Denkov, N.D.; Ivanov, I.B.; Campbell, B. *Coalescence stability of emulsions containing globular milk proteins. Adv. Colloid Interface Sci.* **2006**, *123*, 259-293.
- (11) van Vliet, T.; Martin, A.H.; Bos, M.A. *Gelation and interfacial behaviour of vegetable proteins. Curr. Opin. Colloid Interface Sci.* **2002**, *7*, 462-468.
- (12) Day, L.; Augustin, M.A.; Batey, I.L.; Wrigley, C.W. *Wheat-gluten uses and industry needs. Trends Food Sci. Technol.* **2006**, *17*, 82-90.
- (13) Matsudomi, N.; Kato, A.; Kobayashi, K. *Conformation and surface-properties of deamidated gluten. Agri. Biol. Chem.* **1982**, *46*, 1583-1586.
- (14) Flores, I.; Cabra, V.; Quirasco, M.C.; Farres, A.; Galvez, A. *Emulsifying properties of chemically deamidated corn (zea mays) gluten meal. Food Sci. Technol. Int.* **2010**, *16*, 241-250.
- (15) Gharsallaoui, A.; Cases, E.; Chambin, O.; Saurel, R. *Interfacial and emulsifying characteristics of acid-treated pea protein. Food Biophys.* **2009**, *4*, 273-280.
- (16) Day, L.; Xu, M.; Lundin, L.; Wooster, T.J. *Interfacial properties of deamidated wheat protein in relation to its ability to stabilise oil-in-water emulsions. Food Hydrocolloids* **2009**, *23*, 2158-2167.

- (17) Howell, N.K. *Chemical and enzymatic modifications*, in *Food proteins: Properties and characterization*, Nakai S., Modler, H.W.; VCH Publishers, Inc: New York, 1996. p. 235-280.
- (18) Berecz, B.; Mills, E.N.C.; Tamas, L.; Lang, F.; Shewry, P.R.; Mackie, A.R. *Structural stability and surface activity of sunflower 2S albumins and nonspecific lipid transfer protein. J. Agric. Food Chem.* **2010**, *58*, 6490-6497.
- (19) Keerati-u-rai, M.; Corredig, M. *Heat-induced changes occurring in oil/water emulsions stabilized by soy glycinin and β -conglycinin. J. Agric. Food Chem.* **2010**, *58*, 9171-9180.
- (20) Webb, M.R.; Naeem, H.A.; Schmidt, K.A. *Food protein functionality in a liquid system: a comparison of deamidated wheat protein with dairy and soy proteins. J. Food Sci.* **2002**, *67*, 2896-2902.
- (21) Murray, B.S. *Rheological properties of protein films. Curr. Opin. Colloid Interface Sci.* **2011**, *16*, 27-35.
- (22) Ridout, M.J.; Mackie, A.R.; Wilde, P.J. *Rheology of mixed β -casein/ β -lactoglobulin films at the air-water interface. J. Agric. Food Chem.* **2004**, *52*, 3930-3937.
- (23) Kelly, S.M.; Jess, T.J.; Price, N.C. *How to study proteins by circular dichroism. Biochim. Biophys. Acta: Proteins Proteom.* **2005**, *1751*, 119-139.
- (24) Caessens, P.W.J.R.; De Jongh, H.H.J.; Norde, W.; Gruppen, H. *The adsorption-induced secondary structure of β -casein and of distinct parts of its sequence in relation to foam and emulsion properties. Biochim. Biophys. Acta* **1999**, *1430*, 73-83.
- (25) Yamamoto, T.; Fukui, N.; Hori, A.; Matsui, Y. *Circular dichroism and fluorescence spectroscopy studies of the effect of cyclodextrins on the thermal stability of chicken egg white lysozyme in aqueous solution. J. Mol. Struct.* **2006**, *782*, 60-66.
- (26) Wu, X.Y.; Narsimhan, G. *Effect of surface concentration on secondary and tertiary conformational changes of lysozyme adsorbed on silica nanoparticles. Biochim. Biophys. Acta: Proteins Proteom.* **2008**, *1784*, 1694-1701.
- (27) Wu, X.; Narsimhan, G. *Characterization of secondary and tertiary conformational changes of β -lactoglobulin adsorbed on silica nanoparticle surfaces. Langmuir* **2008**, *24*, 4989-4998.
- (28) Vermeer, A.W.P.; Norde, W. *CD spectroscopy of proteins adsorbed at flat hydrophilic quartz and hydrophobic Teflon surfaces. J. Colloid Interface Sci.* **2000**, *225*, 394-397.
- (29) Sethuraman, A.; Vedantham, G.; Imoto, T.; Przybycien, T.; Belfort, G. *Protein unfolding at interfaces: Slow dynamics of α -helix to β -sheet transition. Proteins: Struct., Funct., Bioinf.* **2004**, *56*, 669-678.
- (30) Husband, F.A.; Garrood, M.J.; Mackie, A.R.; Burnett, G.R.; Wilde, P.J. *Adsorbed protein secondary and tertiary structures by circular dichroism and infrared spectroscopy with refractive index matched emulsions. J. Agric. Food Chem.* **2001**, *49*, 859-866.

- (31) Zhai, J.; Miles, A.J.; Pattenden, L.K.; Lee, T.-H.; Augustin, M.A.; Wallace, B.A.; Aguilar, M.-I.; Wooster, T.J. *Changes in β -lactoglobulin conformation at the oil/water interface of emulsions studied by synchrotron radiation circular dichroism spectroscopy. *Biomacromolecules* **2010**, *11*, 2136-2142.*
- (32) Miles, A.J.; Wallace, B.A. *Synchrotron radiation circular dichroism spectroscopy of proteins and applications in structural and functional genomics. *Chem. Soc. Rev.* **2006**, *35*, 39-51.*
- (33) Holt, C.; Sawyer, L. *Primary and predicted secondary structures of the caseins in relation to their biological functions. *Protein Eng.* **1988**, *2*, 251-259.*
- (34) Dalgleish, D.G. *The sizes and conformations of the proteins in adsorbed layers of individual caseins on latices and in oil-in-water emulsions. *Colloids Surf., B* **1993**, *1*, 1-8.*
- (35) Kasarda, D.D.; Woodard, K.M.; Adalsteins, A.E. *Resolution of high molecular weight glutenin subunits by a new SDS-PAGE system incorporating a neutral pH buffer. *Cereal Chem.* **1998**, *75*, 70-71.*
- (36) McCann, T.H.; Small, D.M.; Batey, I.L.; Wrigley, C.W.; Day, L. *Protein-lipid interactions in gluten elucidated using acetic acid fractionation. *Food Chem.* **2009**, *115*, 105-112.*
- (37) Farrell, H.M., Jr.; Jimenez-Flores, R.; Bleck, G.T.; Brown, E.M.; Butler, J.E.; Creamer, L.K.; Hicks, C.L.; Hollar, C.M.; Ng-Kwai-Hang, K.F.; Swaisgood, H.E. *Nomenclature of the proteins of cows' milk - sixth revision. *J. Dairy Sci.* **2004**, *87*, 1641-1674.*
- (38) Miles, A.J.; Janes, R.W.; Brown, A.; Clarke, D.T.; Sutherland, J.C.; Tao, Y.; Wallace, B.A.; Hoffmann, S.V. *Light flux density threshold at which protein denaturation is induced by synchrotron radiation circular dichroism beamlines. *J. Synchrotron Radiat.* **2008**, *15*, 420-422.*
- (39) Miles, A.J.; Hoffmann, S.V.; Tao, Y.; Janes, R.W.; Wallace, B.A. *Synchrotron radiation circular dichroism (SRCD) spectroscopy: New beamlines and new applications in biology. *Spectroscopy* **2007**, *21*, 245-255.*
- (40) Miles, A.J.; Wien, F.; Wallace, B.A. *Redetermination of the extinction coefficient of camphor-10-sulfonic acid, a calibration standard for circular dichroism spectroscopy. *Anal. Biochem.* **2004**, *335*, 338-339.*
- (41) Lees, J.G.; Smith, B.R.; Wien, F.; Miles, A.J.; Wallace, B.A. *CDtool - an integrated software package for circular dichroism spectroscopic data processing, analysis, and archiving. *Anal. Biochem.* **2004**, *332*, 285-289.*
- (42) Tatham, A.S.; Shewry, P.R. *The conformation of wheat gluten proteins - the secondary structures and thermal stabilities of α -gliadins, β -gliadins, γ -gliadins and ω -gliadins. *J. Cereal Sci.* **1985**, *3*, 103-113.*
- (43) Graham, E.R.B.; Malcolm, G.N.; McKenzie, H.A. *On the isolation and conformation of bovine β -casein A¹. *Int. J. Biol. Macromol.* **1984**, *6*, 155-161.*

- (44) Whitmore, L.; Wallace, B.A. *Dichroweb, an online server for protein secondary structure analyses from circular dichroism spectroscopic data*. *Nucleic Acids Res.* **2004**, *32*, W668-W673.
- (45) Whitmore, L.; Wallace, B.A. *Protein secondary structure analyses from circular dichroism spectroscopy: methods and reference databases*. *Biopolymers* **2008**, *89*, 392-400.
- (46) Rampon, V.; Genot, C.; Riaublanc, A.; Anton, M.; Axelos, M.A.V.; McClements, D.J. *Front-face fluorescence spectroscopy study of globular proteins in emulsions: Displacement of BSA by a nonionic surfactant*. *J. Agric. Food Chem.* **2003**, *51*, 2482-2489.
- (47) Shewry, P.R.; Tatham, A.S. *Disulphide bonds in wheat gluten proteins*. *J. Cereal Sci.* **1997**, *25*, 207-227.
- (48) Shewry, P.R.; Tatham, A.S.; Forde, J.; Kreis, M.; Mifflin, B.J. *The classification and nomenclature of wheat gluten proteins - a reassessment*. *J. Cereal Sci.* **1986**, *4*, 97-106.
- (49) Tatham, A.S.; Masson, P.; Popineau, Y. *Conformational studies of peptides derived by the enzymic-hydrolysis of a γ -type gliadin*. *J. Cereal Sci.* **1990**, *11*, 1-13.
- (50) Muller, S.; Wieser, H. *The location of disulphide bonds in monomeric γ -type gliadins*. *J. Cereal Sci.* **1997**, *26*, 169-176.
- (51) Piston, F.; Dorado, G.; Martin, A.; Barro, F. *Cloning of nine γ -gliadin mRNAs (cDNAs) from wheat and the molecular characterization of comparative transcript levels of γ -gliadin subclasses*. *J. Cereal Sci.* **2006**, *43*, 120-128.
- (52) Zhai, J.; Wooster, T.J.; Hoffmann, S.V.; Lee, T.-H.; Augustin, M.A.; Aguilar, M.-I. *Structural rearrangement of β -lactoglobulin at different oil-water interfaces and its effect on emulsion stability*. *Langmuir* **2011**, *27*, 9227-9236.
- (53) Lakowicz, J.R. *Principles of fluorescence spectroscopy*, 2nd ed.; Kluwer Academic: New York, 1999.
- (54) Chobert, J.M.; Briand, L.; Gueguen, J.; Popineau, Y.; Larre, C.; Haertle, T. *Recent advances in enzymatic modifications of food proteins for improving their functional properties*. *Nahrung - Food* **1996**, *40*, 177-182.
- (55) Damodaran, S.; Song, K.B. *Kinetics of adsorption of proteins at interfaces - role of protein conformation in diffusional adsorption*. *Biochim. Biophys. Acta* **1988**, *954*, 253-264.
- (56) Norde, W.; Favier, J.P. *Structure of adsorbed and desorbed proteins*. *Colloids Surf.* **1992**, *64*, 87-93.
- (57) Kumosinski, T.F.; Brown, E.M.; Farrell, H.M., Jr. *Three-dimensional molecular modelling of bovine caseins - an energy-minimized β -casein structure*. *J. Dairy Sci.* **1993**, *76*, 931-945.
- (58) Mitchell, J.R., *Foaming and emulsifying properties of proteins*, in *Developments in Food proteins 4*, Hudson, B.J.F.; Elsevier: London, 1986. p.291-338.

- (59) Fang, Y.; Dalgleish, D.G. *The conformation of α -lactalbumin as a function of pH, heat treatment and adsorption at hydrophobic surfaces studied by FTIR. Food Hydrocolloids* **1998**, *12*, 121-126.
- (60) Fang, Y.; Dalgleish, D.G. *Conformation of β -lactoglobulin studied by FTIR: Effect of pH, temperature, and adsorption to the oil-water interface. J. Colloid Interface Sci.* **1997**, *196*, 292-298.
- (61) Green, R.J.; Hopkinson, I.; Jones, R.A.L. *Unfolding and intermolecular association in globular proteins adsorbed at interfaces. Langmuir* **1999**, *15*, 5102-5110.
- (62) Lee, S.-H.; Lefèvre, T.; Subirade, M.; Paquin, P. *Changes and roles of secondary structures of whey protein for the formation of protein membrane at soy oil/water interface under high-pressure homogenization. J. Agric. Food Chem.* **2007**, *55*, 10924-10931.
- (63) McClements, D.J. *Food emulsions: Principles, practices, and techniques*, 2nd ed.; CRC Press: Boca Raton, 2005.
- (64) Miller, R.; Ferri, J.K.; Javadi, A.; Kraegel, J.; Mucic, N.; Wuestneck, R. *Rheology of interfacial layers. Colloid Polym. Sci.* **2010**, *288*, 937-950.
- (65) Murray, B.S. *Rheological properties of protein films. Curr. Opin. Colloid Interface Sci.* **2011**, *16*, 27-35.
- (66) Lin, J.-M.; White, J.W. *Denaturation resistance of β -lactoglobulin in monomolecular films at the air-water interface. J. Phys. Chem. B* **2009**, *113*, 14513-14520.
- (67) Bowie, J.U. *Solving the membrane protein folding problem. Nature* **2005**, *438*, 581-589.
- (68) MacKenzie, K.R. *Folding and stability of α -helical integral membrane proteins. Chem. Rev.* **2006**, *106*, 1931-1977.

Table 1: The secondary structure composition (% α -helix, β -sheet, turns and unordered) of gliadins isolated from wheat gluten (not deamidated), laboratory prepared deamidated gliadins and deamidated gliadins isolated from deamidated wheat protein derived from deconvolution of the respective SRCD spectra.* The results are average of 2 separate measurement of each sample with a difference less than 0.5%.

SRCD	Degree of deamidation	α -Helix	β -Sheet	Turns	Unordered
Gliadins	0 %	35.0	16.0	14.0	35.0
Lab-prepared deamidated gliadins	29 %	22.0	22.3	15.0	40.7
Deamidated gliadins	35 %	16.3	26.0	15.7	42.0

*Analysis algorithm CDSSTR with the reference data set SP175 was used to obtain secondary structure calculation.⁴⁵ The normalised root mean square deviation (NRMSD) for all spectra obtained was below 0.03.

Table 2: The secondary structure composition (% α -helix, β -sheet, turns and unordered) of deamidated gliadins (~35% deamidation) in solution and adsorbed at tricaprln/water or hexadecane/water interface derived from deconvolution of the respective SRCD spectra.* The results are average of 2 separate measurement of each sample with a difference less than 0.5%.

Deamidated gliadins	α -Helix	β -Sheet	Turns	Unordered
In solution:	16.3	26.0	15.7	42.0
At emulsion interfaces:				
tricaprln/water, 0 h	20.0	21.5	17.0	41.5
tricaprln/water, 24 h	19.5	22.3	16.5	41.5
hexadecane/water, 0 h	23.5	18.9	16.5	41.0
hexadecane/water, 24 h	20.5	20.5	17.0	42.0

*Analysis algorithm CDSSTR with the reference data set SP175 was used to obtain secondary structure calculation.⁴⁵ The normalised root mean square deviation (NRMSD) for all spectra obtained was below 0.03.

Table 3: The secondary structure composition (% α -helix, β -sheet, turns and unordered) of β -casein in solution and adsorbed at tricaprln/water or hexadecane/water interface derived from deconvolution of the respective SRCD spectra.* The results are average of 2 separate measurement of each sample with a difference less than 0.5%.

β -casein	α -Helix	β -Sheet	Turns	Unordered
In solution:	5.5	34.5	15.0	44.5
At emulsion interfaces:				
tricaprln/water, 0 h	20.0	23.0	16.0	41.0
tricaprln/water, 24 h	20.0	22.5	16.0	41.0
hexadecane/water, 0 h	22.5	24.0	14.0	38.5
hexadecane/water, 24 h	23.0	23.0	15.0	38.5

*Analysis algorithm CDSSTR with the reference data set SP175 was used to obtain secondary structure calculation.⁴⁵ The normalised root mean square deviation (NRMSD) for all spectra obtained was below 0.03.

Figure Legends

Figure 1: Characterisation of protein fractions prepared using 70% ethanol. (A) SE-HPLC chromatograms of deamidated wheat protein (IWP), its corresponding deamidated gliadin-rich fraction and the glutenin-rich fraction; (B) SE-HPLC chromatograms of wheat gluten (VWG), its corresponding gliadin-rich fraction and the glutenin-rich fraction; (C) SDS-PAGE gel images of IWP (lane 2) and deamidated gliadin-rich fraction (lane 3); (D) SDS-PAGE gel images of VWG (lane 2) and gliadins (lane 3). Lane 1 – protein molecular weight marker.

Figure 2: Far-UV SRCD spectra of gliadins, laboratory deamidated gliadins (29 % deamidation) and deamidated gliadins (35 % deamidation) in solution at pH 8.

Figure 3: Tryptophan fluorescence emission spectra of gliadins and deamidated gliadins (~35 % deamidation) in solution at pH 8.

Figure 4: Mean particle size ($d_{3,4}$) of 20 w/w% oil-in-water emulsions stabilized by deamidated gliadins at protein concentrations ranging from 0.1 – 1.0 w/w%. Measurements were carried out immediately after emulsion preparation and after 24 h. Values are the average of three individual measurements and error bars represent the standard deviations.

Figure 5: (A) Far-UV SRCD spectra and (B) tryptophan emission spectra of deamidated gliadins (35 % deamidation) in solution at pH 8, adsorbed at tricaprins oil/water and hexadecane oil/water interfaces.

Figure 6: (A) Far-UV SRCD spectra and (B) tryptophan emission spectra of β -casein in solution, adsorbed at tricaprins oil/water and hexadecane oil/water interfaces.

Figure 7: Graphic illustrations of conformational changes in protein structure. (A) Wheat gliadins (based on sequence CAB75404 for γ -gliadin⁵¹) upon deamidation and subsequent adsorption at the oil/water interfaces. Gliadins comprise two distinctive domains, an N-terminal repetitive domain rich in β -turns structure and a C-terminal domain globular structure rich in α -helix.^{47,49} Deamidation leads to an increased charge at N-terminal domain and partial unfolding of the C-terminal globular structure resulted in a decrease of α -helix content. No further changes in secondary structure of deamidated gliadins upon adsorption at oil/water interfaces with its C-terminus anchored into the oil phase and highly charged N-terminus extending to the aqueous phase. (B) β -casein with largely random coil structure in solution undergoes structure rearrangement upon adsorption to the emulsion interface with its hydrophobic C-terminus located in the oil phase and hydrophilic N-terminus extended into the aqueous phase.³ Both proteins have similar secondary structure components at emulsion interfaces (Tables 3 and 4).

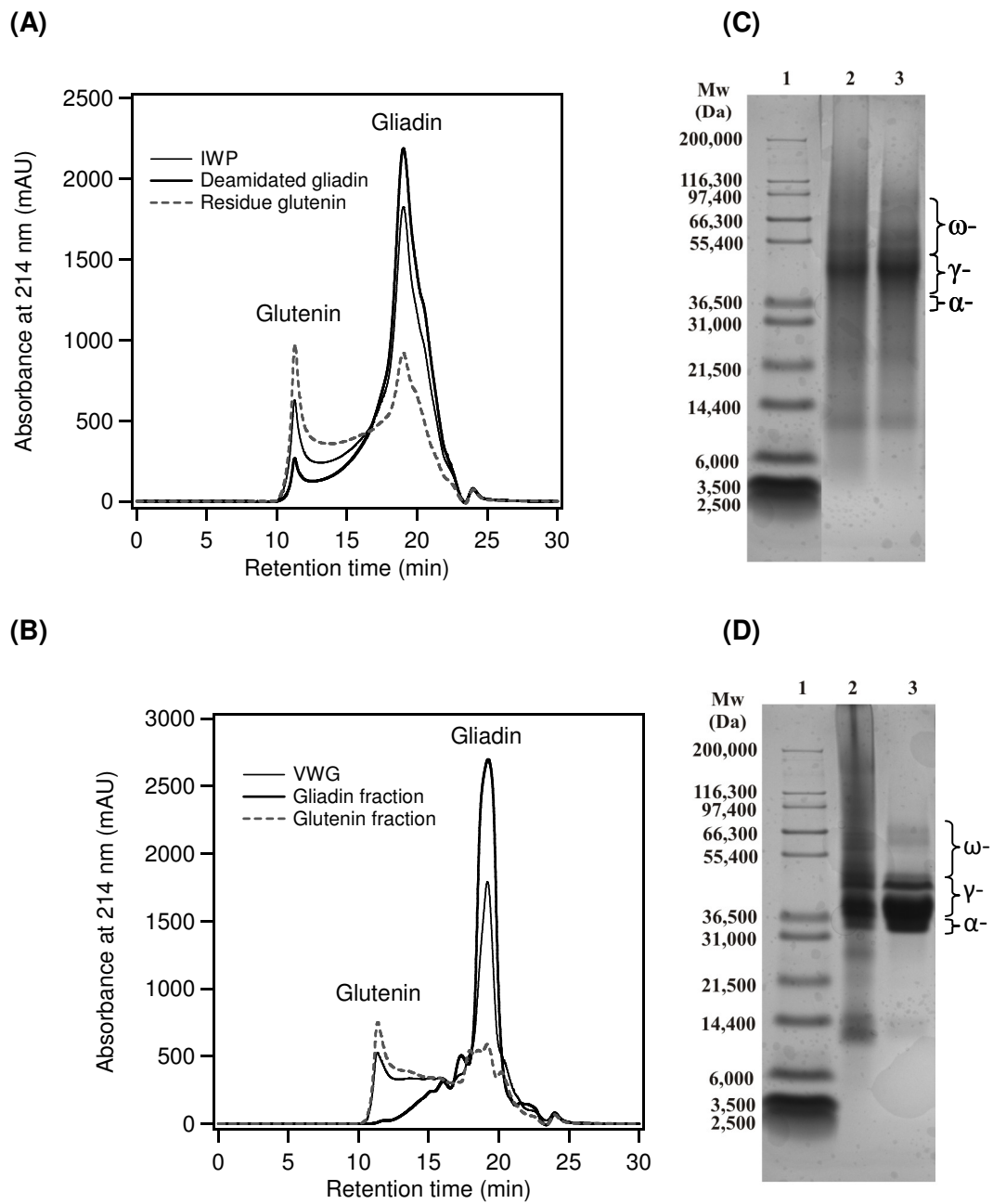


Figure 1

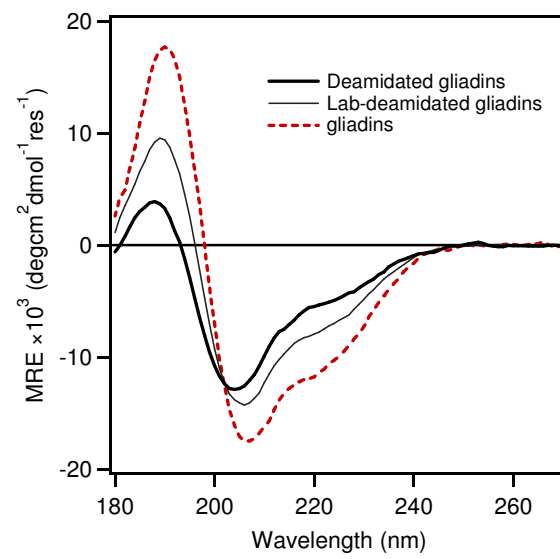


Figure 2

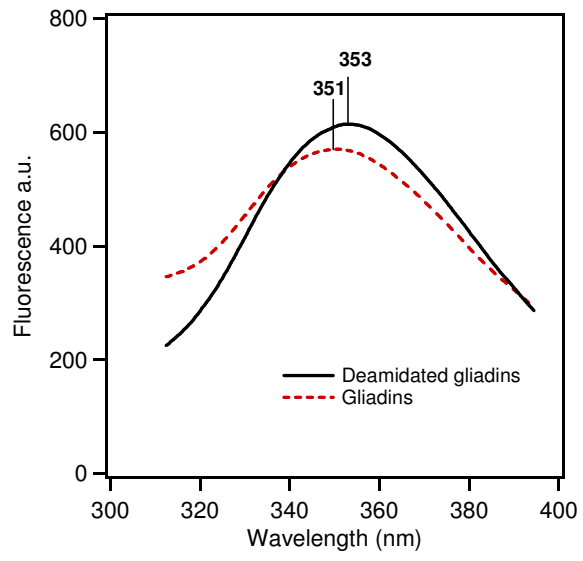


Figure 3

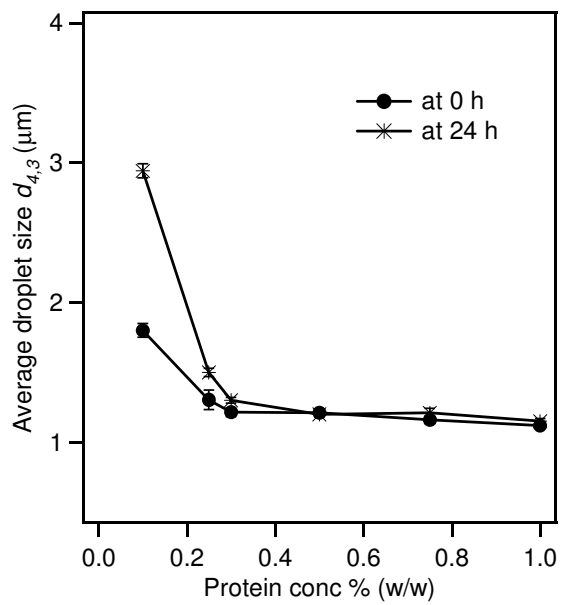


Figure 4

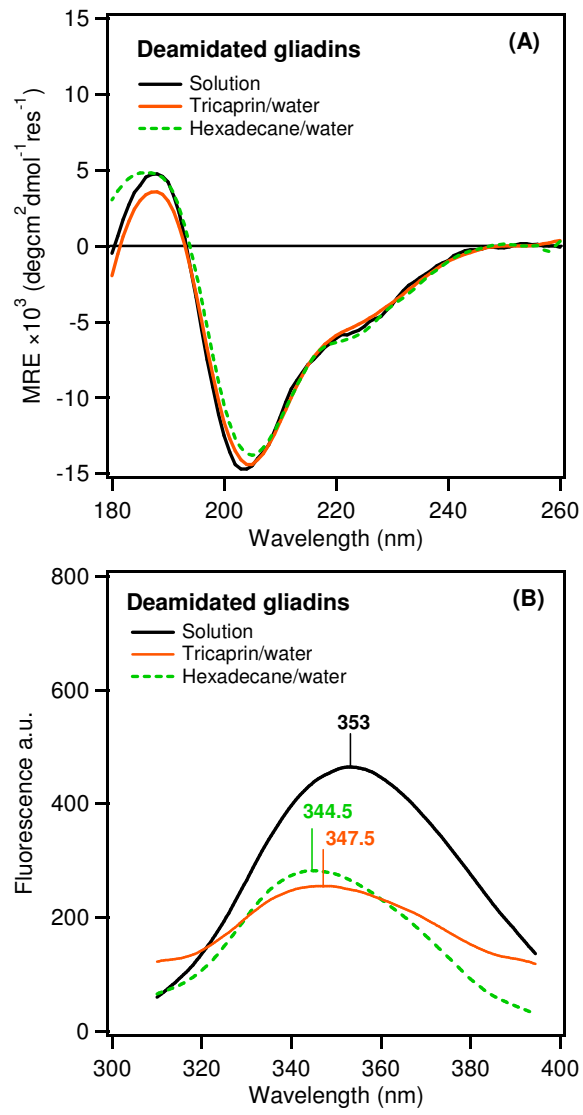


Figure 5

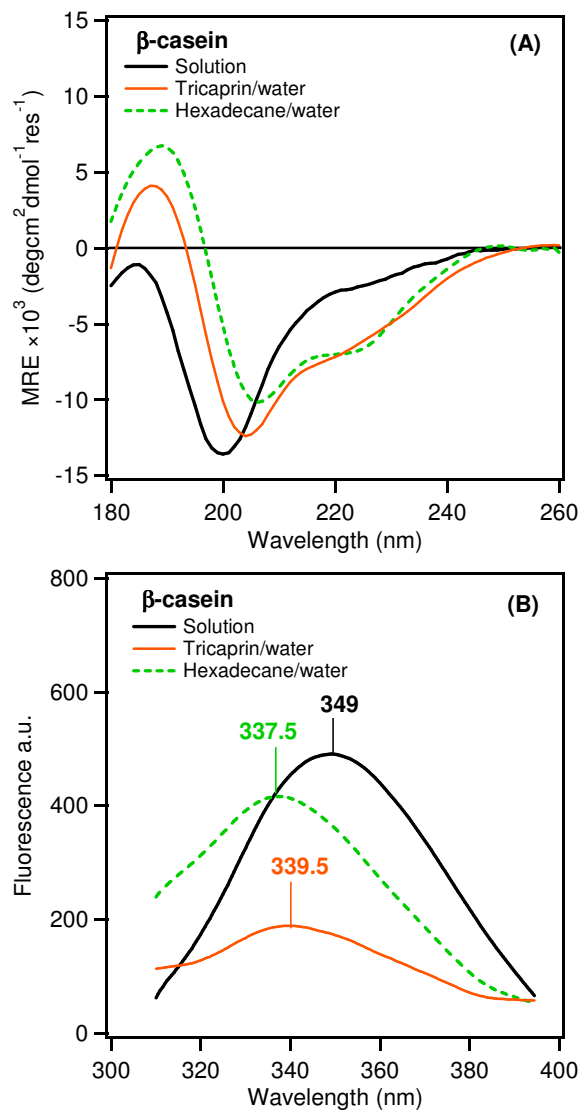


Figure 6

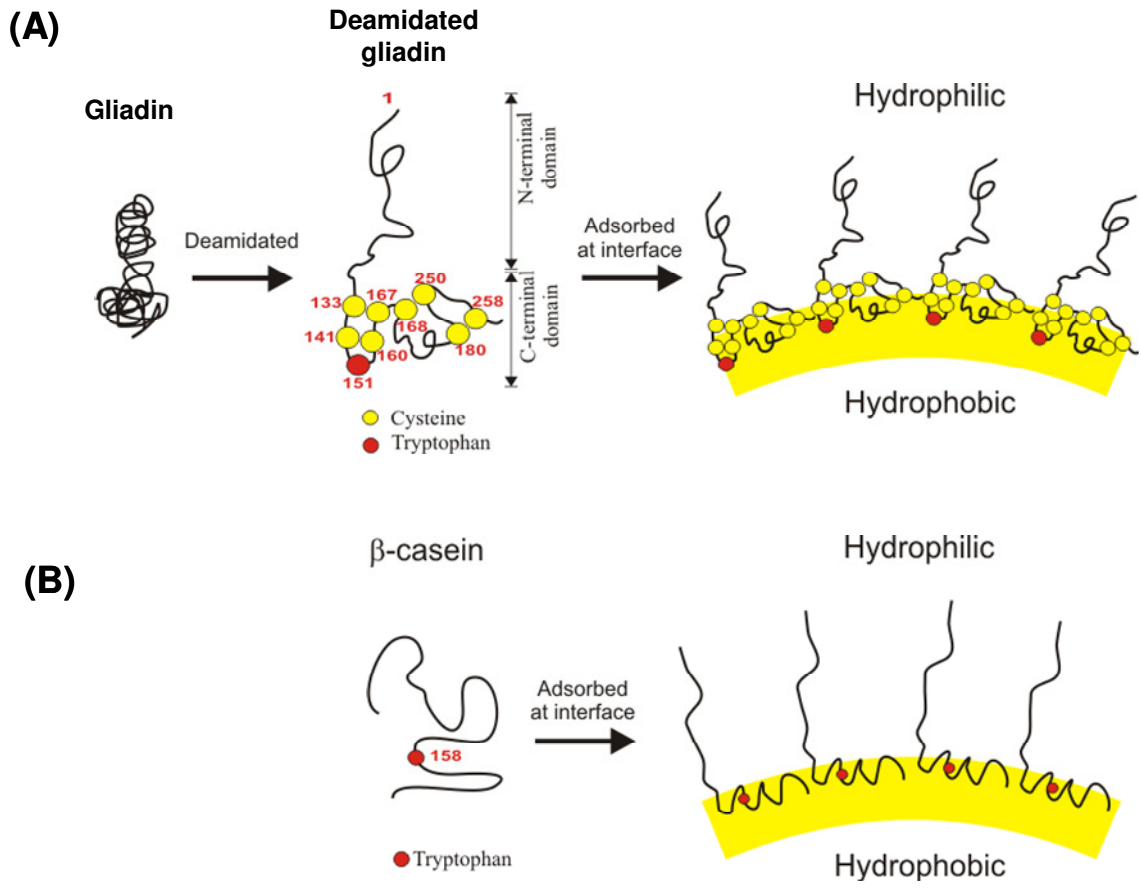
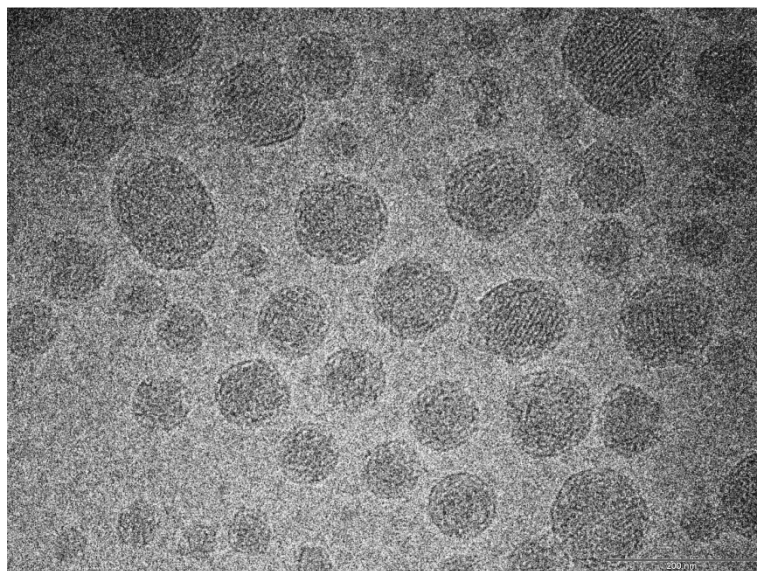


Figure 7

Chapter 6

Revisiting β -casein as a stabilizer for lipid liquid crystalline nanostructured particles



A cryo-TEM image of β -casein-stabilized GMO cubosomes

Revisiting β -casein as a stabilizer for lipid liquid crystalline nanostructured particles

Jiali Zhai^{1,2}, Lynne Waddington³, Tim J. Wooster^{2,#}, Marie-Isabel Aguilar^{1,*} and Ben J. Boyd^{4,*}

¹ Department of Biochemistry and Molecular Biology, Monash University, Clayton, VIC 3800, Australia

² CSIRO Food and Nutritional Sciences, 671 Sneydes Road, Werribee, VIC 3030, Australia

³ CSIRO Materials Science and Engineering, 343 Royal Pde, Parkville VIC 3052, Australia

⁴ Drug Delivery, Disposition and Dynamics, Monash Institute of Pharmaceutical Sciences, Monash University (Parkville Campus), 381 Royal Pde, Parkville VIC 3052, Australia

[#]Present Address: Nestlé Research Centre, CH-1000 Lausanne 26, Switzerland

*Corresponding author:

Prof. Marie-Isabel Aguilar,
Department of Biochemistry & Molecular Biology,
Monash University, Clayton, Vic 3800, Australia
mibel.aguilar@monash.edu
Ph: +61-3-9905-3723
Fx: +61-3-9902-9500

Assoc. Prof. Ben J. Boyd,
Drug Delivery, Disposition and Dynamics,
Monash Institute of Pharmaceutical Sciences,
Monash University (Parkville Campus), 381 Royal Pde, Parkville, Vic 3052, Australia
ben.boyd@monash.edu
Ph: +61-3-99039112
Fx: +61-3-99039560

Abstract

Lipid liquid crystalline nanostructured particles such as cubosomes and hexosomes have unique internal nanostructures that have shown great potential in drug and nutrient delivery applications. The triblock copolymer, Pluronic F127, is usually employed as a steric stabilizer in dispersions of lipid nanostructured particles. In this study, we investigated the formation of glyceryl monooleate (GMO) and phytantriol (PHYT) cubosome dispersions using β -casein compared to Pluronic F127 as the stabilizer. Internal structure and particle morphology were evaluated using small angle X-ray scattering (SAXS) and cryo-transmission electron microscopy (cryo-TEM), while protein secondary structure was studied using synchrotron radiation circular dichroism (SRCD). The GMO cubosome dispersion stabilized by β -casein alone displayed a cubic ($Pn3m$) phase structure and a cubic to hexagonal phase transition at 60 °C. In comparison, Pluronic F127-stabilized GMO dispersion had a cubic ($Im3m$) phase structure and the hexagonal phase only appeared at higher temperature, i.e. 70 °C. In the case of PHYT dispersions, only the cubic ($Pn3m$) phase structure was observed irrespective of the type and concentration of stabilizers. However, β -casein-stabilized PHYT dispersion displayed a cubic to hexagonal to micellar transition behaviour upon heating, whereas Pluronic F127-stabilized PHYT dispersion displayed only a direct cubic to micellar transition. The protein secondary structure was not disturbed by interaction with GMO cubosomes. The results demonstrate that β -casein provides steric stabilization to dispersions of lipid nanostructured particles and avoids the transition to $Im3m$ structure in GMO cubosomes, but also favours the formation of the micellar phase, which has implications in drug formulation and delivery applications.

Introduction

The liquid crystalline phase behaviour of polar lipids in an aqueous environment has been well studied.¹⁻⁵ Some polar lipids, such as glyceryl monooleate (GMO) and phytantriol (PHYT), self-assemble in excess water to form remarkable structures with long-range periodicity, but short-range disorder at atomic distances, termed lyotropic liquid crystalline phases. The chemical structures of GMO and PHYT and illustration of structures that they form in excess water are given in Figure 1. GMO is the most commonly studied lipid known to form liquid crystalline phases in excess water.^{4, 6-8} PHYT is a lipid that has received increasing attention because of its relative stability and purity compared to GMO. Studies have shown PHYT exhibits liquid crystalline phase behaviour very similar to that of GMO.^{9, 10} Both GMO and PHYT in excess water can form an inverse bicontinuous cubic (V_2) phase at ambient temperatures, an inverse hexagonal (H_2) phase and an inverse micellar (L_2) phase at higher temperatures (Figure 1). The V_2 phase consists of a network of two non-intersecting water channels separated by a single continuous lipid bilayer. There are three different geometries identified for the V_2 phase based on infinite periodic minimal surfaces (IPMS). They are primitive, diamond, and gyroid types with an $Im3m$, $Pn3m$, and $Ia3d$ space group respectively. The H_2 phase consists of infinite cylinders of water molecules in a continuous medium of lipid. The cylinders are arranged in a hexagonal array. The L_2 phase consists of water-in-oil micelles with the head groups sequestered in the micelle core and the hydrocarbon chains extend away.

A consequence of the thermodynamic stability of these structures in excess water is that they can be mechanically dispersed to form particles that retain the internal nanostructure of the 'parent' phase at high dilution (Figure 1). Dispersions of cubic and hexagonal phases have been termed 'cubosomes' and 'hexosomes' respectively. To make kinetically stable dispersions, a steric stabilizer is required to prevent rapid aggregation of the particles, which is driven by van der Waals and hydrophobic interactions. Larsson first described this phenomenon using β -casein as a steric stabilizer for GMO-based cubosomes.^{4, 11} However, since the discovery that the block co-polymer Pluronic F127 is a highly effective stabilizer for these dispersions,¹² it has become the stabilizer of choice for studies of cubosomes and hexosomes.^{10, 13-16} However, recent studies have indicated that Pluronic F127 is not necessarily the optimal stabilizer for cubosomes.¹⁷

Both the non-dispersed liquid crystalline phases and the dispersed cubosomes and hexosomes are of particular interest to the pharmaceutical and food industries due to their potential to protect and control the release of cargo molecules.^{5, 7, 18-26} Given the interest in application of these materials in oral drug and nutrient delivery, the development of a biocompatible stabilizer is important. The use of peptides and proteins is a logical option for natural stabilizers for such systems based on the early reports on β -casein,^{4, 11} however they do not appear to have been further

explored. β -Casein is highly amphiphilic and has a flexible, linear structure, which has made it an excellent stabilizer in other dispersion systems such as oil-in-water emulsions.²⁷⁻²⁹ Studies using synchrotron radiation circular dichroism (SRCD) spectroscopy and neutron reflectivity have shown that β -casein adsorbs to the oil-water interface of emulsions and adopts a characteristic interfacial structure to provide steric stabilization to prevent oil particle aggregation.^{30, 31} In the dispersion systems of cubosomes and hexosomes, there is little understanding of the interaction between protein and the lipid-water interface. Moreover, no X-ray diffraction data supporting internal nanostructures of cubosomes and hexosomes dispersed by β -casein have been reported. Further, Larsson's early study using freeze fracture transmission electron microscopy (TEM) indicated that the *Ia3d* gyroid cubic phase structure was present for GMO cubosomes dispersed with caseins, which would be unusual in an excess water environment for GMO systems.¹¹

Consequently, the aims of this study were to investigate the ability of β -casein to replace Pluronic F127 for the dispersion of GMO and PHYT into cubosomes and hexosomes in excess water, and to gain a deeper understanding of its interaction with the internal liquid crystalline structure, and its association with the lipid-water interface. Dispersions were prepared at varying ratios of β -casein and Pluronic F127. The particle size and morphology of the dispersed lipid systems were studied by dynamic light scattering (DLS) and cryo-TEM. Internal liquid crystalline structure was determined using small angle X-ray scattering (SAXS). The effect of increased temperature on the phase transition behaviour was examined to probe the nature of interaction of the stabilizer with the particle structure. Finally, the effect of protein interaction with lipid nanostructured particles on protein secondary structure was studied using SRCD.

Materials and Methods

Materials

Myverol 18-99K was donated by Kerry Bio-Science (Norwich, NY) and was used for glyceryl monooleate (GMO)-based samples. Myverol 18-99K contains 58.3% GMO (C18:1), 12.2% glyceryl monolinoleate (C18:2), 5.1% glyceryl monolinolenate (C18:3), 3.9% glyceryl monopalmitate (C16:0), 1.7% glyceryl monostearate (C18:0), 0.96% glyceryl monogadoleate (C20:1), 0.2% glyceryl arachidonate (C20:4), 0.1% free fatty acids and 0.4% glycerol. Trace amounts of unquantified diglycerides are also believed to be present. Phytantriol (3,7,11,15-tetramethyl-1,2,3-hexadecanetriol, PHYT) was a gift from DSM (Basel, Switzerland), with a nominal purity of >96.6%. β -Casein (BioUltra, $\geq 98\%$ PAGE), Pluronic F127 (F127) and sodium phosphate (monobasic and dibasic) were purchased from Sigma (St. Louis, MO). These chemicals were used without further purification. Milli-Q grade water (Millipore, Billerica, MA) was used for all sample preparation.

Sample preparation

Separate stock solutions of β -casein (1% w/w) and F127 (1% w/w) were prepared in 10 mM sodium phosphate buffer, pH 7. These stock solutions were then mixed at various ratios to obtain the desired ratio of β -casein : F127 (at 1 % w/w) for subsequent preparation of lipid-based dispersions. The ratio α represents the mass fraction of β -casein in the total stabilizer, hence

$$\alpha = \frac{[\text{casein}]}{[\text{casein}] + [\text{F127}]}$$

Lipid dispersions were prepared by drop-wise addition of 0.5 g of molten lipid to 5 g of the stabilizer solution (1% w/w) containing either β -casein, or F127, or mixtures of β -casein and F127. The sample was immediately ultrasonicated for 20 min using a Branson Sonifier at a power of approximately 80 W, resulting in milky dispersions.

Dynamic light scattering and cryo-TEM measurements

The particle size distribution for dispersions was measured using a Malvern Zetasizer Nano ZS (Malvern Instrument, UK). Samples were diluted with Milli-Q water and analyzed in a plastic cuvette at 25 °C. The absorbance of both lipids were set to 0.010 and used for calculations of particle size by the software.

For cryo-TEM imaging a laboratory-built humidity-controlled vitrification system was used to prepare the samples. Humidity was kept close to 80% for all experiments. 200-Mesh copper grids coated with perforated carbon film (Lacey carbon film, ProSci Tech, Australia) were used.

Grids were first glow discharged in nitrogen to render them hydrophilic. 4 μL aliquots of the sample were applied onto each grid. After 30 s adsorption time, grids were blotted manually using Whatman 541 filter paper for approximately 2 s. Grids were then plunged into liquid ethane cooled by liquid nitrogen. The samples were examined using a Gatan 626 cryo-holder (Gatan, Pleasanton, USA) and a Technai 12 Transmission Electron Microscope (FEI, Eindhoven, The Netherlands) at an operating voltage of 120 kV, with a Megaview III CCD camera and AnalySIS camera control software.

SAXS measurements

SAXS measurements were performed on an Anton Paar SAXess instrument with a Cu $K\alpha$ radiation of wavelength 1.542 Å and a line collimation system. The SAXS camera was fitted on a 1D-diode-array detector. The sample-to-detector distance was set to 306.8 mm, which provided a q -range of 0-0.6 Å⁻¹. The SAXS profile of each sample was an average of two frames and the exposure time for each frame was 1800 s. Samples (20 μL) were contained in a quartz flow cell and temperature controlled by Peltier system. Temperature was set to 20 °C for measurements except for thermal ramp experiments. The optics and sample chamber were under vacuum to minimize air scatter. The q scale was calibrated using silver behenate.

The software program SAXSquant was used to conduct baseline subtraction, integration and smoothing. The resulting SAXS profiles were a function of intensity versus the scattering vector q , which is defined by $q = (4\pi/\lambda)(\sin 2\theta)/2$, λ being the wavelength and 2θ the scattering angle. The mean lattice parameter, a , of each liquid crystalline phase was calculated from the interplanar distance, d ($d = 2\pi/q$), using the appropriate scattering law.³² For the L₂ phase, which shows only one broad peak, d is termed the characteristic distance.³³

SRCD measurements

SRCD measurements were performed on the CD1 beam line of the SRCD station at the ASTRID storage ring using methods previously described.^{30, 31, 34} A Suprasil cell (Hellma GmbH & Co., Germany) of 0.01 cm path length was used for far-UV SRCD measurements at 20 °C. The operating conditions were: 1 nm bandwidth, 2.15 s averaging time, 3 scans for solution sample or 8 scans for dispersion sample. F127-stabilized lipid dispersions were used as the baseline. Spectra of β -casein-stabilized lipid dispersions were baseline subtracted and processed using CDtool software.³⁵ The spectra are presented as mean residue ellipticity [θ], based on a mean residue weight of 114.9 for β -casein calculated from its sequence.

Results

β -Casein stabilization of GMO-based nanostructured particles

The GMO-based dispersions formed with $\alpha = 1$, where only β -casein was present, were milky high quality emulsion-like systems, with mean particle size = 262.9 ± 16.2 nm and polydispersity index = 0.282 ± 0.014 . The overall particle size distribution was larger than that with $\alpha = 0$, where only F127 was used as the stabilizer (mean particle size = 181.5 ± 0.7 nm, polydispersity index = 0.106 ± 0.019). GMO-based dispersions containing mixtures of β -casein and F127 had average particle sizes of 180-280 nm and polydispersity indices of < 0.3 (Table S1 in Supporting Information). There was, however, no clear trend in the particle size with change in ratio (α) of β -casein : F127.

Figures 2A and B show two representative cryo-TEM images of the GMO cubosome dispersion stabilized by 1% β -casein ($\alpha = 1$). It can be seen that the cubosomes possessed internal nanostructures consistent with observations for F127-stabilized cubosomes. Interestingly, there was no evidence of other types of lipid self-assembled structures such as liposomes in the field of view. In comparison, cryo-TEM examination of F127-stabilized GMO dispersions has revealed that a large amount of lipid vesicles often co-exist with cubosomes.^{13, 15, 16, 36}

SAXS patterns obtained from the GMO dispersions stabilized by varying ratios of β -casein and F127 are shown in Figure 2C. The GMO dispersion formed without β -casein ($\alpha = 0$) had peaks at q values of 0.0656 \AA^{-1} , 0.0941 \AA^{-1} and 0.115 \AA^{-1} , which correspond to peak spacing ratios $\sqrt{2}$, $\sqrt{4}$, $\sqrt{6}$. This indicated that the nanostructure was the V_2 phase with an $Im3m$ space group (primitive type of IPMS, C_p), commonly observed for F127-stabilized GMO dispersion. Increasing α towards 1 by substitution of F127 by β -casein induced a transition in structure for the GMO dispersions from the $V_2 (Im3m)$ phase to the $V_2 (Pn3m)$ phase (Figure 2C). The $V_2 (Pn3m)$ phase (double diamond type of IPMS, C_D) was identified in SAXS patterns with peaks of spacing ratios $\sqrt{2}$, $\sqrt{3}$, $\sqrt{4}$. The $V_2 (Pn3m)$ phase co-existed with the $V_2 (Im3m)$ phase from between $0.2 \leq \alpha \leq 0.4$. When the fraction of β -casein (α) was above 0.5, the $V_2 (Im3m)$ phase no longer existed. The results therefore indicate that β -casein alone provides similar stabilization to GMO cubosome dispersions as F127, but without perturbation of the $V_2 (Pn3m)$ internal nanostructure.

The corresponding lattice parameters derived from SAXS patterns are shown in Figure 2D. The $V_2 (Im3m)$ phase at $\alpha = 0$ had a lattice parameter of $134 \pm 1 \text{ \AA}$, in agreement with previous studies for GMO dispersions stabilized by F127.^{16, 37, 38} Addition of β -casein resulted in a transition to the $V_2 (Pn3m)$ phase with a smaller lattice parameter (approximately 100 \AA) also consistent with

the lattice parameter for the V_2 ($Pn3m$) structure for the bulk GMO cubic phase in the absence of F127.

β -Casein stabilization of PHYT-based nanostructured particles

The PHYT-based dispersions had average particle sizes of 280-430 nm and polydispersity indices of < 0.5 (Table S1 in Supporting Information). In contrast to the GMO dispersions, β -casein was not able to produce stable cubosome dispersions when present as the sole stabilizer, with rapid aggregation and phase separation occurring under the same preparation conditions as for the GMO dispersions. In fact only at $\alpha \leq 0.8$, where 20% the β -casein was replaced with F127, could stable dispersions be prepared. PHYT generally produces larger particles at equivalent stabilizer concentration compared to GMO dispersions.¹⁰

The overall larger particle size was reflected in the cryo-TEM imaging for PHYT particles in which larger particles were generally observed compared to the images for GMO. Figures 3A and 3B illustrate two representative cryo-TEM images for PHYT cubosome dispersions stabilized by 0.7% β -casein + 0.3% F127 ($\alpha = 0.7$). The morphology of these particles showed internal structure again characteristic of cubic phases.

SAXS patterns obtained from PHYT dispersions stabilized by F127 with an increasing fraction of β -casein up to $\alpha = 0.8$, and the corresponding lattice parameters, are shown in Figures 3C and 3D respectively. The PHYT dispersion formed by PF127 alone had peaks at q values of 0.127 \AA^{-1} , 0.156 \AA^{-1} and 0.180 \AA^{-1} , which correspond to peak spacing ratios $\sqrt{2}$, $\sqrt{3}$, $\sqrt{4}$. This pattern confirmed a V_2 ($Pn3m$) phase with a lattice parameter of $69.8 \pm 0.1 \text{ \AA}$, in agreement with previous studies.^{9, 10} Increasing the fraction of β -casein did not induce any change in the V_2 ($Pn3m$) phase structure, as indicated by the overlapping peak positions in SAXS patterns for all dispersions from $\alpha = 0$ to 0.8 (Figure 3C). The lattice parameter for the V_2 ($Pn3m$) phase was 68-70 \AA (Figure 3D).

Thermal behaviour of β -casein-stabilized liquid crystalline nanostructured particles

The V_2 to H_2 phase transition with increasing temperature in GMO and PHYT systems in excess water is very sensitive to the presence of additives that occupy the hydrophobic volume.^{6, 39} In order to better understand the role of β -casein in dispersing GMO or PHYT, the phase transition behaviour in response to heating was examined. Figure 4A shows the temperature-dependent SAXS patterns of the F127-stabilized GMO dispersion ($\alpha = 0$). The shift in peak positions to higher q values with increasing temperature up to 60 °C indicates no change in the V_2 ($Im3m$) phase structure but a decrease in lattice parameter from $134 \pm 1 \text{ \AA}$ to $105 \pm 1 \text{ \AA}$ between 20 °C and 60 °C (Figure 4B). The SAXS pattern at 70 °C also had peaks at 0.125 \AA^{-1} and 0.219 \AA^{-1} (spacing

ratios $\sqrt{1}$, $\sqrt{3}$), indicating the appearance of the H₂ phase with a lattice parameter of 58 Å, i.e. a transition from cubosomes to hexosomes. This result is consistent with previous studies on Myverol-based GMO systems dispersed by F127.³⁸

In the case of the β -casein-stabilized GMO dispersion ($\alpha = 1$), the peak positions in the SAXS patterns (Figure 4C) also shifted to higher q values with increasing temperature, indicating that the lattice parameter decreased from 100 ± 1 Å to 75 ± 1 Å between 20 °C to 70 °C (Figure 4D). Most importantly, the V₂ to H₂ transition was observed at 60 °C, i.e. 10 °C less than for the F127-stabilized dispersion.

The temperature-dependent phase transition behaviour of the PHYT-based system is shown in Figure 5. The SAXS patterns of the F127-stabilized PHYT dispersion ($\alpha = 0$) upon heating (Figure 5A) showed that from 20 °C to 50 °C, the V₂ ($Pn3m$) phase remained stable but that the lattice parameter reduced with increasing temperature as seen for the GMO systems (Figure 5B). At 60 °C and above, there was a dramatic change in the SAXS pattern, and only one broad peak was observed (Figure 5A). This pattern is characteristic of the inverse micellar L₂ structure with a characteristic distance of approximately 40 Å. This result shows a direct phase transition of the F127-stabilized PHYT dispersion from the V₂ ($Pn3m$) phase to the L₂ phase upon heating to 60 °C without showing the H₂ phase, in agreement with previous studies.³⁸ (It should be noted, however, that with temperature steps of 10 °C it is possible that the H₂ phase existed over a narrow range of temperature between 50-60 °C but was not detected in this study). Interestingly, when β -casein was used as the major stabilizer ($\alpha = 0.8$), the PHYT dispersion displayed a transition to the H₂ phase at 60 °C and then to the L₂ phase at 70 °C (Figure 5C and 5D). The results shown so far clearly indicate that β -casein interacts in a different manner with cubosomes compared to F127, influencing the phase structure and temperature-dependent phase transition behaviour.

Secondary conformation of β -casein in lipid-water systems

Given that β -casein alone ($\alpha = 1$) was effective for stabilization of GMO-based cubosomes, it was likely that β -casein was adsorbed at the lipid-water interface and evidently associated with the cubosomes. It was therefore of interest to determine whether the association could influence the secondary structure of β -casein. SRCD was therefore used to examine the influence of association of the β -casein with GMO cubosomes on protein secondary structure.

The SRCD spectrum for GMO cubosomes stabilized by β -casein ($\alpha = 1$), together with a comparative spectrum for native β -casein are given in Figure 6. Additionally the figure also shows the spectrum for a hexadecane-in-water emulsion stabilized by β -casein for which secondary structure was known to be compromised, thereby serving as a negative control. The far-UV SRCD spectrum of β -casein in 10 mM sodium phosphate buffer had a minimum peak at 200 nm and no

zero-crossing, indicating a large amount of unordered structure. Our previous study revealed the secondary structure of β -casein in buffer consisted of 11% α -helix, 25% β -sheet, 16% turn and 47% unordered structure (data submitted for publication). The previous study also investigated the β -casein secondary structure in an oil-water environment, i.e. the hexadecane-in-water emulsion made by high-pressure homogenization. It was found that β -casein located at the hexadecane-water interface adopted a very different conformation containing non-native α -helix as shown in Figure 6. In the present study where β -casein was incorporated into GMO cubosomes, there was no significant change in the far-UV SRCD spectrum compared to that in buffer, indicating that the adsorption to the lipid-water interface did not induce any change to the ordered secondary structure in β -casein.

Discussion

The complex nanostructures of lipid liquid crystalline particles, such as cubosomes and hexosomes, have received increasing interest in drug and nutrient delivery applications. One of the important issues in formulation of cubosome and hexosome dispersions is colloidal stability. Researchers have primarily used Pluronic F127, a commercially available triblock copolymer, to impart steric stabilization to these particles. However, the need for alternative stabilizers has emerged¹⁷ in the field of oral drug and nutrient delivery. The goal of the current study was to more rigorously investigate proteins, in particular β -casein, as a non-synthetic biocompatible stabilizer. β -Casein is one of the major variants of milk caseins, with 209 amino acid residues and a molecular weight of 24 kDa.⁴⁰ β -Casein has a flexible, polymer-like structure with a large amount of unordered conformation. A characteristic feature of β -casein is that it can be generally divided into a hydrophilic region (0-40 residues at the N-terminus) with many charged residues and a hydrophobic region for the remainder of the chain at the C-terminus. As a result, β -casein is highly amphiphilic and surface-active. β -Casein is known to interact with oil-water interfaces and act as an excellent stabilizer in oil-in-water emulsions.²⁷⁻²⁹

In this study, we explored the potential of using β -casein to disperse two lipids, GMO and PHYT, into cubosome dispersions, subsequently characterized using SAXS and cryo-TEM measurements. It was found that β -casein alone could provide sufficient stabilization to disperse GMO in excess water, whereas for the PHYT-based system, β -casein alone could not disperse the lipid, with lumps of aggregated lipid evident in the sample. A minimum concentration of 0.2% F127, together with 0.8% β -casein ($\alpha = 0.8$), was required to disperse PHYT into cubosomes. This result indicates that β -casein is less effective than F127 in terms of providing steric repulsion between the dispersed cubosomes, at least on a w/w basis. The preservation of the $Pn3m$ space group for the cubic phase at higher β -casein fractions for GMO cubosomes also indicates reduced interaction with the lipid than when F127 is used as the stabilizer. The SRCD measurement showed no change in the secondary conformation of β -casein by incorporation into GMO cubosomes (Figure 6), confirming the relatively weak interaction. Together the results indicate an overall reduction in β -casein association with cubosomes compared to F127, irrespective of which lipid was being dispersed.

This result might be rationalized in terms of differences in the steric barrier provided by β -casein and F127. Neutron reflectivity studies have demonstrated that the hydrophobic region of β -casein is anchored at air-water or oil-water interfaces. The thickness of the steric layer from the hydrophilic region of β -casein was reported to be approximately 5 nm and a surface excess concentration of approximately 2 mg/m².^{41, 42} By way of contrast, F127 has been reported to present an approximate layer of thickness of 9 nm and a surface excess concentration of approximately 3

mg/m² at the air-water interface.⁴³ Hence, although the surface coverage is expected to be similar in mass terms, the higher molecular weight of β -casein means that there are likely to be fewer molecules per unit surface area providing a lower surface coverage and a thinner steric barrier, which would understandably provide less effective colloidal stabilization. Further studies using neutron scattering techniques for this system are expected to provide a deeper understanding of the relative disposition of the stabilizers at the lipid-excess water interface.

We also studied the ability of 1% β -lactoglobulin (β -Lg) to disperse GMO or PHYT cubosomes. For both lipids we discovered that F127 was required to be present for effective dispersion (Figure S1 in Supporting Information). This is understood to be a consequence of its compact globular structure and low surface hydrophobicity at neutral conditions,⁴⁴ slowing adsorption and rendering β -Lg even less effective as a steric stabilizer than β -casein .

The ‘threshold’ fraction for transition from the *Im3m* to *Pn3m* phase of the GMO dispersion occurred with addition of only 0.2% β -casein ($\alpha = 0.2$); meaning that there was an effective F127 concentration of 0.8% (Figure 2D). A previous study has reported that this F127 concentration (0.8%) is well within the concentration range where the *Im3m* phase is expected in the GMO + F127 + excess water system.¹⁶ This means that the transition from the *Im3m* to *Pn3m* phase is not merely a consequence of changing the GMO : F127 ratio, but that the transition is a consequence of the presence of β -casein. The reason is unclear at this time – there is no discernable systematic change in lattice parameters within the same phase structure with changes in stabilizer composition (Figure 2D). These systems do however seem to favour formation of the *Pn3m* phase over the *Im3m* phase, evident from the fact that dispersions of GMO and PHYT in differing ratios of the two lipids require more than 80% (w/w) GMO before a transition from the *Pn3m* phase to the *Im3m* phase is observed.⁴⁵

The favoured formation of the *Pn3m* phase with β -casein as the sole stabilizer for GMO dispersions is at odds with the previous report on this particular system,¹¹ which inferred the gyroid (*Ia3d*) cubic phase structure from freeze-fracture TEM images. The nodular surface is however reminiscent of the texture observed in more recent cryo-field emission scanning electron microscopy (cryo-FESEM) images of the bulk *Pn3m* phase prepared using PHYT in excess water and the corresponding dispersed cubosomes.⁴⁶

The temperature-dependent phase transitions for both GMO and PHYT-based systems provide some further insight into the interaction between stabilizer and internal nanostructure. Generally speaking, lipid chains are usually disordered at elevated temperatures occupying a greater volume, and hence increasing temperature may induce a V₂ to H₂ phase transition.^{47, 48} Using β -casein to stabilize the GMO-based dispersion suppressed the V₂ to H₂ transition by up to

10 °C greater than in the F127-stabilized dispersion (Figure 4). In the case of the PHYT-based system, the β -casein-stabilized dispersion displayed a V_2 to H_2 (60 °C) to L_2 (70 °C) transition whereas the F127-stabilized dispersion displayed a direct V_2 to L_2 transition at 70 °C (Figure 5). The result indicates that the H_2 phase is more favoured in dispersions containing β -casein (or that it at least forms at a lower temperature).

Examination of the structure of the H_2 phase reveals that there is a packing stress arising from the fact that the circular cross-section of the cylindrical interface requires the ‘void’ hydrophobic region be filled to a uniform density with the hydrophobic chains.^{49, 50} The ‘void’ region is energetically unfavourable if the lipid chains are not sufficiently long to reach and occupy the intersection space. Previous studies have shown that the presence of surface active compounds with increased lipid chain volume or hydrophobic compounds may also promote the formation of the H_2 phase at lower temperature by occupying the ‘void’ in the space between hexagonally packed cylinders.^{10, 33, 39} The F127-stabilized GMO system forms the H_2 phase (Figure 4A) because Myverol 18-99K used in this study contains many other amphiphilic compounds in addition to GMO. The impurities allow the formation of the H_2 phase at 70 °C. In contrast, the commercially available PHYT is relatively pure and the F127-stabilized PHYT dispersion did not form the H_2 phase here or in previous reports.¹⁰ The reason for the more favourable formation of the H_2 phase by the β -casein-stabilized dispersions compared to the F127 stabilized dispersions is not clear, however it is apparent that based on the above model of ‘void’ filling stabilizing the H_2 structure that β -casein likely acts more effectively as a space filling agent in the H_2 phase.

The comparison between β -casein- and F127-stabilized lipid liquid crystalline nanostructured particles has revealed that β -casein may have application in substituting for F127 as a functional stabilizer for these systems in the active delivery field. For example, the H_2 phase has shown advantage over the V_2 phase in prolonged release of model drug molecules due to its smaller water channels.^{21, 22, 51} With the presence of β -casein, the lipid dispersed system displays a suppressed temperature required for the V_2 to H_2 transition, which becomes more relevant under physiological conditions. Future studies will investigate the stability of the β -casein-based lipid liquid crystalline nanostructured particles during digestion, the incorporation of model drug molecules into such systems and the controlled release rate *in vitro* and *in vivo*. The studies also highlight a need to better understand the protein-lipid nano-scale interactions to optimize selection of protein-based stabilizers for functionalization of these systems in targeted delivery applications.

Conclusion

This study reported the first SAXS and cryo-TEM studies on β -casein-stabilized cubosomes of GMO and PHYT in excess water. It was found that β -casein could provide effective steric stabilization to disperse GMO into cubosomes with a V_2 ($Pn3m$) internal nanostructure. The β -casein-stabilized GMO dispersion had a lower V_2 to H_2 transition temperature than the equivalent F127-stabilized dispersion. In the case of PHYT cubosomes, β -casein could act as a stabilizer but required the presence of F127 in relatively low proportions to bolster its stabilizing effect. In both cases β -casein filled 'void' space in the H_2 structure, promoting the formation of the H_2 phase in comparison to F127-stabilized dispersions where the H_2 phase was either absent or occurred at elevated temperatures.

Acknowledgement

The authors would like to sincerely thank Professor Matthew Wilce and Dr. Leanne Dyksterhuis for their advice and assistance on the SAXS instrument, Dr. Søren V. Hoffmann for his assistance on the SRCD beam line, the Australia Synchrotron for synchrotron travel funding (Reference No. AS/IA112/3989) and the Australian Research Council and Dairy Innovation Australia Limited (through ARC Linkage Grant No. LP0774909).

Supporting Information Available

The mean particle size of the GMO and PHYT-based dispersions are given in Table S1. The SAXS data of GMO and PHYT-based dispersions stabilized by β -lactoglobulin/F127 mixtures are given in Figure S1.

References

- (1) Hyde, S.; Andersso, S.; Larsson, K.; Blum, Z.; Landh, T.; Lidin, S.; Ninham, B.W. *The language of shape: The role of curvature in condensed matter: Physics, chemistry and biology*; Elsevier B.V.: New York, 1997. p.199-235.
- (2) Johnsson, M.; Barauskas, J.; Tiberg, F. *Cubic phases and cubic phase dispersions in a phospholipid-based system. J. Am. Chem. Soc.* **2005**, *127*, 1076-1077.
- (3) Larsson, K. *Periodic minimal surface structures of cubic phases formed by lipids and surfactants. J. Colloid Interface Sci.* **1986**, *113*, 299-300.
- (4) Larsson, K. *Cubic lipid-water phases: Structures and biomembrane aspects. J. Phys. Chem.* **1989**, *93*, 7304-7314.
- (5) Sagalowicz, L.; Leser, M.E.; Watzke, H.J.; Michel, M. *Monoglyceride self-assembly structures as delivery vehicles. Trends Food Sci. Technol.* **2006**, *17*, 204-214.
- (6) Clogston, J.; Rathman, J.; Tomasko, D.; Walker, H.; Caffrey, M. *Phase behavior of a monoacylglycerol: (Myverol 18-99K)/water system. Chem. Phys. Lipids* **2000**, *107*, 191-220.
- (7) de Campo, L.; Yaghmur, A.; Sagalowicz, L.; Leser, M.E.; Watzke, H.; Glatter, O. *Reversible phase transitions in emulsified nanostructured lipid systems. Langmuir* **2004**, *20*, 5254-5261.
- (8) Qiu, H.; Caffrey, M. *The phase diagram of the monoolein/water system: Metastability and equilibrium aspects. Biomaterials* **2000**, *21*, 223-234.
- (9) Barauskas, J.; Landh, T. *Phase behavior of the phytantriol/water system. Langmuir* **2003**, *19*, 9562-9565.
- (10) Dong, Y.-D.; Larson, I.; Hanley, T.; Boyd, B.J. *Bulk and dispersed aqueous phase behavior of phytantriol: Effect of vitamin E acetate and F127 polymer on liquid crystal nanostructure. Langmuir* **2006**, *22*, 9512-9518.
- (11) Buchheim, W.; Larsson, K. *Cubic lipid-protein-water phases. J. Colloid Interface Sci.* **1987**, *117*, 582-583.
- (12) Landh, T. *Phase behavior in the system pine needle oil monoglycerides-poloxamer 407-water at 20 °C. J. Phys. Chem.* **1994**, *98*, 8453-8467.
- (13) Abraham, T.; Hato, M.; Hirai, M. *Polymer-dispersed bicontinuous cubic glycolipid nanoparticles. Biotechnol. Prog.* **2005**, *21*, 255-262.
- (14) Almgren, M.; Borne, J.; Feitosa, E.; Khan, A.; Lindman, B. *Dispersed lipid liquid crystalline phases stabilized by a hydrophobically modified cellulose. Langmuir* **2007**, *23*, 2768-2777.
- (15) Gustafsson, J.; Ljusberg-Wahren, H.; Almgren, M.; Larsson, K. *Cubic lipid-water phase dispersed into submicron particles. Langmuir* **1996**, *12*, 4611-4613.
- (16) Gustafsson, J.; Ljusberg-Wahren, H.; Almgren, M.; Larsson, K. *Submicron particles of reversed lipid phases in water stabilized by a nonionic amphiphilic polymer. Langmuir* **1997**, *13*, 6964-6971.

- (17) Chong, J.Y.T.; Mulet, X.; Waddington, L.J.; Boyd, B.J.; Drummond, C.J. *Steric stabilisation of self-assembled cubic lyotropic liquid crystalline nanoparticles: High throughput evaluation of triblock polyethylene oxide-polypropylene oxide-polyethylene oxide copolymers. Soft Matter* **2011**, *7*, 4768-4777.
- (18) Amar-Zrihen, N.; Aserin, A.; Garti, N. *Food volatile compounds facilitating H_{ii} mesophase formation: Solubilization and stability. J. Agric. Food Chem.* **2011**, *59*, 5554-5564.
- (19) Augustin, M.A.; Hemar, Y. *Nano- and micro-structured assemblies for encapsulation of food ingredients. Chem. Soc. Rev.* **2009**, *38*, 902-912.
- (20) Cohen-Avrahami, M.; Libster, D.; Aserin, A.; Garti, N. *Sodium diclofenac and cell-penetrating peptides embedded in H_{ii} mesophases: Physical characterization and delivery. J. Phys. Chem. B* **2011**, in press.
- (21) Fong, W.-K.; Hanley, T.; Boyd, B.J. *Stimuli responsive liquid crystals provide 'on-demand' drug delivery in vitro and in vivo. J. Controlled Release* **2009**, *135*, 218-226.
- (22) Libster, D.; Aserin, A.; Garti, N. *Interactions of biomacromolecules with reverse hexagonal liquid crystals: Drug delivery and crystallization applications. J. Colloid Interface Sci.* **2011**, *356*, 375-386.
- (23) Nguyen, T.-H.; Hanley, T.; Porter, C.J.H.; Larson, I.; Boyd, B.J. *Phytantriol and glyceryl monooleate cubic liquid crystalline phases as sustained-release oral drug delivery systems for poorly water soluble drugs I. Phase behaviour in physiologically-relevant media. J. Pharm. Pharmacol.* **2010**, *62*, 844-855.
- (24) Rizwan, S.B.; Boyd, B.J.; Rades, T.; Hook, S. *Bicontinuous cubic liquid crystals as sustained delivery systems for peptides and proteins. Exp. Opin. Drug Delivery* **2010**, *7*, 1133-1144.
- (25) Solaro, R.; Chiellini, F.; Battisti, A. *Targeted delivery of protein drugs by nanocarriers. Materials* **2010**, *3*, 1928-1980.
- (26) Zhang, L.; Pornpattananangku, D.; Hu, C.M.; Huang, C.M. *Development of nanoparticles for antimicrobial drug delivery. Curr. Med. Chem.* **2010**, *17*, 585-594.
- (27) Dalglish, D.G. *Food emulsions stabilized by proteins. Curr. Opin. Colloid Interface Sci.* **1997**, *2*, 573-577.
- (28) Dickinson, E. *Caseins in emulsions: Interfacial properties and interactions. Int. Dairy J.* **1999**, *9*, 305-312.
- (29) McClements, D.J. *Protein-stabilized emulsions. Curr. Opin. Colloid Interface Sci.* **2004**, *9*, 305-313.
- (30) Zhai, J.; Miles, A.J.; Pattenden, L.K.; Lee, T.-H.; Augustin, M.A.; Wallace, B.A.; Aguilar, M.-I.; Wooster, T.J. *Changes in β -lactoglobulin conformation at the oil/water interface of emulsions studied by synchrotron radiation circular dichroism spectroscopy. Biomacromolecules* **2010**, *11*, 2136-2142.

- (31) Zhai, J.; Wooster, T.J.; Hoffmann, S.V.; Lee, T.-H.; Augustin, M.A.; Aguilar, M.-I. *Structural rearrangement of β -lactoglobulin at different oil–water interfaces and its effect on emulsion stability*. *Langmuir* **2011**, *27*, 9227-9236.
- (32) Hyde, S. *Identification of lyotropic liquid crystalline mesophases*, in *Handbook of applied surface and colloid chemistry*, Holmberg, K.; John Wiley & Sons: Chichester, 2002. p.299-320.
- (33) Yaghmur, A.; de Campo, L.; Sagalowicz, L.; Leser, M.E.; Glatter, O. *Emulsified microemulsions and oil-containing liquid crystalline phases*. *Langmuir* **2004**, *21*, 569-577.
- (34) Eden, S.; Lima-Vieira, P.; Hoffmann, S.V.; Mason, N.J. *VUV photoabsorption in CF₃X (Xl, Br, I) fluoro-alkanes*. *Chem. Phys.* **2006**, *323*, 313-333.
- (35) Lees, J.G.; Smith, B.R.; Wien, F.; Miles, A.J.; Wallace, B.A. *CDtool - an integrated software package for circular dichroism spectroscopic data processing, analysis, and archiving*. *Anal. Biochem.* **2004**, *332*, 285-289.
- (36) Spicer, P.T.; Hayden, K.L.; Lynch, M.L.; Ofori-Boateng, A.; Burns, J.L. *Novel process for producing cubic liquid crystalline nanoparticles (cubosomes)*. *Langmuir* **2001**, *17*, 5748-5756.
- (37) Barauskas, J.; Johnsson, M.; Joabsson, F.; Tiberg, F. *Cubic phase nanoparticles (cubosome): Principles for controlling size, structure, and stability*. *Langmuir* **2005**, *21*, 2569-2577.
- (38) Dong, Y.-D.; Tilley, A.J.; Larson, I.; Lawrence, M.J.; Amenitsch, H.; Rappolt, M.; Hanley, T.; Boyd, B.J. *Nonequilibrium effects in self-assembled mesophase materials: Unexpected supercooling effects for cubosomes and hexosomes*. *Langmuir* **2010**, *26*, 9000-9010.
- (39) Dong, Y.-D.; Dong, A.W.; Larson, I.; Rappolt, M.; Amenitsch, H.; Hanley, T.; Boyd, B.J. *Impurities in commercial phytantriol significantly alter its lyotropic liquid-crystalline phase behavior*. *Langmuir* **2008**, *24*, 6998-7003.
- (40) Fox, P.F.; McSweeney, P.L.H. *Advanced dairy chemistry Volume I Proteins*, 3rd ed.; Kluwer Academic/Plenum: New York, 2003.
- (41) Atkinson, P.J.; Dickinson, E.; Horne, D.S.; Richardson, R.M. *Neutron reflectivity of adsorbed β -casein and β -lactoglobulin at the air/water interface*. *J. Chem. Soc., Faraday Trans.* **1995**, *91*, 2847-2854.
- (42) Dickinson, E.; Horne, D.S.; Phipps, J.S.; Richardson, R.M. *A neutron reflectivity study of the adsorption of β -casein at fluid interfaces*. *Langmuir* **1993**, *9*, 242-248.
- (43) Elisseeva, O.V.; Besseling, N.A.M.; Koopal, L.K.; Cohen Stuart, M.A. *Influence of NaCl on the behavior of PEO-PPO-PEO triblock copolymers in solution, at interfaces, and in asymmetric liquid films*. *Langmuir* **2005**, *21*, 4954-4963.

- (44) Ferry, J.D.; Oncley, J.L. *Studies of the dielectric properties of protein solutions. III. Lactoglobulin.* *J. Am. Chem. Soc.* **1941**, *63*, 272-278.
- (45) Tilley, A.; Dong, Y.-D.; Amenitsch, H.; Rappolt, M.; Boyd, B.J. *Transfer of lipid and phase reorganisation in self-assembled liquid crystal nanostructured particles based on phytantriol.* *Phys. Chem. Chem. Phys.* **2011**, *13*, 3026-3032.
- (46) Boyd, B.J.; Rizwan, S.B.; Dong, Y.-D.; Hook, S.; Rades, T. *Self-assembled geometric liquid-crystalline nanoparticles imaged in three dimensions: Hexosomes are not necessarily flat hexagonal prisms.* *Langmuir* **2007**, *23*, 12461-12464.
- (47) Gruner, S.M.; Tate, M.W.; Kirk, G.L.; So, P.T.C.; Turner, D.C.; Keane, D.T.; Tilcock, C.P.S.; Cullis, P.R. *X-ray diffraction study of the polymorphic behavior of n-methylated dioleoylphosphatidylethanolamine.* *Biochemistry* **1988**, *27*, 2853-2866.
- (48) Templer, R.H.; Seddon, J.M.; Duesing, P.M.; Winter, R.; Erbes, J. *Modeling the phase behavior of the inverse hexagonal and inverse bicontinuous cubic phases in 2:1 fatty acid/phosphatidylcholine mixtures.* *J. Phys. Chem. B* **1998**, *102*, 7262-7271.
- (49) Israelachvili, J.N.; Mitchell, D.J.; Ninham, B.W. *Theory of self-assembly of hydrocarbon amphiphiles into micelles and bilayers.* *J. Chem. Soc., Faraday Trans. 2* **1976**, *72*, 1525-1568.
- (50) Rappolt, M. *The biologically relevant lipid mesophases as "seen" by X-rays*, in *Advances in planar lipid bilayers and liposomes Volume 5*, Liu, A. L.; Academic Press: Amsterdam, 2007. p.253-283.
- (51) Boyd, B.J.; Whittaker, D.V.; Khoo, S.-M.; Davey, G. *Lyotropic liquid crystalline phases formed from glycerate surfactants as sustained release drug delivery systems.* *Int. J. Pharm.* **2006**, *309*, 218-226.

Figure Legends

Figure 1: Chemical structures of GMO and PHYT and the nanostructures formed by the lipids in excess water. Dispersions of lipid particles with the internal nanostructures of bulk phases can be achieved with the aid of steric stabilizers.

Figure 2: (A) and (B) Representative cryo-TEM images of GMO-based cubosomes stabilized by 1% β -casein ($\alpha = 1$). The scale bar represents 200 nm. (C) SAXS patterns from GMO-based dispersions stabilized by various ratios of β -casein : F127. Total stabilizer concentration in all cases was 1% (w/w). (D) Phase identity and lattice parameter of GMO-based dispersions derived from SAXS data in (C) as a function of the fraction of β -casein to total stabilizer (α).

Figure 3: (A) and (B) Representative cryo-TEM images of PHYT-based cubosomes stabilized by a 70% β -casein + 30% F127 mixture ($\alpha = 0.7$). The scale bar represents 200 nm. (C) SAXS patterns from PHYT-based dispersions stabilized by various ratios of β -casein : F127. Total stabilizer concentration in all cases was 1% (w/w). (D) Phase identity and lattice parameter of PHYT-based dispersions derived from SAXS data in (C) as a function of the fraction of β -casein to total stabilizer (α).

Figure 4: (A) and (C) Temperature-dependent SAXS patterns of GMO-based dispersions stabilized by F127 ($\alpha = 0$) and β -casein ($\alpha = 1$) respectively. Total stabilizer concentration in all cases was 1% (w/w). (B) and (D) The corresponding temperature-dependence of phase identity and lattice parameter of GMO-based dispersions stabilized by F127 ($\alpha = 0$) and β -casein ($\alpha = 1$) respectively.

Figure 5: (A) and (C) Temperature-dependent SAXS patterns of PHYT-based dispersions stabilized by F127 ($\alpha = 0$) and an 80% β -casein + 20% F127 mixture ($\alpha = 0.8$), respectively. (B) and (D) The corresponding temperature-dependence of phase identity and lattice parameter of PHYT-based dispersions stabilized by F127 ($\alpha = 0$) and an 80% β -casein + 20% F127 mixture ($\alpha = 0.8$) respectively.

Figure 6: Far-UV SRCD spectra of β -casein under various conditions: in aqueous solution (solid line); in β -casein-stabilized GMO cubosomes ($\alpha = 1$) (dotted line); in β -casein-stabilized hexadecane-in-water emulsions (dashed line).

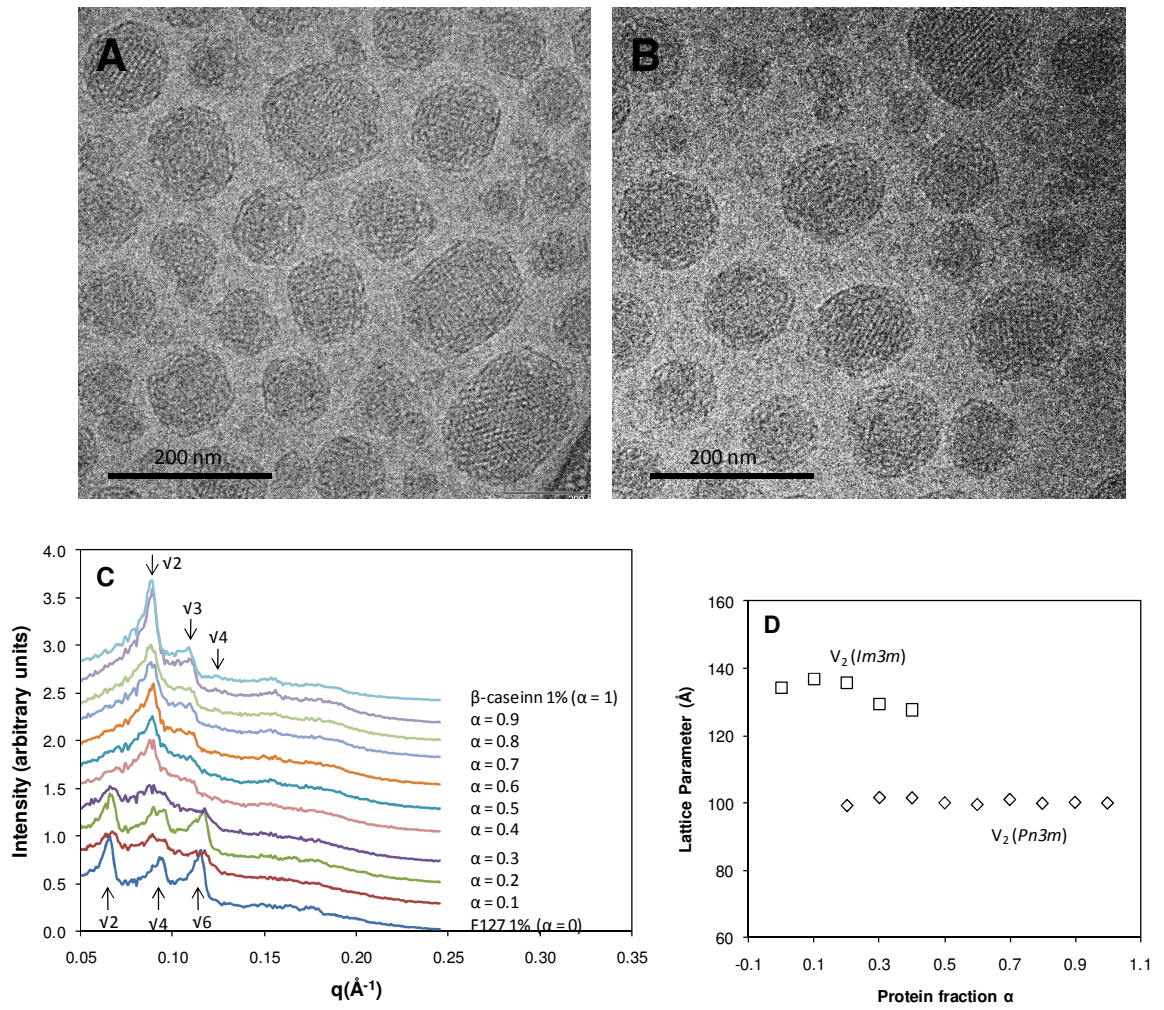


Figure 2

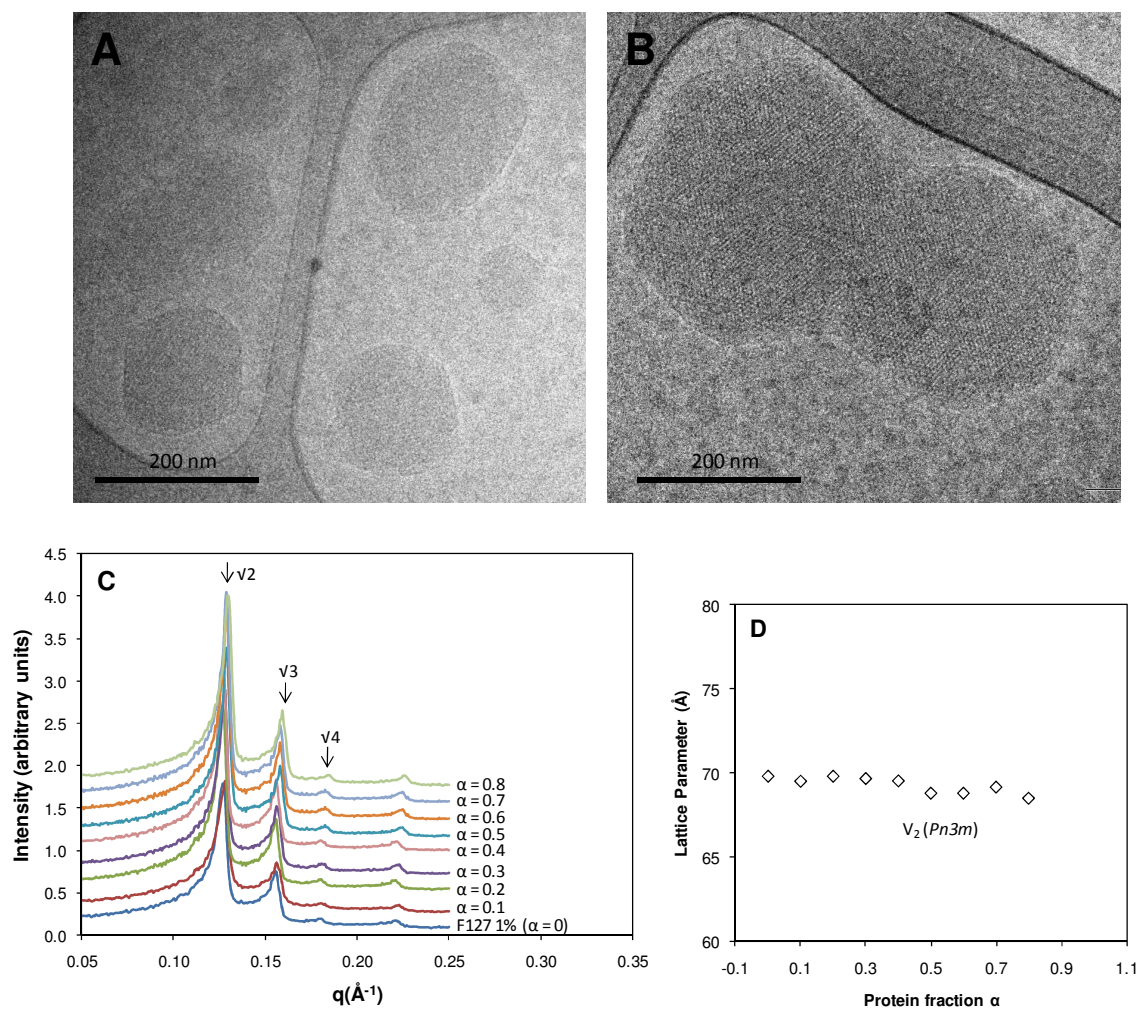


Figure 3

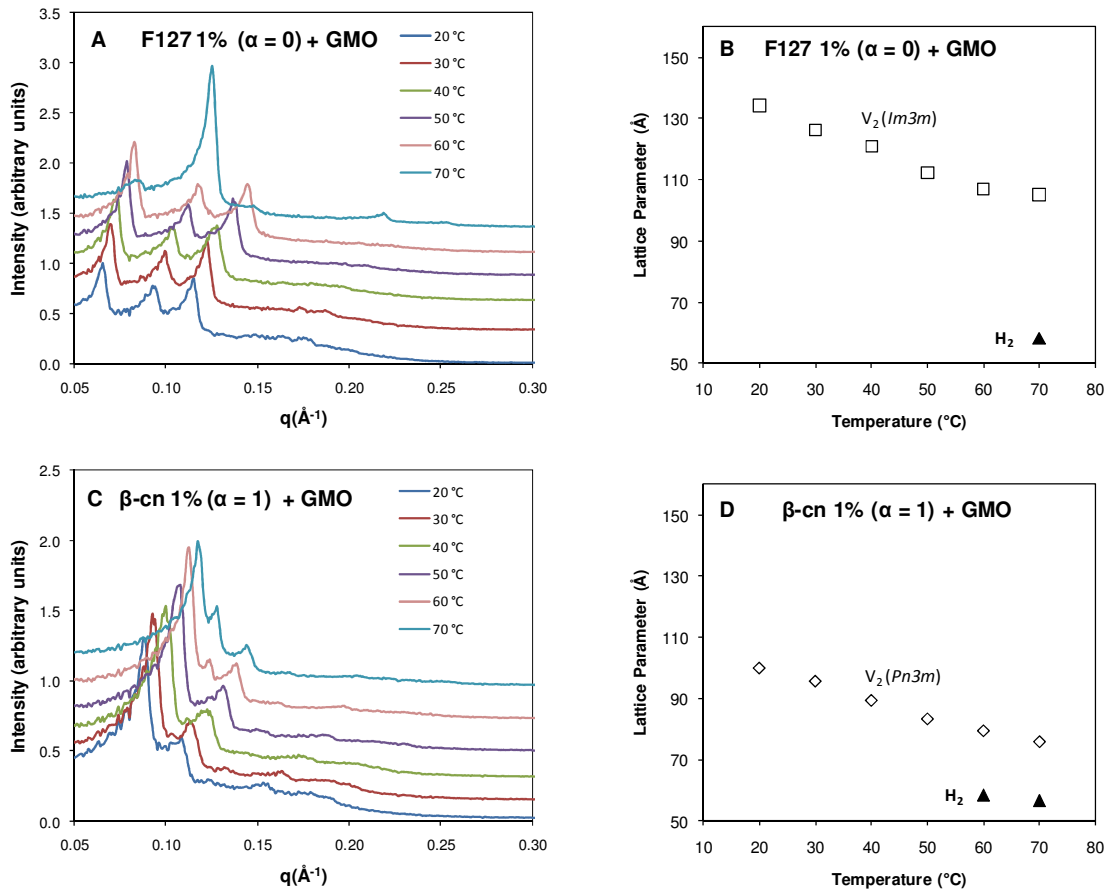


Figure 4

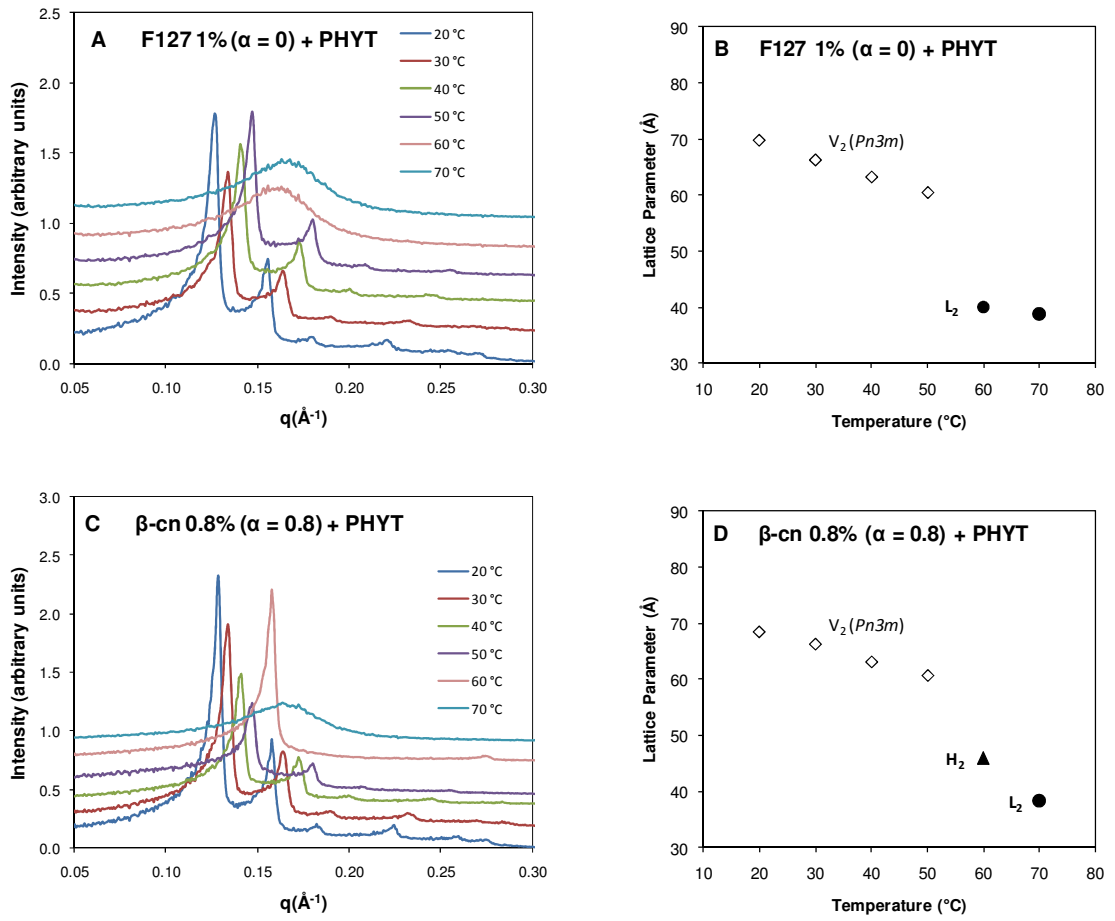


Figure 5

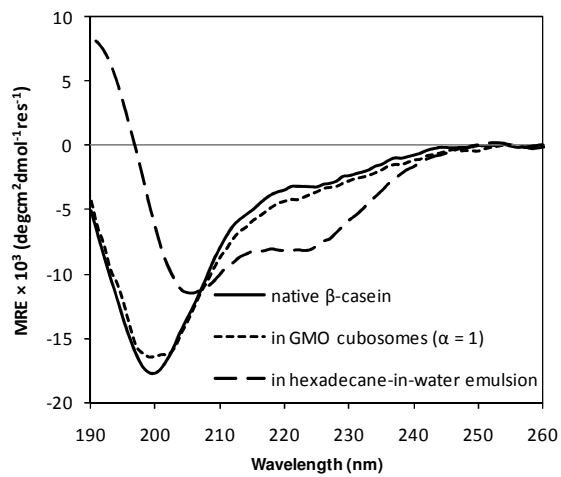


Figure 6

Appendix 6.1: Supporting information

Table S1: The mean particle size and polydispersity index (Pdi) of β -casein-stabilized GMO or PHYT dispersions.

α	GMO		PHYT	
	Size (nm)	Pdi	Size (nm)	Pdi
1	262.9±16.2	0.282±0.014	-	-
0.9	233.3±4.3	0.166±0.021	-	-
0.8	192.1±0.9	0.135±0.006	345.7±38.7	0.306±0.121
0.7	232.1±34.8	0.239±0.073	338.9±7.0	0.312±0.065
0.6	188.4±2.1	0.122±0.017	389.1±19.9	0.486±0.066
0.5	185.5±5.6	0.139±0.017	398.6±17.7	0.343±0.206
0.4	199.6±0.4	0.143±0.002	425.0±8.1	0.350±0.093
0.3	207.6±2.4	0.132±0.011	374.0±4.3	0.196±0.119
0.2	275.1±1.4	0.251±0.010	359.2±14.4	0.347±0.078
0.1	218.0±15.8	0.198±0.072	275.1±27.7	0.206±0.114
0:1	181.5±0.7	0.106±0.019	348.7±8.4	0.415±0.016

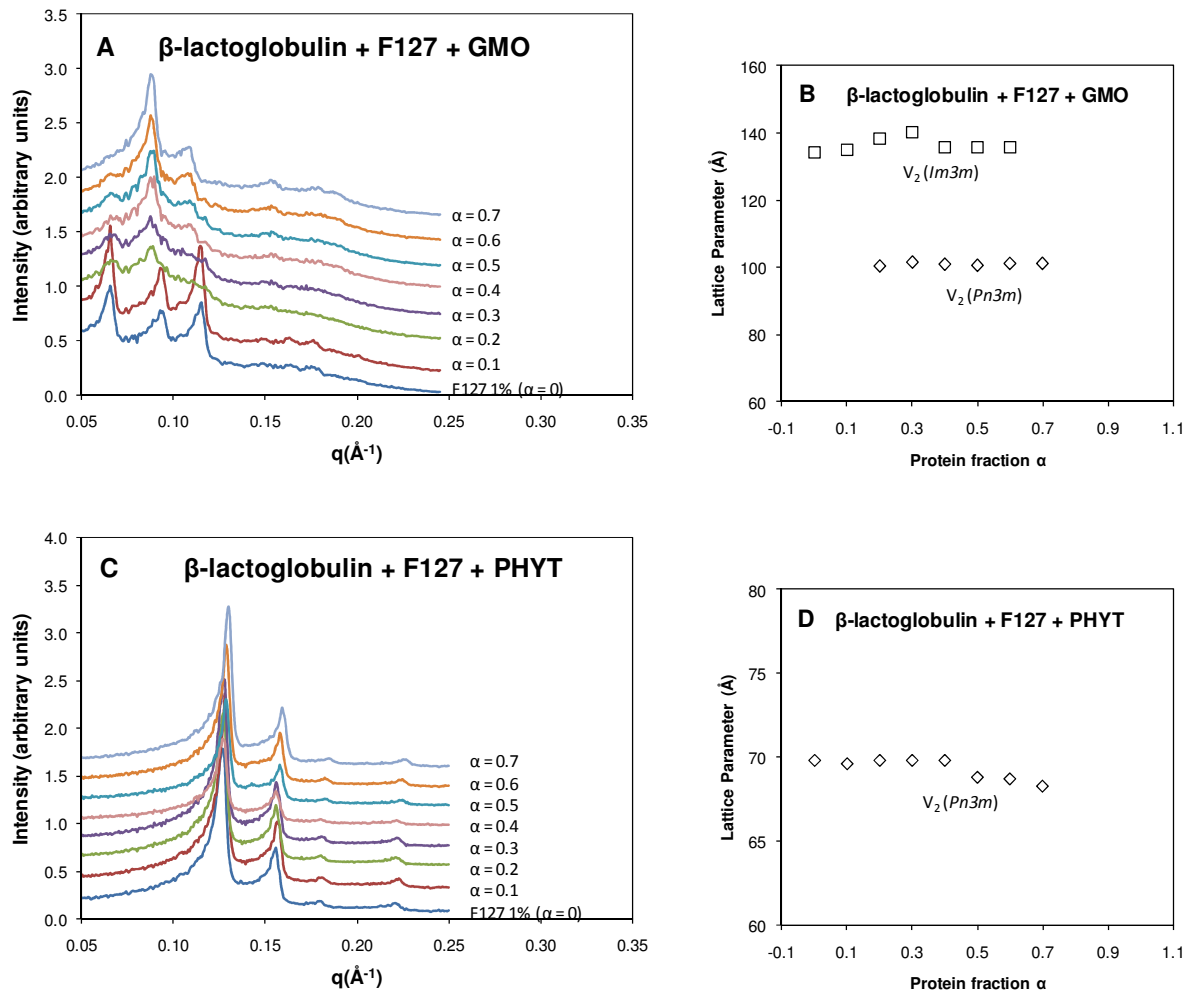
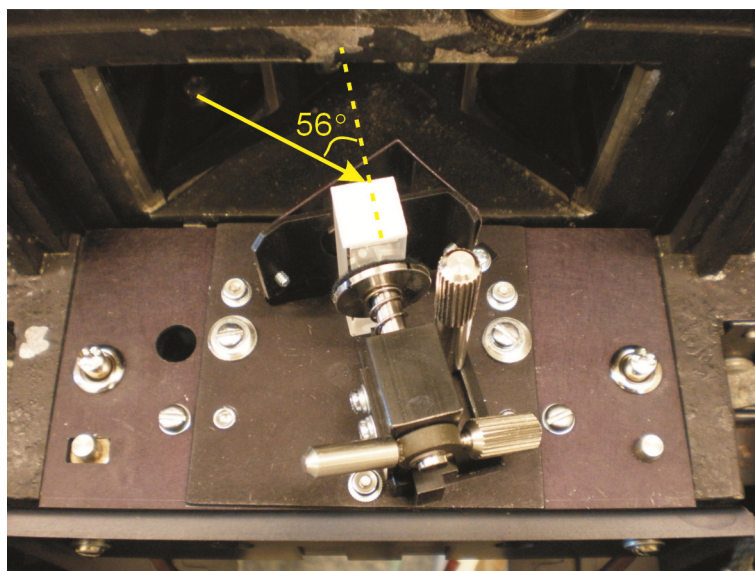


Figure S1: (A) and (C) SAXS patterns of GMO-based and PHYT-based dispersions stabilized by various ratios of β -lactoglobulin : F127. (B) and (D) Phase identity and lattice parameter derived from SAXS data in (A) and (C) respectively as a function of the fraction of β -lactoglobulin to total stabilizer (α).

Chapter 7

Discussion and conclusion



The front-face mode of a fluorimeter where the light strikes a sample at 56°

The interfacial structure of proteins adsorbed at oil-water interfaces of emulsions is a key factor controlling the physical stability as well as other physiochemical properties of oil-in-water emulsions (Chapter 1 Sections 1.3.2 & 1.4). This project set out to investigate the adsorption of milk proteins to the oil-water interface of emulsions. The principal aim was to understand the interfacial structure-function relationship of milk proteins by studying how the structure of proteins adsorbed at the oil-water interface correlates with their ability to maintain the physical stability of emulsions under conditions of heating to 90 °C and/or addition of 120 mM NaCl.

Chapter 2 describes the design of a new experimental approach based on synchrotron radiation circular dichroism (SRCD) spectroscopy to allow in situ measurements of the interfacial structure of proteins in turbid emulsion samples.¹ Specifically, the study investigated the secondary and tertiary structure of β -lactoglobulin (β -Lg) adsorbed at the interface of a model hexadecane-in-water emulsion made by high pressure homogenization. It was found that the high photon intensity from the synchrotron source allowed the secondary structure of β -Lg in the turbid emulsion to be measured directly in the far-UV region of SRCD without the need for further sample preparation. A dramatically improved SRCD signal-to-noise ratio was obtained compared to conventional bench-top CD instruments. Most importantly, a surfactant-based emulsion was used to correct for droplet light scattering which affected the baseline of each SRCD spectrum of the emulsion. This method differentiated the signal arising solely due to the protein in the emulsion from the signal arising from droplet light scattering. A parallel experiment on β -Lg in a refractive index matched emulsion (RIME) was also conducted using a previous method developed by Husband et al. (2001) (Chapter 1 Section 1.3.3.5).² These RIME experiments generated results consistent with those obtained from the direct measurement in the unmatched emulsion and validated the new SRCD method. Overall, the study found that adsorption to the hexadecane-water interface induced the disruption of β -Lg globular structure, which corresponded to a decrease in the β -sheet structure and an increase in the non-native α -helical structure. This study provided the basis for subsequent studies of the structural changes of proteins in turbid samples, including four studies of the application of SRCD spectroscopy to directly measure the interfacial conformation of proteins in emulsions (Chapters 3-5)³⁻⁵ and lipid liquid crystalline nanostructured particles (Chapter 6).⁶

Chapter 3 describes a study of how the adsorption-induced changes in the interfacial structure of β -Lg affected its ability to stabilize oil-in-water emulsions under conditions of heating and salt addition.⁴ The secondary and tertiary structure of β -Lg adsorbed at the interfaces of two different oil-in-water emulsions (hexadecane-in-water and tricaprilyn-in-water emulsions) were studied using SRCD spectroscopy and front-face tryptophan fluorescence (FFTF) spectroscopy. The results showed that β -Lg adsorbed to both oil-water interfaces and changed from a globular structure (3.6 nm in diameter) rich in the β -sheet, into an interfacial secondary structure with a large amount of the non-native α -helix. Analysis of the stability of the secondary structure found

that the non-native α -helical-rich conformation of β -Lg adsorbed at oil-water interfaces only underwent a minor change upon heating to 76 °C in comparison to the dramatic change in the β -Lg conformation in solution as the temperature was increased. Protein structural rearrangement was found to be more dramatic upon adsorption to the more hydrophobic hexadecane-water interface than the tricaprylin-water interface. Moreover, the conformation of β -Lg at the hexadecane-water interface was more resistant to further changes upon heating than that of β -Lg at the tricaprylin-water interface. The geometric dimensions of β -Lg adsorbed at a planar C18-water interface mimicking the oil-water interface of the emulsion were investigated using dual polarization interferometry (DPI). It was found that the β -Lg layer adsorbed at the planar C18-water interface was thin (~ 1 nm) and dense (~ 1 g/cm³). These results highlight that the hydrophobic effect, i.e. the interaction between the hydrophobic region of the protein and the oil-water interface, is a significant thermodynamic driving force for protein structural rearrangement. A parallel study of the emulsion stability upon heating and salt addition was then performed by measuring the emulsion ζ -potential and mean particle size. The structural change of β -Lg induced by adsorption to the oil-water interface resulted in thin interfacial layer around the droplet surfaces, which were negatively charged (approximately -60 mV of ζ -potential). This interfacial layer provided electrostatic repulsion between the droplets of the β -Lg-stabilized emulsion, which was resistant to flocculation upon heating to 90 °C in the absence of salt. However, once exposed to elevated ionic strength by addition of 120 mM NaCl, the electrostatic repulsion between the droplets was reduced via the electrostatic screening effect (Chapter 1 Section 1.2.2.3) to the point where droplet flocculation occurred with heating to temperatures above 60 °C. Overall, this study provided insight at a detailed molecular level into the relationship between the structural rearrangement of β -Lg upon adsorption at oil-water interfaces of emulsions and the physical stability of emulsions under conditions of heating and salt addition.

Chapter 4 presents a study of the relationship between the interfacial structure of α -lactalbumin (α -La) and its ability to stabilize hexadecane-in-water and tricaprylin-in-water emulsions using experimental approaches established in Chapters 2 and 3 for β -Lg. α -La was chosen as the second globular protein to investigate because it has more α -helix and lacks free thiol groups in its native conformation in comparison to β -Lg. The SRCD and FFTF results showed that adsorption to the hexadecane-water and the tricaprylin-water interfaces disrupted the compact globular structure of α -La ($2.5 \times 3.2 \times 3.7$ nm in the crystal structure dimension) and caused a considerable increase in the α -helical conformation, which was resistant to further changes upon heating. The α -La layer adsorbed at the planar C18-water interface was thin (~ 1 nm) and dense (~ 1 g/cm³) as indicated by DPI. The fact that the more hydrophobic environment of the hexadecane-water interface induced a larger conformational change in α -La compared to the tricaprylin-water interface was consistent with the β -Lg study. These results confirmed that the hydrophobic effect is

the thermodynamic driving force for protein structural rearrangement at oil-water interfaces, where the hydrophobic region of the protein interacts closely with the oil phase and the hydrophilic region locates within the aqueous phase. This new conformation of α -La adsorbed at oil-water interfaces was found to be very different from its well-known conformation in the molten globule state in solution. Subsequent analysis of the emulsion stability revealed that the thin, dense and negatively charged α -La layer (approximately -49 mV of ζ -potential) provided strong electrostatic repulsion between the emulsion droplets, resulting in the resistance of emulsion droplets to heat-induced flocculation. Moreover, when salt was added prior to heating, α -La-stabilized emulsions were more stable to droplet flocculation than β -Lg-stabilized emulsions. This can be due to the lack of free thiol groups in α -La resulting in the lack of inter-droplet sulfhydryl-disulfide interactions between emulsion droplets. This study has therefore provided new information at a molecular level that enhances our understanding of how the interfacial structure of α -La influences the physical stability of emulsions under conditions of heating and salt addition.

Chapter 5 extends the study of the interplay between protein interfacial structure and the emulsion stability to a third protein, i.e. β -casein. β -Casein differs largely from both β -Lg and α -La in that it is a flexible protein with a large amount of unordered secondary structure and no well-defined tertiary structure. The SRCD and FFTF results showed that β -casein adsorbed at oil-water interfaces of hexadecane-in-water and tricaprylin-in-water emulsions underwent a structural change, where the α -helical conformation was increased and the tryptophan-containing C-terminal region moved to a more hydrophobic environment, i.e. the oil phase. The DPI results showed that the β -casein layer at a hydrophobic C18 surface was 2.5-5.0 nm thick, which was thinner than the β -casein layer (5-10 nm) adsorbed at air-water or hexane-water interfaces as measured by neutron reflectometry (Chapter 1 Section 1.4.3).⁷⁻⁹ Nevertheless, this study showed that adsorption of β -casein to oil-water interfaces resulted in a protein layer that was negatively charged (approximately -40 mV of ζ -potential) and thicker (~5 nm) and more diffuse (0.4 g/cm^3) than the β -Lg and α -La layers. This interfacial β -casein layer provided a combination of electrostatic and steric repulsion between the emulsion droplets, which imparted excellent stability of β -casein-stabilized emulsions under conditions of heating and salt addition. Together with the results of β -Lg and α -La studies, this study of β -casein has enriched our understanding of the influence of intrinsic molecular properties on protein structural rearrangement upon adsorption as discussed below.

Chapter 6 explored the stabilizing function of β -casein in a different colloidal system, i.e. a lipid liquid crystalline nanostructured particle system.⁶ Since β -casein has an interfacial structure that imparts steric stabilization to oil-in-water emulsions, it was hypothesized that β -casein can also act as a stabilizer in lipid liquid crystalline nanostructured particles, which are commonly stabilized by polymeric emulsifiers such as Pluronic F127. The study used β -casein on its own or in a mixture with Pluronic F127 to disperse two lipids, glyceryl monooleate (GMO) and phytantriol (PHYT),

into cubosomes and to investigate the thermally induced phase behaviour of the resulting dispersions. The major results from this study were: 1) β -casein on its own was able to disperse GMO in excess water into cubosomes with an internal structure of a cubic ($Pn3m$) phase; 2) β -casein as a sole stabilizer was not able to disperse PHYT and a threshold fraction of Pluronic F127 (20%) was needed to produce stable PHYT cubosomes with a cubic ($Pn3m$) phase; 3) β -casein-stabilized dispersions for both GMO and PHYT strongly favoured the transition from the cubic phase to the hexagonal phase compared to Pluronic F127-based dispersions; and 4) adsorption of β -casein to the GMO-water interface did not induce significant conformational changes of β -casein. These results suggested that compared to Pluronic F127, β -casein interacted more weakly with the lipid-water interface and provided less steric stabilization to lipid liquid crystalline nanostructured particles. However, the very feature of the flexible structure of β -casein allowed it to act as a space filling agent in the hexagonal phase. Since the hexagonal phase has shown advantages over the cubic phase in terms of prolonged release of drug molecules and nutrients due to their smaller water channels (Chapter 1 Section 1.5), reducing the cubic to hexagonal phase transition temperature via the presence of β -casein can have implications in formulation science with high relevance to physiological conditions.

From the summary above, it can be seen that this project has demonstrated the complex interplay between the interfacial structure and function of proteins in colloidal systems. This has been achieved through the development of biophysical methods that were applied to the analysis of proteins adsorbed at oil-water or lipid-water interfaces, yielding high-resolution data of the interfacial secondary and tertiary structure. The following discussion highlights the advantages of the involved biophysical techniques, the effect of both intrinsic molecular properties and external factors on protein structural rearrangement upon adsorption and how different interfacial structures of proteins predict their ability to provide physical stabilization to colloidal systems.

This project reported the first application of far-UV SRCD spectroscopy (Chapter 1 Section 1.3.3.5) to milky colloidal samples of emulsions and lipid particles with high light absorbance and scattering properties. The combination of the strong light intensity from a synchrotron source and the scattering background correction from suitable control samples has allowed the direct characterization of the secondary structure of β -Lg, α -La and β -casein adsorbed at oil-water interfaces (Chapters 2-5) as well as at lipid-water interfaces (Chapter 6), which were not possible before. In the emulsion studies, the SRCD results identified the formation of the non-native interfacial conformations of proteins with an increased amount of α -helix and the stability of these interfacial conformations upon heating. These SRCD studies reported that high-quality SRCD spectra of the secondary structure of proteins in turbid colloidal samples can be measured directly. Together with the analysis of the secondary structural content, these studies provide a high degree

of confidence in the secondary structural changes of proteins that occur upon adsorption to oil-water or lipid-water interfaces.

SRCD spectroscopy in the near-UV region (Chapter 1 Section 1.3.3.5) was employed to obtain information on protein tertiary structural changes upon adsorption to oil-water interfaces of emulsions. The near-UV SRCD spectrum of a globular protein has a characteristic shape and magnitude depending on the number of each type of aromatic amino acids present, their position in the protein and more importantly the nature of their hydrophobic environment. Thus, the spectrum provides a fingerprint of the tertiary structure of the protein, as seen in the β -Lg and α -La studies (Chapters 3 & 4). The loss of the near-UV SRCD signals of β -Lg and α -La upon adsorption to oil-water interfaces clearly indicated a strong perturbation of their tertiary structures. However, the refractive index matching method developed by Husband et al. (2001)² was needed to make the emulsion sample transparent in order to obtain high quality near-UV SRCD spectra. FFTF spectroscopy (Chapter 1 Section 1.3.3.4) was also employed as an important complementary technique to near-UV SRCD spectroscopy for characterization of the tertiary structure of globular proteins adsorbed at oil-water interfaces of emulsions. The advantage of FFTF is that it can measure proteins in emulsion samples without further sample preparation. The λ_{max} in FFTF spectra is sensitive to the hydrophobic environment of tryptophan residues. The FFTF results showed that upon adsorption to oil-water interfaces, the two tryptophan residues in β -Lg (one deeply buried and one partially exposed in native conformation) moved to a more hydrophobic environment (Chapter 3), whereas the four tryptophan residues of α -La (all deeply buried) moved to a more hydrophilic environment (Chapter 4). These results confirmed the perturbation of the globular structures of β -Lg and α -La upon adsorption to oil-water interfaces as seen in the near-UV SRCD experiments.

DPI is a biosensing technique which allows real-time measurements of the mass, thickness and density of a protein layer adsorbed at different solid-liquid interfaces (Chapter 1 Section 1.3.3.2). This project utilized DPI to examine the geometric dimensions of protein layers adsorbed at two different interfaces, a hydrophobic C18-water interface and a hydrophilic silicon oxynitride-water interface. The DPI results showed how globular proteins, β -Lg and α -La, either retained their native structural dimensions at the hydrophilic silicon oxynitride-water interface or underwent significant structural changes forming a thin (~ 1 nm), dense (~ 1 g/cm³) protein layer at the hydrophobic C18-water interface (Chapters 3 & 4). When DPI was applied to the β -casein study, the adsorption to the C18 surface resulted in a relatively diffuse (~ 0.4 g/cm³) protein layer of 2.3-5 nm thick (Chapter 5). This thickness of the β -casein layer obtained with DPI was lower than that derived from neutron reflectivity studies, which have reported a 5-10 nm thickness for the β -casein layer adsorbed at air-water or hexane-water interfaces.⁷⁻⁹ Cowsill et al. (2011) compared parallel measurements of the bovine serum albumin (BSA) layer adsorbed at silicon-water interfaces using both DPI and neutron reflectivity.¹⁰ They also reported a difference between the measured

thickness values with the BSA layer being 2-4 nm thinner when measured by DPI than by neutron reflectivity.¹⁰ This difference may have arisen because the DPI analysis uses a simplified single-layer model that assumes a uniform protein layer at the sensor surface, whereas neutron reflectivity uses a two-layer model. Thus, neutron reflectivity is more suitable for calculating the thickness and density profile of adsorbed protein layers consisting of a dense inner layer and a diffuse outer layer such as the β -casein layer. Nevertheless, DPI provides a range of sensor surfaces of different properties, which allows parallel studies to examine the mechanism of interface-mediated protein structural changes as seen in the β -Lg and α -La studies.

Using these biophysical methods, the interfacial structures of β -Lg (Chapter 3), α -La (Chapter 4) and β -casein (Chapter 5) adsorbed at oil-water interfaces of emulsions was characterized. A significant result was the increase in the α -helical conformation in the interfacial secondary structure of all three proteins. Taking the hexadecane-water interface as an example, the amount of the increase in the α -helical conformation followed the extent of β -Lg (34%) > α -La (28.6%) > β -casein (12%). β -Casein is the most flexible of the investigated three proteins. Although it is generally thought to be a more flexible protein that adsorbs to the interface and undergoes structural changes more readily than rigid proteins, the results from the current studies showed that the increase in α -helix of β -casein was the lowest of the three proteins. This is likely due to the fact that β -casein contains the largest number of proline residues, 17% proline content in β -casein compared to 4.9% in β -Lg and 1.6% in α -La.¹¹ It is thus difficult for β -casein to adopt the α -helical conformation even when adsorbed at oil-water interfaces because proline is a known helix breaker due to its ring structure. Therefore, the amino acid content of a protein also affects adsorption-induced conformational changes.

The thermal stability of the secondary structure of β -Lg and α -La adsorbed at oil-water interfaces was also investigated. The results showed that the non-native α -helical-rich conformations of β -Lg and α -La at oil-water interfaces were resistant to further changes upon heating to 76 °C (Chapters 3 & 4). In contrast, at a similar temperature in solution, β -Lg and α -La underwent significant conformation changes. The difference in the thermal stability of proteins in solution and at oil-water interfaces highlights the dominant forces in determining protein conformation, i.e. the hydrophobic effect and the conformational entropy (Chapter 1 Section 1.3.1). When proteins are free in solution, thermal energy causes a large gain of conformational entropy, which disrupts the hydrogen bonding and hydrophobic interactions essential for native folding structures. When proteins adsorb to the oil-water interface, the hydrophobic effect drives protein structural rearrangement, where the hydrophobic regions of the protein interact with the oil phase. This structural rearrangement has already 'denatured' the protein into a preferred conformation, which is anchored at the oil-water interface limiting the number of conformations the protein can

adopt. Increasing temperature may therefore have little impact on the interfacial conformation of proteins at oil-water interfaces.

This project also studied the effect of the oil phase on adsorption-induced structural changes of β -Lg (Chapter 3), α -La (Chapter 4) and β -casein (Chapter 5) by using two oil-water interfaces: the hexadecane-water interface and the tricaprylin-water interface. The results showed that: 1) the more hydrophobic hexadecane always induced a larger degree of conformational changes compared to tricaprylin; and 2) the conformation of proteins at the hexadecane-water interface was more resistant to further changes upon heating. These results also highlight the important role of the hydrophobic effect in determining the preferred conformation of the protein at the interface. When proteins adsorb to the oil-water interface, the hydrophobic effect drives the structural change of proteins, where the hydrophobic regions face toward the hydrophobic oil phase and polar residues are exposed to the aqueous phase.

In contrast to adsorption at oil-water interfaces of emulsions, there was no dramatic increase in ordered secondary structure of β -casein upon adsorption to the GMO-water interface of cubosomes (Chapter 6). Given the large surface area in cubosomes, it is unlikely that a large amount of β -casein remained in the bulk phase. The lack of secondary structure changes of β -casein adsorbed at the GMO-water interface can be due to the fact that the commercial GMO sample used in the study contains only 58.3% GMO and many other amphiphilic ingredients (Chapter 6 Materials and Methods) and thus is much more polar than hexadecane and tricaprylin. The more polar environment of the GMO-water interface may require less conformational changes for β -casein adsorption.

The oil phase also displayed an effect on droplet flocculation under conditions of heating and salt addition in the studies of the physical stability of emulsions stabilized by β -Lg (Chapter 3) and α -La (Chapter 4). The results revealed that the hexadecane-in-water emulsions were always more stable than the tricaprylin-in-water emulsions. The reason can be that colloidal van der Waals attractive interactions between emulsion droplets are weaker in the hexadecane-in-water emulsions than the tricaprylin-in-water emulsions. The strength of colloidal van der Waals interactions between the droplets in a particular emulsion depends on factors such as the droplet size and the refractive index of the oil phase (Chapter 1 Section 1.2.2.1). According to the Hamaker function, a smaller difference in the refractive indices between the oil and continuous phases results in a smaller strength of the van der Waals attraction between emulsion droplets. As discussed in Chapter 3, the refractive indices of hexadecane and tricaprylin are 1.435 and 1.449 respectively. The difference between oil and water was therefore 0.102 for hexadecane and 0.116 for tricaprylin. The smaller refractive index of hexadecane and the smaller initial droplet size of the hexadecane-

in-water emulsions lead to smaller van der Waals attraction between hexadecane-in-water droplets than the attraction between tricaprilyn-in-water droplets, resulting in greater emulsion stability.

Overall, the studies presented in this thesis revealed the interplay between the interfacial structure and stabilizing function of proteins in emulsions. The colloidal stability of an emulsion is determined by colloidal interactions, such as van der Waals attractive forces, electrostatic repulsive forces and steric repulsive forces (Chapter 1 Sections 1.2.2 & 1.2.3). In the case of β -Lg (Chapter 3), the structural study revealed a very thin protein layer with negative charges around the droplet surfaces of emulsions. The major colloidal interaction of β -Lg-stabilized emulsions was thus a balance between van der Waals attractive forces and electrostatic repulsive forces. Therefore, β -Lg-stabilized emulsions were prone to flocculation upon heating in the presence of salt when electrostatic repulsive interactions were largely screened and the inter-droplet hydrophobic and sulfhydryl-disulfide interactions occurred between the β -Lg interfacial layers. In the case of α -La (Chapter 4), structural studies showed a high similarity between the adsorbed α -La layer and the β -Lg layer, i.e. thin, dense and negatively charged. The main stabilization mechanism to oppose colloidal van der Waals attractive forces was therefore still electrostatic repulsion in α -La-stabilized emulsions. Moreover, the lack of the inter-droplet sulfhydryl-disulfide interactions in the α -La-stabilized emulsions made the droplets more resistant to flocculation upon heating even in the presence of salt.

In the case of β -casein (Chapter 5), the presence of a negatively charged and thick layer of β -casein adsorbed at oil-water interfaces gave the most stable emulsions under conditions of heating and/or the presence of salt as compared to β -Lg and α -La-stabilized emulsions. The combination of electrostatic and steric repulsive forces strongly opposed the van der Waals attraction between the droplets in β -casein-stabilized emulsions. In the final study of this project, β -Lg and β -casein were investigated to stabilize a second colloidal system, i.e. the lipid liquid crystalline nanostructured particles (Chapter 6). The results showed that only β -casein, whose interfacial structure provide both steric and electrostatic stabilization, can oppose the van der Waals and hydrophobic attraction in such systems and therefore form stable cubosomes.

In conclusion, this project employed a range of biophysical techniques, i.e. SRCD spectroscopy, FFTF spectroscopy and DPI, for measurement of the interfacial structures of proteins adsorbed at oil-water or lipid-water interfaces and planar C18-water interfaces. These methods demonstrated great advantages in terms of in situ characterization of protein interfacial structure at three different levels, i.e. the secondary structure, the tertiary structure and the geometric dimensions. The structural studies in this thesis provided insight into mechanisms of protein structural rearrangement upon adsorption to oil-water or lipid-water interfaces by selecting a range of proteins (β -Lg, α -La and β -casein) and by manipulating external environments (oil polarity and

heating). Furthermore, the studies on the stability behaviour of the protein-stabilized colloidal systems (oil-in-water emulsions and lipid liquid crystalline nanostructured particles) under conditions of heating and/or salt addition revealed the interplay between the interfacial structure and the stabilizing function of these proteins in colloidal systems.

The ability to determine protein conformations in colloidal systems at a high molecular level opens great potential for research on protein adsorption to liquid-liquid or solid-liquid interfaces. Future studies may investigate a wider range of proteins, interfaces and environmental conditions (pH, ionic strength, etc.) to gain a better understanding of how intrinsic molecular properties (internal disulfide bonding, flexibility, surface hydrophobicity, etc.), interfacial properties (hydrophobicity, etc.) and the environment mediate protein structural rearrangement and in turn the colloidal stability. These studies may help exploit an interesting phenomenon revealed in the studies in this thesis, i.e. the increase in the non-native α -helical conformation upon protein adsorption to oil-water interfaces. Furthermore, these studies may lead to protein engineering in order to improve their interfacial function, particularly through control of the surface-induced secondary structure, and to tailor the stability and physicochemical properties of emulsions.

Emulsions used in food and pharmaceutical industries are more complex than the model systems studied in this thesis. Thus, studying more complex systems containing a mixture of proteins and/or surfactants as emulsifiers will be essential to further advance our understanding and apply the knowledge arising from basic research to industrial applications. Research in the field of food emulsion and drug delivery sciences has also focused on the physiological effects of the stability and properties of emulsions and lipid-based drugs once they are in the gastrointestinal tract. Studying the conformational changes of plasma proteins and enzymes such as lipases upon adsorption to the interface of emulsions and lipid particles may provide new information on how these proteins mediate the release of the cargo nutrients and drugs by these colloidal systems. Thus, emulsion engineering may well benefit from these types of studies. Overall, this project has characterized the adsorption of proteins to oil-water or lipid-water interfaces in colloidal systems of emulsions and lipid liquid crystalline nanostructured particles, which are commonly used or have great potential in food and pharmaceutical industries. New information obtained from this project and ongoing future work will therefore have significant implications in the development and improvement of the formulation and quality of products based on proteins in emulsions and lipid particles.

References

- (1) Zhai, J.; Miles, A.J.; Pattenden, L.K.; Lee, T.-H.; Augustin, M.A.; Wallace, B.A.; Aguilar, M.-I.; Wooster, T.J. *Changes in β -lactoglobulin conformation at the oil/water interface of emulsions studied by synchrotron radiation circular dichroism spectroscopy. *Biomacromolecules* **2010**, *11*, 2136-2142.*
- (2) Husband, F.A.; Garrood, M.J.; Mackie, A.R.; Burnett, G.R.; Wilde, P.J. *Adsorbed protein secondary and tertiary structures by circular dichroism and infrared spectroscopy with refractive index matched emulsions. *J. Agric. Food Chem.* **2001**, *49*, 859-866.*
- (3) Wong, B.T.; Zhai, J.; Hoffmann, S.V.; Aguilar, M.-I.; Augustin, M.A.; Wooster, T.J.; Day, L. *Conformational changes to deamidated wheat gliadins and β -casein upon adsorption to oil-water emulsion interfaces. *Food Hydrocolloids*, in press.*
- (4) Zhai, J.; Wooster, T.J.; Hoffmann, S.V.; Lee, T.-H.; Augustin, M.A.; Aguilar, M.-I. *Structural rearrangement of β -lactoglobulin at different oil-water interfaces and its effect on emulsion stability. *Langmuir* **2011**, *27*, 9227-9236.*
- (5) Zhai, J.; Hoffmann, S.V.; Day, L.; Lee, T.-H.; Augustin, M.A.; Aguilar, M.-I.; Wooster, T.J. *Conformational changes of α -lactalbumin adsorbed at oil-water interfaces: Interplay between protein structure and emulsion stability. Submitted to *Langmuir*, **2011**.*
- (6) Zhai, J.; Waddington, L.; Wooster, T.J.; Aguilar, M.-I.; Boyd, B.J. *Revisiting β -casein as a stabilizer for lipid liquid crystalline nanostructured particles. Submitted to *Langmuir*, **2011**.*
- (7) Atkinson, P.J.; Dickinson, E.; Horne, D.S.; Richardson, R.M. *Neutron reflectivity of adsorbed β -casein and β -lactoglobulin at the air/water interface. *J. Chem. Soc., Faraday Trans.* **1995**, *91*, 2847-2854.*
- (8) Dickinson, E.; Horne, D.S.; Phipps, J.S.; Richardson, R.M. *A neutron reflectivity study of the adsorption of β -casein at fluid interfaces. *Langmuir* **1993**, *9*, 242-248.*
- (9) Fragneto, G.; Thomas, R.K.; Rennie, A.R.; Penfold, J. *Neutron reflection study of bovine β -casein adsorbed on OTS self-assembled monolayers. *Science* **1995**, *267*, 657-660.*
- (10) Cowsill, B.J.; Coffey, P.D.; Yaseen, M.; Waigh, T.A.; Freeman, N.J.; Lu, J.R. *Measurement of the thickness of ultra-thin adsorbed globular protein layers with dual-polarisation interferometry: A comparison with neutron reflectivity. *Soft Matter* **2011**, *7*, 7223-7230.*
- (11) Farrell, H.M., Jr.; Jimenez-Flores, R.; Bleck, G.T.; Brown, E.M.; Butler, J.E.; Creamer, L.K.; Hicks, C.L.; Hollar, C.M.; Ng-Kwai-Hang, K.F.; Swaisgood, H.E. *Nomenclature of the proteins of cows' milk - sixth revision. *J. Dairy Sci.* **2004**, *87*, 1641-1674.*